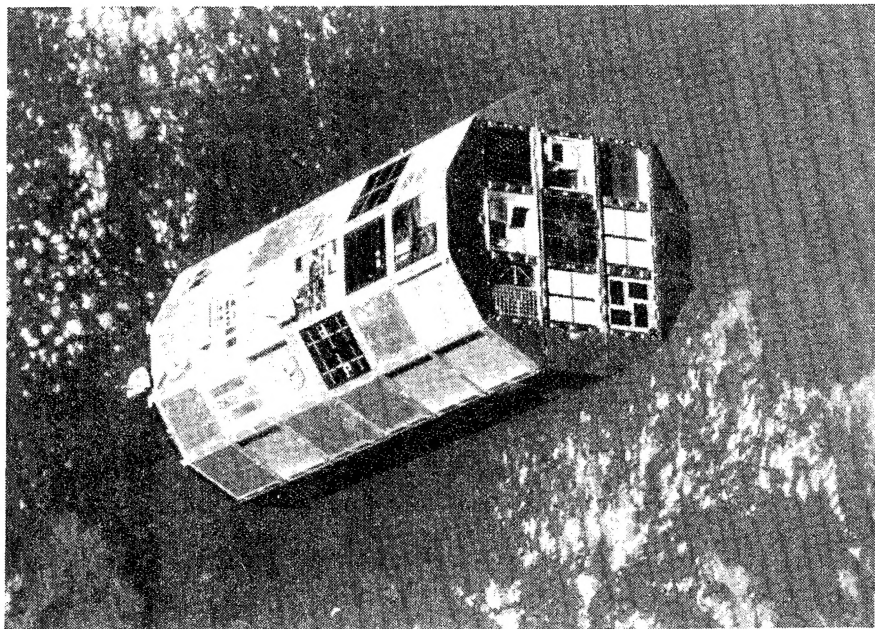
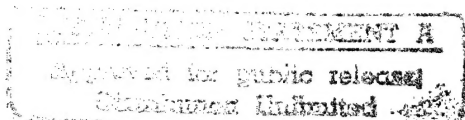


NASA/SDIO Space Environmental Effects on Materials Workshop



19960628 147

Proceedings of a workshop held at
NASA Langley Research Center
Hampton, Virginia
June 28-July 1, 1988



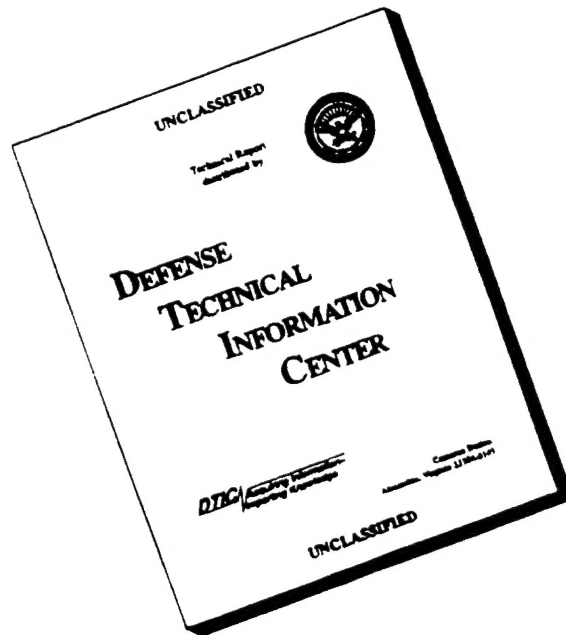
NASA

S

DECEMBER 1988

PLASTED
052884
(PL-052885-PL-052886)

DISCLAIMER NOTICE



**THIS DOCUMENT IS BEST
QUALITY AVAILABLE. THE
COPY FURNISHED TO DTIC
CONTAINED A SIGNIFICANT
NUMBER OF PAGES WHICH DO
NOT REPRODUCE LEGIBLY.**

*NASA Conference Publication 3035
Part 2*

NASA/SDIO Space Environmental Effects on Materials Workshop

*Compiled by
Louis A. Teichman and Bland A. Stein
NASA Langley Research Center
Hampton, Virginia*

Proceedings of a workshop jointly
sponsored by the National Aeronautics
and Space Administration and the
Strategic Defense Initiative
Organization, and held at
NASA Langley Research Center
Hampton, Virginia
June 28–July 1, 1988



National Aeronautics and
Space Administration
Office of Management
Scientific and Technical
Information Division

1989

PREFACE

Until now, most satellites have been launched with limited life expectancies (at most 3-5 years) and the materials used and the operating orbits selected for "long-term" flights have evolved from many successful shorter duration flights. During the 1990's, the Strategic Defense Initiative Organization (SDIO) plans to launch various platforms and satellites, and NASA plans to deploy Space Station Freedom and other large space structures. All of these spacecraft are expected to remain in space for 10 to 30 years at altitudes varying from low Earth orbit to geosynchronous orbit. The materials community is concerned that these systems will be vulnerable to environmentally induced degradation that will result in reduced performance. The environments of major concern are particulate radiation, atomic oxygen, micrometeoroids and debris, contamination, spacecraft charging, and solar radiation (ultraviolet (UV) and thermal cycling).

Although many spacecraft have performed successfully for relatively short periods of time, the effects of these environments, both individually and synergistically, on long-term materials performance is virtually unknown, and terrestrial facilities and tests are unable to resolve the uncertainties. In late 1987 opportunities for piggy-back or getaway special experiments or even a dedicated spaceflight seemed possible. Immediately, questions of which experiments to conduct and in what order of priority arose.

The primary objective of this workshop was to identify and prioritize candidate spaceflight experiments; that is, which materials experiments must be conducted in space to achieve maximum assurance that SDIO and NASA space assets will survive and perform for 10-30 years.

A secondary objective was to provide concise but authoritative tutorials describing each environmental factor. These tutorials would present current knowledge on topics such as each factor's applicable orbital ranges, its variations with time, how it interacts with various materials, and the subsequent consequences to materials or system performance. In addition, assessments of the sources of this knowledge (derived from true space exposure data or from modeling and laboratory simulations), the availability and authenticity of terrestrial test facilities, and the current understanding of interactions (synergisms) between these environmental effects would be offered.

The workshop was cosponsored by SDIO and NASA. It was organized by Charles F. Bersch of the Institute for Defense Analyses; Thomas W. Crooker of the Office of Aeronautics and Space Technology, NASA Headquarters; and Bland A. Stein of NASA Langley Research Center. The papers are published in the order in which they were presented at the Workshop; Section I contains an opening overview session on Environments and Materials Effects, followed by more detailed sessions on past spacecraft experience, and each of the environmental factors mentioned above. Each session was organized by its chairman, who also led the subsequent working group session for his environmental factor and prepared the presentations reproduced in Section II.

Administrative arrangements for the Workshop, as well as the collection of papers for and preparation of these Proceedings, was accomplished under the supervision of Dr. Louis A. Teichman at NASA Langley.

The efforts of the Executive Planning Committee and the Workshop Co-Chairmen are hereby acknowledged. They provided the perspective necessary to define the objectives and to organize a multidisciplinary Space Environmental Effects Workshop. They also planned the technical content of the tutorial presentations and the interactions of the groups representing the individual environmental disciplines. As a result, the objectives of the meeting regarding overall conclusions and recommendations were successfully reached by the collective efforts of all the Workshop participants.

The Executive Planning Committee consisted of

Charles F. Bersch	Institute for Defense Analysis
Herbert A. Cohen	W. J. Schafer Associates
Burton G. Cour-Palais	NASA Marshall Space Flight Center
Thomas W. Crooker	NASA Headquarters
Raymond L. Gause	NASA Marshall Space Flight Center
William Hong	Institute for Defense Analysis
Lubert J. Leger	NASA Johnson Space Center
Ranty H. Liang	Jet Propulsion Laboratory
Carolyn K. Purvis	NASA Lewis Research Center
Fred Smidt	Naval Research Laboratories
Bland A. Stein	NASA Langley Research Center
Louis A. Teichman	NASA Langley Research Center
Jack J. Triolo	NASA Goddard Space Flight Center
James. T. Visentine	NASA Johnson Space Center

The Workshop Co-Chairmen were Charles Bersch, Tom Crooker, and Bland Stein.

The excellence of the meeting facilities at the NASA Langley Activities Center and the continued cooperation of the staff, under the supervision of Ms. Patricia Gates, contributed significantly to the success of the Workshop. Arrangements were coordinated for the Executive Planning Committee by Dr. Louis Teichman.

Mr. Charles F. Bersch provided the primary impetus to the concept and basic goals of this Space Environmental Effects on Materials Workshop. The space environmental effects community owes him a debt of gratitude for his efforts.

CONTENTS

PREFACE	iii
---------------	-----

PART I*

SECTION I - THE TUTORIALS

SESSION 1: Overview: Environments and Materials Effects

Chairman: B. Stein - NASA Langley Research Center

Overview of Environmental Factors	5
C. K. Purvis - NASA Lewis Research Center	
Structural Materials for Space Applications	25
Darrel R. Tenney - NASA Langley Research Center	
Radiation Effects in Spacecraft Electronics	53
James P. Raymond - Mission Research Corporation	
Environmental Effects on Spacecraft Materials	75
J. W. Haffner - Rockwell International	
Surface Treatment Using Metal Foil Liner	87
Ray Garvey - Oak Ridge National Laboratory	
The Long Duration Exposure Facility Material Experiments	101
William H. Kinard and James L. Jones, Jr. - NASA Langley Research Center	

SESSION 2: SPACECRAFT EXPERIENCE

Chairman: J. Triolo - NASA Goddard Space Flight Center

Some Examples of the Degradation of Properties of Materials in Space	109
Frederick E. Betz and Joseph A. Hauser - Naval Research Laboratory	
Trends in Environmentally Induced Spacecraft Anomalies	123
Daniel C. Wilkinson - National Oceanic and Atmospheric Administration	
Returned Solar Max Hardware Degradation Study Results	133
Jack J. Triolo and Gilbert W. Ousley - Goddard Space Flight Center	
EnviroNet: Space Environment for Strategic Defense Initiative Experiments	161
Michael Lauriente - NASA Goddard Space Flight Center	

*Part I presented under separate cover.

†Paper not available at time of publication.

SESSION 3: ATOMIC OXYGEN
Chairmen: L. Leger and J. Visentine
NASA Lyndon B. Johnson Space Center

Environmental Definition of the Earth's Neutral Atmosphere	179
James T. Visentine - NASA Lyndon B. Johnson Space Center	
Atomic Oxygen Effects on Materials	197
Bruce A. Banks and Sharon Rutledge - NASA Lewis Research Center	
Joyce A. Brady - Sverdrup Technology, Inc.	
James E. Merrow - Ohio University	
Atomic Oxygen Effects Applications to Spacecraft	†
Ann Whitaker - NASA George C. Marshall Space Flight Center	
Atomic Oxygen Effects on Spacecraft Materials - The State of the Art of Our Knowledge	241
Steven L. Koontz - NASA Lyndon B. Johnson Space Center	

SESSION 4: MICROMETEORIDS AND DEBRIS
Chairman: Andrew Potter - NASA Lyndon B. Johnson Space Center

The Long-Term Effects of the Micrometeoroid and Orbital Debris Environments on Materials Used in Space	257
Burton G. Cour-Palais - NASA Lyndon B. Johnson Space Center	
Orbital Debris Environment and Data Requirements	281
Donald J. Kessler - NASA Lyndon B. Johnson Space Center	
Microparticle Impacts in Space - Results From Solar MAX Satellite and Shuttle Witness Plate Inspections	301
David S. McKay - NASA Lyndon B. Johnson Space Center	

SESSION 5: CONTAMINATION
Chairman: C. Maag - Jet Propulsion Laboratory

S/C Contamination Environments Overview	†
L. Bareiss - Martin Marietta Corporation	
Spacecraft Contamination Experience	331
E. N. Borson - The Aerospace Corporation	
Effects of the Contamination Environment on Surfaces and Materials	353
Carl R. Maag - Jet Propulsion Laboratory	

PART II

SESSION 6: TRAPPED RADIATION

Chairmen: W. K. Stuckey and A. L. Vampola
The Aerospace Corporation

The Space Particle Environment	367
A. L. Vampola - The Aerospace Corporation	
Effects of Space Radiation on Electronic Microcircuits	383
W. A. Kolasinski - The Aerospace Corporation	
The Radiation Belt Mission on CRRES	†
D. Hardy - Air Force Geophysics Laboratory	

SESSION 7: SOLAR RADIATION

Chairman: Wayne S. Slemp - NASA Langley Research Center

Space Vehicle Thermal Testing: Principles, Practices, and Effectiveness	395
Donald F. Gluck - The Aerospace Corporation	
Ultraviolet Radiation Effects	PL-052885 (425)
Wayne S. Slemp - NASA Langley Research Center	
Effects of Thermal Cycling on Composite Materials for Space Structures	(447)
Stephen S. Tompkins - NASA Langley Research Center	

SESSION 8: SPACECRAFT CHARGING

Chairman: N. John Stevens - TRW

Dielectrics for Long Term Space Exposure and Spacecraft Charging A Briefing	473
A. R. Frederickson - Air Force Geophysics Laboratory	
An Overview of Charging Environments	495
S. B. Gabriel and H. B. Garrett - Jet Propulsion Laboratory	
Surface Phenomena in Plasma Environments	511
C. K. Purvis and D. C. Ferguson - NASA Lewis Research Center	
Influence of Charging Environments on Spacecraft Materials and System Performance	535
N. John Stevens - TRW Space and Technology Group	

SECTION II-A

WORKING GROUP ORAL PRESENTATIONS	543
--	-----

Atomic Oxygen	545
Micrometeoroids and Debris	553
Contamination	559
Trapped Radiation	565
Appendix: Trapped Particle Flux Models at NSSDC/WDC-A-R&S	569
D. Bilitza, D. M. Sawyer, J. H. King	
Solar Radiation	573
Spacecraft Charging	577

SECTION II-B

WORKING GROUP WRITTEN PRESENTATIONS	585
Atomic Oxygen	587
Meteoroid/Orbital Debris Effects on Materials	589
Contamination	†
Trapped Radiation Effects	597
Solar Radiation	607
Spacecraft Charging	609

SECTION II-C

Conclusions and Recommendations to NASA and SDIO	621
As summarized by William Hong - Institute for Defense Analysis	

PART II

SESSION 6: TRAPPED RADIATION

Chairmen: W. K. Stuckey and A. L. Vampola
The Aerospace Corporation

The Space Particle Environment

A. L. Vampola

The Aerospace Corporation, P.O. Box 92957, Los Angeles, CA 90009

ABSTRACT

This paper is a tutorial covering the energetic charged particle environment in the Earth's magnetosphere. It provides an overview of trapped particle morphology, the geometry of the trapping regions, the radiation environmental models, the current status of these models, and future modelling requirements.

INTRODUCTION

The extensive use of space for platforms for communications, surveillance such as weather and Earth resources, science research, military objectives, and manned activities results in a critical requirement for knowledge about the energetic particle environment in space. Radiation damage to circuits and materials, background effects in sensors, hazard to personnel, spurious effects in circuits: all are the result of this energetic particle environment. Utilization of space is continuing to increase. With this increase comes an equivalent increase in the number of personnel who have to have basic knowledge about and access to information about the space particle environment. The material here is intended to provide an overview in the areas of the dynamics of the particle environment, trapped radiation morphology, current trapped radiation models, and future modelling activity in this field. The references accompanying this discussion can serve as a convenient source for more detailed information in this field.

A Geiger-Muller tube launched February 1, 1958 on Explorer I by Dr. James Van Allen is considered to have produced the discovery of the trapped radiation belts surrounding the earth, but such a phenomenon had been predicted prior to the launch of the first artificial Earth satellite. A great flurry of activity aimed at understanding the radiation belts (sometimes called the *Van Allen belts*) ensued. However the myriad of measurements initially resulted in the acquisition of data rather than the acquisition of understanding. Part of the problem was the fact that data were being organized in terms of the orbital parameters longitude-latitude-altitude, a three parameter space, and the quantity of data was insufficient to provide a sufficient density of data points in any part of space to produce a reliable picture of the particle population. In addition to the three spatial parameters, there were also energy, time, and species to contend with. Some instruments made integral energy measurements (detected everything above a particular energy threshold, such as Geiger counters which counted any charged particle which could penetrate its window or walls), some made differential energy measurements, some made unidirectional measurements using collimators, others accepted particles coming from anywhere within a 2π or 4π steradian angle. Some detectors were on spinning vehicles, other on stabilized platforms. Since the particle population is not isotropic (same intensity in all directions), further confusion was possible. The first major step toward producing order out of chaos was taken by Prof. Carl McIlwain when he introduced a new variable, L , based on the second adiabatic invariant of particle motion [1], which with the magnetic field coordinate B formed a two-parameter space to replace the three spatial coordinates used to describe satellite orbits. The variable L is discussed in the next section.

In 1965, NASA funded Dr. James Vette of the Aerospace Corporation to produce model electron and proton environments using the data then available from the various satellites. All the particle data sets available within the US were assembled and incorporated into model environments--AE1 (Aerospace Electron model environment number 1) and AP1 (Aerospace Proton model environment number 1) were the result. These initial models could not be considered to be more than educated guesses. Great effort was expended in translating the various data sets into a common parameter space. (As noted above, different variables controlled the various experimental measurements of the trapped particles.) Since with

sparse data sets differential energy measurements could be converted reliably into integral fluxes and unidirectional measurements into omnidirectional but not vice-versa, the "lowest common denominator" approach was used: fluxes were specified as integral-omnidirectional fluxes as a function of location in B,L space. This is still the mode used for most trapped particle environment models. Two to three orders of magnitude disagreement between ostensibly similar measurements were the norm rather than the exception, even in some cases where the measurements were made at the same time by different instruments on the same satellite. It was realized that producing a reliable environmental model was going to be a gargantuan task. The National Space Science Data Center was set up by NASA at the Goddard Space Flight Center with Dr. Vette as its director and a major effort at space environment modelling was begun, one that continues at a low level to this day. The models produced by those efforts will be discussed later in this presentation.

TRAPPED PARTICLE MORPHOLOGY

In this section, three subjects will be discussed: trapped particle motions, McIlwain's "L" parameter, and the general configuration of the radiation belts. The discussion is at an introductory level: no previous knowledge about the particle radiation environment is assumed. The intent is to provide sufficient background material about radiation belt morphology that the rest of this tutorial and the other presentations in these proceedings which deal with particle radiation effects will be understood in context.

Trapped Particle Motions

An understanding of the dynamics of the radiation belts requires some knowledge of the dynamics of an individual particle. The three basic particle motions in the Earth's magnetosphere with which we are concerned are gyration or cyclotron motion, bounce, and drift. The gyration is about the local magnetic field line, the bounce motion is from one end of the field line to the other (one hemisphere to the other), and the drift is around the world in longitude. These motions are a consequence of the behavior of a charged particle with forces acting on it moving in a non-uniform magnetic field.

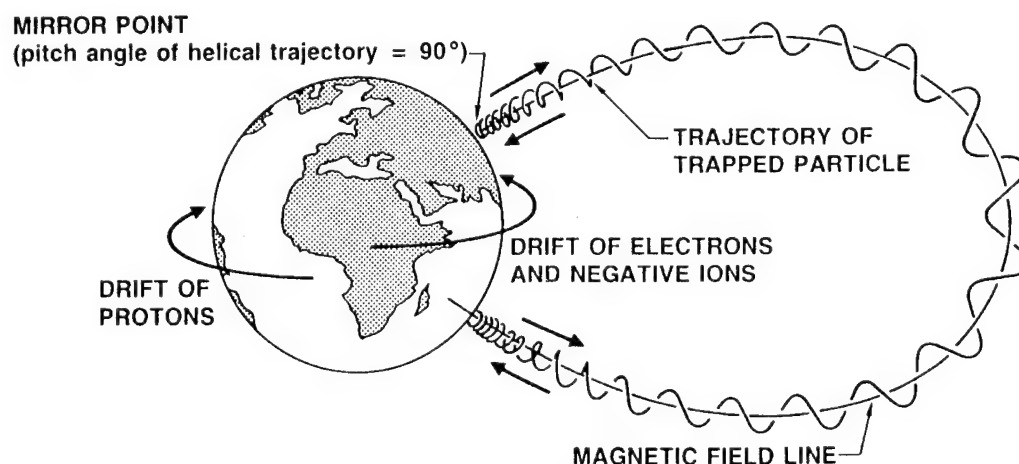


Figure 1. Geomagnetically Trapped Particle Motions

In a uniform magnetic field \mathbf{B} , a charged particle q moving with velocity \mathbf{v} experiences a force which appears as an electric field \mathbf{E} at right angles to both the direction of the field \mathbf{B} and the component of the velocity vector perpendicular to that field ($\mathbf{E} = -q \mathbf{v} \times \mathbf{B}$ in vector notation). Since at each instant this electric field tends to change the direction of the particle, which in turn changes the direction of the effective electric field, the particle executes a circular path---it gyrates about the field. This coupling of forces also results in a complementary behavior: a charged particle initially at rest in a magnetic field which has a force imposed upon it will move in a net direction perpendicular to both the force and the magnetic field

(components of force along the field are ignored here). The three basic motions of trapped particles in the magnetic field are a consequence of these force couplings and of the fact that the geomagnetic field has curvature and intensity gradients. Because of the curvature and intensity gradients, the particle's gyration path does not close upon itself, resulting in a drift motion. The motions are shown in Figure 1.

The direction of gyration follows the "right hand rule" for both electrons and ions; since the charges are opposite for the two types of particles, the direction of gyration is opposite for the electrons and ions, and therefore the direction of drift is also opposite, with electrons and negative ions drifting eastward and protons and other positive ions drifting westward. The frequency of gyration, called the *Larmor frequency*, is given by

$$f_L = \Omega_1 / 2 \pi = -q B / 2 \pi m_0 \gamma c \quad (1)$$

where: q = charge on the electron or ion

B = local magnetic field

m_0 = rest mass of the electron or ion

γ = relativistic mass ratio of the particle, $1/(1-v^2/c^2)^{1/2}$

v = velocity of the particle

c = velocity of light

Note that since the frequency of gyration is proportional to B , it is not constant along the field line. It is a minimum at the magnetic equator and increases as the particle moves away from the equator. Typical equatorial frequencies at 1000 km altitude are around 0.5 MHz for very low energy electrons and about 300 Hz for low energy protons. High energy particles have lower gyrofrequencies because of their greater (relativistic) mass.

The First Adiabatic Invariant

If one analyzes the path of a particle gyrating in a magnetic field, one observes that it encloses a fixed amount of flux which depends on the momentum of the particle perpendicular to the magnetic field. Under static conditions, the flux can't "leak" out of the path. This flux quantity, which is the origin of the magnetic moment of the particle, is *invariant* as long as conditions are adiabatic; i.e., the magnetic field is quiescent and no energy is added to the particle. It is called the *first adiabatic invariant*. The radius of gyration is inversely proportional to B . Thus the total flux enclosed by the path (flux density times area) is inversely proportional to the *square* of the magnetic field. But, if the magnetic field increases, thereby decreasing the radius of gyration, the perpendicular momentum of the particle has to increase to conserve the magnetic moment--to keep any of the flux from leaking out of the enclosed path. Otherwise the flux area enclosed by the gyration path would have decreased by B^2 while the flux density increased by only B . This has two interesting consequences:

First, it produces the bounce motion of particles in the geomagnetic field. A particle starting out at the equator with a component of velocity along the field line will travel a helical path to lower altitude with the field line as a guiding center. As it moves, it is moving in an increasing field. In order to maintain a constant magnetic moment, the momentum component perpendicular to the magnetic field has to increase (in the absence of such an increase, the magnetic moment would be decreasing as $1/B$). The only sources of energy to provide this perpendicular momentum increase are the magnetic field and the particle velocity. In a quiescent field, all of the momentum increase is obtained from the particle motion by converting momentum parallel to the field into momentum perpendicular to the field. When this source is exhausted, the particle motion parallel to the field line is zero and the particle is gyrating at a field intensity B_m , called the *mirror B*. The gradient in the field then reverses the process (called *mirroring*) and the particle travels a helical path to the other hemisphere where it again mirrors at a magnetic field intensity B_m exactly equal to the previous one. The two mirror points are called *conjugate* points because they are joined by the field line which is the guiding center of this helical motion. The particle actually spends most of its time at these mirror points.

The second interesting consequence which follows from conservation of the first adiabatic invariant is acceleration of the particle by an increasing magnetic field. As noted above, the only sources of energy to

maintain a constant magnetic moment in an increasing field are the particle motion and the field. If the field is changing, the particle may maintain its magnetic moment by increasing its perpendicular momentum at the expense of the magnetic field. Consider a particle that is mirroring so that all of its momentum is perpendicular momentum. If the field then increases, the field must accelerate the particle to increase the particle's perpendicular momentum (which must be done to conserve the total flux enclosed within the particle's gyration path). Note that the particle still has the same magnetic moment after it has been accelerated as it had previously, but it is now at a higher energy. The reverse process also works: a decreasing field will decelerate particles. Geomagnetic activity does both, producing radial displacements in the process. If the third adiabatic invariant, discussed below, is violated, the result is radial diffusion (a process in which particles initially on the same field line are transported to higher and lower field lines) which results in a net increase of energetic particles in the outer zone. These energetic particles then diffuse both inward and outward.

The Second Adiabatic Invariant

The bounce motion described above also has an associated invariant, called the *second adiabatic invariant*. Basically it is the total magnetic field energy contained within the envelope of the helical path between mirror points. (This function, like the other invariants, can be evaluated as a line integral. This will be discussed in more detail under *McIlwain's L Parameter*.) Note that if the magnetic field is increased, the energy density is increased. The radius of gyration is reduced to compensate (first invariant, described above), but the path length must also be reduced. Thus the mirror points must be raised. Conversely, if the field weakens, mirror points can also be lowered and the particles could be lost into the atmosphere. The bounce period is only a weak function of the equatorial pitch angle of the particle (the angle between the particle velocity and the magnetic field line at the magnetic equator) since the particles spend most of their time at the mirror points. The bounce period can be approximated by [2]:

$$2\pi/\Omega_2 = (4 L R_e / v) T(y) \quad (2)$$

where: L = McIlwain's parameter

R_e = Earth radius

$y = \sin \alpha$ where α is the equatorial pitch angle

and $T(y)$ is given by [2]:

$$T(y) = 1.3802 - .31985(y + y^{1/2})$$

The Third Adiabatic Invariant

Because the field has a radial gradient and curvature, the radius of curvature of the gyration or orbit about the field line is larger at the top of the orbit than at the bottom (top and bottom referenced with respect to the Earth radial direction). Thus the path does not quite close into a circle and the next orbit starts slightly eastward (for electrons) or slightly westward (for positive ions) from the previous gyration. This advance in position results in a drift motion around the Earth. After one drift period around the Earth, the particle will be back at the same location in the field where it started, provided the field is quiescent. The locus of points through which the particle passes is called its *drift shell*. The total flux enclosed by this shell must again be conserved. It is the conservation of this flux function, or *third adiabatic invariant*, that causes the particle drift shell to close after one drift period. However, during the time required for a particle to drift around the Earth (Figure 2), the magnetic field itself may change. During large magnetic storms, the change can be quite substantial, up to 1%. After one drift period, the particle may find itself on a different drift shell with a different field intensity (and therefore a different energy). The resulting violation of the third adiabatic invariant is the primary source of particle acceleration in the magnetosphere.

The drift frequency is a function of the bounce frequency (note the $T(y)$ in Eqn. 2 shows up in Eqn. 3) and can be approximately represented by [2]:

$$2\pi/\Omega_3 = -(3L/2\pi\gamma)(\gamma^2-1)(c/R_e)^2(m_0/qB_0)D(y)/T(y) \quad (3)$$

where $D(y)$ is given by

$$D(y) = 1/12\{5.5208-4.381y-.6397(y \ln y + y^{1/2})\}$$

and B_0 is the value of the Earth's magnetic field at the surface of the earth at the equator. Figure 2 presents a summary of approximate gyration, bounce, and drift frequencies for electrons and protons as a function of energy and L .

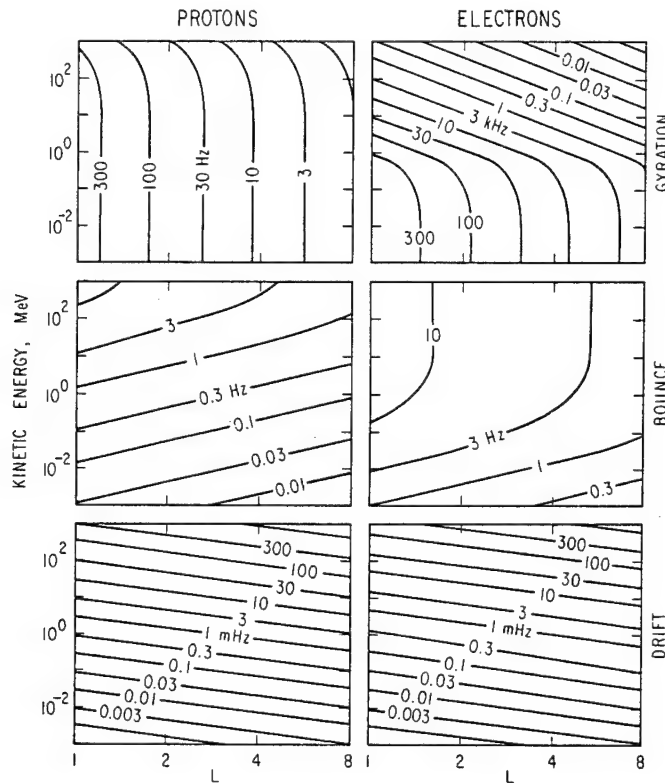


Figure 2. Gyration, Bounce and Drift Frequencies for Electrons and Protons in the Earth's Magnetic Field [2].

McIlwain's L Parameter

As a result of conservation of the first invariant, a particle's instantaneous pitch angle as it moves along a field line can be expressed in the form

$$\sin^2 \alpha_i / B_i = \text{constant} \quad (4)$$

where: α_i is the particle pitch angle at location i
 B_i is the magnetic field intensity at the same location

As a consequence of this relationship between B and α , if one knows the pitch angle of a particle at any point on the field line between the mirror points, one also knows B_m (which is the point at which $\alpha = 90^\circ$). The loci of these mirror points as the particle drifts around the Earth are two rings of constant B_m (one in each hemisphere). Provided one knows the unidirectional flux all along the field line below a point, the relationship expressed by the equation above permits the conversion of unidirectional fluxes to omnidirectional fluxes along the same region of the field line. In a similar manner, one can reconstruct the

unidirectional flux from the omnidirectional flux. However, in practice it is much easier to measure the unidirectional flux along the field line (it can be done from a single equatorial point by using an instrument that scans in the angle α) than to measure the omnidirectional flux distribution (which would have to be done by making measurements at closely-spaced points all along the field line).

As a particle drifts around the earth, the conservation of the second invariant results in the particle's guiding center tracing out a shell which connects the two rings of mirror points. The third invariant produces the result that the shell is closed upon itself--a particle remains on the same shell as it drifts around the earth. Of course, if the magnetic field varies during a drift period (or bounce or gyration), the adiabat associated with that motion will no longer be precisely conserved. As previously stated, such violation of conservation due to magnetic field fluctuations results in pitch angle diffusion, cross-field particle diffusion, and in changes in the energy of the particles.

Mapping of the particle population in the magnetosphere requires multi-dimensional labelling: particle species; energy; pitch-angle; altitude, latitude, longitude. The task of mapping the radiation environment is greatly simplified by reducing the three spatial coordinates to two magnetic coordinates, B and L, which are essentially the drift shells (L) and mirror rings (B_m) described above. The adiabatic invariant associated with the bounce motion, I, is obtained by integrating the function $(1-B/B_m)^{1/2}$ between the mirror points. Since this is awkward to do in a nonuniform field (the field has to be represented by a multipole expansion), an approximate relation is derived which can be related to a dipole field: $L^3 B / M = F(I^3 B / M)$. Here M is the dipole moment of the geomagnetic field. The function F can be calculated at a number of points, generating an interpolation table. L then becomes a simple calculation [1]. Note that for the real magnetic field, L is only an approximate representation of I, although a sufficiently accurate representation for mapping purposes. For a dipole, $L = R$, where R is the normalized distance from the center of the dipole to the equatorial crossing of the field line labeled "L". For our purposes, the dipole approximation will provide some understanding without belaboring the mathematics:

$$R = L \cos^2 \lambda \quad (5)$$

$$B = M/R^3 (4 - 3 R / L)^{1/2} \quad (6)$$

where R and λ are the usual radial distance and magnetic latitude in a dipole field, M is the dipole moment, and L is McIlwain's parameter. Note that R and λ are not sufficient to describe the spatial characteristics of the particle distributions since a given particle does not drift at a constant R or mirror at a constant λ except in a true dipole field where the azimuthal symmetry produces a degeneracy. The above expression shows that in a dipole field, L would correspond to the radial distance from the center of the Earth to the equatorial crossing of the magnetic field ($\lambda = 0^\circ$).

The Radiation Belts

The Earth's magnetosphere contains a wide variety of charged particles, primarily electrons and protons, with energies ranging from the thermal (less than 1 eV) to highly relativistic (tens of MeV for electrons, BeV for protons). The ionosphere contains a cold plasma, in the 1 eV energy range, with densities of the order of $10^6/\text{cm}^3$. The ionosphere is generally considered to consist of the neutral and ion components up to about 1000 km altitude, with the region above this called the plasmasphere (since the constituents there are highly ionized, forming a plasma). The plasmasphere particle density drops slowly until a boundary, called the plasmapause, is reached in which the cold plasma density drops abruptly by about 2 orders of magnitude, from 10^3 to 10^4 per cm^3 to below 100 per cm^3 . The location of the plasmapause is local-time and magnetic-activity dependent but is generally found between $L=4$ and $L=5$ and generally follows the field line to higher latitudes rather than an altitude contour. Beyond this region, hot plasma clouds, with temperatures of the order of 1 to 10 keV or more, are sometimes encountered. The plasma is heated by magnetic processes in the tail and auroral regions of the magnetosphere. In the remainder of this section, we will restrict our discussion to the energetic particle populations >40 keV. They will be discussed by location or zone and by species.

When Prof. Van Allen's detector passed through the magnetosphere in a radial direction, the count rate in the detector first increased, then decreased, and then increased again. Two distinct zones of trapped radiation were being traversed. These were named the *Van Allen belts* and are commonly referred to as the *inner zone* and the *outer zone*, with a region known as the *slot* separating them. Only for electrons are these zones distinct. Figure 3, which presents data from a period when copious fluxes of fission electrons were still present from the Starfish nuclear explosion in space, shows the minimum between the inner zone and outer zone. The inner zone, which is generally considered to cover the region $1.0 < L < 2$, has a peak in flux intensity at about $L=1.5$ for 1 MeV electrons. The region $2.0 < L < 2.8$ is generally considered the slot region where magnetospheric processes result in a low intensity of electrons during magnetically quiet periods. The process which removes the electrons is a resonant interaction between energetic electrons and whistler-mode (right circularly polarized) electromagnetic waves. The interaction results in some of the particles being scattered to lower angles (relative to the magnetic field line) such that their new mirror points are within the atmosphere. The atmosphere absorbs them. Thus the slot region normally contains relatively low fluxes of particles. At times of large magnetic storms, the slot can be refilled and quite high flux levels can be observed there for a few days. The location of the slot is quite variable: during large geomagnetic storms, the minimum between the inner and outer zone can be very narrow and may be displaced to a low L value, even centered as low as $L=2.0$. Immediately after a storm, the slot may be completely filled with electrons and so does not exist. An extensive discussion of these dynamics is available elsewhere [3]. The outer electron zone, which is extremely variable, typically peaks around $3.5 < L < 4.0$. In the outer zone, significant fluxes of electrons with energies in excess of 5 MeV are observed after major magnetic storms. During extended quiet periods, the outer zone may almost disappear at high energies. The difference in flux intensity from minimum to maximum may be as high as 5 orders of magnitude. See, for example, Figure 2 of [3] or Figure 7 of [4].

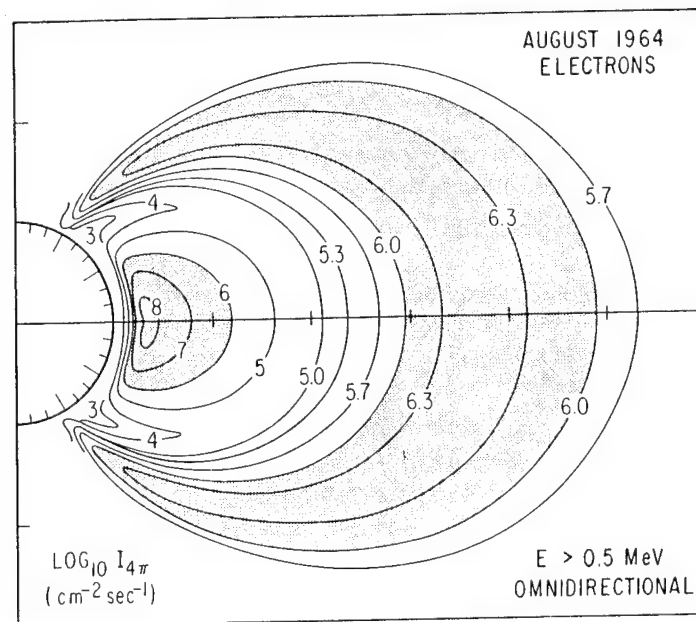


Figure 3. Inner and Outer Zone Electron Belts. The numbers on the contours are the \log_{10} of the integral omnidirectional flux, $I_{4\pi}$. The intense inner zone was due to the Starfish fission source. For times subsequent to 1968, the maximum inner zone intensity is several orders of magnitude lower.

The proton environment is sometimes separated into two constituents also, but in this case the separation is done on the basis of the energy of the protons. The same region of space that constitutes the inner zone for electrons contains very energetic protons, some with energies in excess of 200 MeV, which are also the result of the cosmic-ray albedo neutron decay described in the section on inner zone electrons.

There is another source of trapped protons. Low energy protons, from either a solar wind or ionosphere source, are accelerated similarly to the energetic electrons. Some of the initial acceleration for

ionospheric electrons is produced by electric fields, especially in the auroral zone. The low energy proton belt can be considered to be composed primarily of protons with energies below 10 MeV. These lower-energy protons are present in both the inner and outer zones. There is no slot such as occurs for the electrons. The peak in proton flux intensity depends on the energy, with lower energy protons peaking farther out. The 1 MeV proton flux is at its maximum at about $L = 3$.

TRAPPED PARTICLE POPULATIONS

In this section, we will briefly describe the four major components of the magnetospherically trapped energetic particle population---the inner and outer electron zones, the energetic proton belt, and the low energy proton population. The sources of the particles and their general flux levels as a function of L and energy will be discussed. Solar flare protons, which are discussed in the later section on modelling, will not be discussed in this section because the contribution of flare protons *which become trapped* to the fluences observed in most orbits is negligible. Flare protons in the polar region may be a major concern for some satellites, but those particles are not trapped.

Inner Zone Electrons

The source of the inner zone electrons is a combination of cosmic-ray albedo neutron decay (CRAND) and radial diffusion through the slot from the outer zone. In the CRAND mechanism, cosmic rays interact with air molecules in the upper atmosphere, producing energetic neutrons, some of which escape back into space. Since neutrons are uncharged, they cross magnetic field lines unimpeded. However, some decay while still in the magnetosphere and the decay products, an electron and a proton, are charged and so become trapped. The end-point energy of the electron in neutron decay is slightly under 1 MeV. The contribution of the neutron's velocity to the electron's energy is small. As a result, there are few electrons with energies in excess of 1 MeV in the inner zone. Electrons with higher energies are present in small numbers, especially above about $L=1.65$ after large magnetic storms, but can be ignored as a hazard to space systems except for their background effects in sensors.

Inner zone electrons below about 1000 km have lifetimes that are primarily determined by the scale height of the atmosphere. During solar-active periods, the increased scale height results in a reduced lifetime and lower average fluxes. This is reflected in the models by having a solar maximum and a solar minimum version. Farther out in the inner zone, electrons are quite stable, with typical lifetimes of 400 days [5]. Principle loss mechanisms are probably any or all of the following: radial diffusion into the atmosphere (violation of the second and third invariants caused by magnetic storms); interaction with whistler-mode waves produced by lightning strokes (the resonant interaction between these waves, also known as cyclotron waves, and the electrons results in a lowering of the electron pitch angle, causing it to be absorbed by the atmosphere at the end of the field line); interaction with VLF waves from ground-based transmitters.

The order-of-magnitude of the electron fluxes at $L=1.45$ in the inner zone are as follows: $> 10^8$ for $E_e > 0.1$ MeV; $> 10^6$ for $E_e > 1$ MeV; $> 10^5$ for $E_e > 2$ MeV. The numbers represent the integral, omnidirectional fluxes $\text{cm}^{-2}\text{-sec}^{-1}$. Below about $L = 1.55$, the fluxes are quite stable, with little variation being observed over the solar cycle [6] except for altitudes below 1000 km where atmospheric effects are observed. Above $L= 1.6$, major magnetic storms inject electrons with energies up to at least 1.2 MeV [3]. Figure 4 shows the equatorial omnidirectional inner zone electron flux intensities as a function of L and energy.

Outer Zone Electrons

The outer zone electrons originate either as solar wind electrons in the tail of the magnetosphere or as ionospheric electrons at high latitudes which are accelerated up the field lines. Magnetic field fluctuations cause them to be diffused radially inward, energizing them. The acceleration is a consequence of the conservation of the first adiabatic invariant coupled with violation of the third invariant, discussed earlier, by magnetic activity. As the particles are transported to field lines deeper in the magnetosphere, the increase in the average field intensity has to be compensated by an equivalent increase in particle momentum, or energy. The various fluxes peak at different locations in the outer zone for different energies, with the higher energies peaking at lower L . Representative outer zone fluxes are of the order of: $> 10^8$ for $E_e >$

0.1 MeV, $L = 6$; $> 10^7$ for $E_e > 1$ MeV, $L = 5$; $> 10^5$ for $E_e > 4$ MeV, $L = 4$. Units are as described for the inner zone fluxes.

Outer zone electron fluxes are highly variable, with increases at a given energy on a given L shell being as great as 5 orders of magnitude in less than a day. These large increases are caused by major magnetic storms, where $D_{st} > -150\gamma$. D_{st} is a global magnetic field disturbance index which is generally responsive to low latitude variations caused by a magnetospheric ring current. This ring current is composed of low energy ions accelerated by the magnetic storm. Typical decay constants for outer zone electrons are of the order of 10 days. In addition to the radial diffusion of particles caused by magnetic storms, they also cause pitch-angle scattering of the particles. Thus particles which were previously stably trapped on a field line (had mirror points that were above the atmosphere everywhere along their drift paths), can be perturbed so that they now mirror within the residual atmosphere below 100 km at some point along their drift path. At this altitude, the atmosphere absorbs the particles. A low altitude satellite which is normally below the trapped radiation zones (except when traversing the South Atlantic Anomaly) may suddenly find itself bathed in large fluxes of energetic electrons at midlatitudes when it encounters these particles which show up low on the outer zone field lines (sometimes called the *horns* of the outer zone). The South Atlantic Anomaly is a region of anomalously low magnetic field strength. Since particles mirror at a constant B_m , they attain at their lowest mirror altitude in the South Atlantic Anomaly.

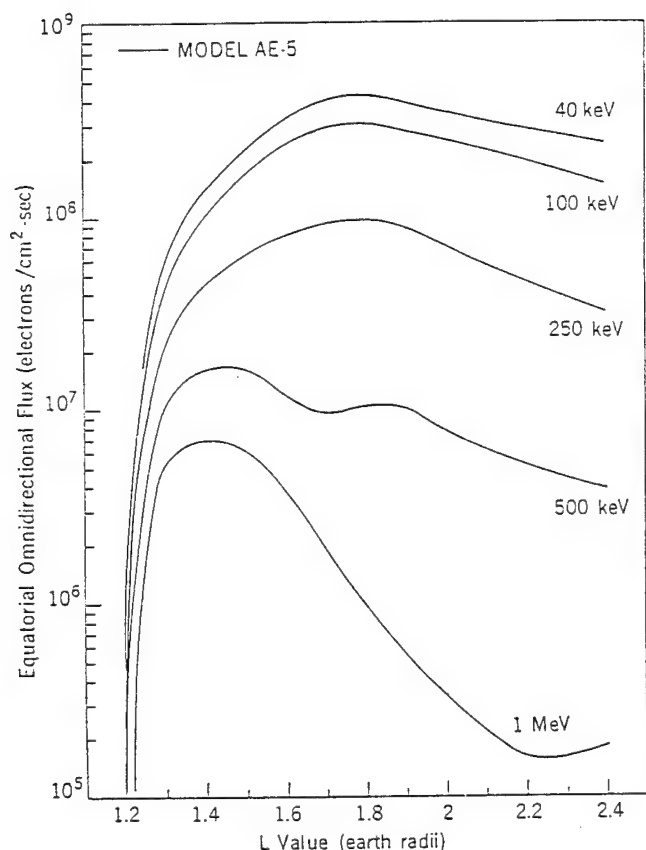


Figure 4. Inner Zone Electron Flux Intensities [6]

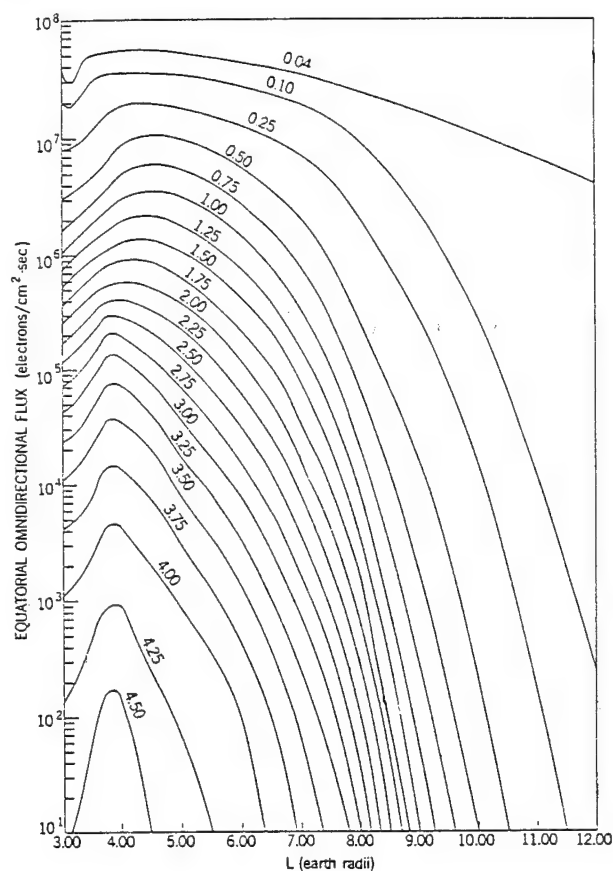


Figure 5. Outer Zone Electron Flux Intensities [7]

Energetic Protons

The source of the energetic protons which are present in the inner zone is CRAND, the mechanism mentioned previously. They are quite stable, with minor variations in intensity occurring at low altitudes due to variations in the atmospheric density due to solar activity. Typical intensities are of the order of

$> 10^4$ for $E_p > 100$ MeV and $> 10^3$ for $E_p > 300$ MeV, both at $L = 1.45$. Due to the secular variation in the magnetic field, a very slow decrease which may be an indication that the earth's field will undergo a reversal in the geologically-speaking near future (10^4 years?), the energetic proton environment is also exhibiting a small decrease (the decreasing field intensity is driving the protons into the atmosphere, again due to conservation of the adiabatic invariants). A serious problem in particle modelling due to this secular decrease in field intensity will be discussed in the section on models.

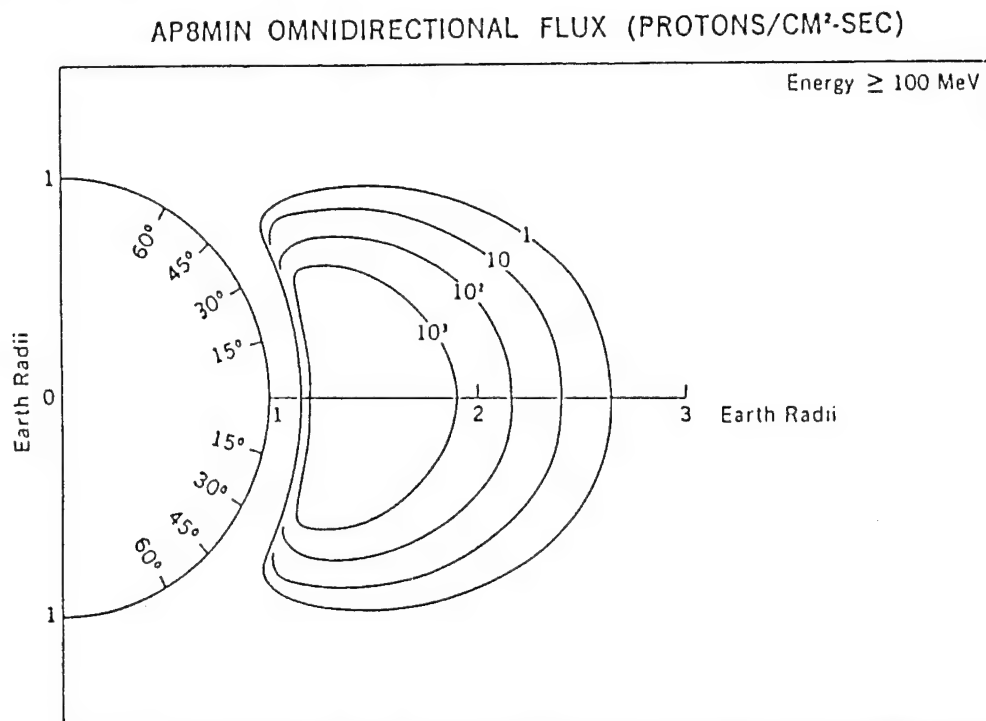


Figure 6. High Energy Protons in the Inner Zone [8]

Low Energy Protons

The low energy protons with which we are concerned here are in the 0.5 to 5 MeV range, since there are large fluxes of such particles in both the inner and outer zone and they have significant materials effects. Particles with these energies can originate in a number of sources: radial diffusion and energization of solar wind particles which enter the geomagnetic tail, similar to the outer zone electrons; ionospheric acceleration up field lines, with subsequent radial diffusion and acceleration; direct access of solar flare protons. Typical intensities in the outer zone are $> 10^8$ for $E_p > 0.1$ MeV; $> 10^7$ for $E_p > 1$ MeV; $> 10^5$ for $E_p > 10$ MeV; $< 10^2$ for $E_p > 100$ MeV. Again, these are omnidirectional, integral fluxes in units of $\text{cm}^{-2}\text{-sec}^{-1}$. While the fluxes are subject to variation due to magnetic storm activity, the variations are much smaller than for electrons. The primary loss mechanisms are deenergization through collisions with the residual atmosphere and charge-exchange, which results in an energetic neutral particle which is not trapped by the magnetic field.

CURRENT STATUS OF PARTICLE MODELS

In this section, we will cover the currently recommended particle models, their ranges and estimates of accuracy, discuss briefly their sources, availability, future modelling plans, and requirements for additional data. A more extensive discussion of the modelling efforts at the National Space Science Data Center is presented elsewhere [9].

Inner Zone Electron Models

The current NSSDC models which provide useful inner zone ($L = 1.2$ to 2.4) electron data are AE5 [6], for solar minimum, AE6 [10], for solar maximum, and AE8 [9] for either solar minimum or maximum. The energy range of these models is from 0.04 MeV to 5 MeV, although present techniques can not make reliable measurements of electrons with energies above 2 MeV below about $L=1.55$ in the inner zone. They are empirical models, being based on in-situ measurements of the fluxes. To produce the models, data is acquired from investigators, corrected, edited, averaged, interpolated, extrapolated, etc; in other words, it is all very thoroughly massaged. Some estimate of its reliability is also made, but such a step is very subjective. In general, the temporal coverage for any data set is six months or longer. The measurements were made between 1964 and 1977 (although data up to 1968 include Starfish electrons). Starfish contamination has been removed from the data in generating the above models. Newer data are available for incorporation into models [9]. The accuracy of the models is very good, better than a factor of two, for energies below 1 MeV and $L < 1.65$. Above $L=1.65$, the variability of the flux levels themselves produce uncertainty. Above 2 MeV, the fluxes are extrapolations and their accuracy is unknown.

The models, and codes for running them, are available from NSSDC. In addition to a tape format, the codes are also available as files on a VAX at NSSDC. The VAX is a SPAN (Space Physics Analysis Network) node. Thus, anyone with access to SPAN or other networks which can connect to SPAN (such as TELENET, ARPANET, BITNET, etc.) can access these files to download them to their home computer via the network. Dr. James Green is in charge of SPAN at NSSDC. Alternatively, the codes can also be run interactively on the NSSDC VAX at no charge to the user (other than his own costs of connecting to the SPAN network). An alternate interactive resource is EnviroNET [11], which is resident on a MicroVAX at GSFC and is accessible as the SPAN node ENVNET. To access EnviroNET, the user name ENVIRONET and password HENNIKER are used.

Future plans for the inner zone modelling activity are to incorporate newer data bases and also perhaps include some storm-time dynamics. It may not be possible to accomplish the latter task with presently available data bases, but the CRRES mission [12] has as one of its objectives the acquisition of the data required for producing dynamic particle models.

Outer Zone Electron Models

In-situ electron flux data in the outer zone are far from satisfactory for generating electron models. Most of the data used are extrapolations in both energy and altitude. At the geosynchronous region, measurements up to 1.7 MeV have been available from ATS-1. Near the equator, S³ provided measurements from about $L=2.5$ to $L=6$, but only up to 300 keV. OGO-5 had an electron channel at 2.7 MeV but the satellite orbit inclination was 27° so it made no measurements near the equatorial region. All other satellites which traversed the equatorial region at high altitude either had no high energy electron measurements ($E_e > 1.5$ MeV) or the energy threshold and detector efficiency were not known with sufficient accuracy to be usable in modelling. The source of the orders-of-magnitude discrepancies seen in comparisons of energetic outer zone electrons (e.g., Figure 12 of [4]) are these uncertainties. All other sources of data used in the models are extrapolations of measurements made low on the field line.

The current NSSDC outer zone models ($L > 2.4$) which provide useful results are the following: AE7-Lo and AE8 for solar minimum and AE7-Hi for solar maximum or long duration missions (> 5 years). For geosynchronous satellites, another model is still relatively valid--AE3 [13]. For long term missions, AE7-Hi is probably accurate to within a factor of two, especially for $L < 6$ and $E < 5$ MeV. However, if the mission includes the period a year or two following the sunspot maximum when the magnetic storm activity is greatest, AE7-Hi will err on the low side (actual integrated fluences can be expected to be greater than the model prediction). AE7-Hi was generated in response to criticisms that the earlier models, AE4 and AE6, were deficient in high energy electrons, and seriously so. In fact, in those models the energy spectra were truncated at 5 MeV, as is also done in AE8. A comparison of the models with in-situ data [4] showed that the models predicted fluxes that were low by about a factor of three, but almost the entire deficiency was in electrons > 1.5 MeV. The result was a prediction of dose in heavily shielded satellite components that was low by an order of magnitude. AE7-Hi, which truncates the energy spectrum at 7.5 MeV, has also been criticized for truncating the spectrum, since electrons with energies up to 10 MeV have been

measured at geosynchronous orbit [14]. Figure 7 shows the equatorial flux contours as a function of L and energy which are contained in AE7-Hi [15].

AE8 exists in two forms, AE8MIN and AE8MAX, which are supposed to represent the environment during solar minimum and maximum. However, both are truncated at 5 MeV and cannot properly model the solar maximum period when large fluxes of very energetic electrons appear. AE8 uses a single outer zone model and uses AE5 and AE6 solar minimum and solar maximum inner zone models. The major difference between AE8 and AE7-Hi is in the high energy electron flux at around $L = 4$. The AE7-Hi model contains about a factor of two greater flux at 3 MeV and about a factor of 10 greater flux at 4.5 MeV. At solar minimum, there are relatively few energetic electrons and any of the later models, AE7-Hi, AE7-Lo, AE8MIN, and AE8MAX are satisfactory for any use except calculating background rates in detectors. The models are probably accurate to a factor of three for dose calculations.

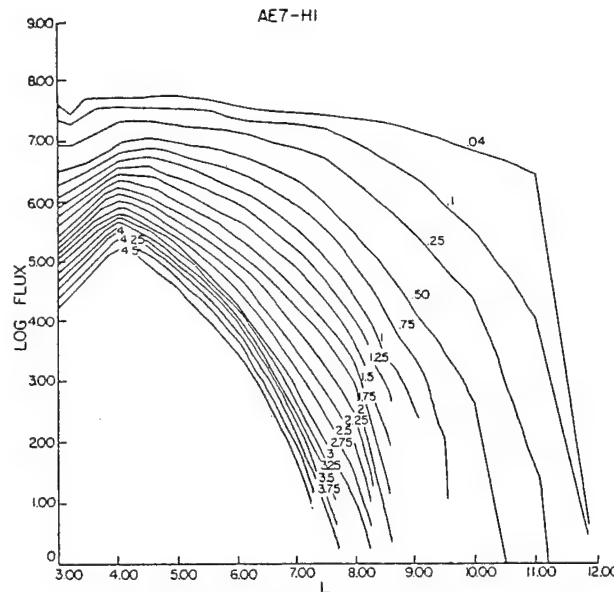


Figure 7. AE7-Hi Equatorial Electron Flux Contours [15].

As in the inner zone case, future plans are to incorporate new data in an attempt to increase the accuracy of the models and to include a dynamic model (addressing both the prediction of electron increases due to magnetic storms and the evolution of the fluxes after the increases). The Radsat portion of the CRRES mission [12] has two outer zone electron modelling goals: obtain data in the outer zone nearer to the equator than has been done previously in order to reduce the amount of extrapolation that has been necessary for model generation; obtain a data base which can be used to generate a dynamic model.

Proton Models

The current proton models are AP8MIN and AP8MAX, again representing the solar minimum and maximum periods. The major effect of the solar variation is the variation in atmospheric density at lower altitudes: at solar maximum, the higher scale height of the atmosphere decreases the energetic proton fluxes. The models are probably accurate to 50% or better. They cover the energy range from 100 keV to 400 MeV and the L range from 1.17 to 7. The data were obtained during the same time period that the inner zone electron data was obtained. Figure 8 shows the equatorial flux contours as a function of L and energy provided by AP8MIN. Since the MIN model predicts slightly more flux than the MAX model, it can be used during solar maximum or for long term missions as a conservative model.

One major problem with the energetic proton models is the fact that they are organized in terms of B,L. The secular variation in the earth's magnetic field (the dipole term is diminishing) causes the energetic proton ensemble, which is nominally very stable, to be carried to lower altitude. The model does not take into account the increased atmospheric density the protons will encounter at the lower altitude. As a result, if calculations are made with the magnetic field projected well into the future (more than ten to fif-

teen years), totally invalid results are obtained for low altitudes such as the Space Station orbit [16]. Since the source of the energetic protons is the decay of energetic neutrons produced in the upper atmosphere by cosmic rays, the geometry of the production process relative to the atmosphere will not change. The future configuration of the inner zone proton belt probably will not change relative to the present configuration, provided both are described in terms of L and B/B_0 , where B is the magnetic field at the point in question and B_0 is the equatorial intensity on the same field line. One will almost certainly get a more accurate result for a calculation of the proton environment for Space Station in the year 2025 by making the calculation with the present field model than by extrapolating the field 35 years into the future.

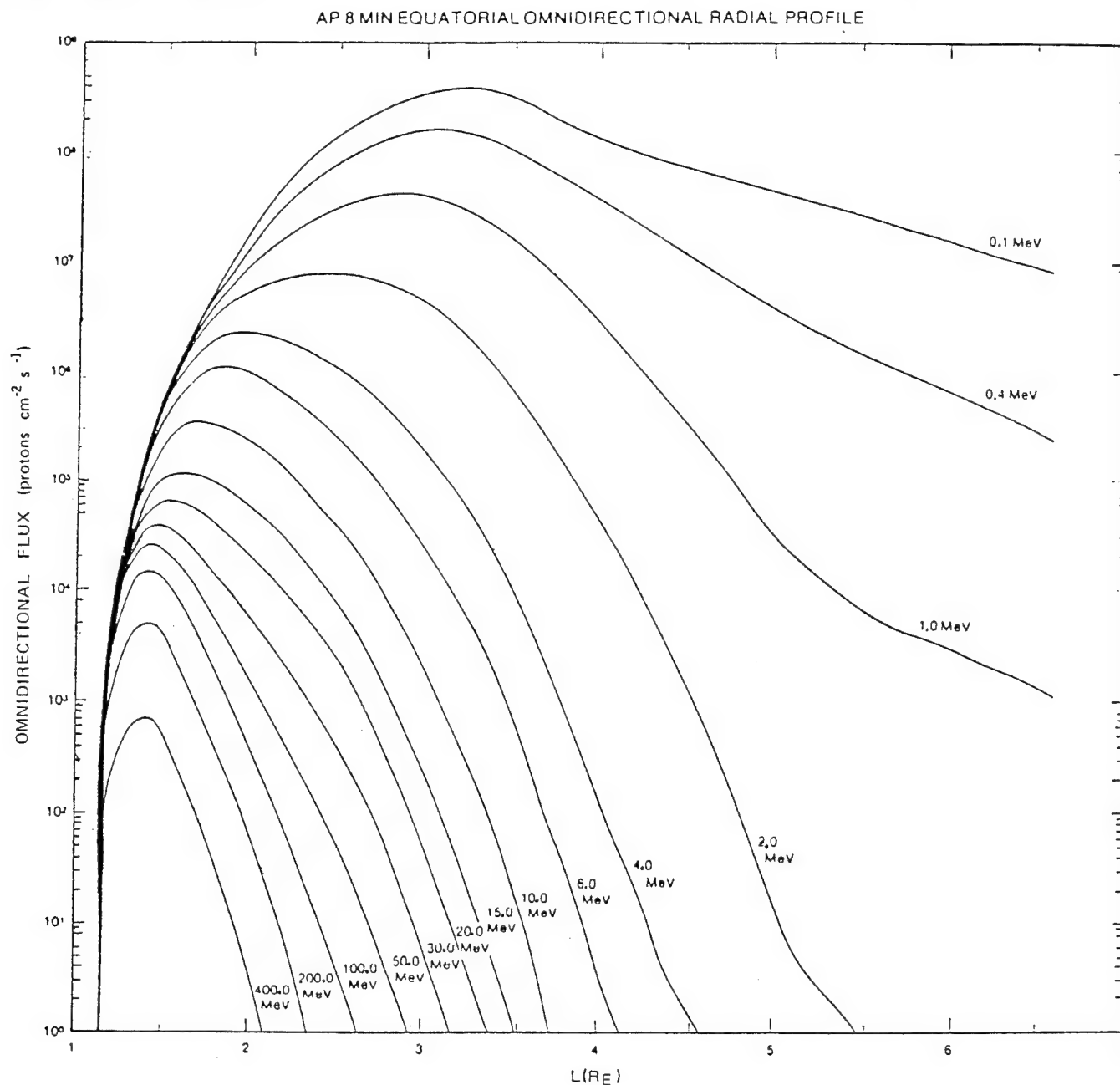


Figure 8. AP8MIN Equatorial Proton Flux Contours [15].

Solar Flare Proton Models

Solar flare protons are treated separately because they are transient and show up in the outer zone only in relatively small numbers. Their major impact is in the case of low altitude polar-orbiting satellites which normally receive relatively little particle irradiation--and almost all of that in short infrequent traversals of the South Atlantic Anomaly region. For some satellites, the major portion of the particle environment they encounter during their lifetime may occur during one or two major solar flare particle events, each lasting only a few days. In a typical solar cycle of 11 years, 90% of the energetic proton fluence is the result of a single anomalously large flare. The integrated fluence over the polar caps from the one event can be of the order of $2 \times 10^9/\text{cm}^2$ $P+ > 30$ MeV. Averaged over a solar cycle, the annual fluence is about $5 \times 10^8/\text{cm}^2$ $P+ > 30$ MeV over the polar cap. At 100 MeV, these numbers are about a factor of 30 lower. A low altitude polar orbiting satellite spends roughly 40% of its time at latitudes where these protons can gain access. Thus such a satellite may receive virtually all of its energetic proton dose from solar flares rather than from the magnetospherically-trapped protons.

FUTURE MODELLING REQUIREMENTS

The major efforts in modelling must be directed toward the electron environments, since the energetic inner zone protons are relatively stable and well understood and the outer zone protons can be described well statistically. Within limits, their evolution after a storm is also generally predictable. This is primarily due to the relative ease with which proton measurements can be made. Also, the studies of the physics of the protons have been more productive. The CRRES mission [12] is expected to provide additional high-quality data for the proton dynamics modelling.

While a large amount of data is available which has not yet been used to update the various trapped radiation models, there are significant gaps in the electron data bases. A major reason for this is the difficulty of separating the signal from a small flux of these particles from the large background of protons and cosmic rays. One of these gaps was mentioned previously: No useful data base has ever been obtained in the outer zone for electrons above 300 keV between about $L=2.8$ and geosynchronous orbit at geomagnetic latitudes below about 20° . CRRES will lower this limit to 10° . Above 2.8 MeV no data is available for altitudes above 8000 km except for some geosynchronous orbit measurements [14]. In the inner zone above 2 MeV, no usable measurements are available because of tremendous penetrating proton background problems in detectors. CRRES will not be able to furnish this type of data, either, because its primary radiation mission is an engineering one and electrons above 2 MeV in the inner zone can be ignored. (If you have problems measuring them, they are unlikely to cause a problem on operational vehicles.)

One major area which has not been modelled is the dynamics of the radiation belts in response to magnetic activity. One report [17] attempts to correlate the response of the outer zone to the magnetic index K_p , but the particle data were all obtained at geosynchronous orbit and the field lines that are represented in the K_p index are high latitude field lines which thread through the geosynchronous region. Hence, that study is limited in validity to the geosynchronous region. Low altitude measurements indicate that in general the outer zone does not correlate with K_p , except incidentally when major magnetic storms occur, but does have some relationship with D_{st} , the low latitude index mentioned previously. The intention is to get the type of data base from CRRES that one needs to address the dynamics modelling.

In order to be useful, the dynamics models have to address three issues *quantitatively*: a) The prediction of magnetic storms which produce increases in the outer zone energetic electron and proton populations; b) The energy spectra and L profiles of the fluxes as a function of the magnetic storm parameters; and c) The evolution of the distribution as a function of time (and magnetic activity) post-storm. The first of these requires a better understanding of the solar-terrestrial coupling physics and may have to await completion of the Global Geophysics Program (aka International Solar-Terrestrial Physics program) which is scheduled to start launching satellites in the 1993 time period [12]. A first step for b) and c) would be to make a statistical model of particle storm and post-storm behavior from a large data base. Again, CRRES is designed to provide the data base for such an effort and current plans include developing such a statistical model.

REFERENCES

- [1] McIlwain, Carl E., Coordinates for Mapping the Distribution of Magnetically Trapped Particles, *J. Geophys. Res.*, 66, 3681-3691, 1961.
- [2] Schulz, M. and L. J. Lanzerotti, *Particle Diffusion in the Radiation Belts*, Springer, New York, 1974.
- [3] Vampola, A. L., "Natural Variations in the Geomagnetically Trapped Electron Population," in *Proceedings of the National Symposium on Natural and Manmade Radiation in Space*, NASA TM X-2440, E. A. Warman, Ed., 1972.
- [4] Vampola, A. L., J. B. Blake and G. A. Paulikas, "A New Study of the Magnetospheric Electron Environment," *J. Spacecraft and Rockets*, 14, 690, 1977.
- [5] Stassinopoulos, E. G. and P. Verzariu, General formula for decay lifetimes of Starfish electrons, *J. Geophys. Res.*, 76, 1841, 1971.
- [6] Teague, M. J., and J. I. Vette, *The Inner Zone Electron Model AE-5*, NSSDC WDC-A-R&S 72-10, 1972.
- [7] Singley, G. W., and J. I. Vette, *A Model Environment for Outer Zone Electron*, NSSDC WDC-A-R&S 72-13, 1972.
- [8] Sawyer, D. M., and J. I. Vette, *AP-8 Trapped Proton Environment*, NSSDC WDC-A-R&S 76-06, 1976.
- [9] Bilitza, D., D. M. Sawyer, and J. H. King, Trapped Particle Models at NSSDC/WDC-A-R&S, NASA CP-3035, p. 569, May 1989.
- [10] Teague, M. J., K. W. Chan and J. I. Vette, *AE-6: A Model Environment of Trapped Electrons for Solar Maximum*, NSSDC WDC-A-R&S 76-04, 1976.
- [11] Lauriente, M., EnviroNET: Space Environments for SDIO Experiments, this proceedings.
- [12] Hardy, D. A., The Radiation Belt Mission on CRRES, Presented at the Space Environmental Effects on Materials Workshop, June 1988.
- [13] Vette, J. I. and A. B. Lucero, Models of the Trapped Radiation Environment, Vol. III: Electrons at Synchronous Altitudes, NASA SP-3024, 1967.
- [14] Baker, D. N., R. D. Belian, P. R. Higbie, R. W. Klebesadel, and J. B. Blake, "Hostile Energetic Particle Radiation Environments in Earth's Outer Magnetosphere," in *The Aerospace Environment at High Altitudes and its Implications for Spacecraft Charging and Communications*, AGARD CP 406, p. 4-1, 1986.
- [15] *Handbook of Geophysics and the Space Environment*, A. S. Jursa, Ed., AFGL/AFSC, 1985. NTIS Accession No. ADA 167000.
- [16] Konradi, A. and A. C. Hardy, "Radiation Environment Models and the Atmospheric Cutoff" *J. Spacecraft and Rockets*, 24, p. 284, 1987.
- [17] Nagai, T, "Space weather forecast: Prediction of relativistic electron intensity at synchronous orbit," *Geophys. Res. Lett.*, 15, 425, 1988.

EFFECTS OF SPACE RADIATION
ON
ELECTRONIC MICROCIRCUITS

W. A. Kolasinski
Space Sciences Laboratory
The Aerospace Corporation
El Segundo, California

INTRODUCTION

Originally, as the title of my talk implies, I was going to discuss briefly the cumulative effects of radiation dose on integrated microcircuits and then cover in some detail the instantaneous Single Event Phenomena (SEP) associated with energetic, individual particles (protons or heavier ions) striking the device sensitive region(s). However, since Jim Raymond has covered in admirable fashion the subject of total dose effects in his talk yesterday, it would be presumptuous and ill-advised on my part to belabor the subject; instead, I shall avail myself of the opportunity to address topics which are more closely related to the work I am currently involved in. Before leaving the subject of total dose behind, I would like to mention that because of the large populations of energetic protons and electrons in the radiation belts, displacement damage in solid state devices can play a larger role here than in other regions of space. Furthermore, the penetrating nature of the trapped radiation precludes in general the use of shielding as a means of mitigating total dose damage.

Without further ado, let us now turn to single event effects or phenomena (SEP), which so far have been observed as events falling in one or another of the following three classes:

1. Single Event Upset (SEU),
2. Single Event Latchup (SEL) and
3. Single Event Burnout (SEB).

Single event upset is defined as a lasting, reversible change in the state of a multistable (usually bistable) electronic circuit such as a flip-flop or latch. In a computer memory, SEUs manifest themselves as unexplained bit flips. Since latchup, as discussed yesterday by Jim Raymond is in general caused by a single event of short duration, the "single event" part of the SEL term is superfluous. Nevertheless, it is used customarily to differentiate latchup due to a single heavy charged particle striking a sensitive cell from more "ordinary" kinds of latchup. Single event burnout (SEB) refers usually to total instantaneous failure of a power FET when struck by a single particle, with the device shorting out the power supply. Needless to say, an unforeseen failure of this kind can be catastrophic to a space mission.

SINGLE EVENT PHENOMENA: EARLY HISTORY

Figure 1 is a summary of the early events leading up to and resulting in our preoccupation with SEP. During the early 1960's, reverse-biased silicon diodes came into widespread use as nuclear particle detectors both on the ground and in

Early History

- 1962
 - UPSET BY COSMIC RAYS PREDICTED
- 1975
 - UPSETS OBSERVED ON INTELSAT IV
- 1978
 - UPSETS PRODUCED BY BEVELAC IRON BEAM
 - PAPERS ON COSMIC RAY UPSET PUBLISHED BY SEVERAL GROUPS
- 1979
 - RESULTS OF EXPERIMENTS ON PROTON AND HEAVY ION ACCELERATORS REPORTED BY SEVERAL GROUPS
 - REPORT ON UPSETS INDUCED BY ALPHAS FROM RADIOACTIVE DECAY

Figure 1. Early History of SEP.

space. The particle-detection process depends on the fact that an energetic ion, while passing through the depletion region of a reverse-biased p-n junction, generates electron-hole pairs along its track. These are swept out of the region by the electric field across the junction and produce a current pulse at the diode output. The amount of charge collected at the output is proportional to the energy lost by the particle in passing through the junction.

In 1962, Wallmark and Marcus¹ made the logical deduction that the same physical process which allows nuclear particle detection by semiconductor devices could lead to a spurious response by ever smaller silicon devices being used with increasing frequency in space systems. They correctly predicted that the problem would emerge when device miniaturization reached a certain critical level beyond which circuit elements would become sensitive to spurious charge

pulses created by the passage of heavy cosmic rays through vulnerable regions. D. Binder and coworkers² reported observations of upsets in JK Flip-Flops on board Intelsat IV. After a careful study they attributed these upsets to cosmic rays. In 1978 upsets of dynamic RAMs in space were reported by Pickel and Blandford³ who explained the observed upset rate in terms of the known cosmic ray environment and its effect on the devices in question. Later that year Kolasinski et al⁴ simulated directly the effect of heavy cosmic rays on solid state memories with the use of a very energetic iron beam from the Lawrence Berkeley Laboratory (LBL) Bevalac accelerator. They continued the work in 1979 using the 88-in. Cyclotron at LBL and discovered SEL in the process⁴. In approximately the same time frame investigators at the Naval Research Laboratory⁵ and the Air Force Geophysical Laboratory⁶ were actively studying upsets caused by protons with energies like those of protons trapped in the inner Van Allen belt. Since that time, numerous manifestations of the various SEP have been observed in semiconductor devices both on the ground and in space-borne systems. Figure 2 is a summary of

SEU Rates in Space
UPSETS PER 10^6 BITS PER DAY
(COURTESY OF E.C. SMITH, HUGHES AIRCRAFT CO)

PROGRAM	PART TYPE	RATE
INTELSAT IV	J-K FLIP-FLOP	16.0*
PIONEER VENUS	PMOS SHIFT REGISTER	7.0
PV/O	SCHOTTKY TTL 64 BIT RAM	12.0
EO	MISC ANOMALIES	10.0
GPS	4096 BIT NMOS RAM	10.0

Fig. 2. Observations of SEU in Space.

Idealized SEU Events

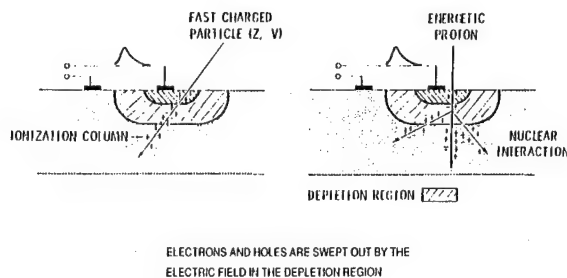


Fig. 3. Pictorial View of the SEP Process.

some of the early observations of SEU in space. An excellent review of the early days of SEP studies, together with a bibliography up to 1982 has been written by Sanderson et al.⁷

THE NATURE OF SINGLE EVENT EFFECTS

When considering any single event effect associated with an integrated circuit chip, it is important to keep firmly in mind the instantaneous and microscopic nature of the underlying process. In other words, the time during which charges are generated in the sensitive region is negligible compared with the time for charge collection; also, the initial diameter of the charge column is smaller than or comparable to the size of the sensitive region. This is in contrast to other common radiation effects such as cumulative total dose damage or response to a short burst of flash x-rays or particles, where the whole chip is bathed in radiation.

Figure 3 above depicts in schematic form the essential features of the mechanism responsible for SEP. At left on Fig.3, a heavy ion traversing the reverse-biased junction depicted on the chip produces a dense track of ionization (electron-hole pairs). The charges move to the electrodes under the electric field within the so-called depletion region, which to first order is the sensitive region for SEU. Upon being collected, the charges produce a current pulse at the circuit node. The linear charge density along the track is proportional to the rate at which the particle loses its energy, or its "linear energy transfer" (LET) in technical jargon. The higher the particle LET and track length within the sensitive region, the higher the deposited charge and hence the node current which may result in a single event upset or other phenomenon.

An upset occurs when a certain minimum amount of charge (the critical charge) has been collected at the circuit node in a time small in comparison with the circuit response time. Generally this prompt charge-collection time is in the pico-second domain, while the circuit time constants are measured in nanoseconds. The circuit critical charge divided by the longest dimension (track length) within the sensitive volume is defined as the threshold LET for a given SEP.

On the right hand side of Figure 3 we see a somewhat different phenomenon taking place. Here, an energetic proton like those trapped in the radiation belt collides with a silicon nucleus within the depletion region, and a nuclear reaction in the form of scattering, neutron emission, fragmentation etc. takes place. As we shall see in a moment, the proton LET is too low to produce enough current for an upset, but by transferring its energy and momentum to the nuclear reaction products whose LET is much higher, the proton can produce an upset. Clearly, the lower the threshold LET of the device for upset with heavy ions, the more vulnerable will the device be to upset by protons. Since the trapped radiation zones contain large fluxes of energetic protons, spacecraft traversing these zones are subject to an increased rate of SEP.

Figure 4 summarizes the process of ion interaction with matter. As we can see, dE/dx and hence LET varies as the

square of the nuclear charge (atomic number) and inversely as the square of the ion velocity. The table at the bottom of

Charged Particle Interaction with Matter

- PARTICLE LOSES ENERGY BY IONIZATION OF ATOMS IN MATERIAL BEING PENETRATED
- ENERGY LOSS PER UNIT PATHLENGTH $\frac{dE}{dx} \propto \frac{Z^2}{V^2}$
 - Z^2 — PARTICLE NUCLEAR CHARGE
 - V^2 — PARTICLE VELOCITY
- THE VALUE OF $\frac{dE}{dx}$ RELATIVE TO HYDROGEN FOR SEVERAL IONS AT A GIVEN VELOCITY IS GIVEN IN THE TABLE

ION	dE/dx (H = 1)
He	4
O	64
Ar	324
Fe	676
Pu	8836

Fig. 4. Ion Interaction with Matter.

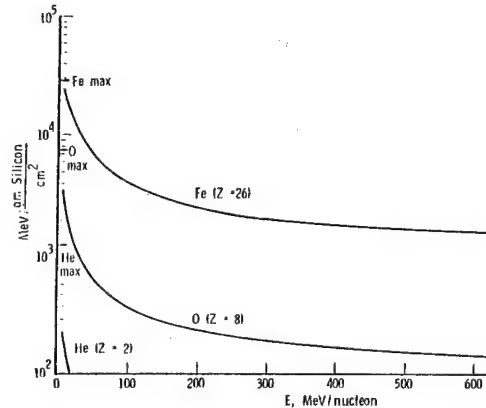


Fig. 5. Energy Dependence of LET.

Figure 4 shows the LETs of several ions relative to protons. We see that the linear charge density along an iron track is almost 700 times that produced by a proton with the same velocity. The increase of LET with increasing atomic mass can be shown more dramatically by multiplying the numerator and denominator of the expression for dE/dx in Fig. 4 by M , the nuclear mass. The denominator now becomes the ion energy, and we note that the rate of energy loss or LET varies directly as the product of ion mass and the square of its charge, and inversely with the energy. Another way of looking at the inverse-square dependence of LET on ion velocity is to remember that velocity squared is essentially energy divided by the ion mass, where the latter equals the mean bound nucleon (ie, proton or neutron) mass times the number of nucleons. Thus LET varies as the square of the nuclear charge and inversely as the energy per nucleon.

This functional form of LET is shown in Fig. 5 for the three major cosmic-ray constituents, not counting protons. Note that LET (vertical axis) is expressed here in units of MeV/(g/cm²), ie. the energy lost in traversing a thickness of material weighing 1 g/cm². In some applications it is more useful to express LET in units of pC/micron. I shall leave it as an exercise for the reader to show that 1 pC/micron in silicon is equivalent to 98 MeV/(mg/cm²). Looking at the oxygen curve in Fig. 5, we note that at 100 MeV/nucleon (1.6 GeV total energy), the oxygen nucleus loses roughly 300 MeV in traversing 1 g/cm² of silicon. To stop it completely would require several g/cm² of shielding. Thus at these energies, shielding against energetic ions in space is impractical except in a few very special cases.

SPACE-RADIATION ENVIRONMENTS RESPONSIBLE FOR SINGLE EVENT EFFECTS

Single event effects in microelectronics are caused primarily by three types of radiation environments in space: galactic cosmic rays, solar cosmic rays and trapped charged particles. While this session is devoted to the effects of trapped

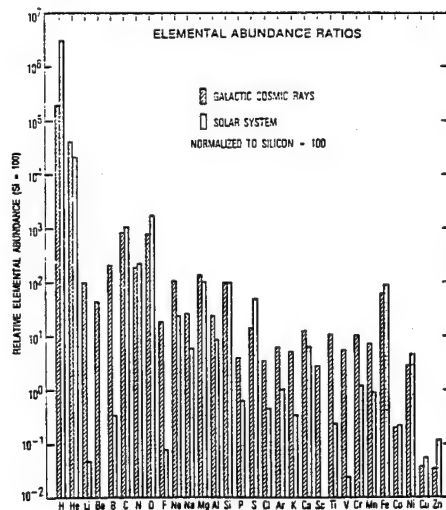


Fig. 6. Cosmic Ray Abundance Ratios.

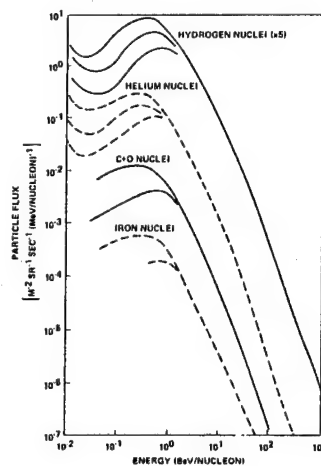


Fig. 7. Cosmic Ray Energy Spectra.

radiation, I shall briefly discuss the other two environments, since to a greater or lesser extent they coexist with the third in many regions of space and are the major contributors to SEP. In the previous talk, Al Vampola presented a very thorough description of the trapped environment, so I shall only comment briefly on its aspects pertaining to SEP.

Galactic Cosmic Rays

Figures 6 and 7, respectively, show the relative abundances and energy spectra of the galactic cosmic rays. The most prominent in this environment are protons, alpha particles, nuclei in the carbon and oxygen group and finally the nuclei with atomic numbers close to that of iron. A very exhaustive and detailed description of the environment has been given by J. H. Adams⁸, including an analytical formulation and review of the experimental data on which it is based. It is important to note that the environment is most severe at spacecraft-orbit altitudes exceeding a few thousand kilometers. At lower altitudes and inclinations below approximately 50 degrees, the earth's magnetic field keeps out a large portion of the low to medium energy flux of the heavy ions. In the polar regions, however, these ions reach low altitudes by spiralling along magnetic field lines, so that the flux intensity is not reduced very much over that at high altitude.

The galactic cosmic ray intensity is modulated by the 11-year cycle of solar flare activity, with the maximum flux occurring during minimum solar activity and vice-versa. Hence the term "solar-minimum flux" refers to the highest intensity flux and so implies the most severe environment. This can be confusing to someone uninitiated to the technical jargon. The degree of solar cycle modulation of the flux is shown by the branches in the spectra of Figure 8.

Solar Flare Particles

An example of heavy ion fluxes associated with a solar flare is shown in Fig. 8. Since solar flares occur sporadic-

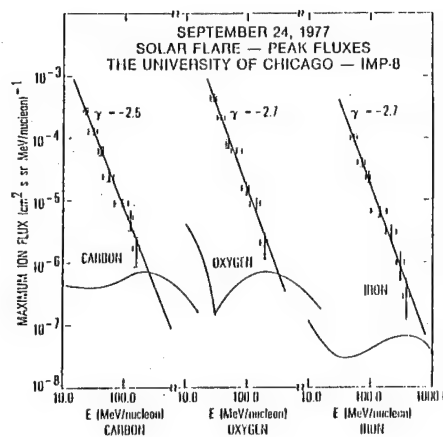


Fig. 8. Particle Fluxes in a Heavy Ion Rich Solar Flare.

ally, so does the associated environment. As in the case of galactic cosmic rays, it is the energetic charged particles, accelerated near the sun during some solar flare events, that cause single event phenomena and total dose damage. Our understanding of solar activity is too rudimentary for us to be able to predict far in advance the exact onset time of a solar flare. Individual flare occurrences appear to be quite random, except that their frequency follows the 11-year sunspot cycle mentioned above.

Most solar flares produce proton fluxes which do not contribute significantly to the single event rate. Generally, the flux of the heavier ions in those flares also is not very significant. However, as the example in Fig. 8 shows, flares rich in heavy ions do occur sometimes, and the flux of medium energy heavy ions from such a flare can exceed the galactic background by more than one order of magnitude. Finally, a "monster" flare like the one in August, 1972 can cause general havoc in spacecraft systems. It is indeed fortunate that these events are rare and of relatively short duration (a few hours to a day or so). A summary of recent solar flare environment data of interest in single event effects work has been published by Chenette and Dietrich⁹.

In regions around the Earth, only the inner Van Allen belt is of concern, and even then only for devices with relatively low degree of immunity against single event effects. The trapped proton flux in the inner belt is many orders of magnitude higher than the flux of galactic cosmic rays. However, as was pointed out above, protons can cause single event effects in currently available devices only indirectly, by way of nuclear reactions in or near the device sensitive regions. Since the probability of these reactions taking place is extremely small, only a few of the devices currently used in space are vulnerable to proton induced single effects. More will be said on this subject later.

EXPERIENCE IN ORBIT

Early observations of SEU on various spacecraft with payloads containing MSI and LSI devices have already been shown in Figure 2. Here the data all seem to cluster around an upset rate of approximately 1 upset per day for a 100,000-bit memory and the rate does not appear to depend strongly on the device technologies used in the various spacecraft.

More recently, Blake and Mandel¹⁰ have published upset rates in CMOS/bulk RAMs on board a spacecraft in a low altitude, polar orbit. The observed rate of approximately 3×10^{-7} per bit per day is considerably lower than the values appearing in Figure 3. At the other end of the scale, upset rates in the neighborhood of 3×10^{-3} per bit per day have been observed in low power bipolar RAMs on board the LEASAT vehicle¹¹.

Upsets have also been observed in devices flown by the NASA Goddard Space Flight Center on the Space Shuttle as part of the Cosmic Ray Upset Experiment (CRUX). The payload flew in an orbit with 57 degrees inclination. It contained complements of VLSI, NMOS dynamic and static RAMs, as well CMOS non-volatile PROMs. No upsets were observed in the PROMs, while the RAM SEU rates fell in the range of 10^{-7} - 10^{-6} upsets per bit per day. Clearly, there appears to be a large range of vulnerability to SEU among the various device technologies.

SUMMARY OF GROUND-TEST AND MODELING ACTIVITY

In view of the fact that the severity of single event effects in space can range from inconsequential to catastrophic,

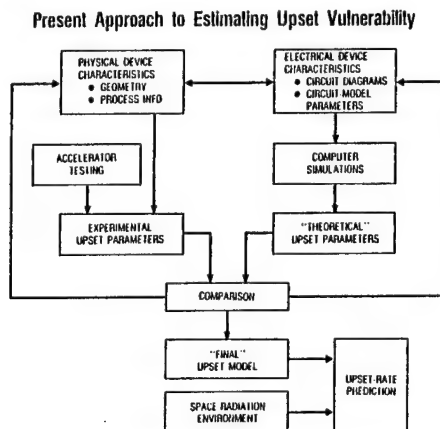


Fig. 9. Flowchart of Modeling Effort.

it is not surprising that during the past decade considerable effort has been expended in testing, modeling and hardening devices against single event effects. The ultimate objectives of these efforts are to acquire the capability of predicting the single event effect rates in orbit for commercially available devices, to harden existing payload designs wherever feasible, and to develop new device technologies resistant to single event effects. Attempts to attain these objectives have concentrated on device modeling, circuit analysis, ground testing of devices and test structures, and acquisition of on-orbit data. This work is briefly summarized below. Figure 9 is an idealized flow-chart of the activities which result in a prediction of single event rate in space.

The parameters absolutely necessary for predicting the single event rate are the minimum charge(s) needed to induce a single event such as an upset, the geometry of the sensitive region(s) and the charge-collection efficiency at the relevant circuit node(s). Because of the fast and microscopic nature of the single event process, circuit parameters like the critical charge or the current-pulse shape cannot be simulated and measured with conventional electronic test equipment.

Instead, theoretical computer models of field configuration and current flow originating from the ion track are developed and used to determine the extent of the sensitive region and minimum charge density along the ion track needed to initiate a particular type of single event.

Ground tests are then performed to validate the model predictions of minimum charge density and probability of upset (SEU cross-section) in the ion beam. Figure 10 summarizes in schematic form the test activities and type of data ob-

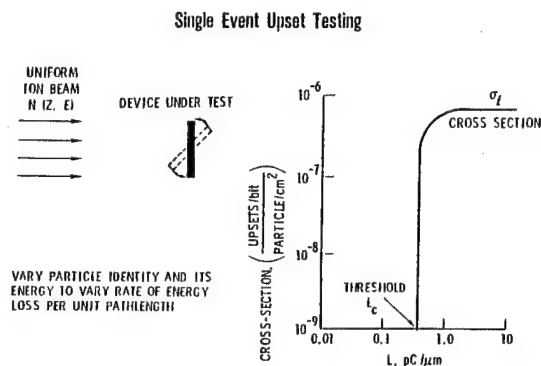


Fig. 10. Summary of Test Procedures.

tained. The devices under test are placed in a uniform beam of protons or heavy ions and exercised in appropriate fashion while being irradiated. The number of bit errors or other upsets, as well as the beam fluence, are recorded and the cross-section computed using the expression

$$\sigma_L = N \sec(\theta) / F,$$

where σ_L , N , θ and F are, respectively, the upset cross-section in cm^2 , number of errors, beam angle of incidence with respect to the chip-surface normal and the total beam fluence in particles/ cm^2 . This process is repeated at various angles of beam incidence and with particles having the range of LETs needed to determine the threshold value of LET. More often than not, the parts have to be de-lidded in order to allow the ions to penetrate into the sensitive region of the device.

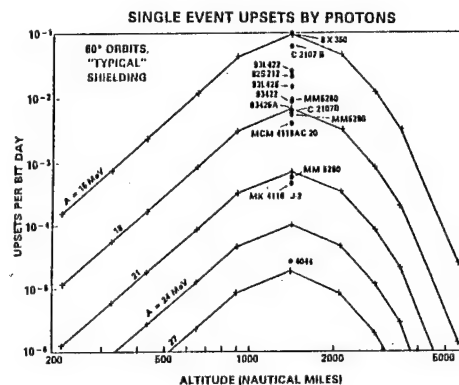
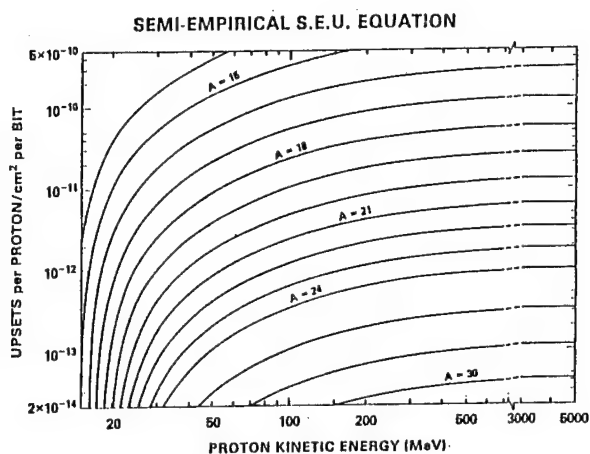
After one or more iterations of theoretical simulation and ground testing, heavy ion upset rates are predicted for specific environments using computer programs like J. C. Pickell's Cosmic Ray Induced Error (CRIER)¹² or J. Adams' Cosmic Ray Upset Model (CRUM)¹³ codes. In these calculations, LET spectra for orbits of interest are first generated in the presence of shielding appropriate for the payload under consideration. The dimensions of the sensitive regions and critical charges for upset, generated in the modeling and test efforts are then provided to the programs which generate random path-length distributions and determine which particles within the calculated LET spectrum deposit enough charge to induce the single event effect.

Petersen et al.¹⁴ have developed a simple and useful expression for estimating the upset rate of microcircuit memories in the so-called "10 percent worst case" galactic cosmic ray environment of Adams⁸. The upset rate R , measured in upsets per cell per day, is computed from the expression

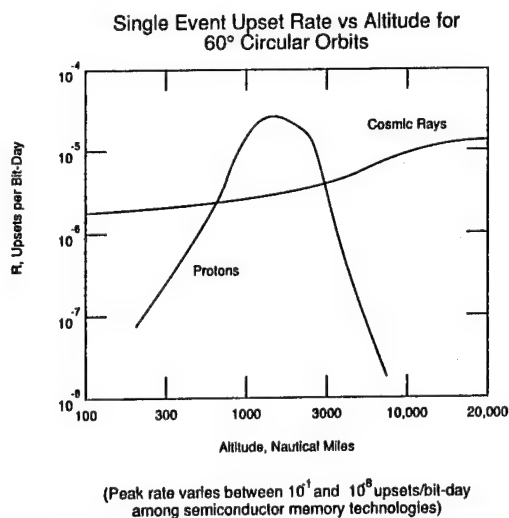
$$R = 5 \times 10^{-10} \sigma_L / L_c^2,$$

where σ_L is the upset cross-section expressed in square microns and L_c is the critical LET expressed in pC/micron. This useful "Figure of Merit" is valid in regions of space where the galactic cosmic ray environment is not significantly affected by the Earth's magnetic field. In regions where trapped radiation is dominant, upsets due to galactic cosmic rays will be in general less, and the contribution from trapped protons has to be computed.

We have seen that proton upsets are induced indirectly via nuclear reactions and so the techniques outlined above for calculating heavy ion upset rates in space do not apply in the case of protons. A semi-empirical method for estimating proton induced upsets in spaceborne memories has been developed by Bendel and Petersen¹⁵. Upon examining trends in proton test data obtained on a large variety of devices and reconciling these trends with nuclear reaction data at the low and high proton-energy extremes, they came up with a rather simple and elegant equation for the proton-upset probability or cross-section which depends on just two variables, viz. E , the proton energy and the parameter A which is equivalent to the apparent threshold at low energy. Their result is shown in Figure 11, plotted as a function of proton energy for various fixed



values of the parameter A. Note that in this model, the measurement of the upset cross-section at a single proton energy significantly above threshold is enough to determine the device upset cross-section at all energies and hence the upset rate in any given proton space environment. Figure 12 shows the upset rates predicted by Bendel and Petersen for some devices flying in a 60 degree inclination orbit, at 1400 nm altitude. In Figure 13, the proton SEU rate in a part with A=25 MeV is



compared with the upset rate induced by galactic cosmic rays. In general, we would expect the trapped proton contribution to upset rate to dominate in low inclination orbits within the inner Van Allen belt, while in highly inclined orbits the rate should be comparable to the galactic cosmic ray contribution.

Validation of the model predictions is, of course, obtained from observations of single event rates in space. Unfortunately, while some data showing that the predictions are "in the right ballpark" exist, there are not nearly enough of such data, particularly of those acquired under carefully controlled conditions, so that their validity and correlation with an actual environment can be established.

In concluding this talk, I would like to give you an idea of the range of vulnerability of existing device technologies, as determined in the studies outlined above. Figures 14 and 15 show the predicted heavy ion upset rates for some representative device types in bipolar and MOS technologies, respectively. The comparisons listed in Figs. 14 and 15 are based on the Petersen et al. "Figure of Merit"¹⁴ and do not reflect the proton induced SEU rates in the inner Van Allen radiation belt. However, devices showing upset rates of less than 10^{-6} per bit-day can be expected in general to be quite hard against proton-induced SEU. I base this statement on the empirical observation that devices with threshold LETs above

10 Mev-cm² do not in general upset with protons, while with heavy ions, according to the Petersen formula, they upset at rates comparable to or less than 10⁻⁶/day.

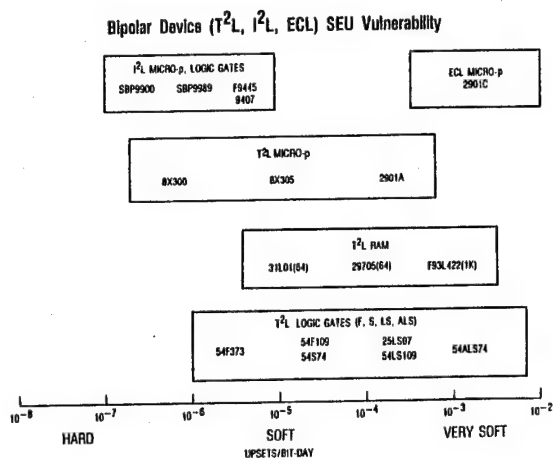


Fig. 14. SEU Rates for Bipolar Devices.

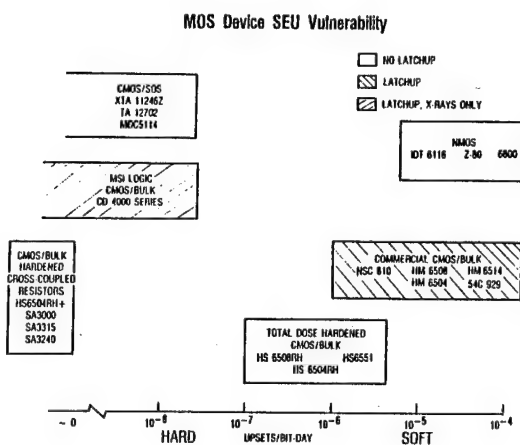


Fig. 15. SEU Rates for MOS Devices

REFERENCES

1. J. T. Wallmark and S. M. Marcus, "Minimum size and maximum packing density of nonredundant semiconductor devices", *Proc. IRE* March, 286-298 (1962).
2. D. Binder, E. C. Smith and A. B. Holman, "Satellite Anomalies from Galactic Cosmic Rays", *IEEE Trans Nucl. Sci.*, NS-22, 2675-2680 (1975).
3. J. C. Pickel and J. T. Blandford, "Cosmic Ray Induced Errors in MOS Memory Cells", *IEEE Trans Nucl. Sci.*, NS-25, 1166-1171 (1978).
4. W. A. Kolasinski, J. B. Blake, J. K. Anthony, W. E. Price and E. C. Smith, "Simulation of Cosmic Ray Induced Soft Errors and Latchup in Integrated Circuit Computer Memories", *IEEE Trans Nucl. Sci.* NS-26, 5087-5091 (1979).
5. C. S. Guenzer, E. A. Wolicki and R. G. Allas, "Single Event Upset of Dynamic RAMs by Neutrons and Protons", *IEEE Trans Nucl. Sci.*, NS-26, 5048-5052 (1979).
6. R. C. Wyatt, P. J. McNulty, P. Toumbas, P. L. Rothwell and R. C. Filz, "Soft Errors Induced by Energetic Protons", *IEEE Trans. Nucl. Sci.* NS-26, 4905-4910 (1979).
7. T. K. Sanderson, D. Mapper and J. H. Stephen, "Effects of space radiation on advanced semiconductor devices", *Interim Report for the European Space Agency*, G 2532, December, 1982.
8. J. H. Adams, R. Silberger and C. H. Tsao, "Cosmic Ray Effects on Microelectronics. Part 1: The near-earth particle environment", *NRL Memorandum Report* 4506, 1981.
9. D. L. Chenette and W. F. Dietrich, "The solar flare heavy ion environment for single-event upsets: a summary of observations over the last solar cycle, 1973-1983", *IEEE Trans. Nucl. Sci.* NS-31, 1217-1222 (1984).
10. J. B. Blake and R. Mandel, "On-orbit observations of single event upset in Harris HM-6508 1K RAMs", *IEEE Trans. Nucl. Sci.*, NS-33, 1616-1619 (1986).
11. M. Shoga, P. Adams, D. L. Chenette, R. Koga, and E. C. Smith, "Verification of single event upset rate estimation methods with on-orbit observations", *IEEE Trans. Nucl. Sci.*, NS-34, 1256-1259 (1987).
12. J. C. Pickel and James T. Blandford Jr., "Cosmic-ray induced errors in MOS devices", *IEEE Trans. Nucl. Sci.* NS-26, 1006-1015 (1980).
13. James H. Adams, Jr., "Cosmic ray effects on Microelectronics, Part IV", *NRL Memorandum Report* 5901, December, 1986.
14. E. L. Petersen, J. B. Langworthy and S. E. Diehl, "Suggested Single Event Upset Figure of Merit", *IEEE Trans. Nucl. Sci.* NS-30, 4533-4539 (1983).
15. W. L. Bendel and E. L. Petersen, "Proton Upsets in Orbit", *IEEE Trans. Nucl. Sci.*, NS-30, 4481-4485 (1983).

SESSION 7: SOLAR RADIATION

Chairman: Wayne S. Slemp
NASA Langley Research Center

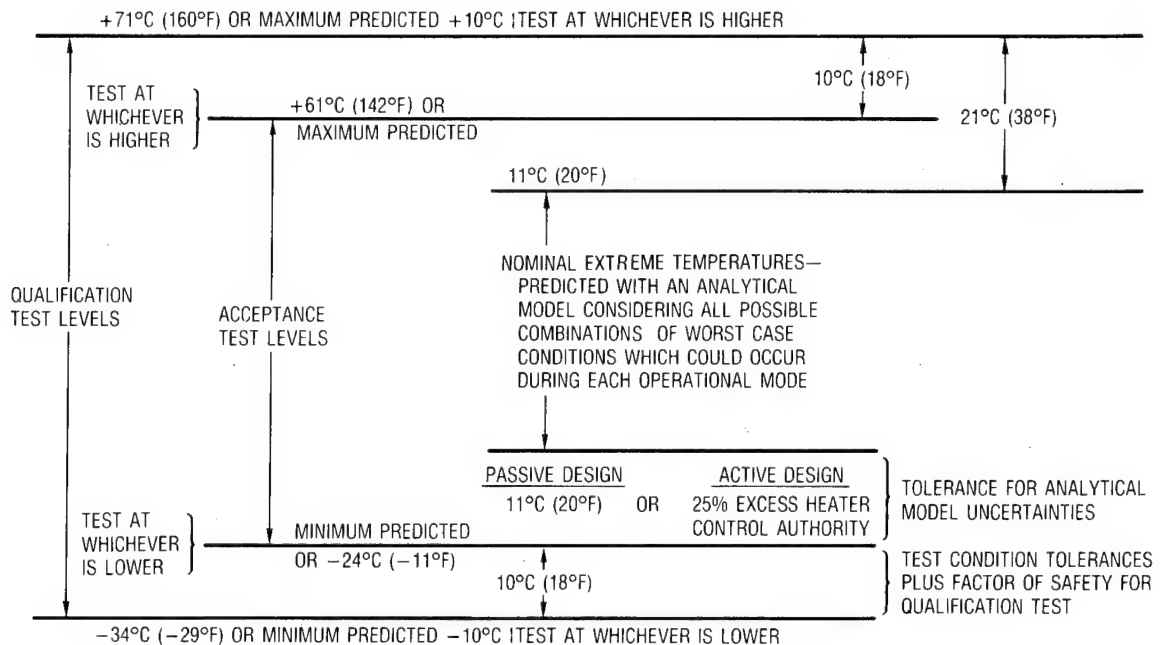
SPACE VEHICLE THERMAL TESTING: PRINCIPLES, PRACTICES,
AND EFFECTIVENESS

Donald F. Gluck
Thermal Control Department
The Aerospace Corporation
El Segundo, California

MIL-STD-1540B TEST REQUIREMENTS FOR COMPONENTS

Component qualification and acceptance temperatures are derived from worst case thermal analyses and analytic uncertainty margin subject to certain specified temperature extremes. Nominal extreme temperatures are predicted by applying an analytical model (e.g., SINDA computer program TMM) to each operational mode which considers worst case combinations of equipment operation, space vehicle attitude, solar radiation, eclipse conditions, degradation of thermal surfaces, et cetera. This must be done component by component, as a worst combination of conditions for one component may not prove to be worst for another. To these results an uncertainty margin is added. This margin, which can be quite large at the beginning of a program (e.g., 20 to 40°C), is reduced as the design and analytic process progresses. Following successful correlation of the thermal analysis with thermal balance test data, this uncertainty margin can be reduced to as little as $\pm 11^\circ\text{C}$. If a component is heater controlled, 25% excess heater control authority is required in lieu of an 11°C temperature margin. These temperatures set component acceptance test levels, subject to the requirement that the mounting plate or case temperature be at least as cold as -24°C and at least as hot as 61°C . These specified extremes are required in order to (a) provide adequate environmental stress screening, (b) demonstrate component survival capability, and (c) assure that temperature-insensitive and high-quality parts and materials are used in component design. Component qualification tests are conducted at temperatures 10°C colder (even if heaters are used for temperature control) and 10°C hotter than the acceptance test temperatures.

For some temperature-sensitive components such as batteries, propellant valves, and inertial reference units, the specified extremes are waived.



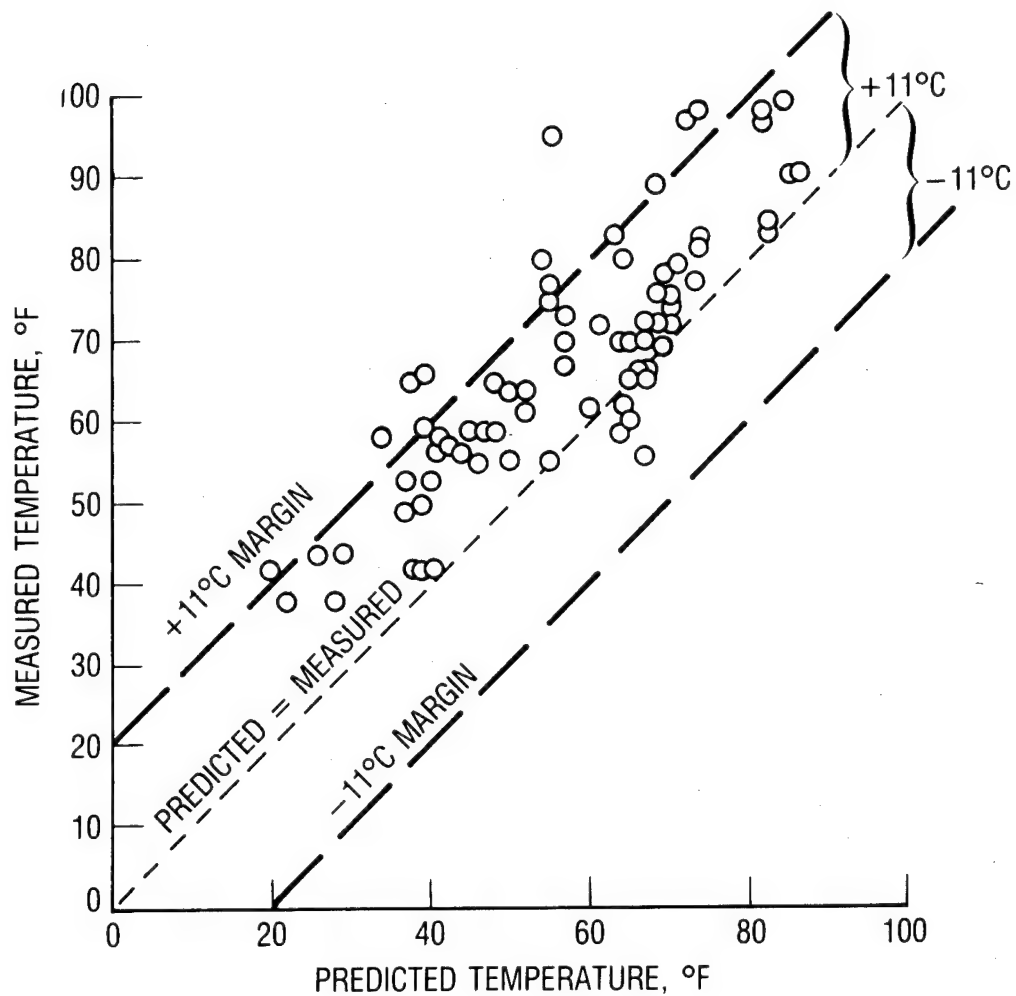
REPRESENTATIVE SPACE VEHICLE THERMAL CONTROL REQUIREMENTS

Temperature requirements are shown for equipment operation within specification and for survival and turn-on (need not operate within specification, but must not experience any degradation when returned to operational range). Temperature excursions for most equipment are seen to be 20 to 50°C above and below room temperature. Components without active electronics which are mounted outboard, such as solar arrays and antennas, are usually designed to withstand wider temperature excursions, particularly at the cold end. Batteries are tightly controlled at cold temperatures to increase life. Payload components such as extremely accurate clocks for precise navigation are controlled over a relatively narrow temperature range.

<u>COMPONENT/SUBSYSTEM</u>	<u>OPERATING TEMPERATURE RANGE (°C)</u>	<u>SURVIVAL/TURN-ON TEMPERATURE RANGE (°C)</u>
DATA HANDLING AND TT&C SUBSYSTEMS	-28.9/60	-28.9/60
ELECTRIC POWER AND DISTRI- BUTION SUBSYSTEM	-28.9/60	-28.9/60
EPDS REGULATOR	-28.9/60	-28.9/60
STABILIZATION AND CONTROL COMPONENTS	-28.9/60	-28.9/60
COMPUTER	-28.9/43.3	-28.9/60
DIPOLE RING ARRAY ANTENNA	-150/100	-150/100
CONE ANTENNA	-150/110	-150/110
BICONE ANTENNA	-150/110	-150/110
SOLAR ARRAY	-141/61	-141/61
SOLAR ARRAY DAMPERS	-45.5/55.5	TBD/55.5
PAYLOAD ELECTRONICS	-12.2/43.3	-28/60
PAYLOAD ELECTRONICS	-6.7/43.3	-28.9/48.9 (SURVIVAL) -6.7/48.9 (TURN-ON)
BATTERIES	0 → 5 (TRICKLE CHARGE) 21.1 (DEEP DISCHARGE)	0/30
PROPULSION SUBSYSTEM	-3.9/26.7	TBD/40
THRUSTERS	-3.9/26.7	TBD/40
RUBIDIUM CLOCK	20/45	-19/45
CESIUM CLOCK	20/45	-19/45

FLTSATCOM-F1 PREDICTED TEMPERATURES VERSUS MEASURED TEMPERATURES,
EQUINOX DIURNAL EXTREMES

The Aerospace Corporation's Thermal Control Department personnel, B. J. Smith and A. L. Bavetta, compared thermal balance test correlated model predictions with on-orbit measurements for the space vehicle FLTSATCOM-F1. Equinox data showed that measured temperatures were skewed towards being higher than predicted. Of 74 temperature measurements, 65 were within $\pm 11^\circ\text{C}$ of prediction, with a maximum deviation of 22°C . While the skewing was not necessarily experienced on other space vehicles, the pattern and spread were typical.



STP P78-1 SATELLITE (NO THERMAL BALANCE TEST)
COMPARISON OF ON-ORBIT TEMPERATURE MEASUREMENT WITH
CONTRACTOR ANALYTIC PREDICTIONS

Air Force Space Test Program Satellite P78-1 was launched without a thermal balance test. A comparison has been made of 12th day on-orbit measurements with contractor predictions. The temperature of 10 of 17 components within the wheel (rotating portion of the space vehicle) and 5 of 8 components within the sail (sun-fixed portion of the space vehicle) were within 11°C of the predicted values. The temperature of seven wheel components and three sail components exceeded prediction by more than 11°C, with the largest deviation being 24°C. Agreement between prediction and measurement was substantially poorer than for a typical satellite which had received a thermal balance test.

WHEEL EQUIPMENT, °C

	BATTERIES			ELECTRIC CHARGE CNTR.	POWER SHUNT REQ.	19V REG	TAPE RECORDERS			TELEMETRY DISTRIBU- TION UNIT	TRANS- MITTERS		COMMAND & DATA PROCESSOR	SPIN ASSEMBLY	AZIM. DRIVE ASSEMBLY	REFRIGERATOR PAA ELECTRONICS	
	1	2	3				A	B	C		1	2				GAMMA 3	GAMMA 4
ON-ORBIT TEMPERATURE MEASUREMENT 12th DAY AFTER LAUNCH	17	18	17	18	15	18	20	27	15	16	17	25	31	27	18	7.5	10
CONTRACTOR PREDICTION, NORMAL RESOLUTION	11	11	10	13	6	7	15	15	8	8	0	8	7	10	11	-9	-6

SAIL EQUIPMENT, °C

	REMOTE COMMAND AND DATA PROCESSOR		AMPLIFIER		AUXILIARY CONTROL ELECTRONICS	TRUNNION	NUTATION DAMPER	SOLAR ARRAY
	1	2	SERVO	POWER				
ON-ORBIT TEMPERATURE MEASUREMENT 12th DAY AFTER LAUNCH	21	16	28	24	30	24	25	63
CONTRACTOR PREDICTION, NORMAL RESOLUTION	14	21	15	19	7	16	2	55

THE BASIS OF MIL-STD-1540's TEMPERATURE UNCERTAINTY MARGIN

The table is supported by The Aerospace Corporation's data base. An uncertainty margin of 11°C is used in MIL-STD-1540 for analytic predictions correlated to thermal balance test results. Note that the intent of the standard is to provide 95% confidence that acceptance test temperatures will not be exceeded during mission life.

STANDARD DEVIATION	PERCENT OF CONFIDENCE	TEMPERATURE UNCERTAINTY (°C)	
		UNVERIFIED ANALYTICAL PREDICTIONS	PREDICTIONS VERIFIED BY TESTING
1.0	68%	8.3	5.6
1.4	85%	12.2	7.8
2.0	95%	16.7	11.0
3.0	99%	25.0	16.7

MIL-STD-1540 COMPONENT TEST BASELINE

MIL-STD-1540 defines a component as "a functional unit that is viewed as an entity for purposes of analysis, manufacturing, maintenance, or record-keeping. Examples are hydraulic actuators, valves, batteries, electrical harnesses, and individual electronic boxes such as transmitters, receivers, or multiplexers." Components are made up of modules and assemblies which, in turn, are made up of piece parts. Test and screens are conducted at these lower levels of assembly. However, the lowest level of assembly addressed in MIL-STD-1540 is the component level.

These tables are abstracted from tables in this Standard. Thermal vacuum, thermal cycling, and burn-in are component thermal tests and screens. MIL-STD-1540 requires thermal cycling rather than elevated temperature burn-in. Functional tests, while not considered here as thermal tests, are required at temperature extremes during thermal cycling and thermal vacuum tests.

COMPONENT QUALIFICATION TESTS

TEST	REFERENCE PARAGRAPH	SUGGESTED SEQUENCE	ELECTRONIC OR ELECTRICAL EQUIPMENT	ANTENNAS	MOVING MECHANICAL ASSEMBLY	SOLAR PANEL	BATTERIES	VALVES	FLUID OR PROPULSION EQUIPMENT	PRESSURE VESSELS	THRUSTERS	THERMAL EQUIPMENT	OPTICAL EQUIPMENT
FUNCTIONAL	6.4.1	1 ⁽¹⁾	R	R	R	R	R	R	R	R	R	R	R
THERMAL VACUUM	6.4.2	9	R	R	R	R	R	R	R	O	R	R	R
THERMAL CYCLING	6.4.3	8	R	O	O	O	O	O	O	—	—	—	—

COMPONENT ACCEPTANCE TESTS

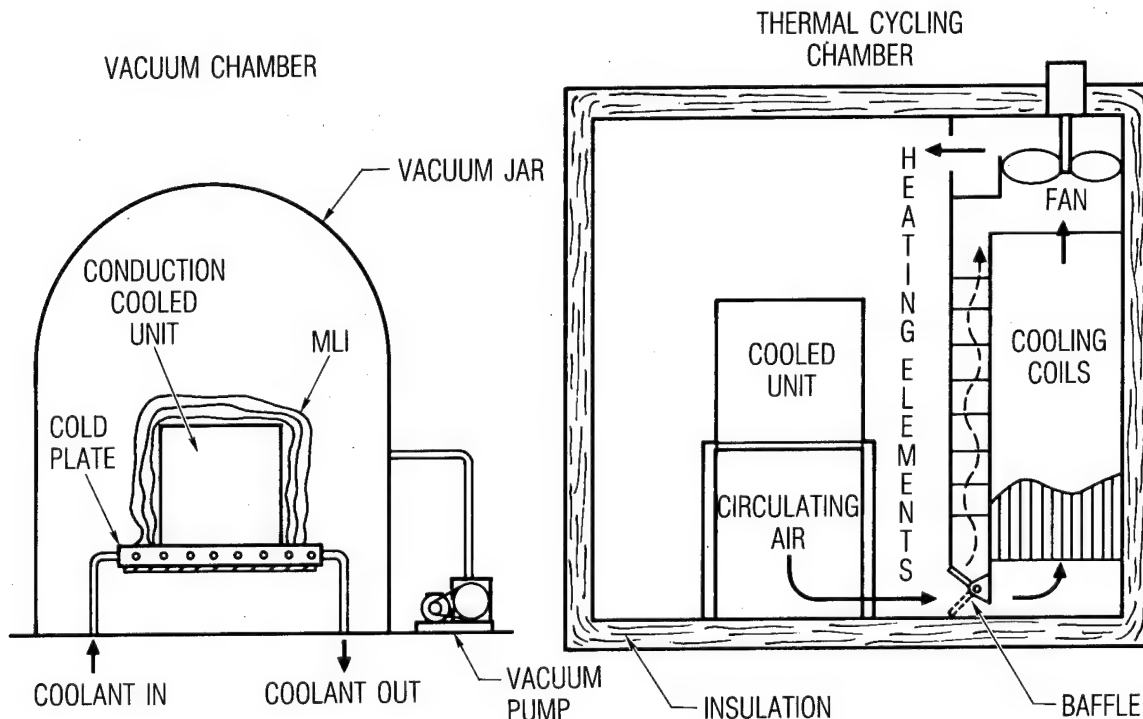
TEST	REFERENCE PARAGRAPH	SUGGESTED SEQUENCE	ELECTRONIC OR ELECTRICAL EQUIPMENT	ANTENNAS	MOVING MECHANICAL ASSEMBLY	SOLAR PANEL	BATTERIES	VALVES	FLUID OR PROPULSION EQUIPMENT	PRESSURE VESSELS	THRUSTERS	THERMAL EQUIPMENT	OPTICAL EQUIPMENT
FUNCTIONAL	7.3.1	1 ⁽¹⁾	R	R	R	R	R	R	R	R	R	R	R
THERMAL VACUUM	7.3.2	7	R ⁽²⁾	O	R	O	R	R	R	O	R	R	R
THERMAL CYCLING	7.3.3	6	R	O	O	O	O	O	O	—	—	—	—
BURN-IN	7.3.9	8	R	—	O	—	—	R	—	—	R	—	—
LEGEND: R = REQUIRED O = OPTIONAL TEST — = NO REQUIREMENT Notes: (1) Functional tests shall be conducted prior to and following environmental test (2) Required only on unsealed units and on high power, RF equipment													

COMPONENT THERMAL ENVIRONMENTS

A wide variety of test chambers are available for thermal cycling tests. Nitrogen or humidity-controlled air is used to prevent water vapor condensation. Heating, cooling, and a rapid air or gas flow are required. A rapid rate of temperature change at the base plate or case of the component of interest is often difficult to achieve. This may be the major technical challenge faced in thermal cycling testing.

Thermal vacuum tests are divided into two categories: (1) those where conduction to a mounting plate is the dominant mode of cooling, and (2) those where radiation to the surroundings dominates or where cooling is by both conduction and radiation. The former has proved to be the more likely occurrence. Conduction cooling is usually accomplished by torquing the component down onto a monolithic, thermally-controlled plate. This is not truly representative of actual component installation, which may, for example, have delron inserts in an aluminum honeycomb with face sheets. However, this is usually acceptable for component testing and buy-off, provided the differences between test mounting and flight mounting are accounted for by analysis and verified by testing at the subsystem or the system level.

Many components are cooled primarily by radiation or by both conduction and radiation. Such components include control moment gyroscopes, horizon sensors, and inertial reference units. Here, control of the heat loss paths should be such that radiation and conduction occur in the same proportion as calculated for the flight environment. This is necessary so that module and piece part temperatures and component temperature gradients duplicate those which occur in actual usage. This can be achieved, for example, by the use of heated baffles and shields and the control of mounting plate temperatures.



OBJECTIVES OF COMPONENTS THERMAL CYCLING, THERMAL VACUUM, AND BURN-IN TESTS

The specified tests (thermal cycling, thermal vacuum, and burn-in) can be construed as having three functions: environmental stress screening (ESS), demonstration of survival and turn-on capability, and performance verification. ESS, by subjecting hardware to physical stresses, forces flaws which are not ordinarily apparent into observable failures. Flaws are latent defects in design, workmanship, parts, processes, or materials which could cause premature component failure. The defective elements are repaired or removed prior to usage. The intent of the survival and turn-on function is to demonstrate that the equipment can be soaked, started, and operated at cold and hot survival temperature limits without experiencing permanent damage or performance degradation when returned to the operational temperature range. Survival/ turn-on temperature limits derive from ascent, safemode and threat mission phases, and factory and launch site checkout. Finally, the tests verify that the component electronic and mechanical performance is within specification.

● ENVIRONMENT STRESS SCREENING

- FINDS FAULTS IN COMPONENT DESIGN. WORKMANSHIP, PARTS, MATERIALS, AND PROCESSES

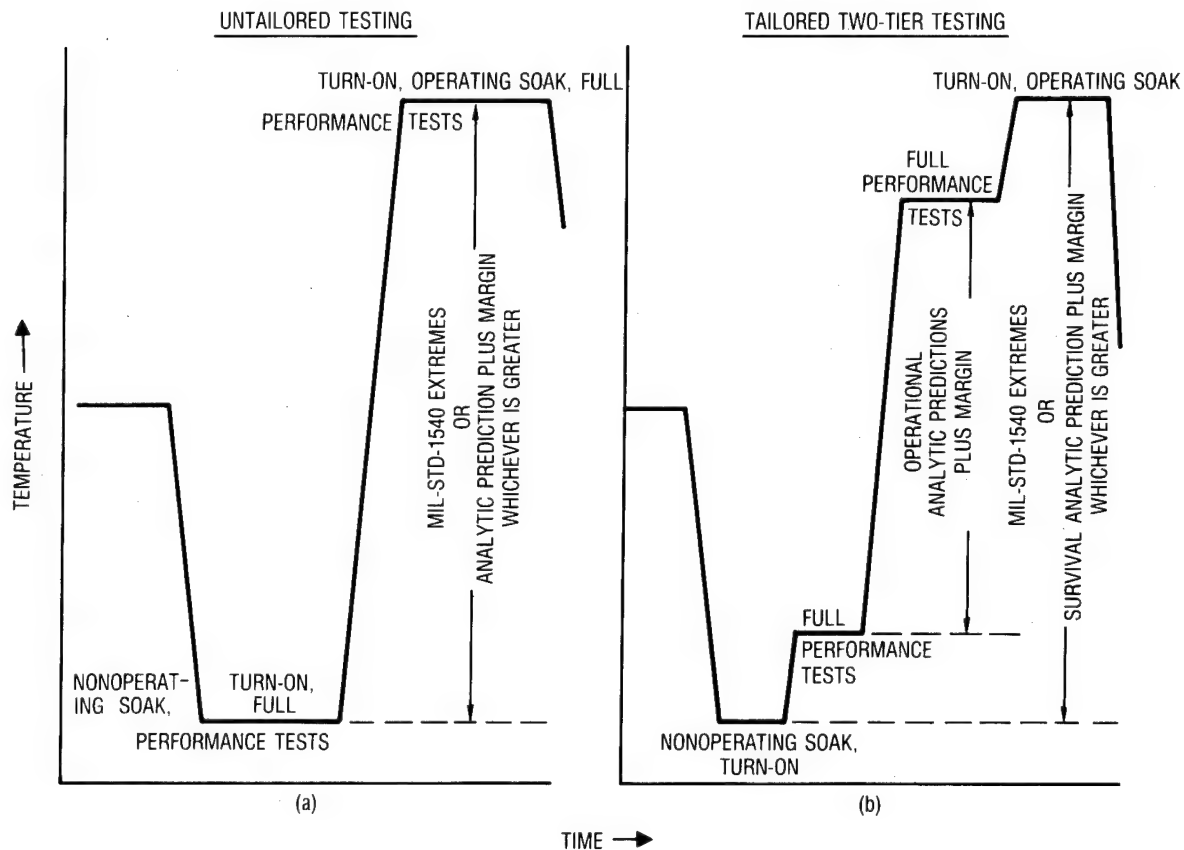
● VERIFICATION OF SURVIVAL AND TURN-ON CAPABILITY

- DEMONSTRATION THAT COMPONENT CAN BE TURNED ON AND OPERATED OVER SURVIVAL TEMPERATURES WITHOUT EXPERIENCING PERMANENT DAMAGE OR PERFORMANCE DEGRADATION WHEN RETURNED TO OPERATIONAL TEMPERATURE RANGE

● VERIFICATION THAT COMPONENT PERFORMANCE IS WITHIN SPECIFICATION OVER ITS OPERATIONAL TEMPERATURE RANGE

TEMPERATURE TIMELINES

Test temperature limits are the same for performance, screening, and survival/turn-on, if MIL-STD-1540 is applied without tailoring. In this case, component thermal tests are conducted at cold and hot limits determined from analytic predictions plus analytic uncertainty margin or at specified extremes whichever is greater. Some suppliers have requested a waiver for units originally built and qualified before the Standard was issued and for a limited number of new units with special temperature sensitivity; they have proposed, in lieu of the Standard, that tailored two-tier testing be conducted as in Figure b. For such testing, performance is verified over the narrower regime of operational analytic predictions plus margin, while screening is accomplished and survival/turn-on are demonstrated over the wider range of MIL-STD-1540 specified extremes or survival temperature analytic prediction. Unfortunately, this waiver request has propagated, so that it is now being requested for many units regardless of heritage, temperature sensitivity, and the like. Additionally, the outer tier tests and temperature levels have been weakened.



COMPARISON OF MIL-STD-1540 ACCEPTANCE TEST REQUIREMENTS
WITH RECOMMENDATIONS

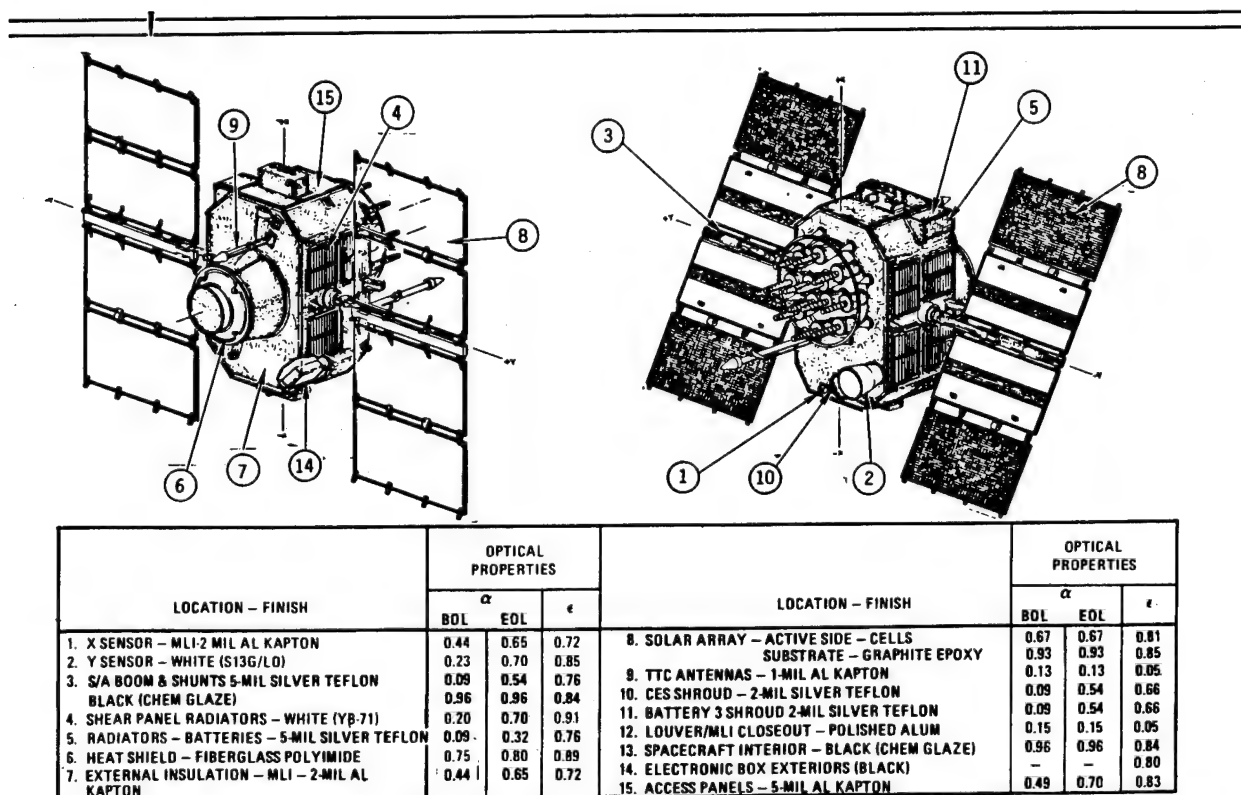
Key Parameter	Recommendations		MIL-STD-1540B Requirements	Conclusions										
	IES Guidelines (Ref. 1)	MMC Study (Ref. 2)												
No. of thermal cycles	12 cycles	<table><tr><td>Part Count</td><td>Recommended No. of Cycles</td></tr><tr><td>100</td><td>1</td></tr><tr><td>500</td><td>3</td></tr><tr><td>2000</td><td>6</td></tr><tr><td>4000</td><td>10</td></tr></table>	Part Count	Recommended No. of Cycles	100	1	500	3	2000	6	4000	10	Thermal cycling -8 cycles Thermal vacuum -1 cycle For TC and TC conduct full functional test at high and low temperature extreme, first and last cycles Burn-in -18 cycles (includes thermal cycling and thermal vacuum)	MIL-STD requirements consistent with industry practice No. of cycles not excessive, may be insufficient
Part Count	Recommended No. of Cycles													
100	1													
500	3													
2000	6													
4000	10													
Temp. extremes and range	-40 to +70°C	-54 to +55°C	-24 to +61°C	MIL-STD requirements within design and performance capability and within experience base of suppliers Makes sense for space vehicles because of unattended long-life requirement										
Temp. transition rate of change	5°C/minute of surrounding media	-	At least 1°C/minute measured at baseplate of unit	MIL-STD requirements more work is needed on subject Rate of change probably too low; should be at least as great as maximum predicted rate										
Operation/non-operation profile	Power ON	-	Power ON during transition Cycles through operational modes Monitor perceptive parameters Cold start/hot start	MIL-STD-1540 requirements are sound and well founded										
Dwell	-	-	One hour minimum dwell at high and low temp. extreme, long enough to obtain internal temp. equilibrium	MIL-STD-1540 requirements seem reasonable										

THERMAL CONTROL SURFACES AND FINISHES

Surfaces and finishes are the most basic thermal control hardware. Some are illustrated for a typical space vehicle. Solar absorptance, α , tends to increase with mission life because of contamination and attack by ultra-violet radiation and charged particles. The composite Kapton-H/aluminum film is widely used as the external surface of structure and multilayered insulation because it has good handling and bonding characteristics and experiences relatively minor mechanical damage due to the natural environment. Teflon/silver film has lower values of α/ϵ than the Kapton film, but it is seeing less use as a flexible second surface mirrors because of mechanical degradation in the natural environment. This satellite did not use the more durable fused silica/silver rigid second surface mirrors commonly called OSRs. White paint such as S13S/L0, composed of zinc oxide pigment and RTV-602 (organic) binder, degrade more rapidly than the newer YB-71 white paint, which is composed of zinc orthotitanate pigment and PS7 potassium silicate (inorganic) binder. The YB-71 paint, sometimes called "ZOT," also appears to have good survival characteristics in some threat environments.

High emissivity white and black paints are widely used for interior surfaces. Polished aluminum, with its low emissivity, is usually employed in applications where there is no direct solar incidence and where low thermal coupling to space and to spacecraft surfaces is desired.

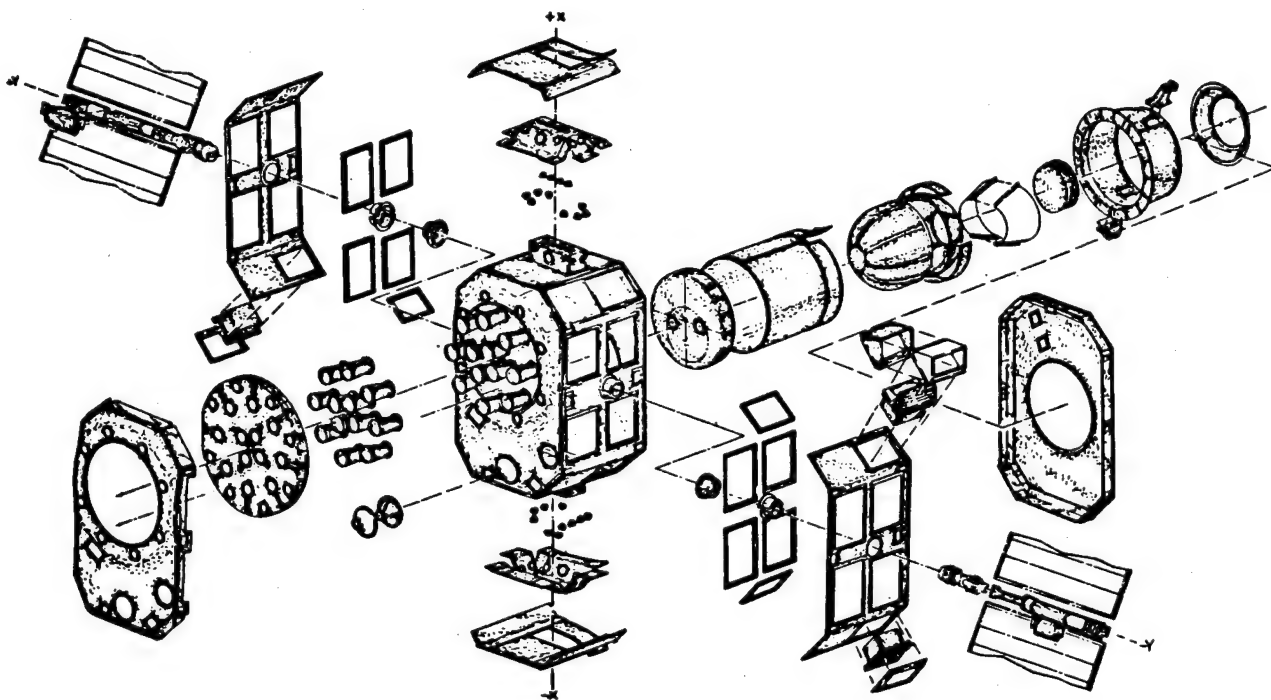
TCS COATINGS



INSULATION BLANKETS

The exploded insulation illustration shows the wide variety of multilayered insulation blankets used on space vehicles. These blankets use a layered approach to reduce conduction and radiation heat transfer to low values. Typically, alternate layers of aluminized Mylar or Kapton and a highly porous spacer material control radiation and conduction, respectively.

Blanket construction and installation can cause performance degradation. Heat shorts can be introduced by blanket compression over curved surfaces (especially those with compound curvature or small radii of curvature); penetration of support posts; blanket electrical grounding, venting and outgassing provisions; and stitching, pinning, and binding. Such problems are usually more severe with smaller blankets and those with cutouts, where the ratio of edge length to surface is large. A well-instrumented, properly controlled thermal balance test, using a qualification space vehicle or subsystem which is a true facsimile of the flight article, is necessary to determine blanket effective emissivity.

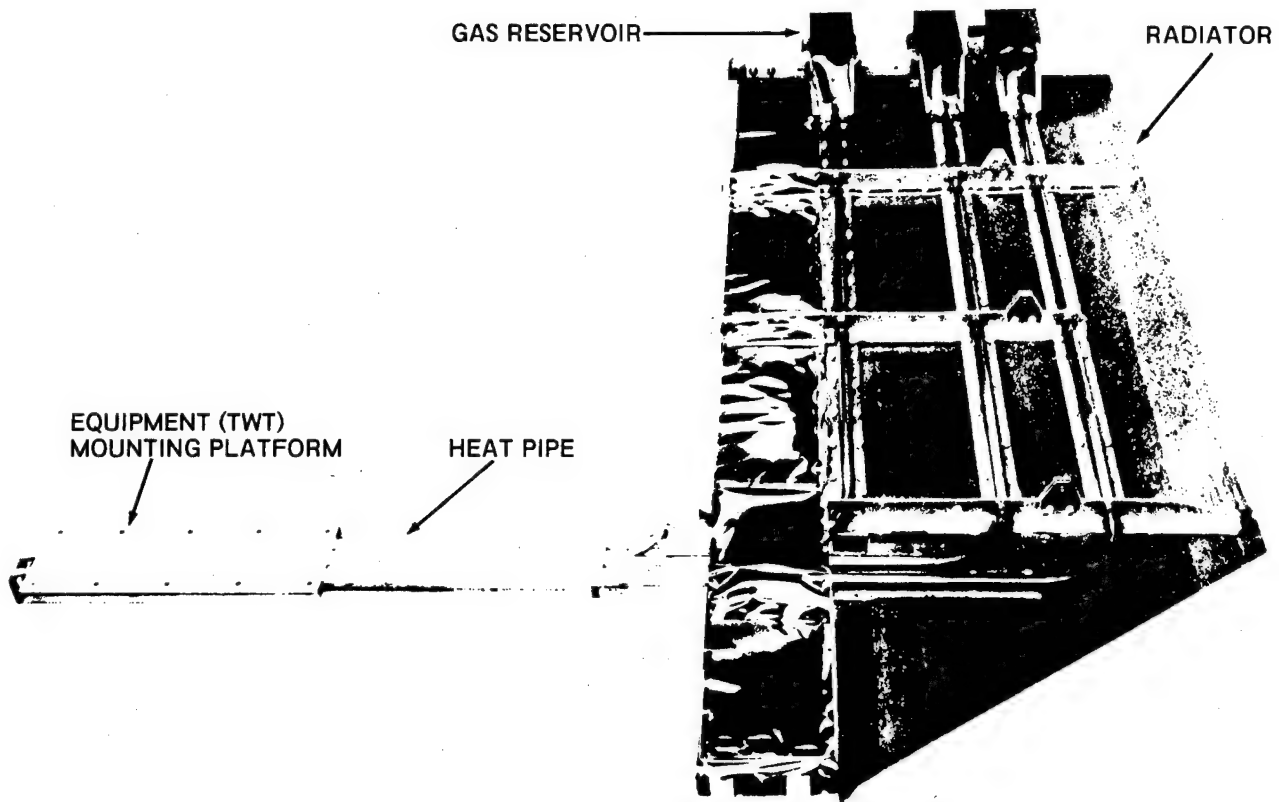


HEAT PIPE ASSEMBLIES

Heat pipes (tubes containing internal wicks and liquid and vapor phase working fluid) are coming into extensive use on space vehicles. Newer vehicles may use more than 100 heat pipes of five to 15 different configurations and types. Evaporation in the region of equipment heat dissipation causes menisci contraction to small radii of curvature. The evaporated vapor condenses in the cold radiator portion of the heat pipe. The differential pressure caused by evaporator menisci pumps the condensed liquid within the wicking grooves to the evaporator end of the heat pipe. A countercurrent convection loop is thereby set up in the pipe which transfers heat at substantially higher rates than a solid aluminum tube of the same diameter. More complex designs offering greater control precision and reduced cold case heater power usage are possible (e.g., the variable conductance heat pipe assembly illustrated here). It employs inert gas within gas reservoirs to block portions of the condenser during mission phases with reduced equipment heat dissipation or environmental loading. For higher heat load applications, capillary pumped loops are receiving consideration. Operation and control of such loops entails yet a higher level of complexity.

Heat pipe performance, as it depends on relatively small capillary forces, is sensitive to body (gravitational) forces. Consequently, a heat pipe which will work excellently in the near zero gravity space environment, could be rendered inoperative by evaporator height exceeding condenser height by a fraction of an inch during ground tests. The effect on vehicle design and ground testing is profound. Precise tolerance control of the design and the test set up may be required to assure that a heat pipe meets leveling requirements. Because of design requirements and allowable test configurations, some heat pipes cannot possibly be tested in the horizontal configuration during space vehicle tests. The thermal performance of such heat pipe assemblies must be verified at the subsystem level; here, it is often possible to rotate the assembly so that the heat pipes of interest are horizontal. A space test may prove to be the ideal way to verify the performance of new capillary pumped loop designs.

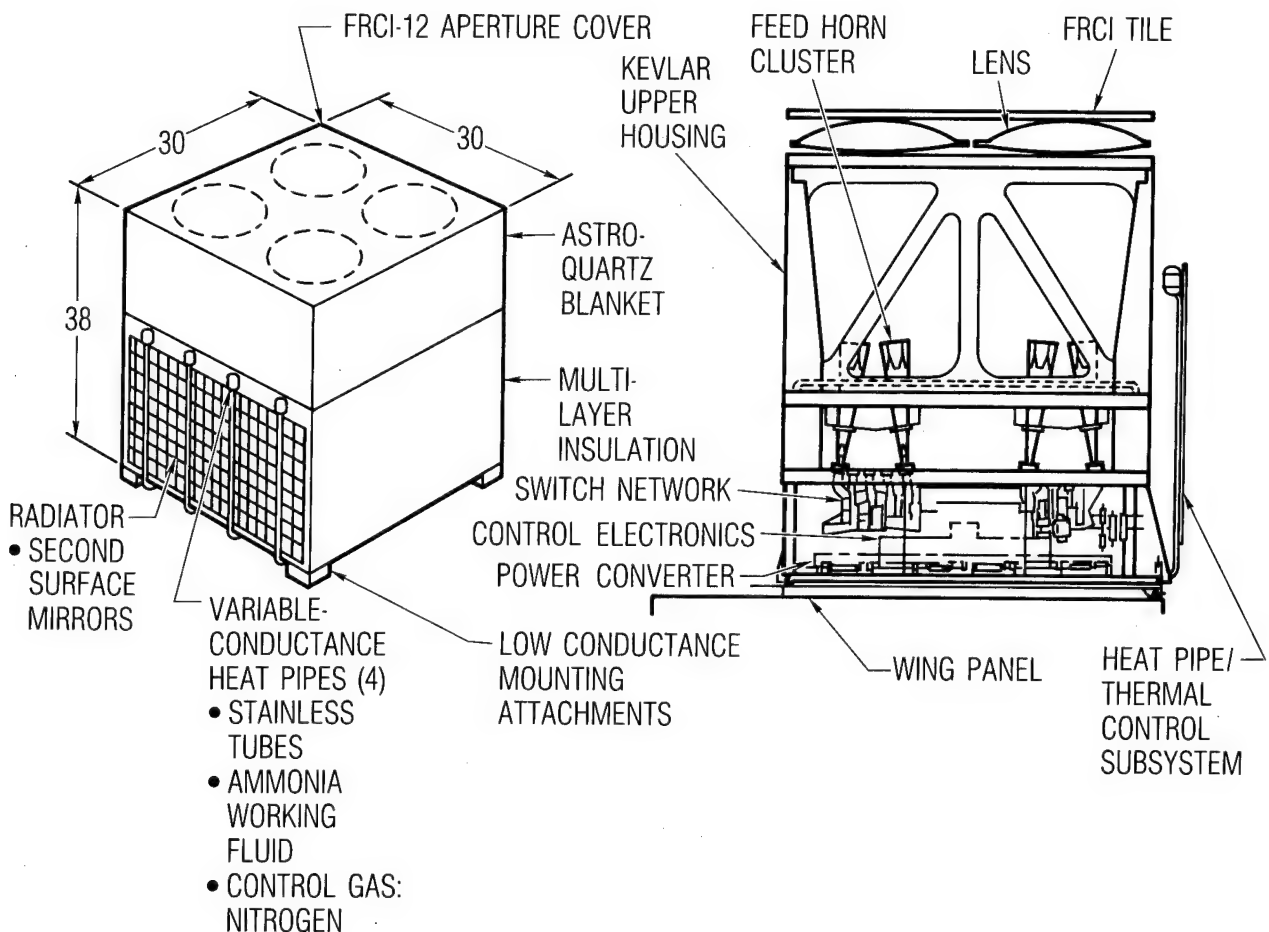
SATELLITE VARIABLE CONDUCTANCE
HEAT PIPE ASSEMBLY



SUBSYSTEM AND ASSEMBLY THERMAL VACUUM TESTS

As spacecraft size and complexity has grown, and buildup time has lengthened, the need has developed for intermediate tests between component and space vehicle testing. Such tests may be conducted on all or part of a subsystem. For example, the thermal design of the depicted antenna assembly is sufficiently complex to warrant an assembly level thermal vacuum test. Design features include multilayered insulation, a second surface mirror radiator, conduction coupling to active electronics, variable conductance heat pipes, and heaters and controllers. The test will verify the ability of the thermal design to hold components within allowable temperatures under specified hot and cold conditions.

Subsystem and assembly tests allow use of smaller test facilities than required for the space vehicle tests, and make it easier to tailor the thermal environment to the specific requirements of the components under test. Usually, configuration and leveling requirements can be more readily met in a subsystem, rather than in a space vehicle test. Results are obtained in a more timely manner, facilitating necessary remedial action.



SPACE VEHICLE THERMAL TESTS

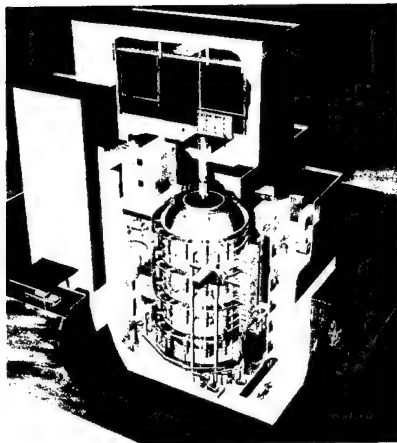
Space Vehicle (SV) qualification thermal tests are more demanding than the SV acceptance tests in that there is a wider temperature range, more thermal cycles, and the inclusion of a thermal balance test. The qualification tests are formal contractual demonstrations that the design, manufacturing, and assembly of hardware have resulted in conformation to specified requirements. The acceptance tests are required formal tests which demonstrate the acceptability of an item for delivery. They are intended to demonstrate performance to specified requirements and to act as environmental screens to detect deficiencies of workmanship, material, and quality. Acceptance test temperature levels should encompass all specified flight environments.

The thermal vacuum test consists primarily of system level functional performance tests (e.g., payload performance, electrical, mechanical, and thermal) between and at temperature extremes. Emphasis is on component and subsystem interaction and interfaces; integrity of mounting, cabling, and connectors; and on end-to-end system performance. An optional thermal cycling test functions as a high level environmental screen. The thermal balance test, conducted as part of the thermal vacuum test for the qualification vehicle, is a dedicated thermal test to correlate the thermal analytic models and demonstrate the design and functional capability of thermal control hardware.

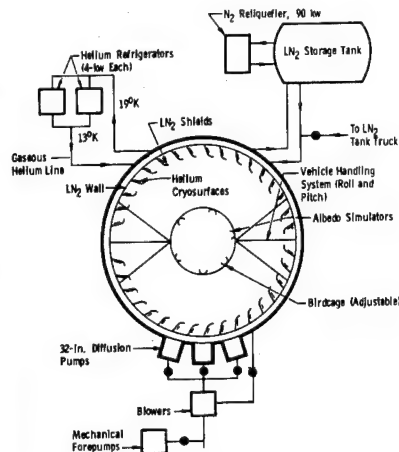
A variety of components, often tested to different temperature extremes during component qualification and acceptance, must be accommodated during SV thermal vacuum testing. The approach taken is to drive as many components as possible (but at least one component per vehicle equipment zone) to their qualification or acceptance temperature extremes, with the constraint that no component should exceed its component level test temperature extremes. This requires pretest analysis, use of test equipment and instrumentation, and local heating or cooling within the chamber. Safeguards are necessary to avoid damage during handling and testing.

ARNOLD ENGINEERING DEVELOPMENT CENTER
AEROSPACE ENVIRONMENTAL CHAMBER (MARK I)

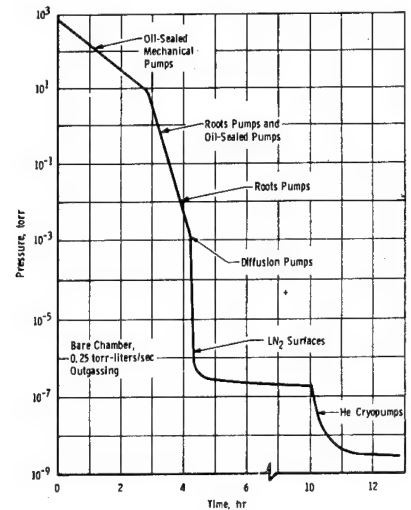
The AEDC Mark I Chamber, in Manchester, Tennessee, is described in order to illustrate a large thermal vacuum facility. The 42-ft diameter, 82-ft high chamber is housed in a 10-story building. It features a 20-ft diameter top hatch for vehicle entry and an 8-ft bottom hatch for personnel access. The cool-down and pump-down systems are shown in the schematic. They feature an 8 kW gaseous helium refrigeration system and a 90 kW nitrogen reliquification system. Diffusion pump capability is 2×10^5 l/sec at 10^{-7} torr and cryopump nitrogen capability is 15×10^6 l/sec.



Mark I Facility Arrangement



Mark I Schematic



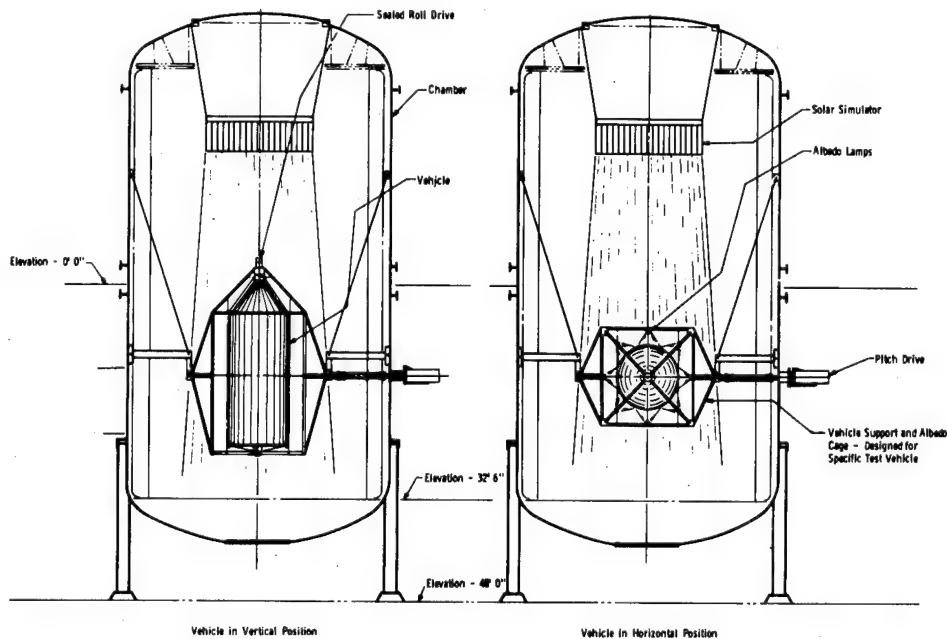
Mark I Pumpdown Curve

MARK I CHAMBER: THERMAL ENVIRONMENTS AND VEHICLE HANDLING

The vehicle handling system accommodates moderate size, symmetric shape test articles to 50,000 lb. A pitch drive and slip-ring assembly is used for power transfer. The handling system is capable of simultaneous real time motion about two axes. However, wire bundles and test instrumentation leads may make this impractical. The Block II GPS-NAVSTAR, recently tested in this chamber, utilized motion about one axis to simulate the time-varying solar vector for the beta-equals-zero orbit.

Solar simulation is accomplished using an array of modules, each containing a 1-kW quartz-iodine lamp and a water-cooled collimator tube. As the created spectrum approximates a 3000°K blackbody, with the sun more nearly like a 5800°K blackbody, augmenting xenon short-arc lamps can be used to improve spectral matching. The Mark I system is capable of continuously variable radiation for 0 to 110% of the solar constant with $\pm 3\%$ uniformity. Solar simulation is the preferred method of spacecraft heating, as this technique allows the natural blockage and cavity effects to occur, while imposing direct and reflected solar-like radiant heating. This method also creates infrared sources, which can approximate actual self heating by virtue of reradiation of absorbed solar energy. Because of cost and complexity, spacecraft heating is often done by methods that do not simulate the spectral content and directionality of the sun, but do attempt to impose the proper intensity and distribution of heating.

The cold environment of space is well-simulated by a liquid nitrogen-cooled high emissivity internal wall. Because of the fourth power dependence of radiant energy interchange, a wall at 77°K constitutes only a minor radiant energy source for a room temperature spacecraft.



SPACE VEHICLE (SV) THERMAL BALANCE TEST

This test formally qualifies the Thermal Control Subsystem (TCS). It is used to correlate the analytic thermal models; to verify the design and performance of TCS hardware such as insulation blankets, louvers, heat pipes, and heaters/thermostats; and to demonstrate that the TCS maintains all payloads and equipment within allowable temperature limits for all mission phases under worst case environments. This test should be conducted for one-of-a-kind spacecraft; the lead vehicle of a series of spacecraft; and a block change in a series of vehicles, upper stages, and sortie pallets designed to fly with the Shuttle.

The thermal balance test is conducted in a cryogenically cooled thermal vacuum chamber. The tests should simulate worst case combinations of equipment usage (primary and redundant), bus voltage, and solar angles and intensities. During these largely steady state tests all important internal heat flow paths and external radiative surfaces should be exercised. Some tests typically involve simulation of non-operational or transient mission phases: transfer orbit cooldown, eclipse, safemode entry or exit. Large appendages such as solar arrays, booms, and antennas are sometimes not part of the tested configuration. Both stowed and deployed vehicle configurations may be tested, requiring vacuum break. Environmental heating is usually simulated by infrared lamps, heated (radiating) plates, and/or test heaters affixed to external surfaces. Solar simulation is less frequently used.

The contractor should compare pretest temperature predictions with corresponding test data. The Aerospace Corporation has proposed, as a guideline, that those differences that fall outside a $\pm 3^{\circ}\text{C}$ band require either a good explanation or a model adjustment, depending on the size of the deviation. In practice, deviations as large as $\pm 6^{\circ}\text{C}$ are often accepted, with narrower limits for temperature-sensitive or mission-critical components.

SPACE VEHICLE (SV) THERMAL BALANCE TEST (Continued)

A variety of test-related factors contribute to a fairly large residual analytic uncertainty after completion of the thermal balance test. These include imperfect spectral matching, inadvertent test heat losses, end-of-life properties not simulated, test set radiation blockage, and measurement and calibration error.

Model correlation to test data may not be effective if an incorrect heat transfer mechanism is employed. Some design changes that were made because of thermal balance test results are not test verified until the acceptance test of the first flight vehicle and, sometimes, unfortunately there is no test validation.

Overall, the thermal balance test has proved successful in correcting major thermal modeling errors, in reducing the standard deviation between prediction and flight measurements, and in providing physical insight into heat transfer mechanisms.

The thermal balance test and portions of the thermal vacuum test serve to verify the design and performance of thermal control hardware. Primary and redundant heaters and thermostats are exercised and the circuitry is proven, location and response time is verified, and 25% excess heater control authority is demonstrated for the cold case. Radiator surface emissive power and insulation blanket effective emissivity are verified. Performance of louvers and heat pipes (if horizontal) is characterized. The ability of the TCS to maintain SV components within their specified temperature extremes under worst hot and cold case conditions is demonstrated.

THERMAL CONTROL REQUIREMENTS TO SUPPORT FACTORY AND LAUNCH SITE CHECKOUT AND FUNCTIONAL TESTING

Checkout and functional tests are required at various stages during the buildup of a space vehicle. Such tests often are not part of the formal developmental, qualification, and acceptance process. For example, these tests: (1) allow checkout at intermediate stages during the buildup process, (2) can verify that a subsystem has not been damaged or degraded during shipment, and (3) allow continuity, checkout, and limited functional tests during and after assembly at the launch site. Thermal control (i.e., gas or liquid cooling) often is required to ensure that components do not overheat during these tests. Compounding the difficulty of this requirement is the fact that the subsystem or space vehicle configuration and surrounding environment can encumber the cooling process. The cold radiation sink for which the space vehicle is designed is lacking during these tests, and natural convection cooling is not very efficient. Moreover, the subsystem or space vehicle may be oriented so that heat pipes are inoperative and may be enveloped with contamination covers, shrouds or the like, so that there is limited accessibility to fluid cooling.

It is important to identify, early in a program, factory and launch site cooling requirements for checkout and functional tests. This is especially important for sensitive components such as batteries. Space vehicle design accommodations and auxiliary ground equipment which may be required to allow adequate cooling should be specified. This may include ducting and fans, piping and pumps, and leveling hardware and instrumentation.

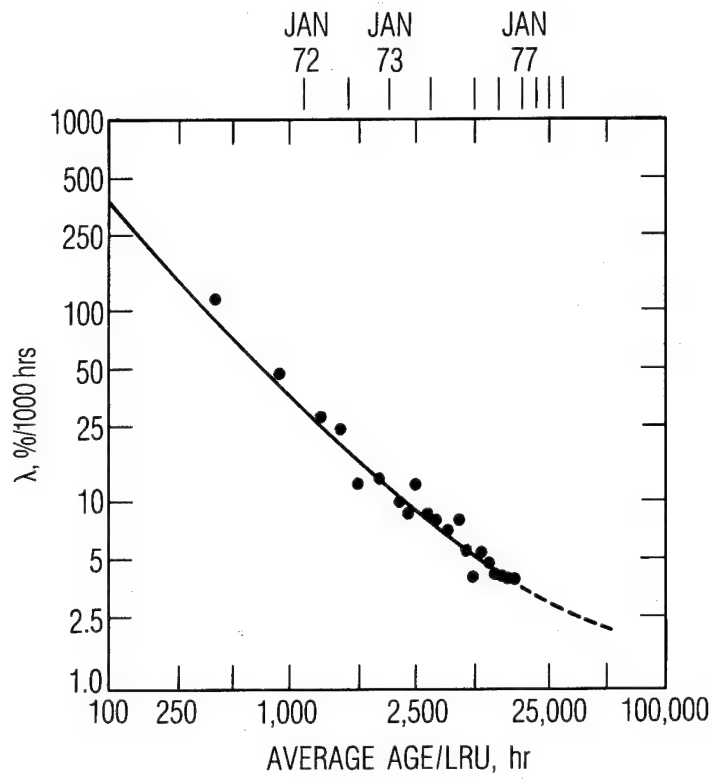
UNIFIED FAILURE THEORY - DEMISE OF THE BATHTUB CURVE

Bezatz and Montague (Ref. 3) have used laboratory and field failure data for the Honeywell Digital Air Data Computer to develop the failure rate curve below. The data base encompassed 6.5 years of revenue service and 11×10^9 part hours. The authors point out that the decreasing failure rate with time is consistent with their experience with semi-conductor devices. Herbert and Myron Hecht (Ref. 4) report a similar trend for spacecraft. Their data base was obtained from over 300 satellites, comprising 96 programs, launched between the early 1960s through January 1984. Primary data sources were The Aerospace Corporation's Orbital Data Analysis Program (ODAP) and the On-Orbit Spacecraft Reliability (OOSR) data compiled by the Planning Research Corporation for NASA. This and other data were the basis for Wong's paper, "Unified Field (Failure) Theory - Demise of the Bathtub Curve" (Ref. 5). Wong points out that the same failure pattern is seen in the laboratory, manufacturing screening, in the field, and that failure rate for electronic equipment trends downward (although the path may have some bumps) for all times of practical interest.

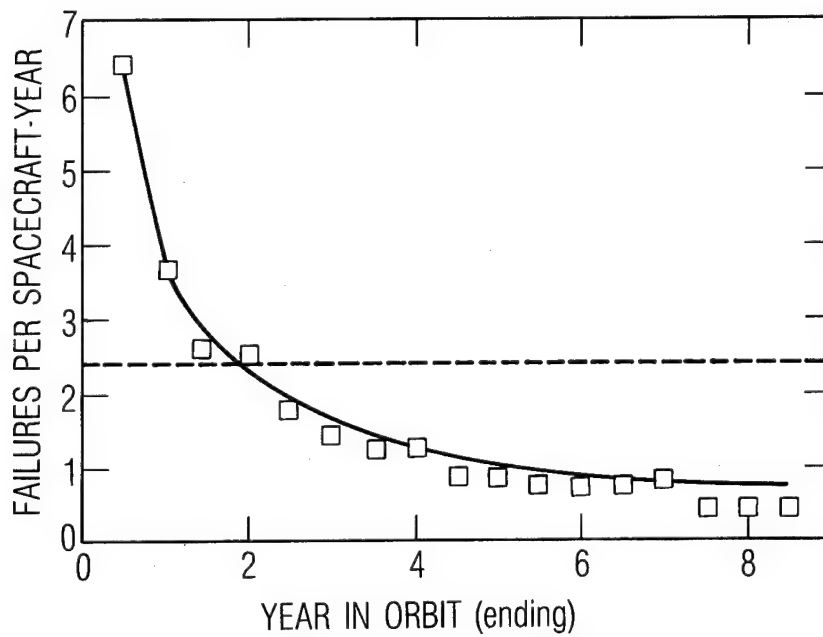
The implications for spacecraft testing and reliability, as we see it, are as follows:

1. No amount of testing will prevent infant mortality failures.
2. Testing can reduce the initial failure rate of this downward trending curve.
3. Provided that failures are detected and repaired, electronic equipment cannot be worn out by testing.
- 4a. Accelerated testing at high stress levels (even beyond flight levels) may be very beneficial for long term reliability.
- 4b. Ambient temperature burn-in with little monitoring is ineffective in screening defective equipment.
5. Quality standards and testing requirements fall off very slowly as mission duration decreases.

Honeywell Digital Air Computer Failure Rate Curve

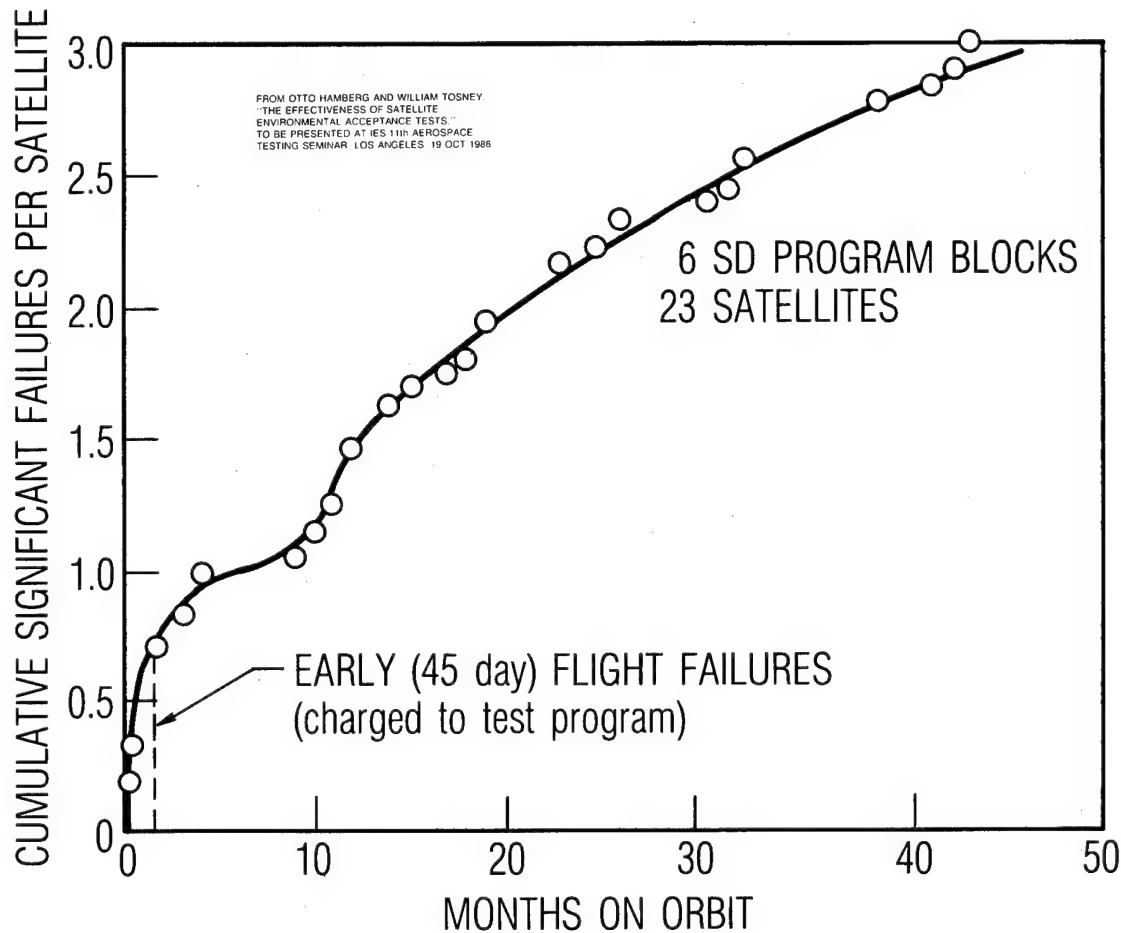


Hecht Study-Satellite Failure History



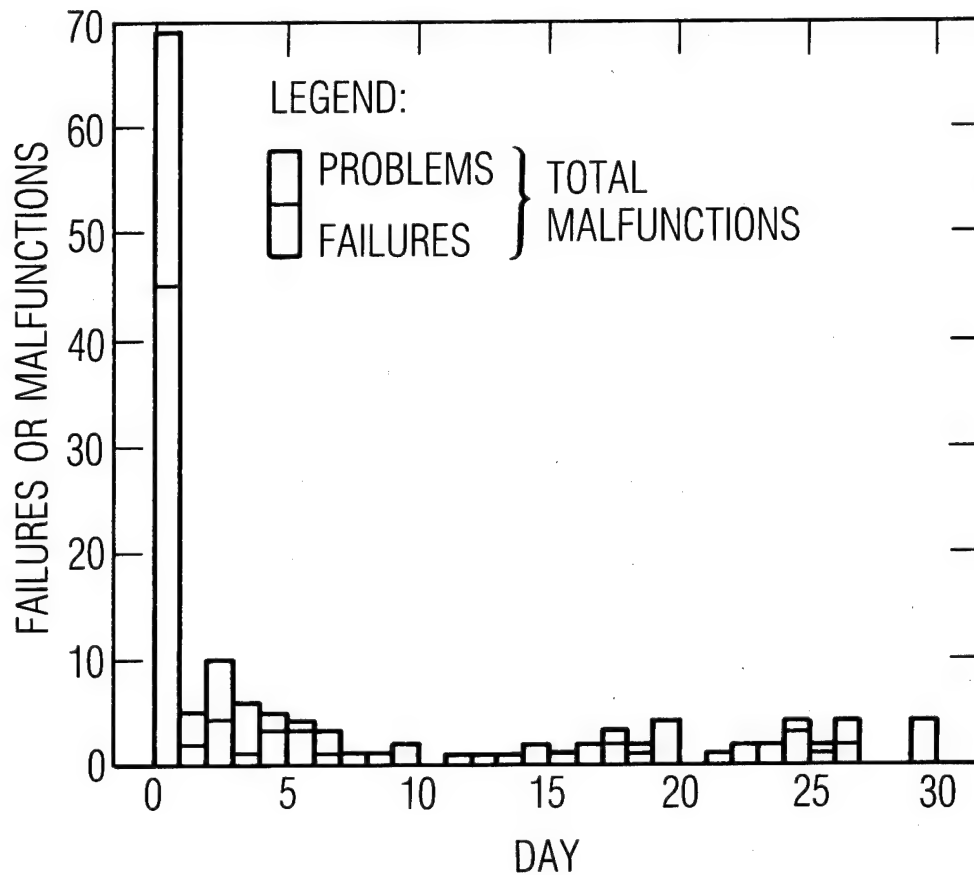
AEROSPACE ON-ORBIT FAILURE DATA

The flight failure history of six Air Force program blocks and 23 satellites is shown (Ref. 6). Only the initial four satellites from each program block were included to minimize the effect of program maturity, and only mission degrading (changes satellite reliability) failures are included. The data were obtained from The Aerospace Corporation's ODAP. It can be noted that the initial high failure rate has moderated somewhat by 45 days. This timeframe coincides with satellite launch, ascent, and the in-orbit operational performance tests. This high failure rate period is considered to be related to the imperfection of the ground test program. The infant mortality period appears to extend out to approximately 12 months of operational flight time. The failure rate after 12 months shows a slowly decreasing rate which is in agreement with the work of the Hechts (Ref. 4).



NASA/GODDARD EARLY ON-ORBIT FAILURE DATA

The work of Timmins (Ref. 7) on NASA/Goddard programs shows that early failures are dominated by first day failures. No corresponding day-by-day failure data has been assembled by The Aerospace Corporation. However, a cursory review by Tosney shows a similar trend, with first day of usage failures quite high.



DEFINITION OF TEST EFFECTIVENESS

The premise underlying the definition of test effectiveness (Ref. 8) is that failures found in environmental tests would have occurred early in flight (first 45 days); these early failures are charged to the test program. Aerospace's ODAP data base was used with only significant test and early flight failures considered. Such failures potentially reduce mission life. Generic failures were counted only once and induced failures not counted. This first order method attempts to account for test sequence as illustrated below.

● QUANTITATIVE MEASURE TO EVALUATE/COMPARE TESTS

TEST FAILURES
TEST PLUS FLIGHT FAILURES

● EXAMPLE PROGRAM A FAILURES PER SATELLITE (average of satellite group)

TESTS			FLIGHT
ACOUSTIC	THERMAL CYCLING	THERMAL VACUUM	45 day
0.9	1.4	1.6	0.6

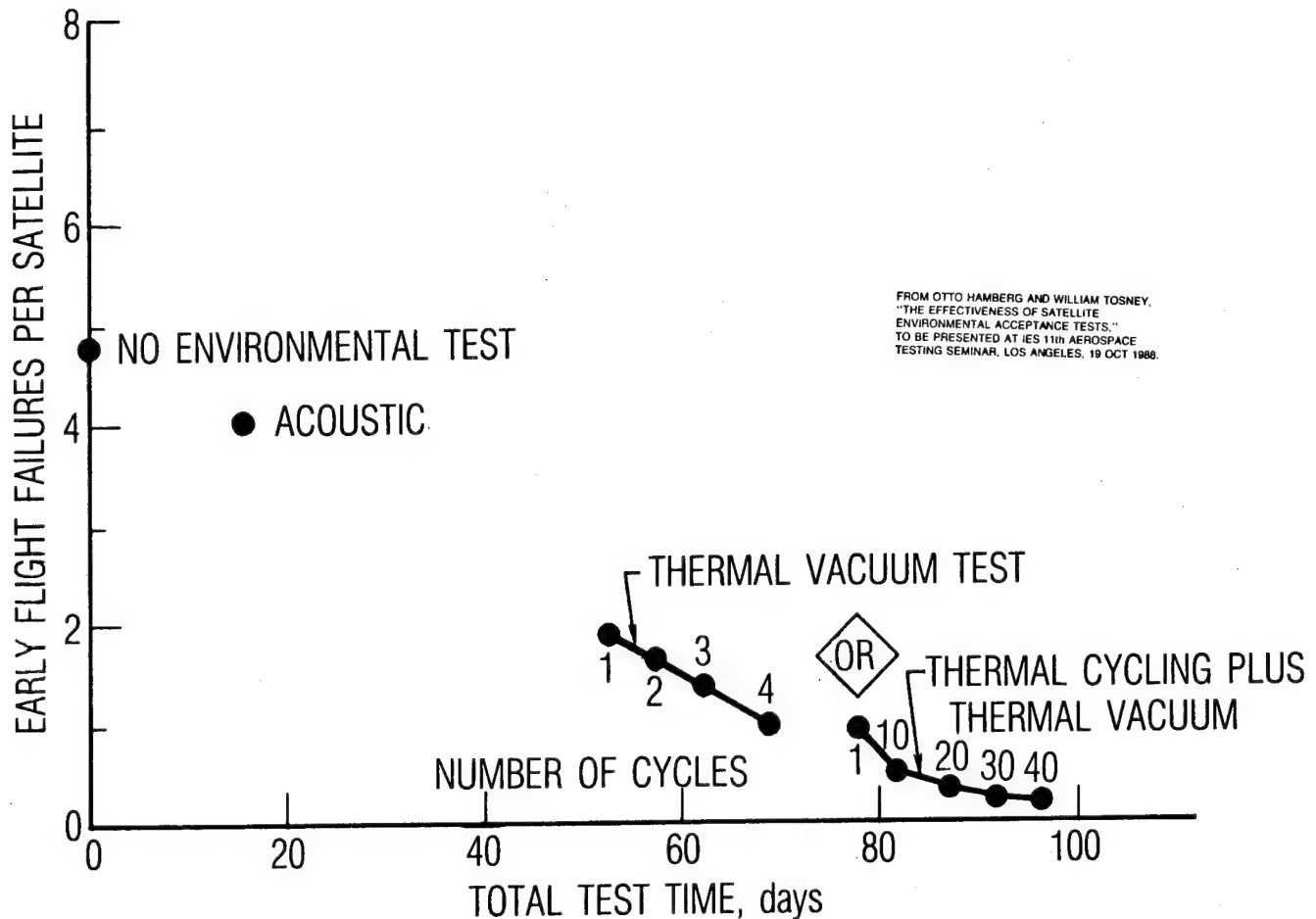
● TEST EFFECTIVENESS

PERCENT

– ACOUSTIC	$= (0.9)(100)/(0.9 + 1.4 + 1.6 + 0.6)$	$= 20$
– THERMAL CYCLING	$= (1.4)(100)/(1.4 + 1.6 + 0.6)$	$= 39$
– THERMAL VACUUM	$= (1.6)(100)/(1.4 + 0.6)$	$= 73$
– COMBINED	$= (0.9 + 1.4 + 1.6)(100)/(0.9 + 1.4 + 1.6 + 0.6)$	$= 87$

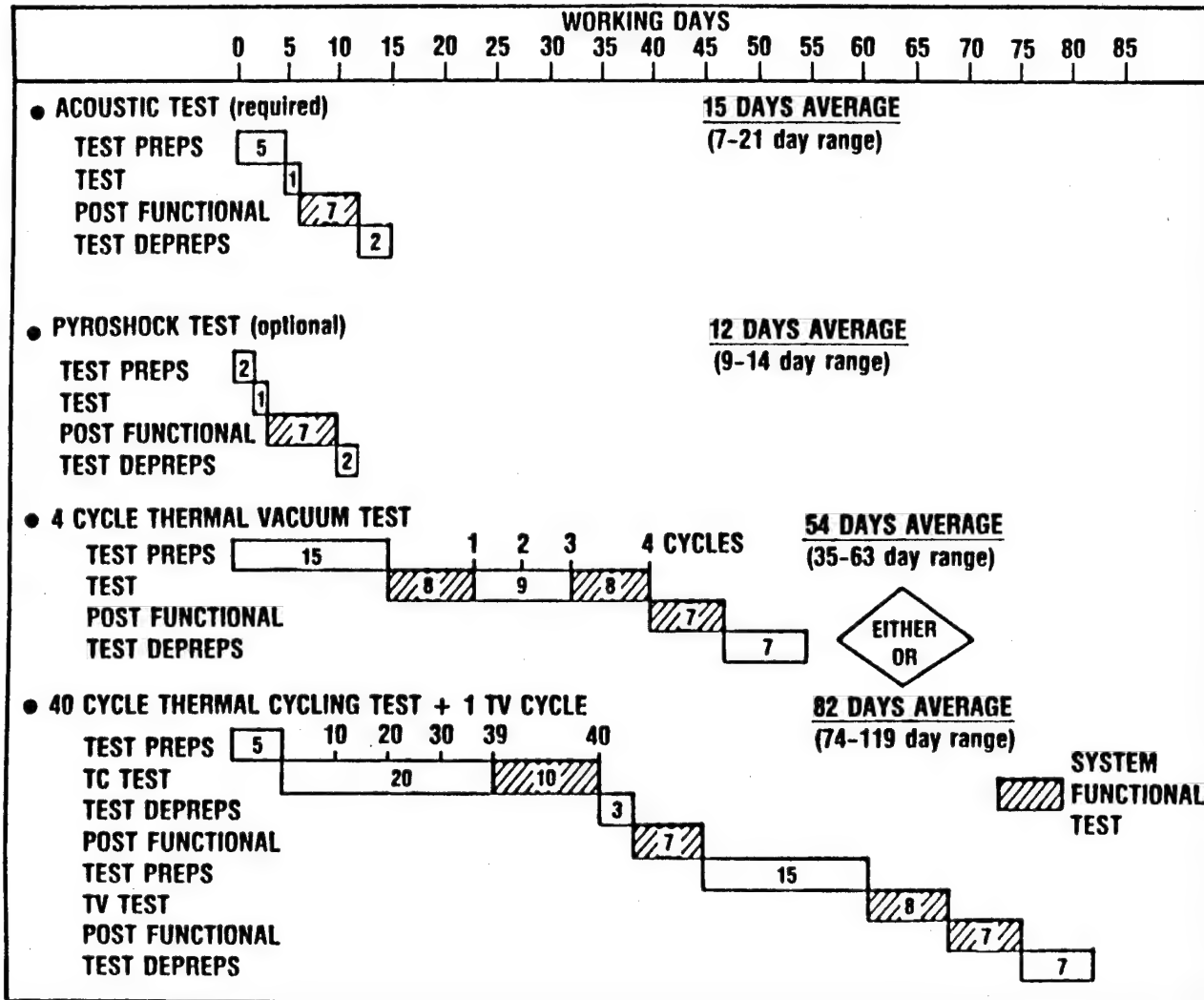
ENVIRONMENTAL TEST VALUE

The data bank (Ref. 8) developed by Laube has been used by Hamberg and Tosney (Ref. 6) to generalize about the effectiveness of space vehicle environmental acceptance tests in eliminating first-45-day mission degrading failures. On the average, in the absence of any environmental tests, 4.5 early failures per satellite are anticipated. The acoustic test while only moderately successful at eliminating early failures (0.63 per satellite) is a relatively short test, 15 days. The four cycle thermal vacuum test or the optional 40 cycle thermal cycling test plus one cycle thermal vacuum test, while markedly more successful at eliminating early failures, are time consuming. As a rule of thumb environmental testing avoids about 0.05 early flight failures per day of test.



Generalized Failure Data

Typical Timelines



REFERENCES

1. Mandel, C. E., "Environmental Stress Screening Guidelines for Assemblies," Institute of Environmental Sciences, September 1984.
2. Burrows, R. W., "Special Long-Life Assurance Studies," Long-Life Assurance Study for Manned Spacecraft Long-Life Hardware, Martin Marietta Report No. MCR-72-169, Vol. IV, September 1972.
3. Bezat, A. G. and L. L. Montague, "The Effect of Endless Burn-in on Reliability Growth Projections," Proceedings 1979 Annual Reliability and Maintainability Symposium.
4. Hecht, Herbert and Myron Hecht, "Reliability Prediction for Spacecraft," RADC-TR-85-229, December 1985.
5. Wong, Kam, "Unified Field (Failure) Theory -- Demise of the Bathtub Curve," 1981 Proceedings Annual Reliability and Maintainability Symposium.
6. Hamberg, Otto and William Tosney, "The Effectiveness of Satellite Environmental Acceptance Tests," IES 11th Aerospace Testing Seminar, Los Angeles, 19 October 1988.
7. Timmins, A. R., and R. E. Heuser, "A Study of First-Day Space Malfunctions," NASA TN D-6474, September 1971.
8. Laube, R. B., "Test Data Bank," The Aerospace Corporation, TOR-0084(4902-06)-1, October 1983.

BIBLIOGRAPHY

Gluck, D. F., "Thermal Testing of Space Vehicle Electronic Components," The Aerospace Corporation, TOR-0084A(5404-10)-2, 31 May 1985.

MIL-HDBK-340 (USAF), Military Handbook, "Application Guidelines for MIL-STD-1540B; Test Requirements for Space Vehicles," 1 July 1985.

Gluck, D. F., "Space Vehicle Thermal Testing: Environments, Related Design and Analysis, Requirements, and Practice," The Aerospace Corporation, TOR-0086A(2902-08)-1, 27 September 1987.

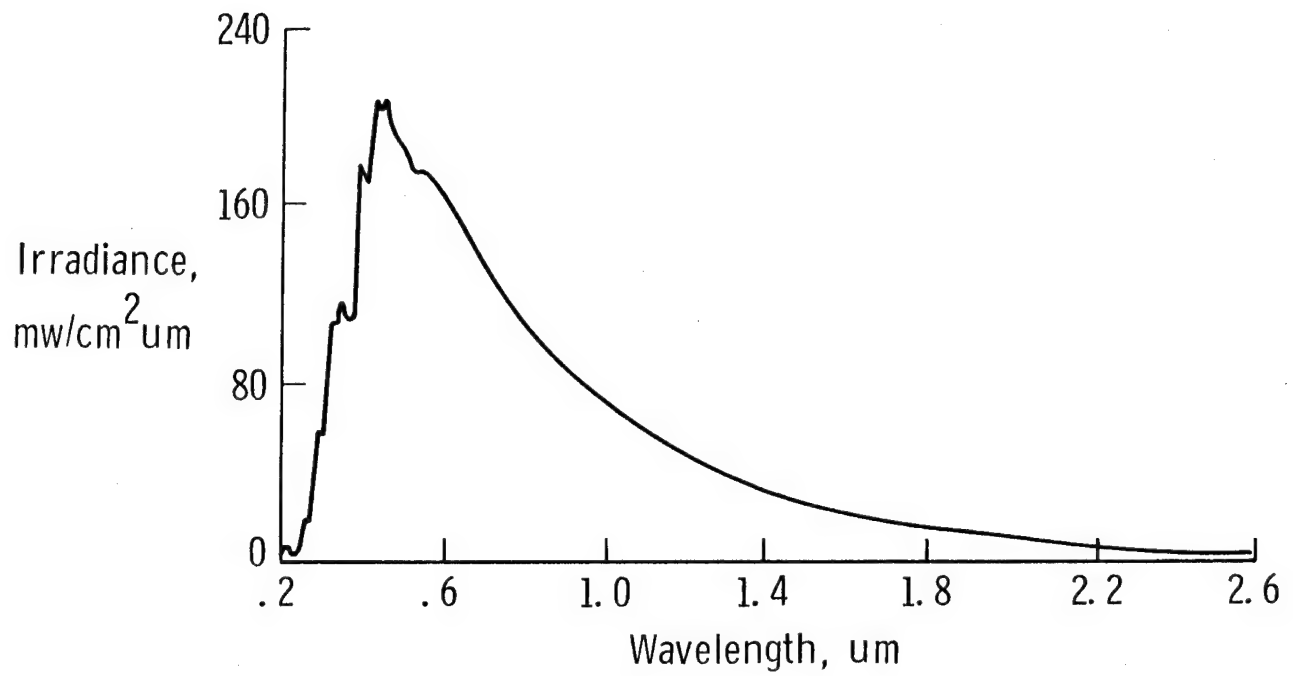
MIL-STD-1540B (USAF), Military Standard, "Test Requirements for Space Vehicles," 10 October 1982.

ULTRAVIOLET RADIATION EFFECTS

Wayne S. Slomp
Materials Division
NASA Langley Research Center
Hampton, Virginia 23665-5225

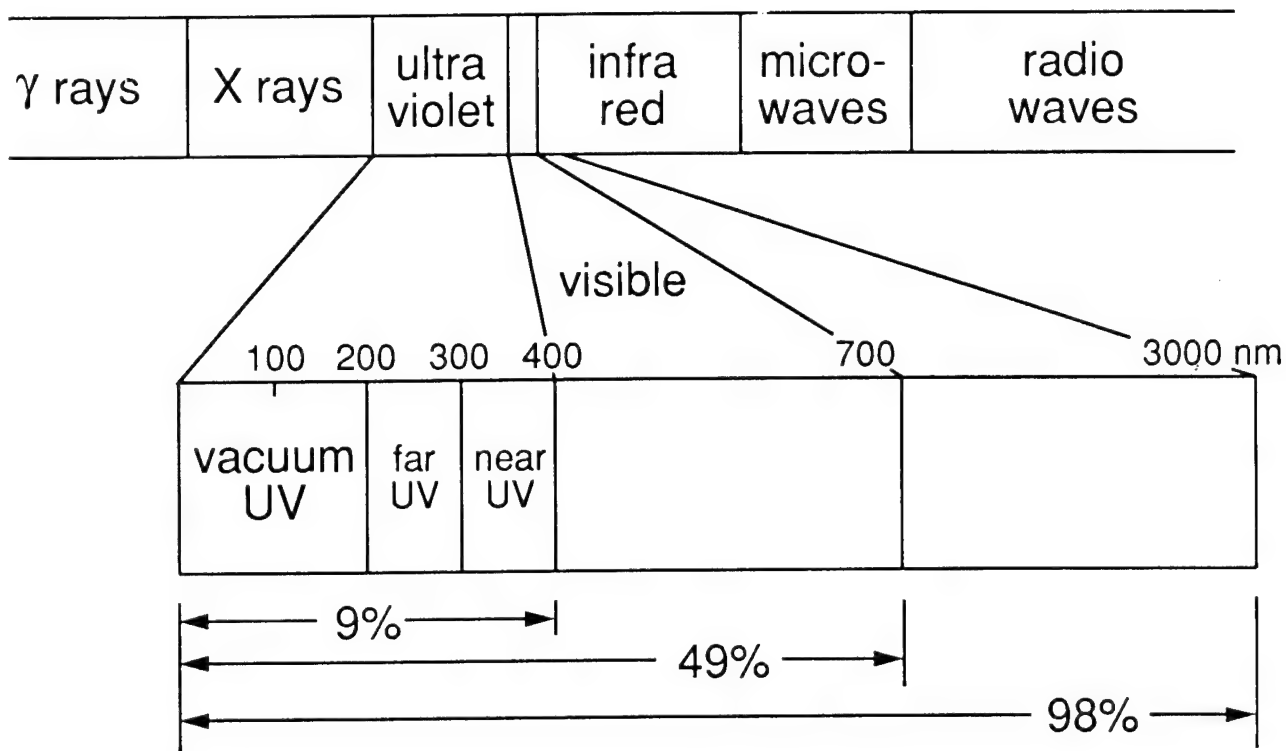
SOLAR SPECTRUM

The irradiance of the solar spectrum for air mass 0 is presented in the figure for the wavelength range of 0.2 micrometers to 2.6 micrometers.



THE ELECTROMAGNETIC SPECTRUM

The electromagnetic spectrum from gamma rays to radio waves is represented in the figure. The ultraviolet, visible, and near-infrared radiation found in the space solar spectrum is only a small part of this electromagnetic spectrum. The UV spectrum is divided into three parts--the vacuum or extreme UV below 200 nm, the far UV from 200 nm to 300 nm, and the near UV from 300 nm to 400 nm. Nine percent of the solar energy is found in the UV.



ULTRAVIOLET ABSORPTION AND PHOTOCHEMICAL EFFECTS

The chemical changes resulting from exposure of a polymer to ultraviolet light are illustrated in the figure. The first law states that only those radiations that are absorbed by a material can produce a chemical change. If a material does not absorb the particular wavelength of UV incident upon the material, then UV cannot cause a chemical change in the material. The second law states that each molecule taking part in a reaction absorbs one quantum ($h\lambda$) of energy. If moles are substituted in the Stark-Einstein law, the Bohr law is obtained. Since this equation is divided by wavelength, the smaller the UV wavelength, the greater the UV energy.

- 1) Only those radiations that are absorbed by a material can produce a chemical change (Grotthuss-Draper)
- 2) Energy absorbed by a reacting molecule is given by $h\lambda$ (Plank's const. x freq. of absorbed light) (Stark and Einstein)
- 3) Change molecules to moles (Bohr Law)

Equation: $E = Nh = N h c / \lambda$

N - Avagadro's No.

$E = 2.86 \times 10^5 / \lambda \text{ k cal/mole}$

C - Velocity of light

λ - Wavelength, angstroms

Examples:

$\lambda = 4000\text{\AA}$ the Einstein is 71 k cal/mole

$\lambda = 2537\text{\AA}$ the Einstein is 113 k cal/mole

TYPICAL VALUES OF BOND ENERGIES

The typical values of bond energies are shown in this table. This illustrates that several chemical bonds can be broken by the 113 k cal/mole energy of the 2537A wavelength of UV radiation. Since the solar radiation in space extends to wavelengths as low as 1000A, most polymer bonds can be broken with UV radiation.

CHEMICAL BOND ENERGY

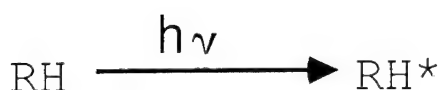
<u>Bond</u>	<u>Bond Energy Term E (K cal./mole, 25°)</u>
C-C	82.6
C=C	145.8
C≡C	199.6
C-N	72.8
C=N	147
C≡N	212.6
C-O	85.5
C=O aldehydes	176
C=O ketones	179
C-S	65
N-N	39
N=N	100
Si-O silicones	106? ^b

^aAll values are deduced from aliphatic compounds and are taken from T.L. Cottrell, "The Strengths of Chemical Bonds," Butterworths Scientific Publications, London, 1958, pp. 270-275.

^b? = doubtful value

ULTRAVIOLET RADIATION EFFECTS

Most organic molecules lie in a singlet ground state (RH). Absorption of a photon raises the molecule to an excited singlet or triplet state (RH*). If the molecule has sufficient energy in the excited state, bond dissociation may take place (R. + H.). This decomposition process must compete with other deexcitation processes. The excited molecule may revert to the ground state by emission of heat or energy (hν) in the form of fluorescence or phosphorescence. The later processes allow the excited molecule to return to the ground state without producing a chemical change. Revision to the ground state may also occur by the transfer of electronic energy from one group to another group in the vicinity of the excited molecule. An example of this occurs in polymethylphenylsiloxane where the phenyl group absorbs the UV energy then transfers this to the methyl group where degradation occurs.

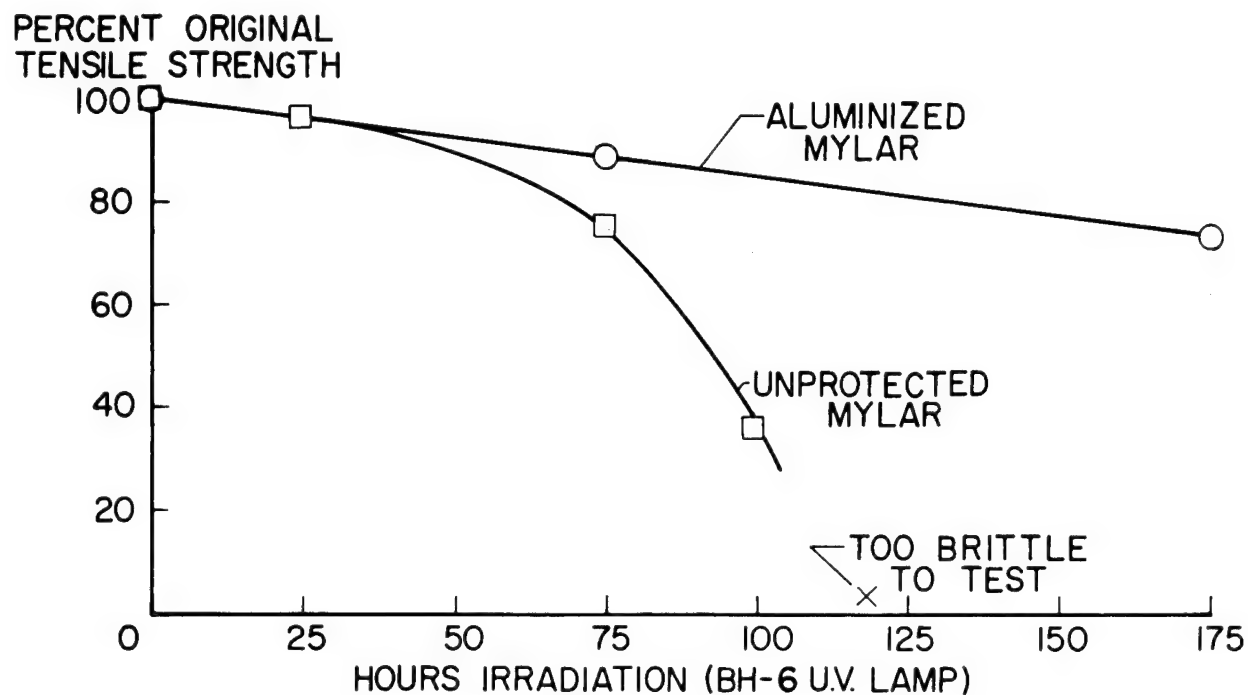


OTHER POSSIBLE REACTIONS



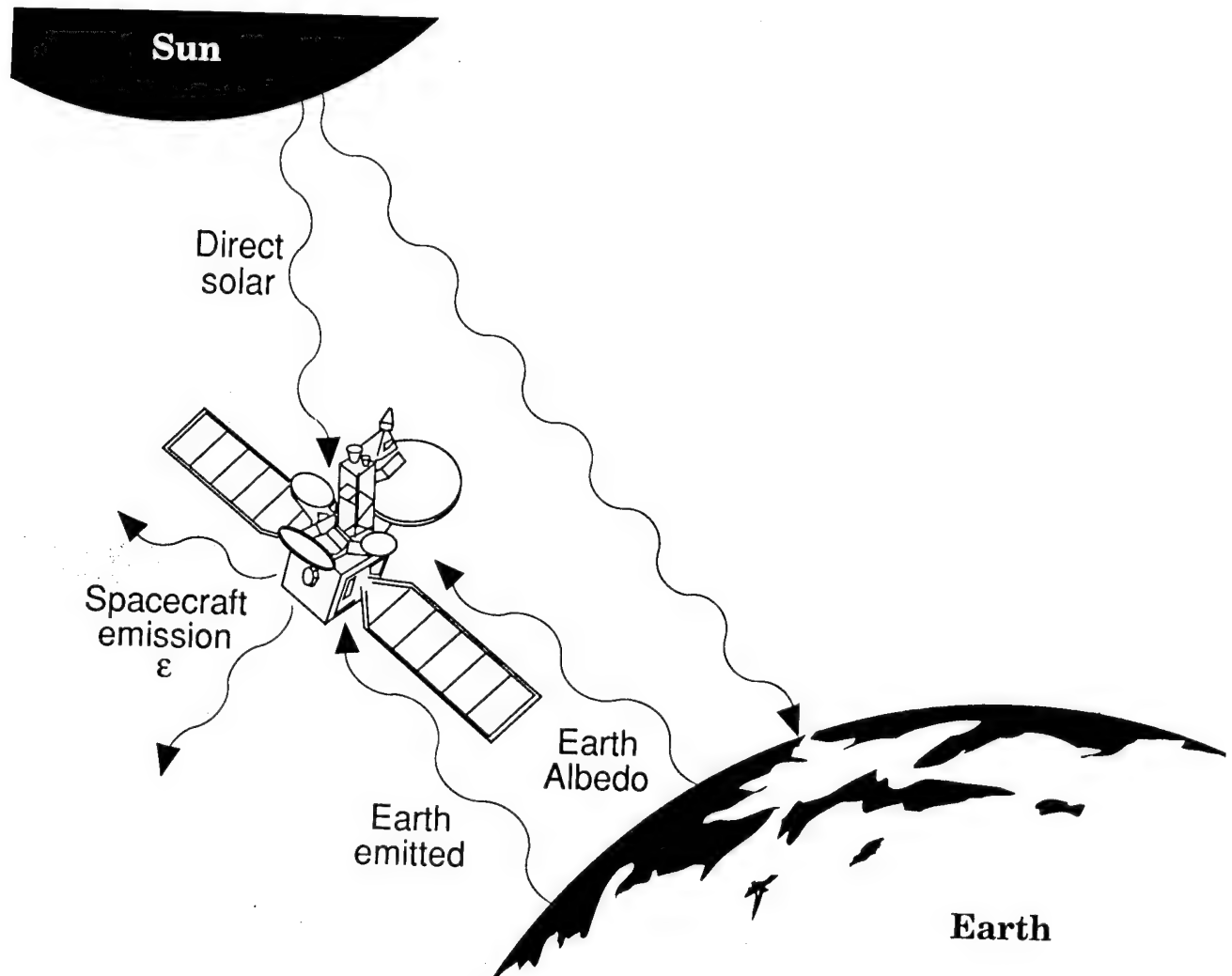
EFFECT OF ULTRAVIOLET RADIATION ON THE TENSILE STRENGTH OF MYLAR

This figure illustrates that UV radiation can degrade the mechanical properties of polymeric materials although the major research emphasis has been on changes in optical properties of polymer films.



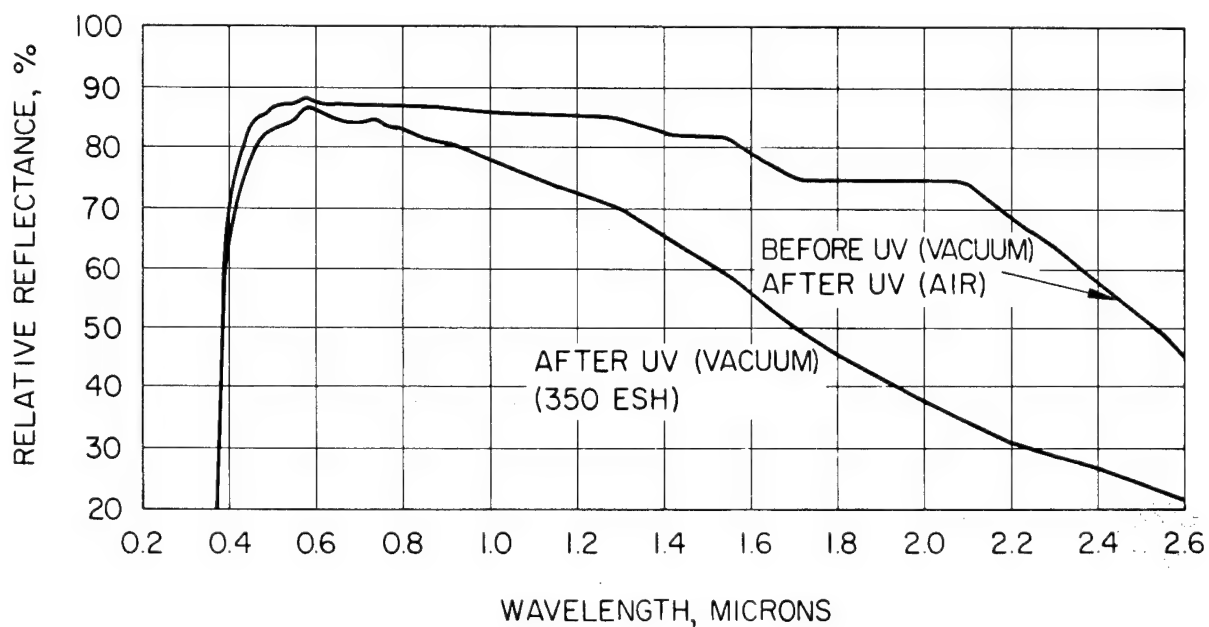
LEO SPACECRAFT THERMAL CONTROL ENVIRONMENT

The thermal control environment for a low Earth orbital satellite consists of the direct solar radiation, the Earth albedo (sunlight reflected from clouds, terrain, and water), and the emitted radiation from the Earth. The absorptance of the spacecraft with its view factor to each of these heat sources is balanced against the emission of heat from the spacecraft.



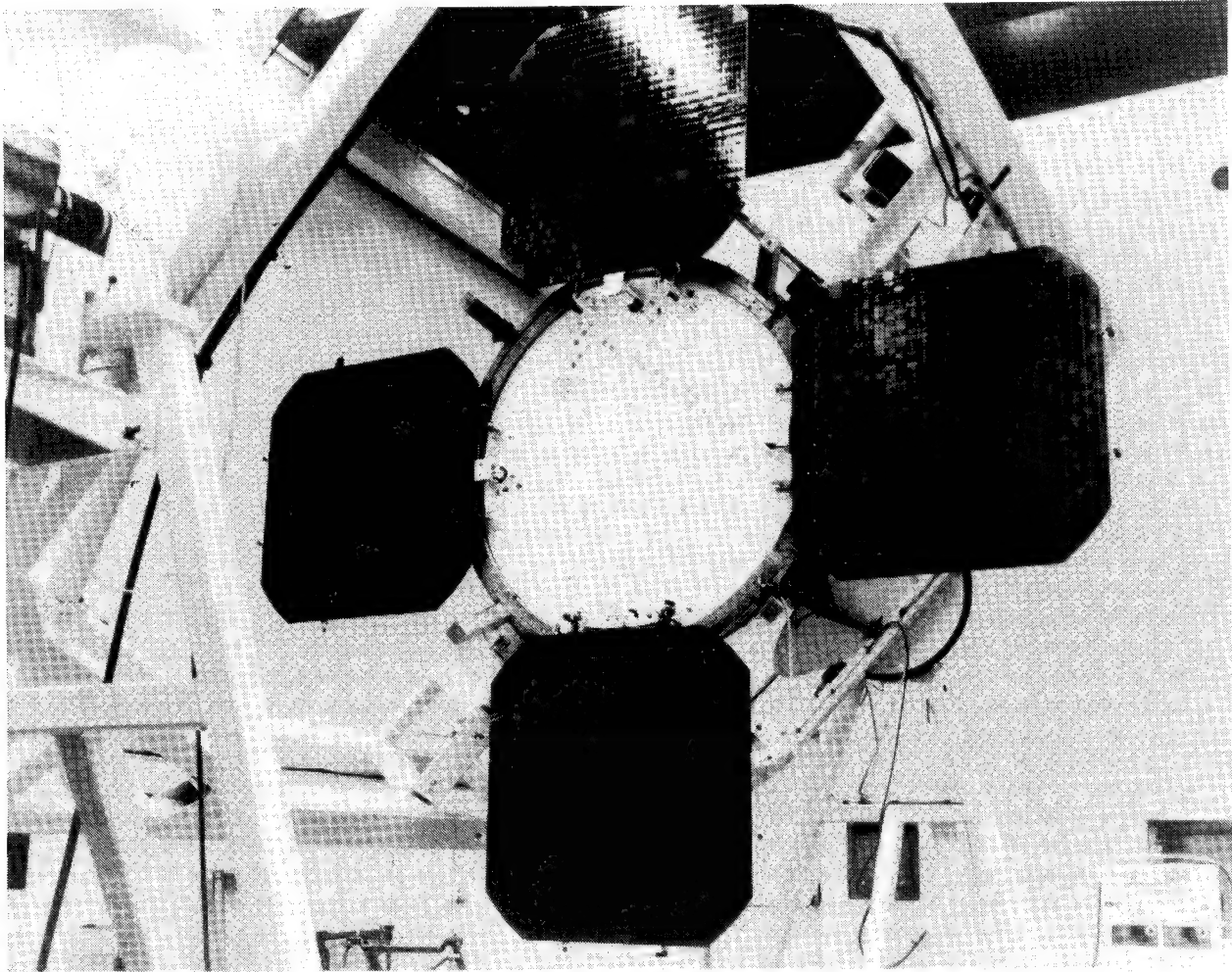
STRUCTURAL REFLECTANCE OF ZINC OXIDE-SILICONE

This figure illustrates the change in spectral reflectance due to UV exposure in vacuum for a zinc-oxide, pigmented silicone paint S-13. The figure also illustrates that upon introduction of air (oxygen) into the vacuum system, bleaching occurs which eliminates the UV degradation to this coating. This bleaching of white paints has led to the need for in situ testing of spacecraft coatings.



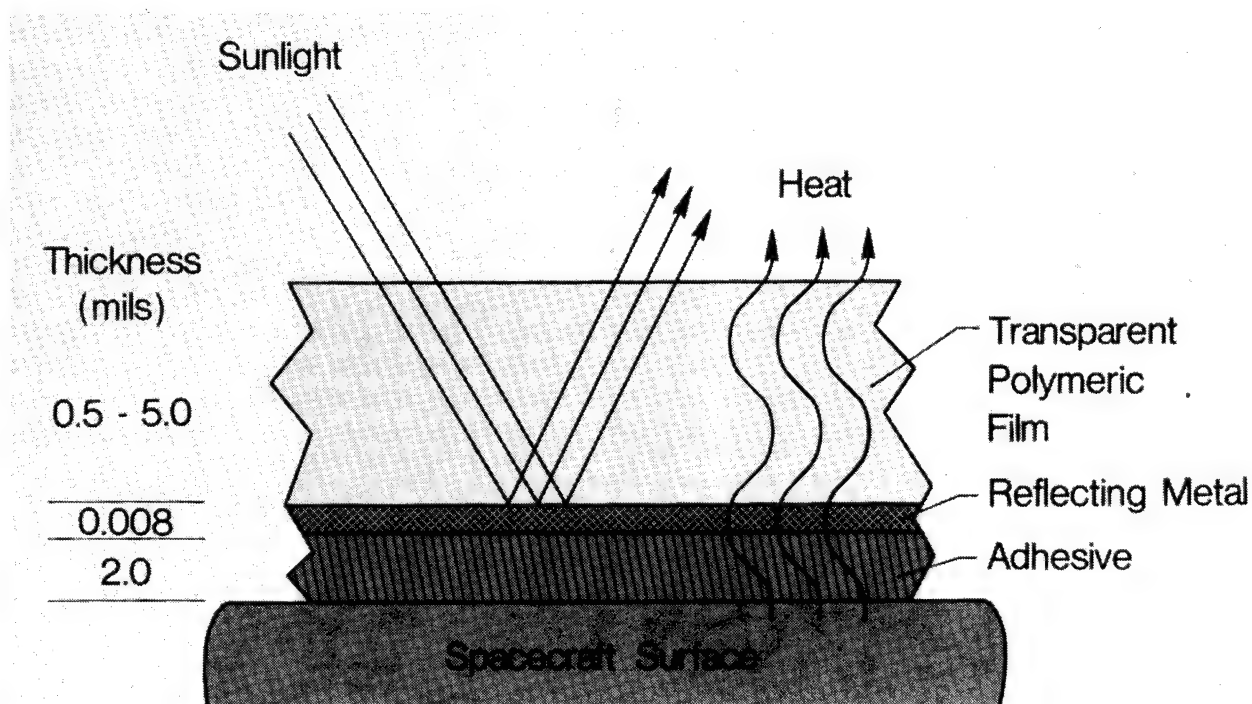
LUNAR ORBITER IV

The radiator on the Lunar Orbiter spacecraft was coated with the S-13 paint before in situ testing was found to be required. Lunar Orbiters I and II experienced very dramatic temperature increases due to UV and solar wind plasma degradation of the coating. To offset the increase in solar absorptance of the white paint, about 20 percent of the radiator area on Lunar Orbiters IV and V were coated with quartz optical solar reflectors.



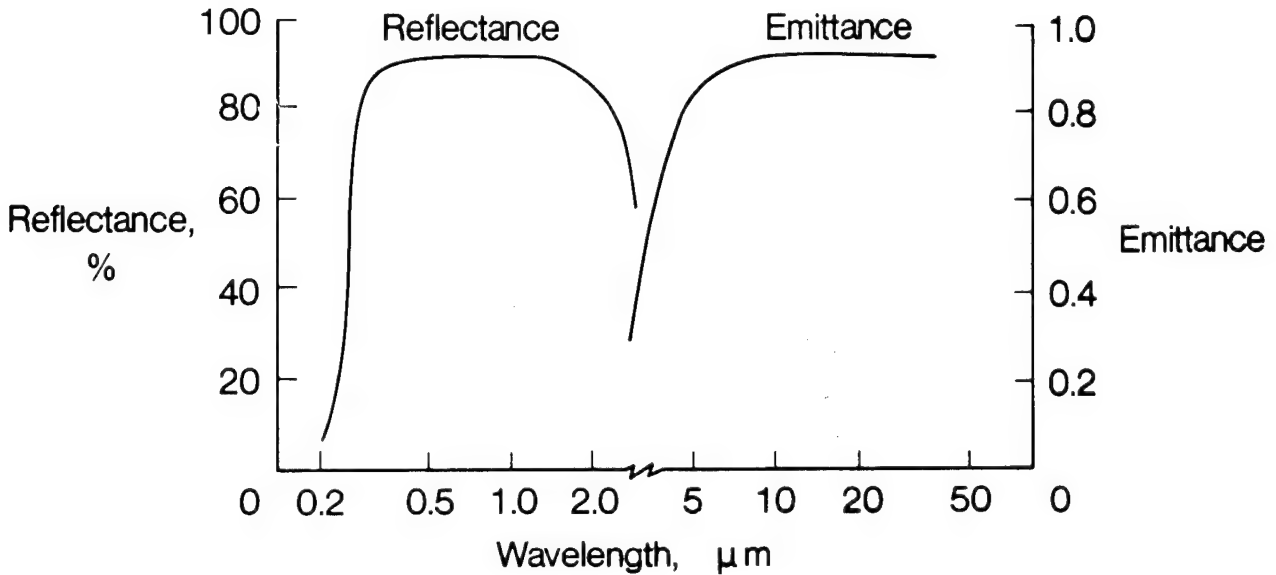
FLEXIBLE SECOND-SURFACE MIRROR (SSM) THERMAL CONTROL COATING

This figure is a schematic of a flexible second-surface mirror coating. The coating consists of a polymeric film that is transparent in the solar wavelength region and is coated on the back side with a reflecting, opaque metal like aluminum or silver. An adhesive is placed behind the metal to hold the coating to the spacecraft. Typically, the larger the thickness of the polymeric film, the stronger the absorption bands are in the infrared, out of the solar wavelength region, and therefore, the higher the emittance of the coating. An example of an SSM coating is silvered - perfluorinated ethylene propylene copolymer (FEP) Teflon.



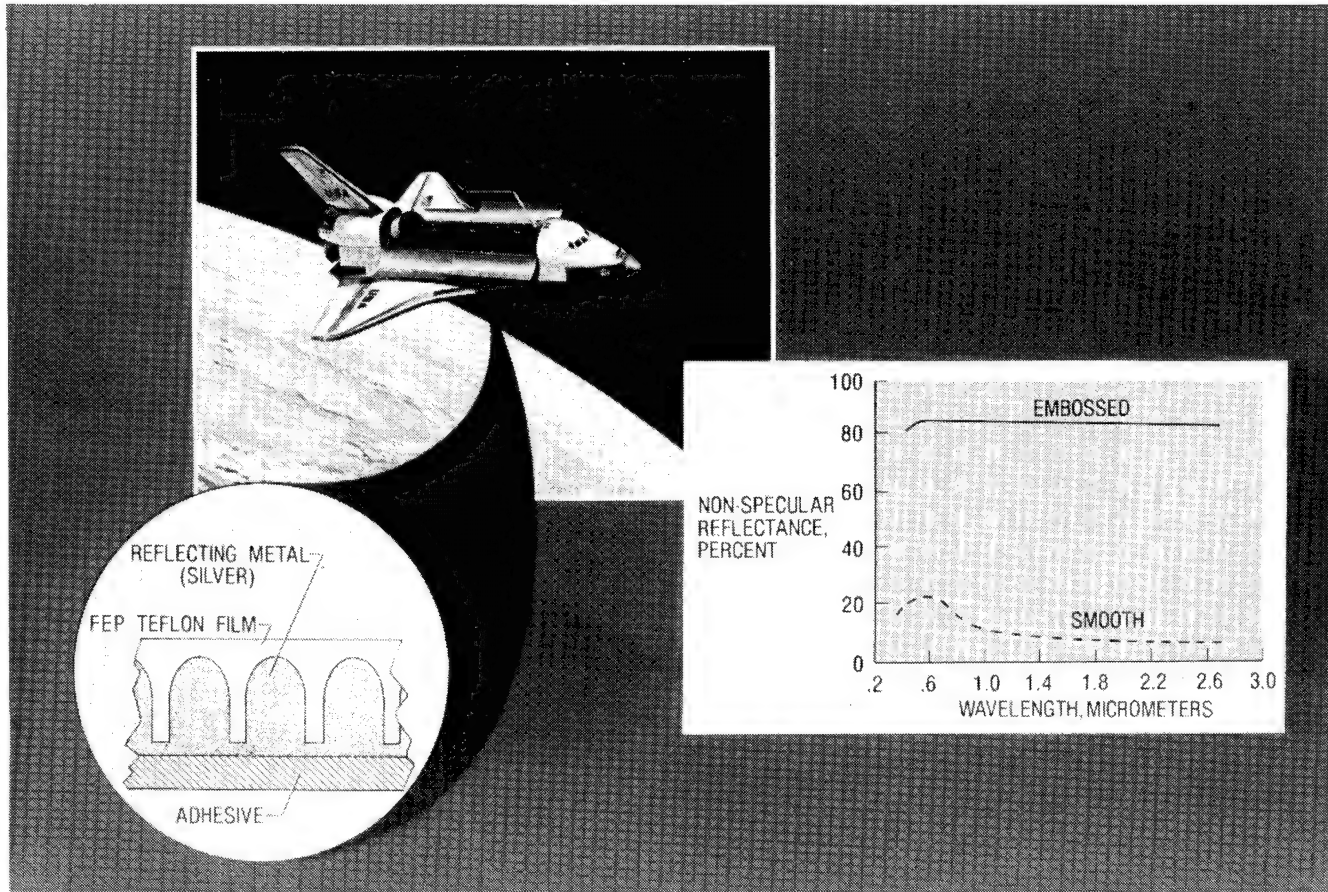
CHARACTERISTICS OF THERMAL CONTROL COATINGS

The figure helps to explain the radiation characteristics of the SSM coating in the previous figure. The reflectance of this coating and the transparency of the polymeric film must occur from 0.2 to 3.0 micrometers, the region of maximum solar energy. But the coating is radiating heat away from a spacecraft which has a maximum temperature of about 100°C; therefore, this energy is found in the infrared from 10 to 50 micrometers. The characteristic absorption bands of polymers provide this infrared emittance.



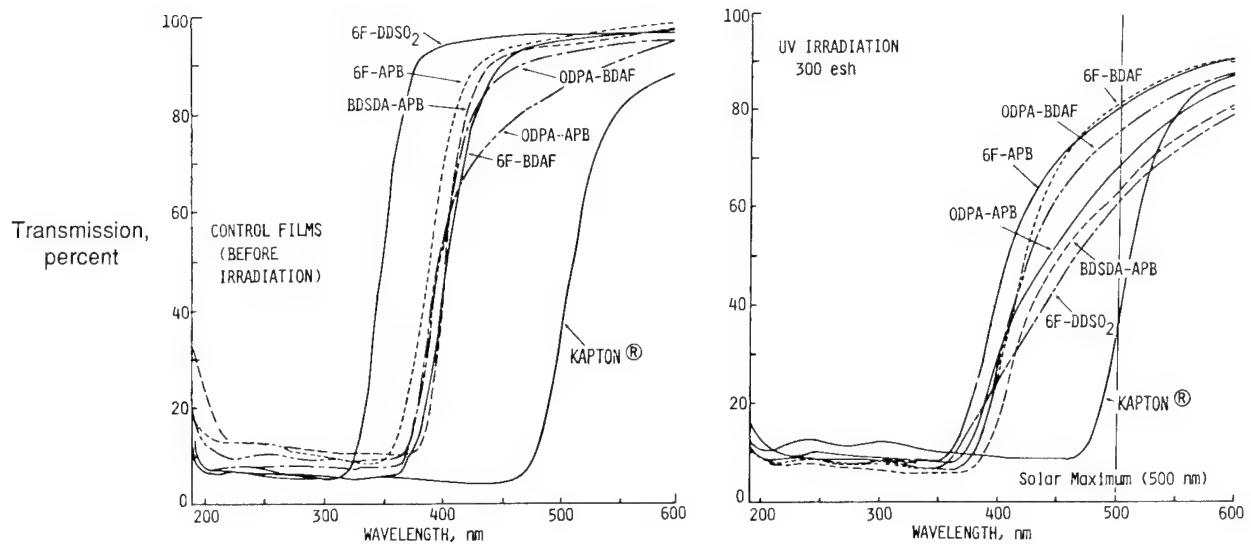
NON-SPECULAR SILVERED TEFLON

The non-specular reflecting silvered Teflon SSM coating used on the Orbiter's radiators was developed at NASA Langley. The FEP Teflon is embossed with a special roller to provide light scattering on the metal coating side leaving the outside smooth to prevent trapping contamination in the Teflon surface. The process reduces the specular reflectance to about 15 percent but maintains the 0.09 solar absorptance of the smooth silvered Teflon SSM.



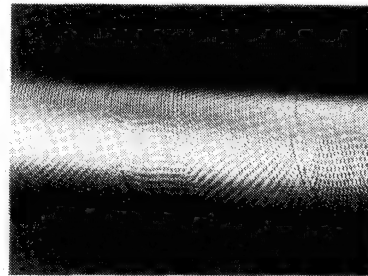
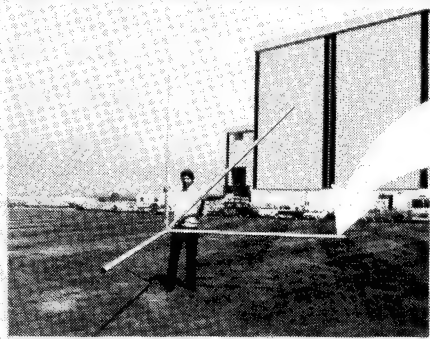
EFFECT OF UV RADIATION ON TRANSMISSION OF TRANSPARENT POLYIMIDE FILMS

This figure illustrates some current studies being conducted at NASA Langley on highly transparent polyimide films. These films are stable to about 300°C and are soluble in the imide form, which means they are sprayable. Some of these experimental films have exhibited high stability to simulated solar UV and high energy electron radiation.



ALUMINUM FOIL COATING FOR COMPOSITE TUBES

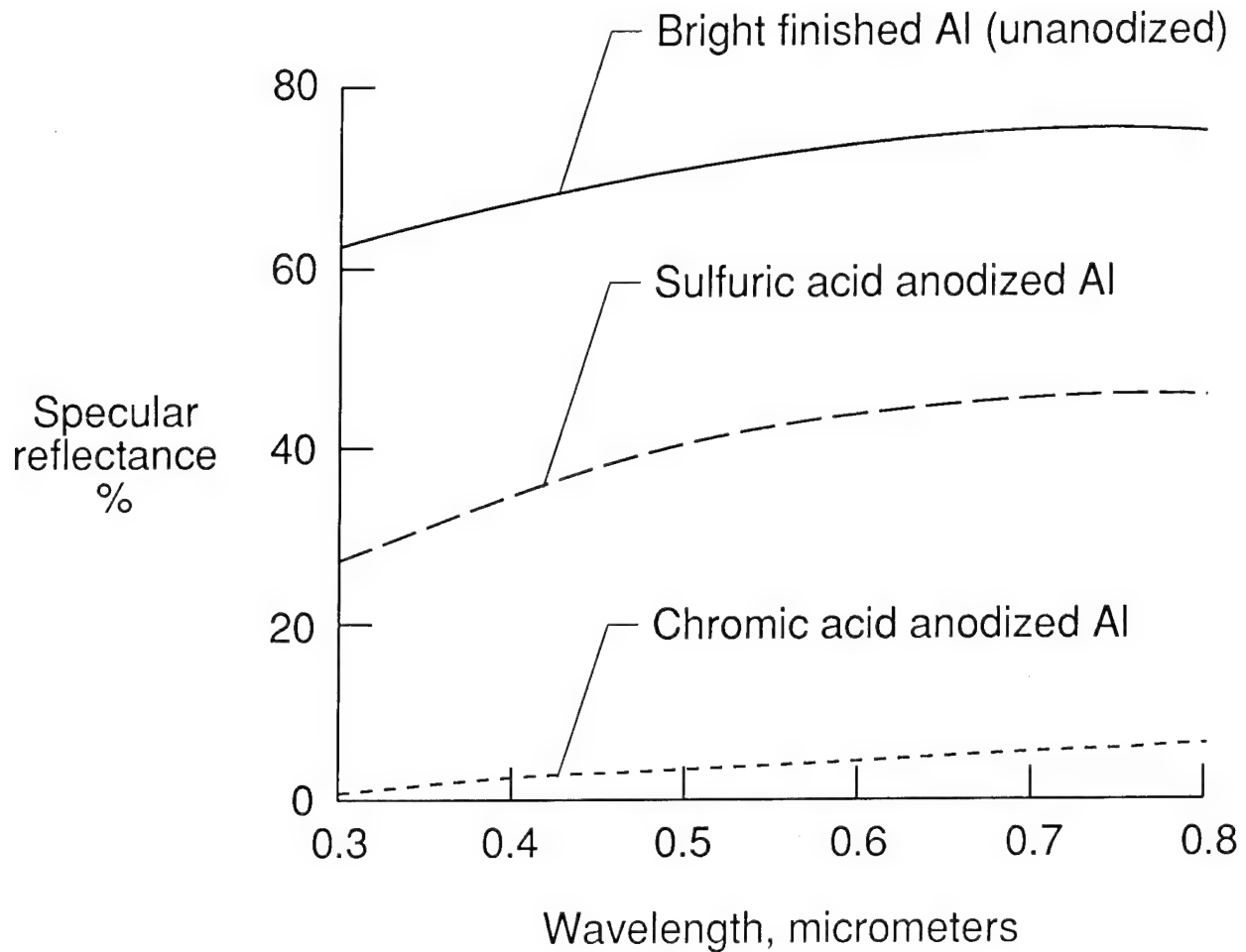
A concept for thermal control and atomic oxygen protection for the composite tubes used as structural elements in the Space Station Freedom has been developed at NASA Langley and demonstrated under contract with Boeing Aerospace Company. Aluminum foil 0.008 cm thick is anodized or sputter coated with SiO_x to achieve the desired radiation properties of 0.3 solar absorptance and 0.65 emittance. This aluminum foil is then adhesively bonded to the exterior of the graphite/epoxy tube. Process specifications have been developed for achieving the radiation properties with chromic acid anodizing.



- Can be anodized or sputter coated to achieve desired optical properties
- Application techniques can provide a non-specular reflecting coating
- Provides atomic oxygen protection for composite tubes
- Resistant to abrasion and UV degradation
- Demonstrated on 2 inch dia. X 8 feet long P75/934 graphite/epoxy composite tubes

SPECULAR REFLECTANCE OF CHEMICALLY TREATED ALUMINUM

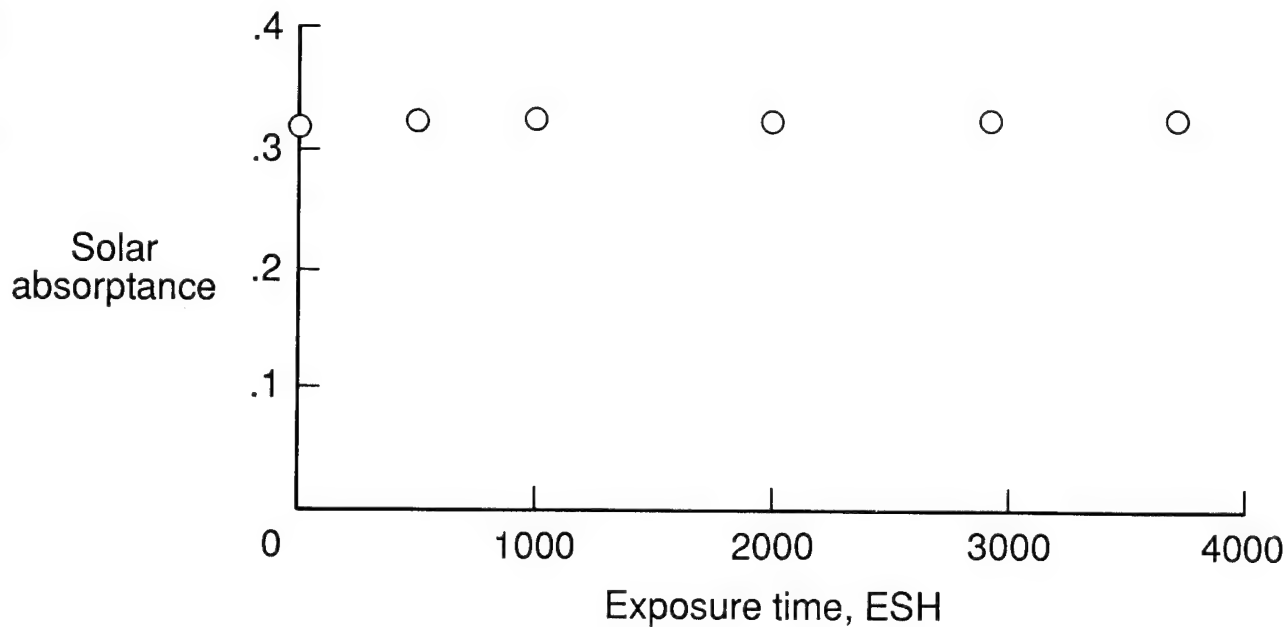
It is highly desirable to have a low solar absorptance coating on the composite structural members which would not be a specular reflector. With the large number of structural members in the Space Station Freedom, sunlight reflected from these members can interfere with optical experiments on the Freedom. This figure shows that the chromic acid anodizing process provides less than 5 percent specular reflectance at 0.5 micrometers, the peak solar wavelength, where the sulfuric acid process has nearly 40 percent specular reflectance.



EFFECTS OF UV ON SOLAR ABSORPTANCE OF
SEALED CHROMIC-ACID ANODIZED 1145 AL 3 MIL FOIL

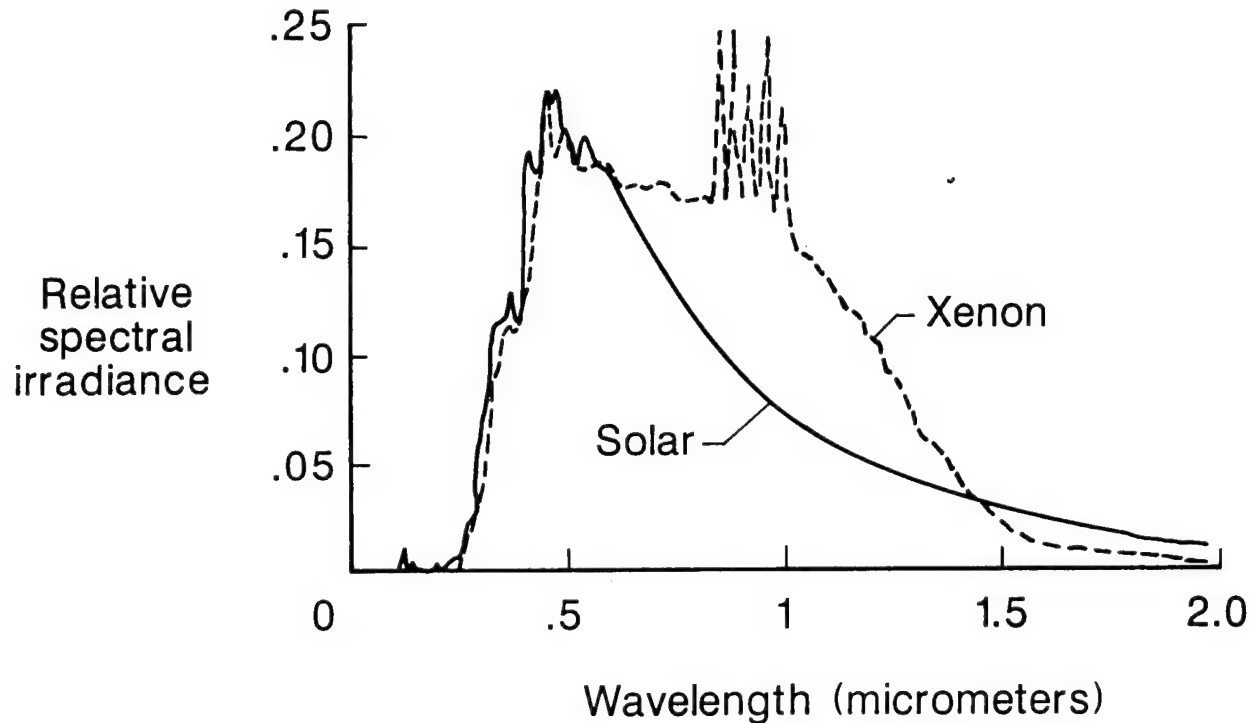
The chromic acid anodized aluminum foil used to coat the composite tubes for the Space Station Freedom has been exposed to simulated solar ultraviolet radiation at NASA Langley. These results show that the coating is very stable to UV radiation having only a 0.02 increase in solar absorptance in 4,000 equivalent solar hours (2,000 hours x 2 solar constants).

2x ESH, air mass zero



SOLAR IRRADIANCE SIMULATION WITH XENON

This figure compares the spectral irradiance of a xenon short-arc lamp with a quartz envelope to the solar irradiance at air mass zero. The figure clearly shows that xenon has a good UV solar match from approximately 0.2 to 0.7 micrometers but is much more intense in the infrared region. This IR radiation leads to over heating of test specimens when accelerated exposure is attempted. Experimental results indicate that acceleration factors of only 3X are possible without substantially overheating the test specimens.



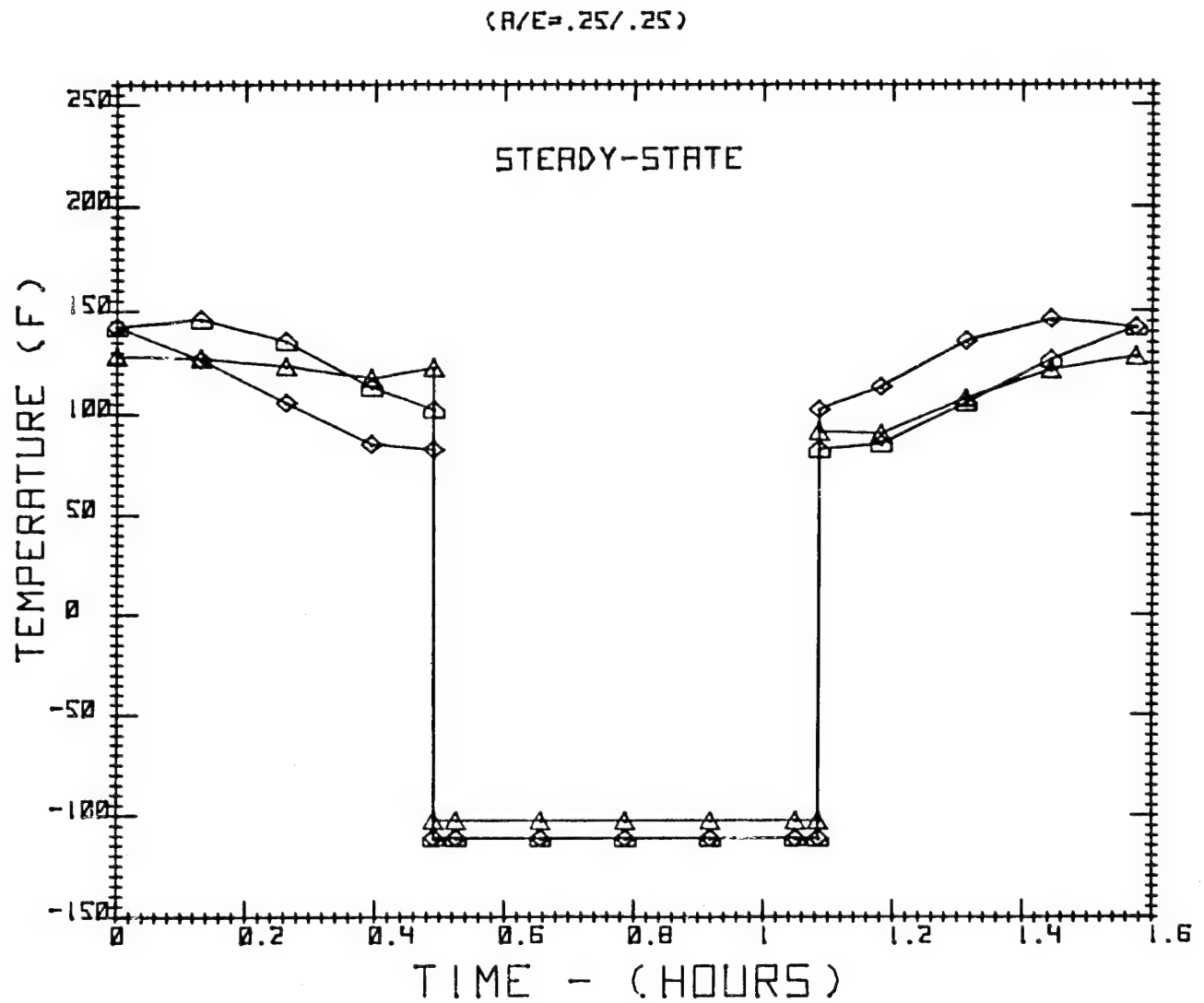
PROBLEMS ASSOCIATED WITH SOLAR SIMULATION

When most investigators expose materials to simulated solar UV, the irradiance of the UV beam is measured and referred to as a percentage of the solar irradiance at air mass 0. Since many spacecraft rotate, then this must be taken into account in calculating one solar constant. Also the shape factor for the spacecraft surface and the orbital parameters must be considered. Many spacecraft will have only 25 percent of their time in orbit in the sun. This would be a 4 to 1 acceleration factor even if the laboratory exposures were conducted at one solar constant.

- **One solar constant assumes nonrotating spacecraft in constant sunlight, but most rotate**
- **Shape factor of 1 where, in reality, shape factor is near 0.5**
- **Near Earth orbit is approximately 90 min. with about 30 min. in solar occult**
- **Reality is 25% to 40% of time in sunlight for spacecraft surfaces**

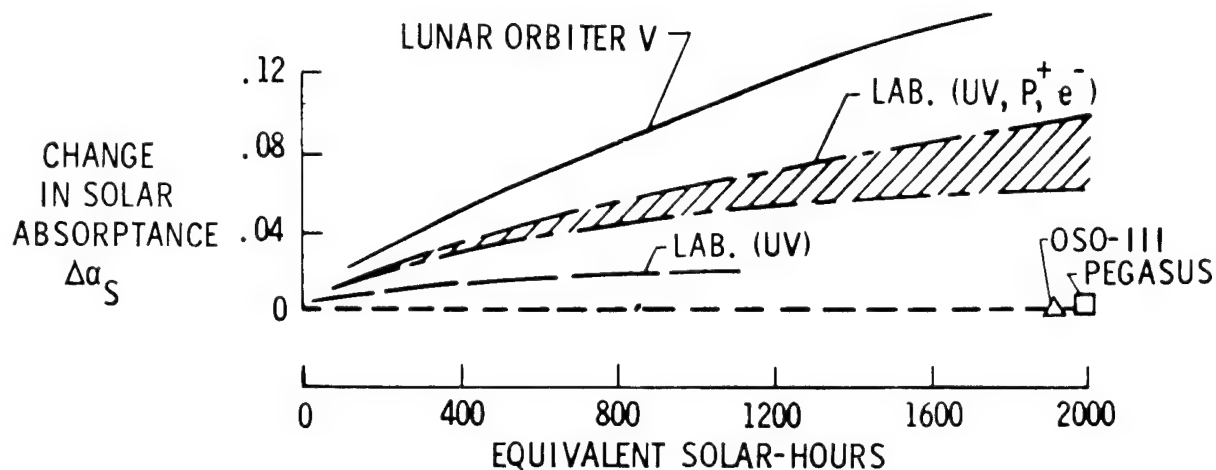
TRUSS TUBE TEMPERATURES

This is a steady state calculation for a composite tube with an α/ϵ of .25/.25 in the proposed Space Station Freedom orbit. This projects the thermal cycle range and shows the typical occurt for these conditions.



COMPARISON OF FLIGHT AND LABORATORY DATA ON ZINC OXIDE-POTASSIUM SILICATE COATING Z-93

This figure was prepared a number of years ago from flight and laboratory data conducted using short arc xenon UV source and a 3 kev solar wind proton source with thermal electrons for charge neutralization. The combined UV and solar wind plasma experienced on Lunar Orbiter V was under simulated in the laboratory. The UV degradation experience by OSD-III and Pegasus was over simulated in the laboratory test. No changes in procedures or equipment which have been made since these tests were conducted would alter these results.



SUMMARY

Solar ultraviolet testing has not been developed which will provide highly accelerated (20 to 50X) exposures that correlate to flight test data. Additional studies are required to develop an exposure methodology which will assure that accelerated testing can be used for qualification of materials and coatings for long-duration space flight.

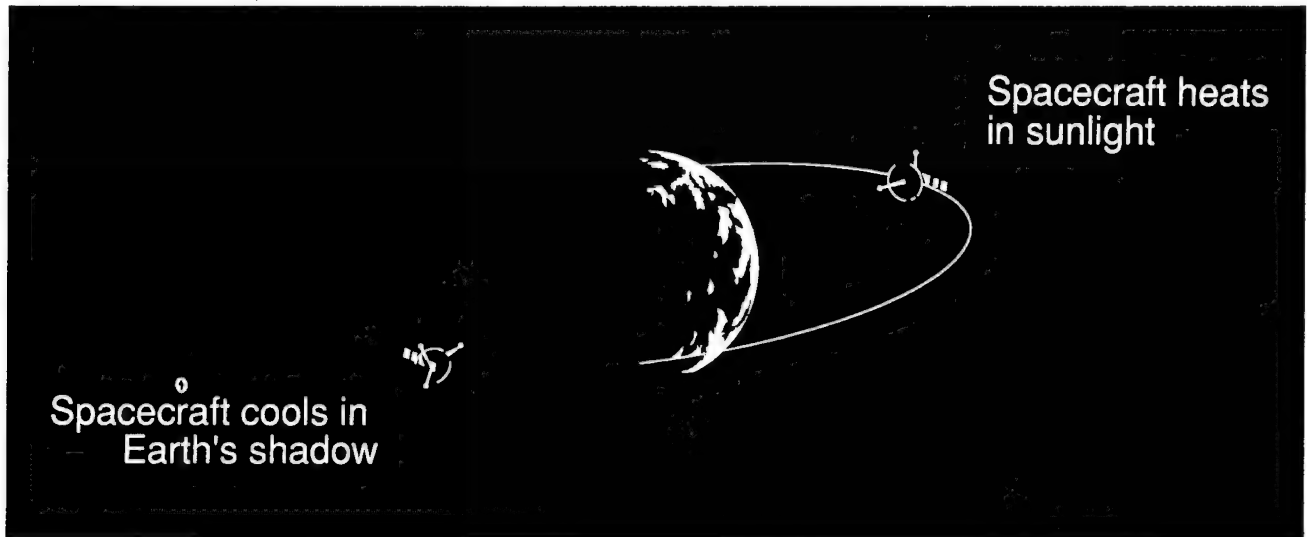
- **Solar UV radiation is present in all orbital environments**
- **Solar UV does not change in flux with orbital altitude**
- **UV radiation can degrade most coatings and polymeric films**
- **Laboratory UV simulation methodology is needed for accelerated testing to 20 UV solar constants**
- **Simulation of extreme UV (below 200 nm) is needed to evaluate requirements for EUV in solar simulation**

EFFECTS OF THERMAL CYCLING ON COMPOSITE MATERIALS FOR
SPACE STRUCTURES

Stephen S. Tompkins
Materials Division
NASA Langley Research Center
Hampton, Virginia 23665-5225

THERMAL CYCLING OF COMPOSITE MATERIALS IN ORBIT

Thermal cycling, which can result from the spacecraft orbiting the Earth, is one of several space service environmental parameters that can affect composite structural materials, ref. 1. As the spacecraft passes in and out of the Earth's shadow, the temperature of the structure rises and falls. The minimum and maximum temperatures reached and the induced effects on the material are directly related to the properties of the material and the thermal control coating. The materials may also experience thermal cycling as a result of structural members casting shadows on other parts of the structure.



OBJECTIVE

The objective of this paper is to briefly describe the effects of thermal cycling on the thermal and mechanical properties of composite materials that are candidates for space structures. The outline for this paper is shown below. The results from a thermal analysis of the orbiting Space Station Freedom will be used to define a typical thermal environment and the parameters that cause changes in the thermal history. The interactions of this environment with composite materials will be shown and described. The effects of this interaction on the integrity as well as the properties of Gr/thermoset, Gr/thermoplastic, Gr/metal and Gr/glass composite materials are discussed. Emphasis will be placed on the effects of the interaction that are critical to precision spacecraft. Finally, ground test methodology will be briefly discussed.

EFFECTS OF THERMAL CYCLING ON COMPOSITE MATERIALS FOR SPACE STRUCTURES

OUTLINE

- Thermal environment
- Material/environment interaction
- Effects on materials:
 - Gr/thermoset
 - Gr/thermoplastic
 - Metal - matrices
 - Glass - matrices
- Ground test methodology

SPACE STATION FREEDOM TRUSS STRUCTURE THERMAL ANALYSIS

The expected thermal history of the Space Station Freedom truss structure will be used to illustrate a typical thermal input to a spacecraft. The temperature history of a single 2-inch diameter, P75 graphite/epoxy tube orbiting the earth at 270 nautical miles was analyzed with the TRASYS orbital mechanics model and the SINDA thermal analyzer assuming no shadowing by other structural members. The tube temperature history is shown below.

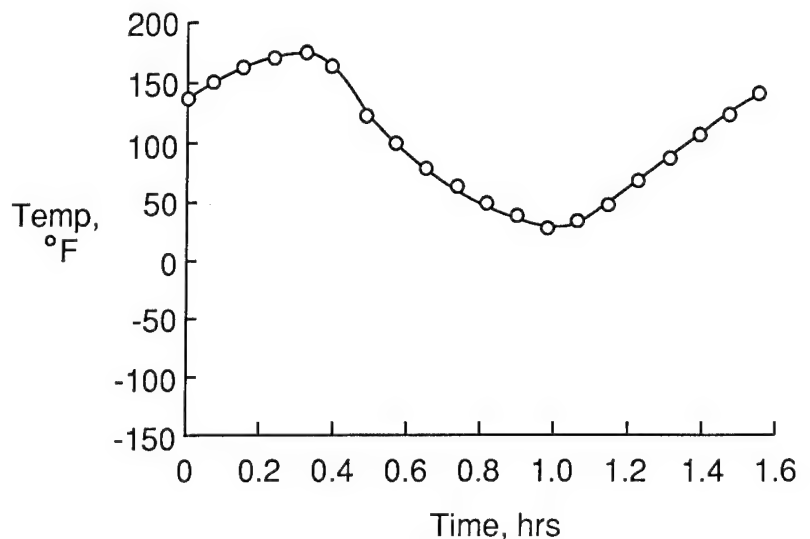
For a tube with a solar absorptance-to-emittance ratio, α_s/ϵ , of 0.3/0.2, the temperature varies between about 175°F to about 25°F over a period of about 90 minutes. The period of the thermal cycle depends upon the altitude of the orbit and the amplitude of the cycle depends upon the α_s/ϵ ratio.

Thermal analysis

- Single tube (9 ft long, 2 in. ID)
- P75 graphite/epoxy
- Orbital parameters
 - Beta = 0 deg.
 - Altitude = 270 N. miles
- TRASYS and SINDA models

Typical tube temperature cycling range

Solar absorptance/emittance = .3/.2

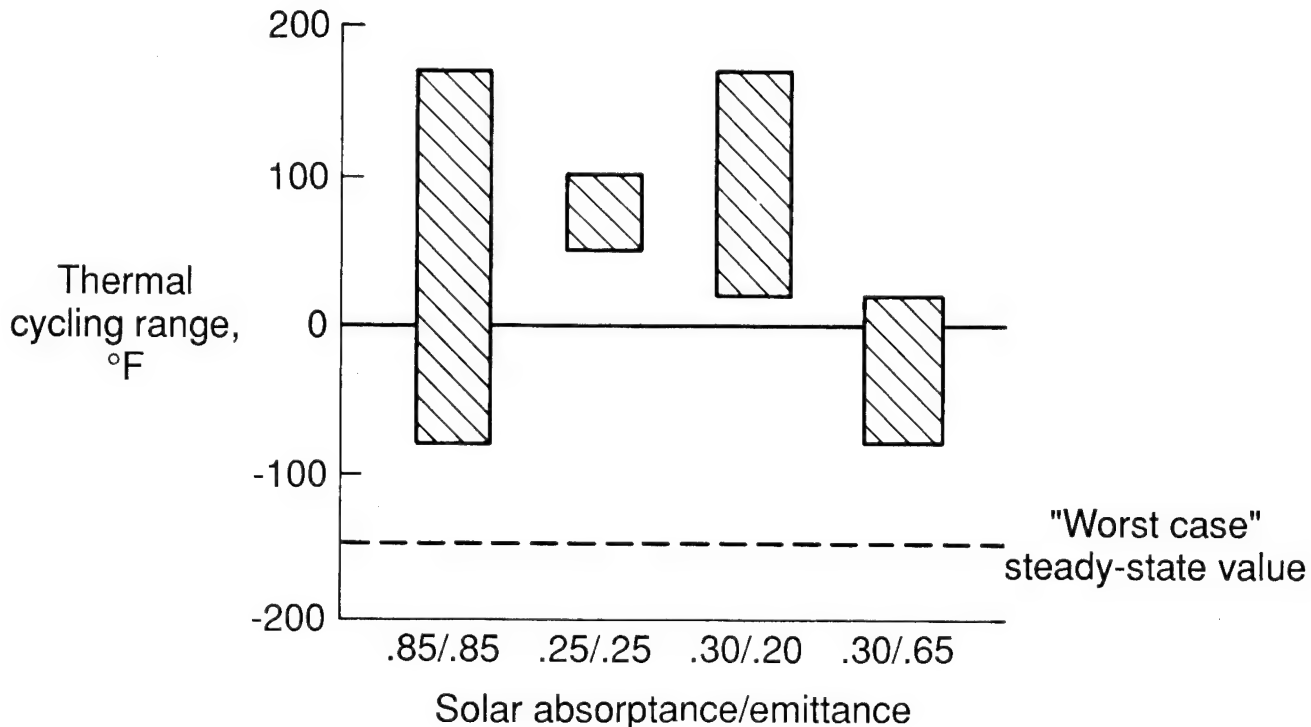


EFFECTS OF SOLAR ABSORPTANCE/EMITTANCE ON TEMPERATURE RANGE

The effects of material surface solar absorptance/emittance ratio, α_s/ϵ on the amplitude of the thermal cycle is shown in the figure below. These results are from a transient analysis of a 2-inch diameter, P75S Gr/Ep composite tube orbiting the Earth. The data shows that the temperature range is very sensitive to α_s/ϵ . For a bare Gr/Ep tube, $\alpha_s/\epsilon = 0.85/0.85$, the temperature range is from about 175°F to about -80°F. The ideal range would be small and centered around room temperature. However, degradation of the thermal control coating could change the α_s/ϵ ratio and significantly change the range. For example, degradation from 0.25/0.25 to 0.30/0.20, causes the temperature range to change from 50°F to 100°F to about 20°F to 175°F. For Space Station Freedom the steady-state cold temperature is estimated to be -150°F; however, some spacecraft could reach as low as -250°F.

SPACE STATION TRUSS STRUCTURE THERMAL CYCLING RANGE

Single 2 in. i.d., P75 Gr/Ep tube



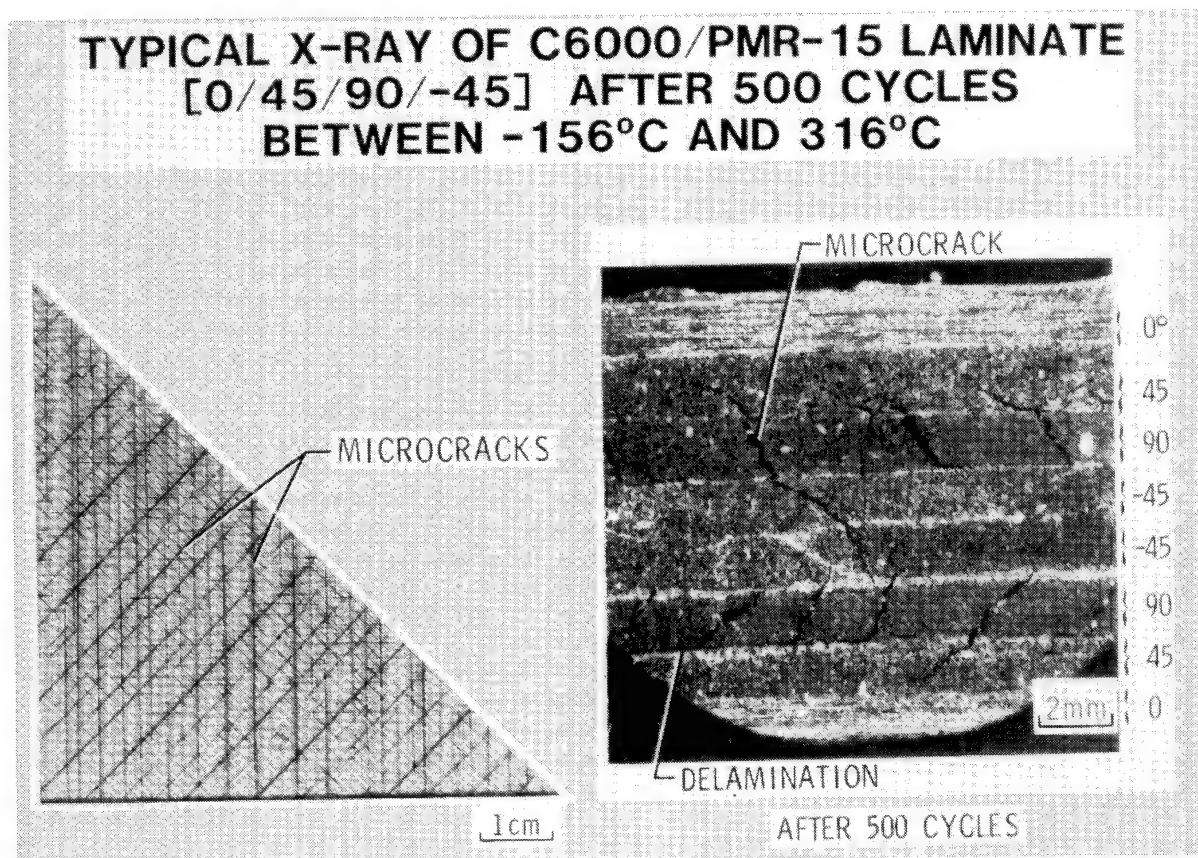
COMPOSITE CONSTITUENT AND LAMINA PROPERTIES

Composite materials are made by combining fibers and matrix materials to form a simple lamina. Laminae are then stacked in various ways to form laminates with the desired properties. Typical room temperature thermal and mechanical properties of continuous graphite fibers, matrix and laminate considered for space structures are shown below. Both high strength and modulus fibers are candidates. The orthotropic character of the fibers becomes evident when the axial and radial properties are compared. Note that the axial coefficients of thermal expansion (CTE), A_1 , are small and negative. The matrix materials have low strength and low modulus and, except for the glass, have large, positive CTE. When combined, the fibers and matrices form highly orthotropic unidirectional lamina. The large differences in the CTE of the fiber and matrix as well as the differences in the directional CTEs of the lamina can result in very high stresses induced by thermal cycling in the laminates as well as the lamina.

Material	Modulus		Strength		CTE	
	E1 Msi	E2 Msi	Xt ksi	Yt ksi	A1 ppm/F	A2 ppm/F
Fibers						
T300	33.8	3.35	350	--	-0.30	5.6
HMS	55.0	0.90	250	--	-0.55	3.80
P75	79.8	1.38	300	--	-0.75	3.80
P100	115.5	1.05	325	--	-0.78	3.80
Matrix						
934	0.67	--	8.5	--	24.4	--
PMR 15	0.5	--	8	--	20.0	--
2024 Al	10.6	--	60	--	12.9	--
Glass	9.1	--	--	--	1.8	--
Lamina						
T300/934	18.9	1.4	223	9.37	-0.01	16.13
P75/934	42.0	0.83	102	3.51	-0.58	19.18
HMS/Glass	24.	1.1	86.3	2.6	-0.23	2.1
P100/2024	47.8	3.6	92.2	8.89	0.800	14.51

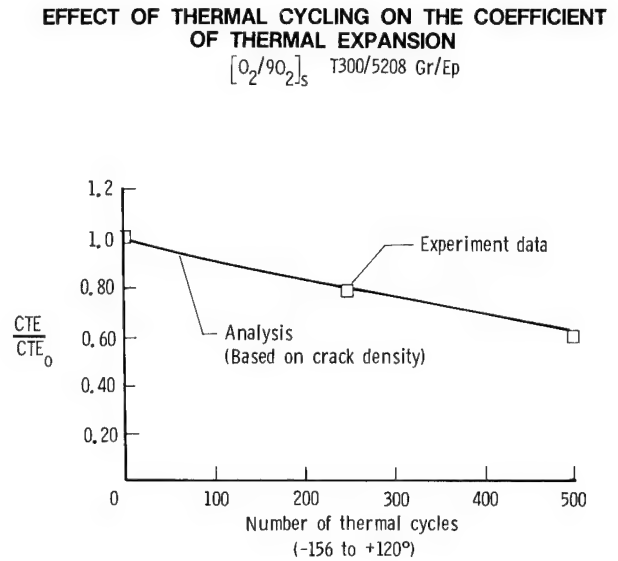
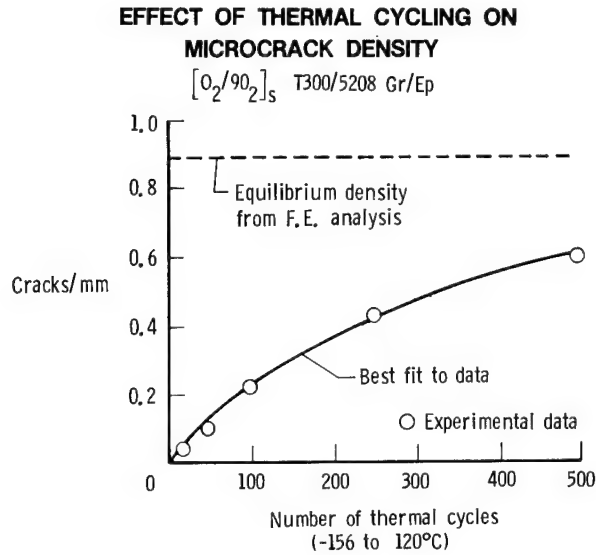
TYPICAL THERMAL INDUCED MICRODAMAGE

The primary effect of thermal cycling on composites is the induced thermal stresses and the resulting damage. Typical microdamage induced by thermal cycling of continuous graphite reinforced polymers is shown in the figure below. The micrograph shows microcracks and delaminations formed in a $[0/45/90/-45]_s$ laminate of C6000/PMR-15 after 500 cycles between -156°C and 316°C , as viewed along a polished edge of the specimen. The thermal cycling in orbit can be considered low amplitude thermal fatigue with the net material effects (microdamage) changing with time. The microcracks began as intraply cracks and grew to interply cracks as the number of cycles increased. Delaminations appeared as the number of cycles increased. An X-ray of the top of the specimen is also shown below. The dark lines are the cracks, enhanced with a dye, that run parallel to the fibers in each lamina over the entire width and length of the specimen. Although this composite material is very brittle, has a high cure temperature (resulting in high residual stresses), and the temperature range is large, similar cracks have been observed in composites with lower cure temperatures even after cycling between a smaller temperature range, -100°C to 66°C .



THERMAL CYCLING EFFECTS ON GRAPHITE/EPOXY COMPOSITES

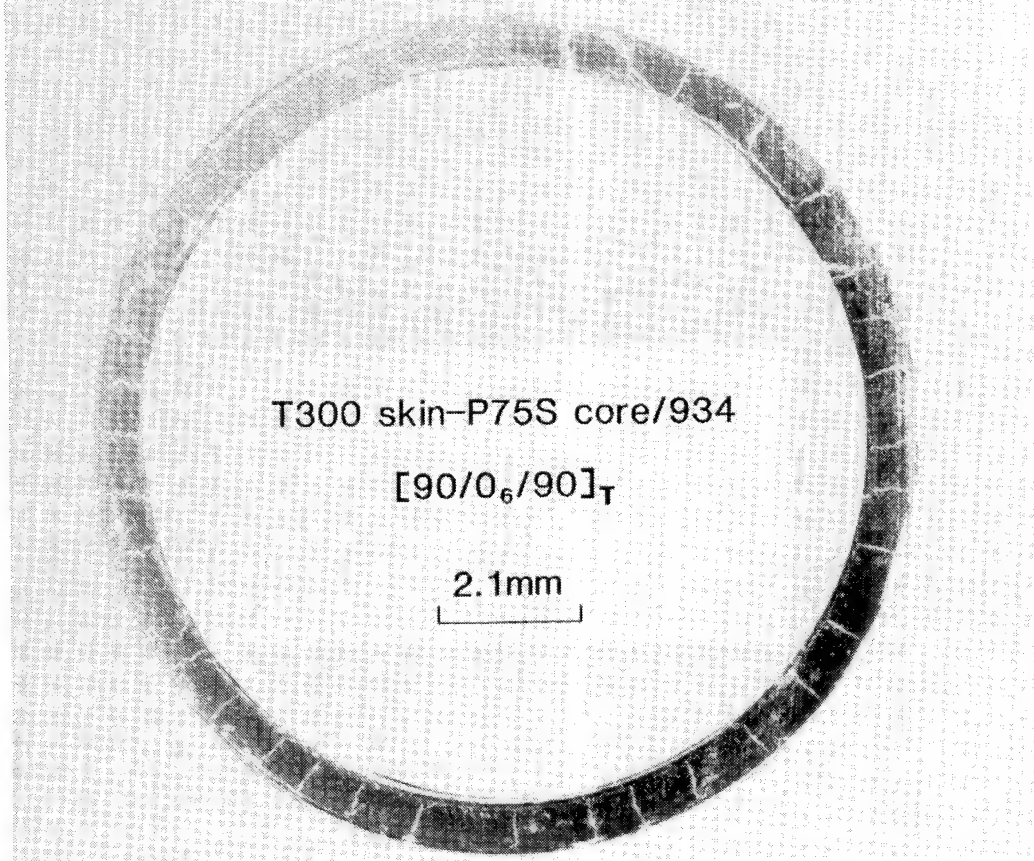
The increase in the crack density (cracks/length of specimen) as thermal fatigue progresses, is shown below. As the number of cycles increases, the crack density asymptotically approaches an equilibrium value. For the T300/5208 $[0_2/90_2]_s$ graphite/epoxy laminate shown here, the equilibrium density may not be reached for several thousand cycles. The coefficient of thermal expansion, CTE, is one of the laminate properties that can be greatly affected by microcracking. For this laminate, the CTE was reduced by about 40% after 500 thermal cycles. Additional reduction may be expected since the laminate had not reached its equilibrium crack density for this temperature range.



MICRODAMAGE IN GRAPHITE/EPOXY TUBES

The data discussed in the previous figures has been for flat specimens. Microdamage can also be induced in composite tubes. The cross section of a 0.5-inch diameter composite tube that was cycled 500 times between -156°C and 94°C is shown below. The radial cracks induced in the wall by the thermal cycling can be clearly seen. Some delamination along the inside and outside diameters was also induced. After 500 cycles, the crack morphology is very similar to that of the flat laminates.

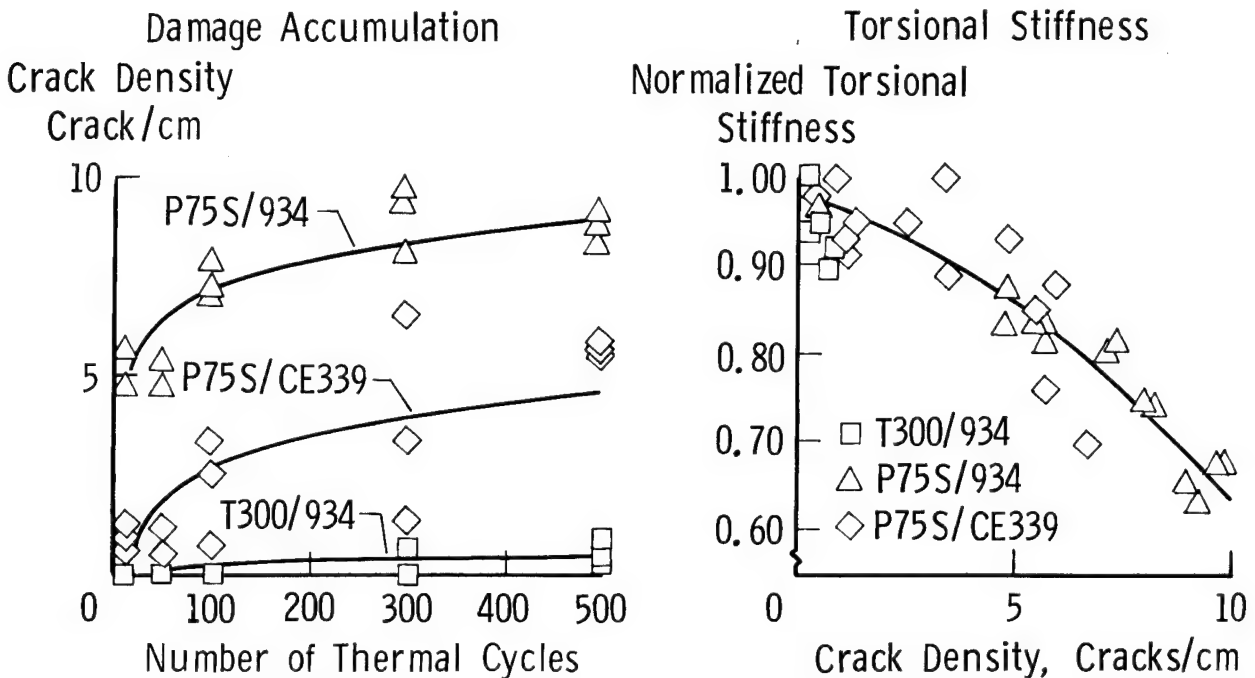
MICRODAMAGE IN Gr/Ep TUBE AFTER 500 THERMAL CYCLES BETWEEN -156°C AND 94°C



EFFECTS OF THERMAL CYCLING ON COMPOSITE TUBES

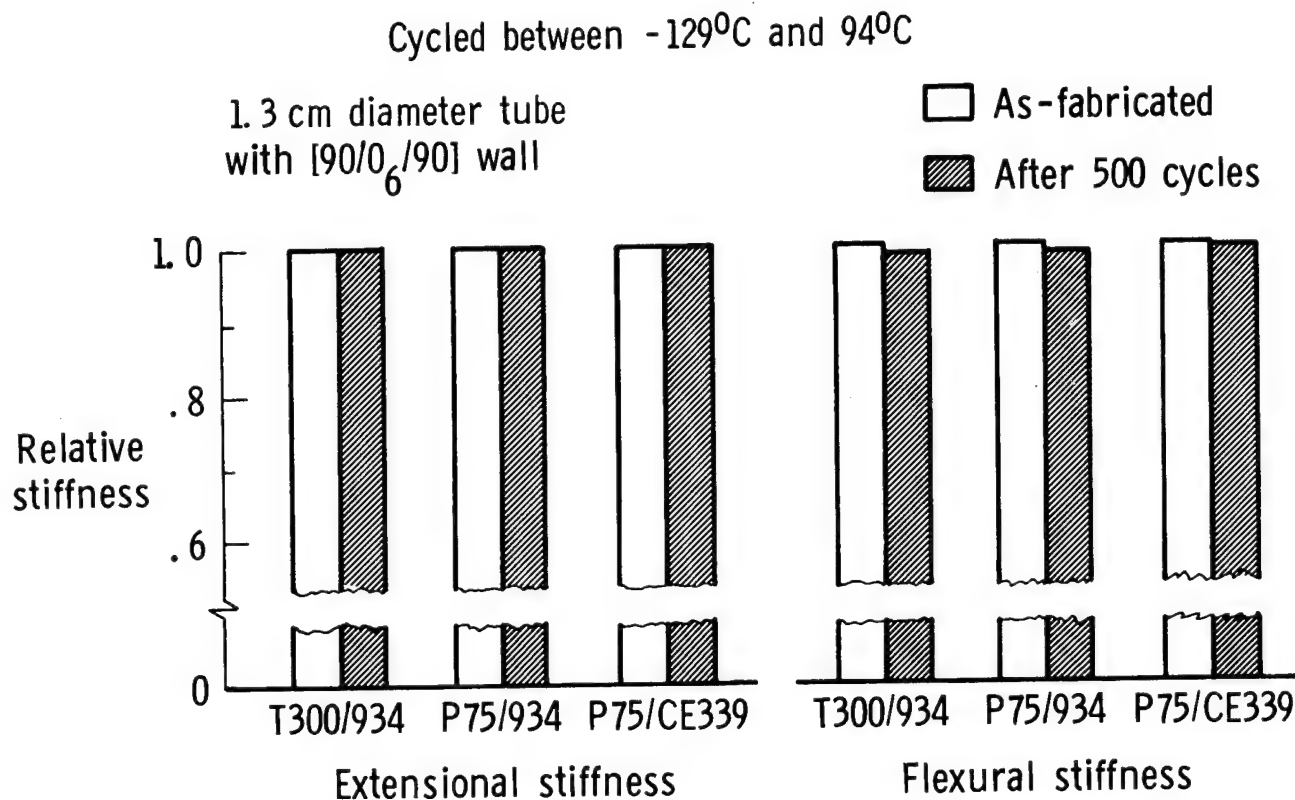
The change in crack density induced in three tubes of different materials, as the number of thermal cycles between -156°C and 94°C increases, is shown in the figure below. The P75S/934 is a high modulus brittle epoxy system, the P75S/CE339 is a high modulus toughened epoxy system, and the T300/934 is a low modulus brittle epoxy system. The crack densities for each material asymptotically approach equilibrium values as the number of cycles increases. The effects of the thermal cycling or microcracking on the torsional stiffness of these tubes are also shown below. The torsional stiffness of tubes of each of the three materials was reduced by about 40% and the change in the stiffness appeared independent of the composite material system. These data illustrate the sensitivity of matrix dominated properties to microcracking.

(Cycled Between -156°C and 94°C)



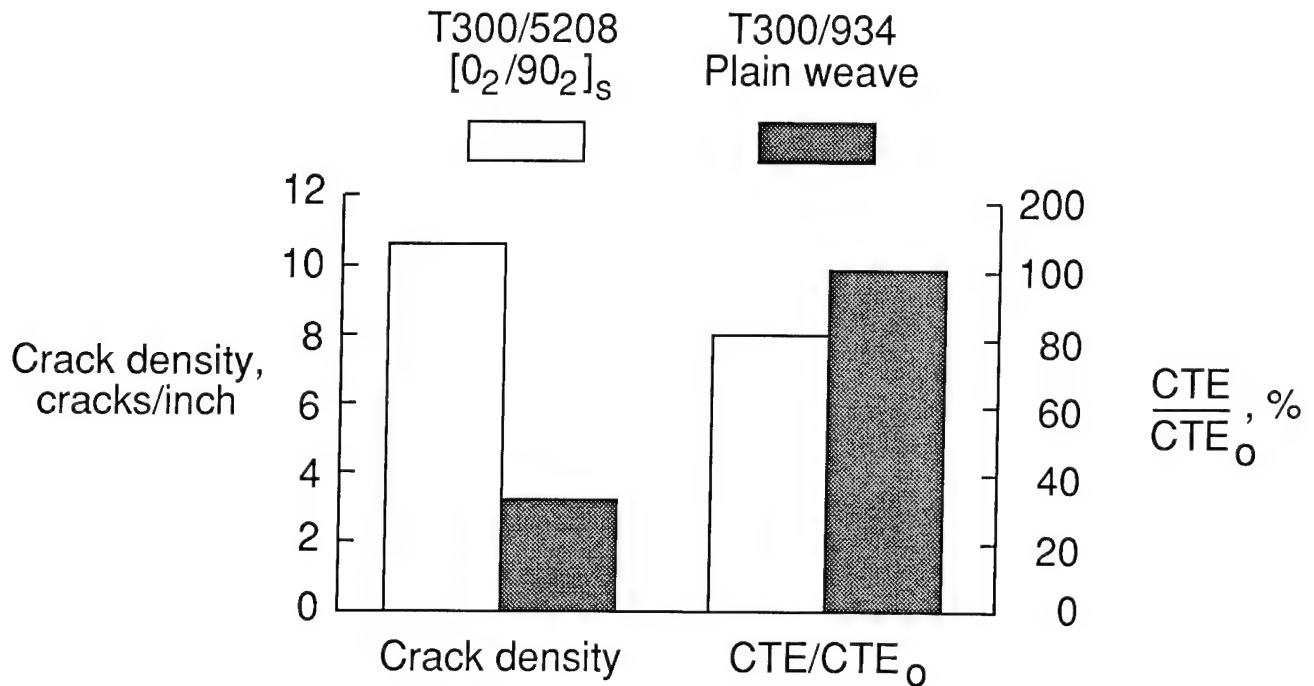
EFFECTS OF THERMAL CYCLING ON EXTENSIONAL AND FLEXURE STIFFNESSES OF Gr/Ep TUBES

The extensional and flexural stiffnesses of the three different Gr/Ep tubes before and after 500 thermal cyclings between -129°C and 94°C are shown below. These are the same materials shown in the previous figure. The data show no significant effects of thermal cycling on these stiffnesses; this was expected since, for this wall configuration, the extensional and flexural stiffnesses are fiber dominated properties, which are not sensitive to matrix damage.



EFFECTS OF FABRIC ON THERMAL CYCLING STABILITY OF Gr/Ep COMPOSITES

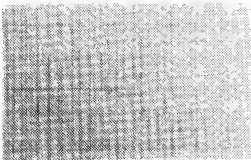
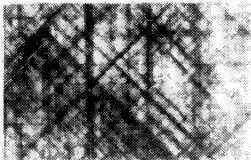
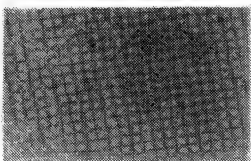

The results from one study to minimize microdamage induced by thermal cycling., ref. 2, are shown in the figure below. Crack densities and changes in CTE for a continuous graphite $[0_2/90_2]_s$ laminate of T300/5208 and a laminate of plain weave T300/934 Gr/Ep are compared. The 5208 epoxy resin and the 934 epoxy resin are very similar in composition and curing and have similar as-fabricated tensile modulus and CTE. The data shows that the fabric significantly suppressed crack formation, as compared to the cross-ply laminate and, therefore, exhibited no significant change in the CTE. These data demonstrate the increase in stability of a woven fabric in a thermal cycling environment as compared to the cross-ply laminate fabricated from unidirectional plies.



SYNERGISTIC EFFECTS OF THERMAL CYCLING AND RADIATION ON MICRODAMAGE IN COMPOSITE MATERIALS

Spacecraft materials are not subjected only to thermal cycling. At GEO, the material can also be exposed to significant dose levels of electron radiation. The effects on induced microcracking in two thermoset and thermoplastic Gr/Ep composites of (1) thermal cycling only and (2) irradiation followed by thermal cycling, ref. 3, are shown in the figure below. Quasi-isotropic laminate, $[0/45/-45/90]_s$, specimens of each material were exposed to either thermal cycling only or 10^{10} rads of electron radiation followed by thermal cycling. When these materials were subjected to only thermal cycling, the toughened epoxy laminate T300/BP907 and the thermoplastic laminate AS4/PEEK, had few or no cracks after 500 cycles between -150°C and 93°C . When exposure to electron irradiation was followed by thermal cycling, the T300/BP907 had a very large increase in the microcrack density whereas the AS4/PEEK had a small increase in the microcrack density. The increase in the microcrack density induced by thermal cycling after irradiation is attributed to radiation-induced embrittlement of the matrix.

(500 THERMAL CYCLES BETWEEN 93°C AND -150°C)

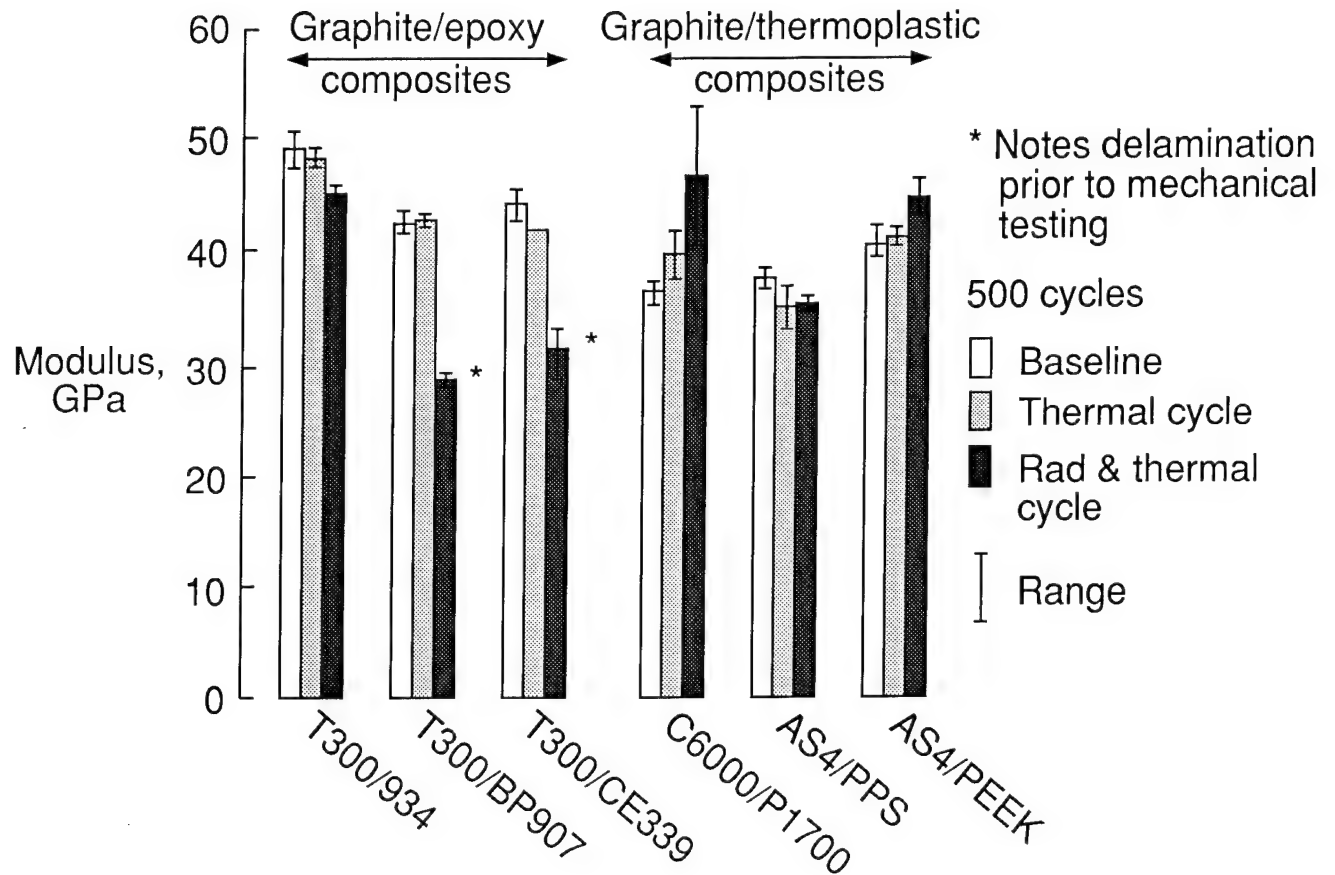
MATERIAL	MICROCRACK DENSITY, CRACKS/CM		
	THERMAL CYCLED	10^{10} RADS AND THERMAL CYCLED	
T300/934	7	17	
T300/BP907	0	> 50	
C6000/P1700	21	24	
AS4/PEEK	1	5	

→ 1 cm ←

THERMAL CYCLING EFFECTS ON TENSILE MODULUS

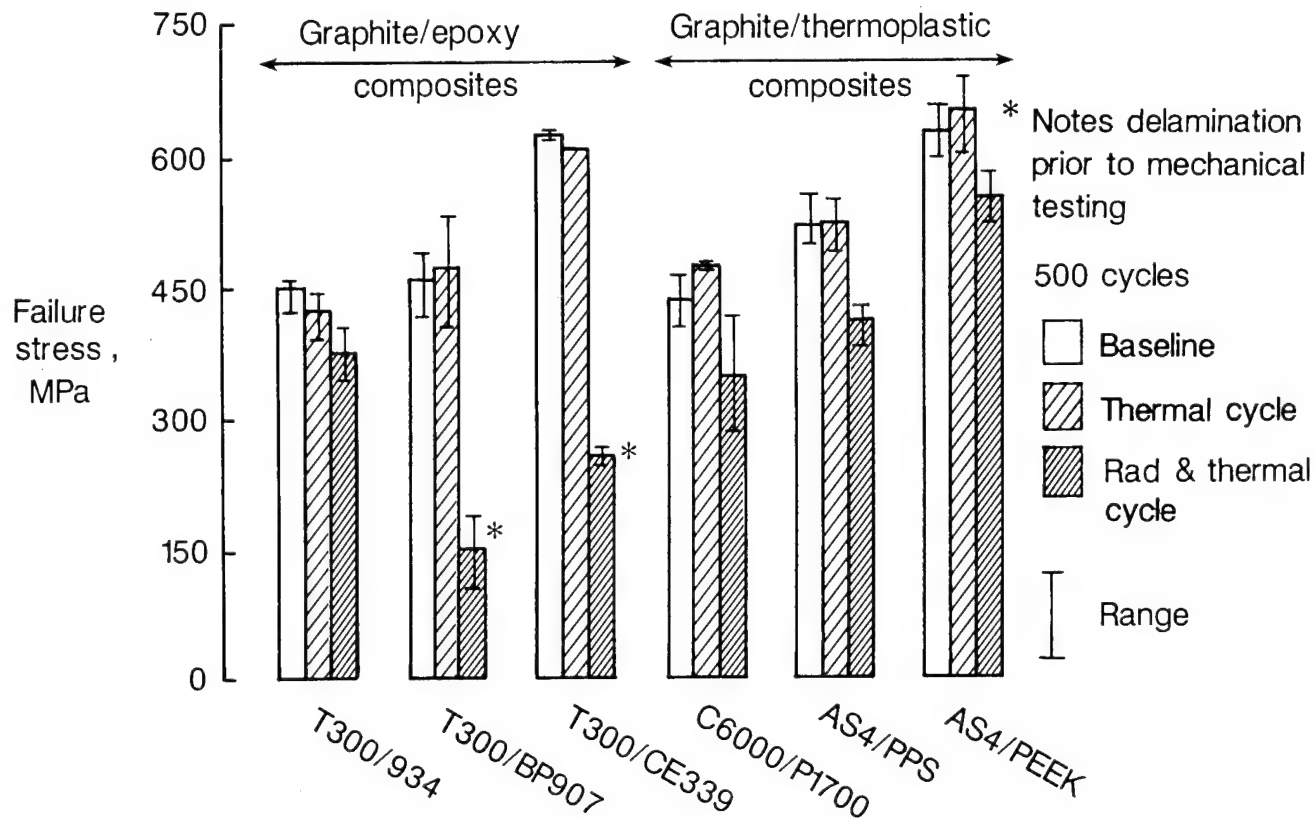
The effects of thermal cycling only and radiation exposure followed by thermal cycling on the tensile modulus of three thermoset and three thermoplastic composite materials, ref. 3, are shown below. Thermal cycling only did not significantly change the tensile modulus of a $[0/+45/-45/90]_s$ laminate made with any one of the six materials. Significant reduction in the modulus caused by radiation followed by thermal cycling was observed only in the T300/BP907 and T300/CE339 toughened epoxy laminates. This reduction in both materials is attributed to matrix embrittlement and resulting damage.

Laminate lay-up $(0/+45/90)_s$



THERMAL CYCLING EFFECTS ON TENSILE STRENGTH

The effects of thermal cycling only and radiation exposure followed by thermal cycling on the tensile strength of three thermoset and thermoplastic composite materials, ref. 3, are shown below. (These are the same materials presented in the previous figure.) Thermal cycling only did not significantly change the tensile strength of the $[0/+45/-45/90]_s$ laminate made with each of the six materials. However, radiation exposure followed by thermal cycling resulted in significant reduction in the tensile strength of the three thermoplastic materials and the two toughened thermoset epoxy materials. These data show that there was detrimental synergism between electron radiation and thermal cycling, at least when thermal cycling follows radiation exposure.

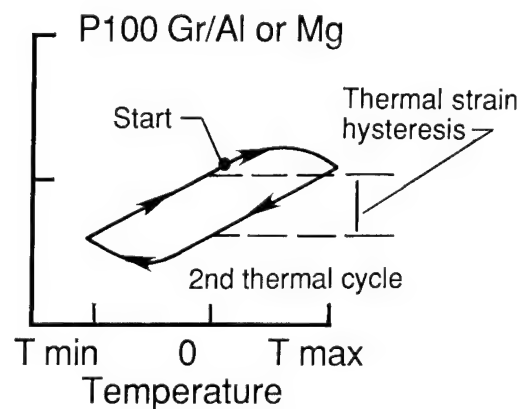
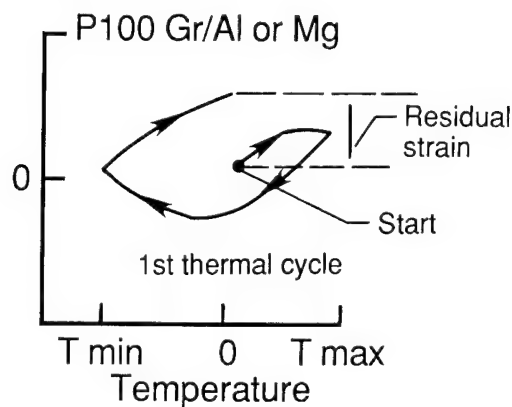


EFFECTS OF THERMAL CYCLING ON METAL-MATRIX COMPOSITES

Advantages of graphite-reinforced metal-matrix composites (MMC) over polymer-matrix composites for space structure applications include higher thermal conductivity and better environmental durability. The standard MMCs considered are continuous graphite-fiber reinforced 6061 Al and AZ91C/AZ61A Mg. However, both of these material systems exhibit thermal strain hysteresis and residual strain during thermal cycling, shown below, which are undesirable for dimensionally critical structures. The response of these materials during thermal cycling is governed by the elastic/plastic deformations of the matrix material, ref. 4. The large residual strain at the end of the first cycle is not seen during subsequent thermal cycles through the same or smaller temperatures ranges because the plastic deformation at the elevated temperatures is offset by the plastic deformation at the low temperatures. There are several potential ways to alter this behavior. The matrix elastic limits could be increased to prevent matrix yielding. Providing the correct matrix alloy chemistry in the final composite could help insure strengthening from heat treatments. Reduction in residual fabrication stresses by thermomechanical treatments could also help reduce total stress levels reached during thermal cycling.

BACKGROUND

- Current state-of-the-art:
 - Standard MMC for space structures: Continuous graphite-fiber reinforced 6061 Al and AZ91C/AZ61A Mg
 - Thermal strain hysteresis and residual strain are recognized problems

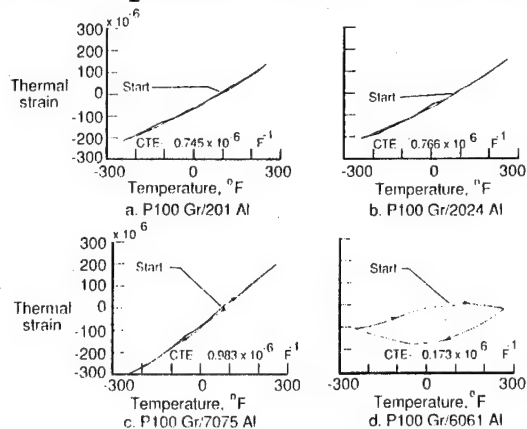


- Potential solutions:
 - Increase matrix tensile and compressive elastic limits
 - Insure correct matrix alloy chemistry
 - Reduce residual fabrication stresses (thermomechanical treatments)

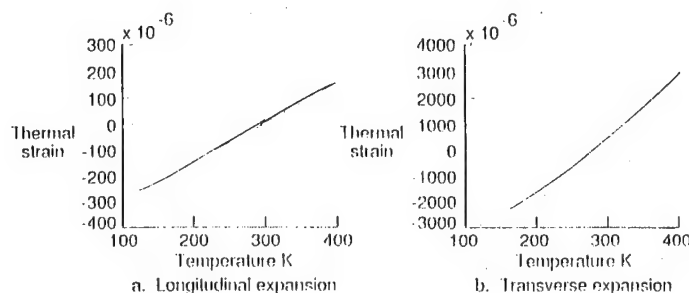
THERMAL EXPANSION BEHAVIOR OF PROCESSED P100Gr/Al [0] COMPOSITES AFTER 1500 CYCLES

The thermal expansion behavior of P100 Gr/Al unidirectional laminates containing high strength aluminum alloys, 201, 2024, and 7075 and the standard 6061, after thermal processing to minimize hysteresis, refs. 4 and 5, is shown in left figure. With the exception of the 6061 Al matrix composite, the P100 Gr/Al laminates show no hysteresis or residual strain even after 1500 cycles. The 6061 Al laminate was not sufficiently strengthened by the heat treatment to eliminate yielding because the chemistry of the alloy was not within specifications. However, when P100 Gr/6061 Al was made with tight control on the chemistry, right figure, processing raised the elastic limit sufficiently to prevent hysteresis. Attempts to heat treat the P100 Gr/Mg MMC with high strength Mg alloys were unsuccessful in eliminating hysteresis. Advancements in high strength Mg alloy development are required to obtain a hysteresis-free P100 Gr/Mg MMC.

THERMAL EXPANSION BEHAVIOR OF THE PROCESSED P100Gr/Al [0] COMPOSITES AFTER 1500 CYCLES



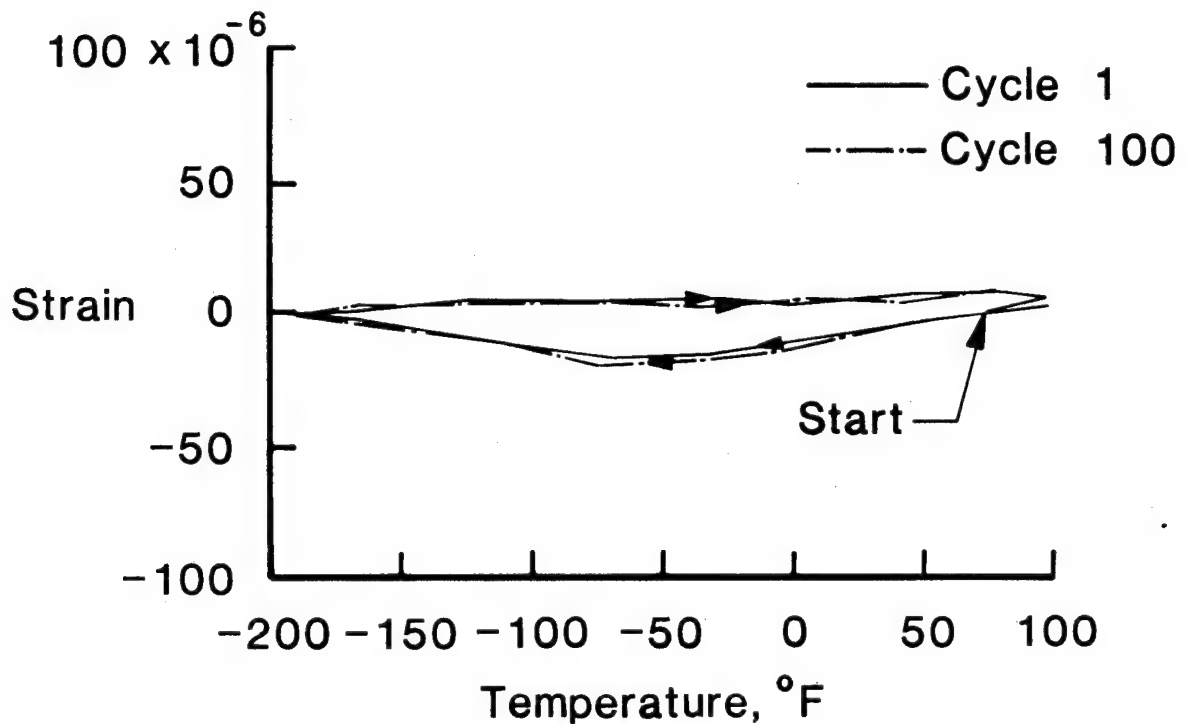
THERMAL EXPANSION OF PROCESSED P100 Gr/6061 Al
1-Ply unidirectional laminate from DOD "Big Buy"



THERMAL EXPANSION OF (0/+ 60)_s HMS/BOROSILICATE GLASS LAMINATE

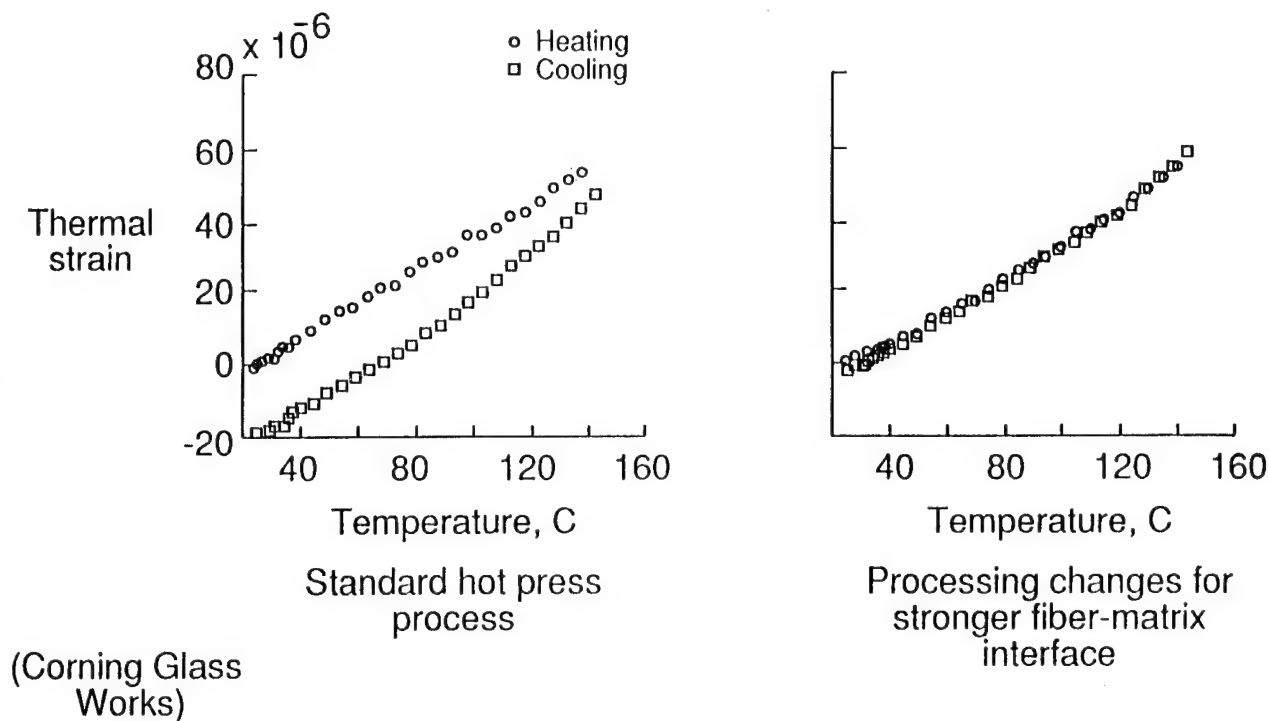
Because of its environmental stability and low outgassing characteristics, graphite-reinforced glass materials are very important for space applications. However, the thermal expansion behavior of this material is characterized by hysteresis which is detrimental to the performance of a precision structure. The thermal expansion of one Gr/glass, HMS/Borosilicate glass, ref. 6, is shown below. The average CTE for this quasi-isotropic laminate is about zero. The expansion behavior before and after 100 cycles exhibits a small hysteresis which is not affected by thermal cycling. The exact mechanism causing this hysteresis is not known but may be the result of the fibers slipping in the glass matrix.

X-Direction



THERMAL EXPANSION OF Gr/ABS GLASS COMPOSITE [0/90]_s LAMINATE

The thermal expansion of a Gr/ABS glass cross-ply laminate before and after processing, ref. 7, is shown below. When the standard hot press process is used, the material exhibits hysteresis when heated from room temperature to about 150°C and cooled back to room temperature. However, when the material is processed in a way to strengthen the fiber-matrix interface, the hysteresis is eliminated. Additional work is needed to investigate the response of the material to verify this behavior and also to determine the behavior when cycled at temperatures below 70°F.



Thermal strain hysteresis eliminated by changes in processing

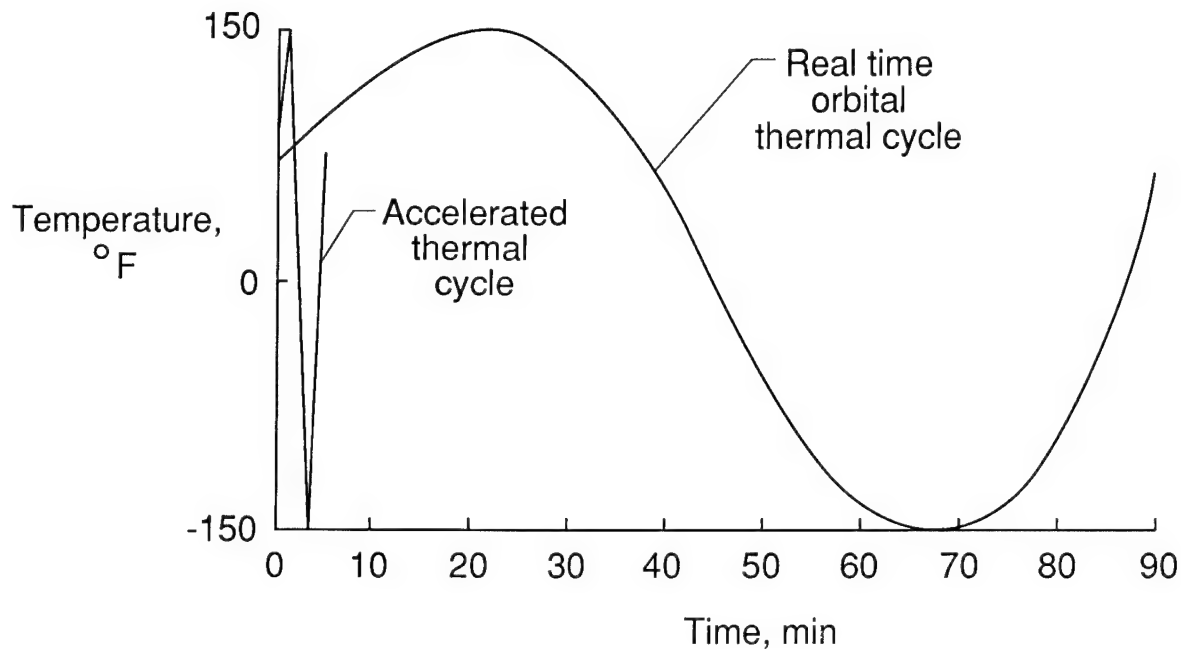
MISSION LIFE VS THERMAL CYCLES

The number of thermal cycles a spacecraft will experience can vary from a little less than 6000 for a one-year life expectancy to as many as 175,000 for a 30-year Space Station. These large numbers of thermal cycles make real time testing impractical. Accelerated testing techniques are required to verify material life assessment and prediction methodologies.

Mission life	No. of 90-min cycles
1 yr.	5840
5 yrs.	29200
10 yrs.	58400
20 yrs.	116800
30 yrs.	175200

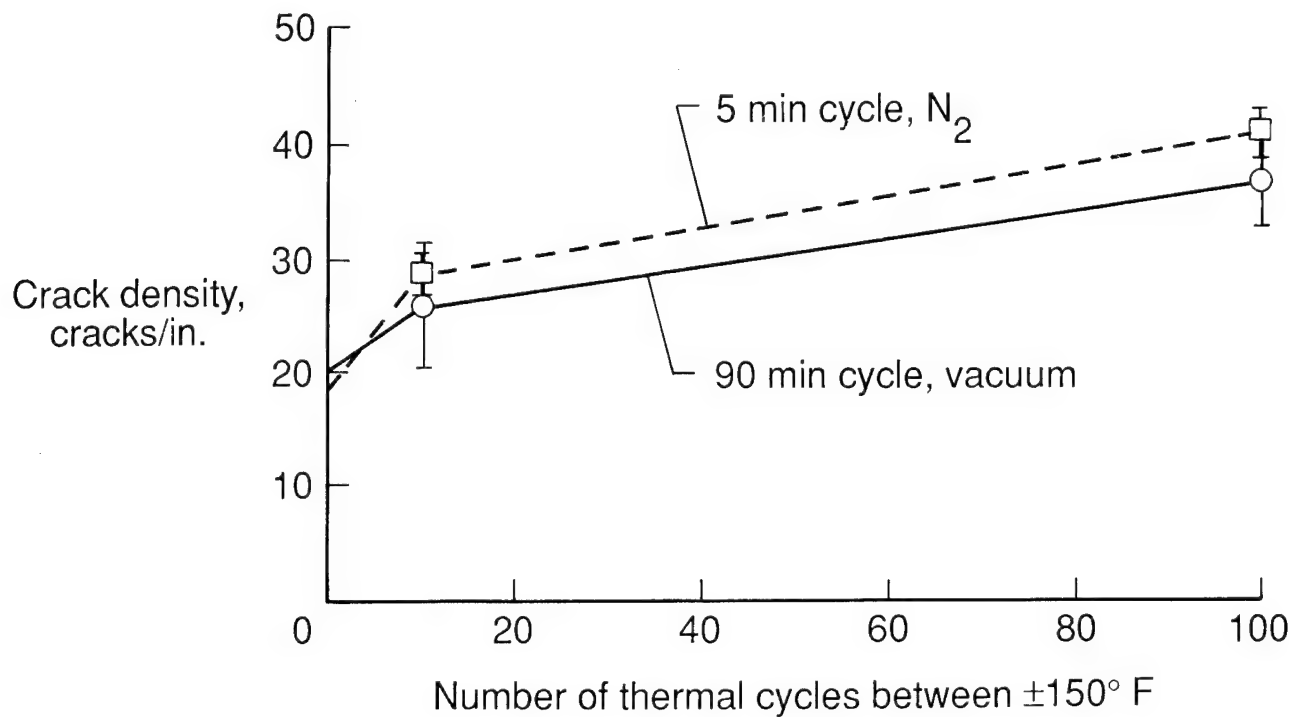
COMPARISON OF ACCELERATED AND REAL TIME THERMAL CYCLES IN SPACE

A comparison of a real time thermal cycle for low Earth orbit and a proposed accelerated thermal cycle is shown in the figure below. The real time cycle takes place in vacuum and has a 90-minute period with an amplitude of $\pm 150^{\circ}\text{F}$. The proposed accelerated cycle has a period of about 5 minutes and an amplitude of $\pm 150^{\circ}\text{F}$. In the accelerated test, a dry nitrogen atmosphere was used instead of vacuum. Heating was therefore done by convection instead of by pure radiation. Composite material samples were exposed to these two environments and the effects on the different environments on a P75 Gr/934 Ep laminate were compared.



EFFECTS OF THERMAL CYCLE RATE AND ATMOSPHERE ON MICROCRACKING IN [0/90/0/90]_s P75 Gr/934 Ep LAMINATE

The validity of the proposed accelerated test technique was established by comparing the microdamage induced in a P75 Gr/934 Ep laminate by a 90-min. cycle in a vacuum and by a 5-min. cycle in nitrogen between $\pm 150^{\circ}\text{F}$, ref. 8. The [0/90/0/90]_s laminate was selected because previous tests have shown that damage was induced in this laminate when it was thermally cycled between $\pm 150^{\circ}\text{F}$. Crack densities in specimens cycled in the slow and accelerated thermal cycles are shown below. The data show that there were no significant differences between the damage induced in this laminate by the two different thermal cycle environments over 100 cycles. This is consistent with similar data obtained by the European Space Agency, ref. 9.



SUMMARY

A brief description of the effects of the space thermal cycling environment on structural composite materials has been given and is summarized below. The material surface optical thermal parameters were shown to have significant effects on the temperature range. The interaction of the environment and the material and the effects of this interaction on resin-matrix (RMC), metal-matrix (MMC), and glass-matrix (GMC) composites were shown and discussed. The primary problem associated with thermal cycling is the microdamage caused by induced thermal stresses. Data were presented that showed accelerated ground tests can simulate the effects of thermal cycling expected in space. The amplitude of the thermal cycle, and therefore the stress levels, can be significantly varied by using a thermal control coating. The effects of thermal cycling are different for the different classes of composite materials. Cycling-induced cracks in RMC caused property changes, and synergistic effects with electron radiation were significant. The MMC exhibited dimensional instability because of plastic deformation. The GMC also exhibited microcracking and thermal strain hysteresis. However, potential solutions to these undesirable effects have been developed for all of the composite material systems studied.

- Primary problem: microdamage caused by induced thermal stresses
- Accelerated ground tests simulate effects on composite materials
- Thermal control coatings will alter the amplitude of the thermal cycle
- Different effects on different classes of materials:
 - RMC - cracking, property changes, synergistic effects with radiation
 - MMC - thermal strain hysteresis, plastic deformation
 - CMC - thermal strain hysteresis, microcracking
- Demonstrated solutions have been developed

REFERENCES

1. Tompkins, S. S.; Sykes, G. F.; and Bowles, D. E.: The Thermal and Mechanical Stability of Composite Materials for Space Structures. IEEE/ASM/ASME/SME Space Technical Conference, Anaheim, CA, Sept. 1985, Technical Paper No. EM 85-979.
2. Bowles, D. E. and Shen, James: Thermal Cycling Effects on the Dimensional Stability of P75-T300 (Fabric) Hybrid Graphite Epoxy Laminate. Proceedings 33rd International SAMPE Symposium and Exhibition, Anaheim, CA, Mar. 1988, Vol. 33, pp 1699-1671.
3. Sykes, G. F.; Funk, J. G. and Slem, W. S.: Assessment of Space Environment Induced Microdamage in Toughened Composite Materials. Proceedings 18th National SAMPE Technical Conference, Seattle, WA, Oct. 7-9, 1986, Vol. 18, pp. 520-534.
4. Dries, G. A. and Tompkins, S. S.: Development of Stable Composite of Graphite Reinforced Aluminum and Magnesium. 12th Conference on Composite Materials and Structures, DOD/NASA Cocoa Beach, FL, Jan. 20-21, 1988.
5. Dries, G. A. and Tompkins, S. S.: Effects of Thermal Cycling on Thermal Expansion and Mechanical Properties of Several Graphite-Reinforced Aluminum Metal Matrix Composites. NASA TP-2701, July, 1987.
6. Tompkins, S. S.; Ard, K. E.; and Sharp, G. R.: Thermal Behavior of Graphite/Glass and Graphite/Magnesium. Proceeding 18th International SAMPE Technical Conference--Materials for Space. Seattle, Washington, Oct. 7-9, 1986, Vol. 18., pp. 623-637.
7. Janas, Victor F.: Thermal Expansion Hysteresis in Graphite/Glass Composites. Proceedings International SAMPE symposium, Anaheim, CA, Mar. 7-10, 1988, Vol. 33, pp. 357-368.
8. Tompkins, S. S.; Bowles, D. E.; Slem, W. S.; and Teichman, L. A.: Response of Composite Materials to the Space Station Orbit Environment. AIAA/NASA Space Station Symposium, Williamsburg, VA, Apr. 21-22, 1988.
9. Reibaldi, G. G.: Thermomechanical Behavior of GERP Tube for Space Structures. Acta Astronautica Vol. 12, No. 5, 1985, pp. 323-333.

SESSION 8: SPACECRAFT CHARGING

Chairman: N. John Stevens
TRW

DIELECTRICS FOR LONG TERM SPACE EXPOSURE
AND SPACECRAFT CHARGING
A BRIEFING

A. R. Frederickson
Air Force Geophysics Laboratory
Space Physics Division
Hanscom AFB, Massachusetts

DEEP DIELECTRIC CHARGE EFFECTS

Charging of dielectrics is a bulk, not a surface property. Radiation driven charge stops within the bulk and is not quickly conducted to the surface. Very large electric fields develop in the bulk due to this stopped charge. At space radiation levels, it typically requires hours or days for the internal electric fields to reach steady state.

The resulting electric fields are large enough to produce electrical failure within the insulator. This type failure is thought, by this author, to produce nearly all electric discharge anomalies.

Radiation also induces bond breakage, creates reactive radicals, displaces atoms and, in general, severely changes the chemistry of the solid state material. Electric fields can alter this process by reacting with charged species, driving them through the solid. Irradiated polymers often lose as much as a percent of their mass, or more, at exposures typical in space. Very different ageing or contaminant emission can be induced by the stopped charge electric fields.

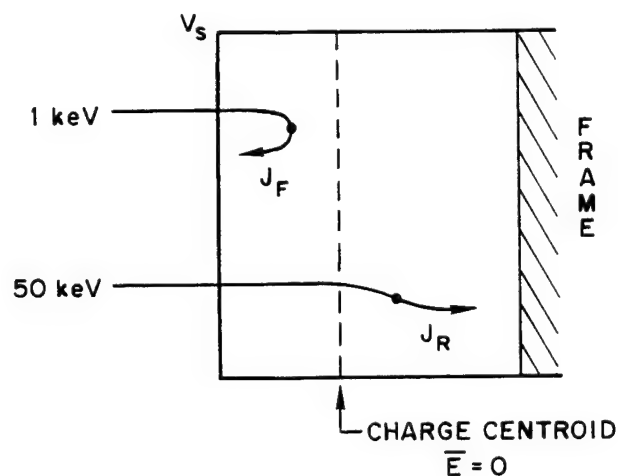
- Modifies or controls surface voltage
- Controls currents within dielectrics
- Increases response time to hours or days
- Causes most electric discharge anomalies
- Modifies properties and ageing of dielectrics
- Modifies emission of contaminants

SURFACE VOLTAGE, V_s

Surface voltage calculations must include the effects of stopped charge. Some of the stopped charge is conducted back to the insulator surface. The rest of the stopped charge is conducted to the satellite frame which, being conductive, is at one potential. The demarcation is marked by the centroid of stopped charge which forms a plane in which the electric field is zero.

The front surface reaches steady state only when these two currents are in steady state and when the position of the zero field plane is constant. For typical insulators, at space radiation levels, it can take hours or days to attain this steady state. However, since space radiations on a given surface of a satellite are not stable in this time interval, steady state is not achieved in most cases.

The major fluctuations in incident radiation are due to sunlight-to-dark transitions, and to passage through differing radiation "belts" during orbit. These fluctuations are sufficient to cause kilovolt excursions relative to frame potential. However, the actual value of surface potential is very dependent on the material properties, thickness, capacitance to frame, etc. but especially to the density of the local space plasma and sunlight intensity. Even when internal fields are large, the surface potential can be clamped to satellite frame potential by sufficient space plasma or sunlight.



- Steady State: $J_F ==$ Surface Charge
 $J_R ==$ Frame Charge
- BUT, Often, Time Constant > Hours
 STEADY STATE NEVER ACHIEVED

IMPORTANCE OF DEEP CHARGE FOR SURFACE VOLTAGE

Stopped charge within the dielectric does not always alter surface potential calculations. In some situations, only the surface secondary emissions term needs to be considered. For example, small area dielectrics may not strongly affect the average satellite potential as long as they are not the most negative tending surface. For very small dielectrics with high secondary emission yields (which is typical) the surrounding material will control the surface potential, even of the dielectric. In addition, for very thick dielectrics, nearly no current will pass through the insulator, most will return to the surface; thus NASCAP procedures are sufficient when considering only surface emission.

However, there are cases where stopped bulk charge is very important. For typical space spectra, we can expect that thicknesses between 1 micron and 1 mm require detailed calculations to determine the relative flows to the insulator surface and through the bulk to the satellite frame. For such thicknesses, then, determination of the insulator surface potential, relative to the satellite frame, is difficult, and requires calculation of electric fields and currents within the insulator.

- NONE: Average Satellite V.
Differential V where:
thickness $> 10 \times$ max range, or
thickness < 2 nd Xover range.
- LARGE: Differential V where insulator
thickness is between 1 mm and
1 micron.

TIME CONSTANT

The time constant for charging within an insulator is similar to the capacitor time constant, RC . However, because each layer of insulator material contacts only other insulator material, the "series resistance" is very high. The effective resistance of space plasma is lower so that the time constants for satellite surface voltages are short compared to the time constants for internal insulator voltages. In the insulator, the time constant, τ , is given by

$$\tau = \epsilon / \sigma = (\text{dielectric constant}) / (\text{conductivity})$$

where σ is a strong function of position depending on dose rate, temperature, UV level, and other factors.

High energy particles stop via atomic collisions, nearly independent of electric field, and produce electric fields. These fields drive conduction carriers thus generating further changes in the fields. The process comes to steady state only when the divergence of current is zero everywhere. Conceptually, the process comes to equilibrium as an exponential but in reality there are many coupled exponentials because of the broad distribution of conductivities throughout the dielectric. It suffices here to warn of some very long time constants in space applications.

$$\tau = RC \rightarrow \epsilon / \sigma$$

- High energy particles' range nearly independent of electric field.
- Conduction currents redistribute stopped charge.

$$d/dx \{J_{\text{fast}} + J_{\text{cond}}\} \rightarrow d/dt \{\text{deep chg}\}$$

$$d/dt \{\text{deep chg}\} \rightarrow d/dt \{E \text{ field}\}$$

$$E \text{ field} \rightarrow 1 - \exp\{-\sigma(x)t/\epsilon\}$$



DISCHARGE ANOMALIES

Dielectric discharge pulses can be characterized in simple ways in order to predict the impact on electronics:

- a) The pulse consists of a transient surge of current producing a classical vector potential about the space of the satellite.
- b) The currents result from the collapse of energy stored in electric fields into which a dense plasma has been injected. The plasma is created by a failure in a dielectric. The collapsing electric fields cause "image charge flows" in surrounding conductors along with displacement currents.
- c) The dense plasma is produced by material responding to the same, or different, electric field. Strong fields separate valence electrons from molecules and thus ionize the material producing a plasma. Field enhancement at a sharp discontinuity continues the process producing a discharge streamer, and the streamer itself becomes a discontinuity and propagates deeply into the material.
- d) Rise times can be bracketed by experience, but can not be predicted. They depend on the rate at which material is ionized and injected into regions of high field. This is a very complex, poorly understood, process. See literature for data, especially papers by K. Balmain, et al.
- e) Coupling of pulse energy into circuits is complex. Prediction would require full modeling of the induced currents and voltages in all elements of the satellite. Because we are in the near fields ($< 5 \lambda$) all modes of coupling are to be considered, not just TEM.
- f) The entire frequency domain is to be considered, from 10^5 to 10^{10} Hertz.

- Electric Pulses Couple to Systems
- Energy Source is Electric Fields:
Deep Charge or Applied Field
- Fast Rise Time
Characteristic of Material Collapse
Not Understood
Analogy to Lightning
- Coupling is a Large Variable
All Near-Field Modes
Energy Limits: I^2R , $1/2\epsilon E^2$, $1/2\mu B^2$
- Pulse widths
Frequency Domain 10^5 to 10^{10} Hz

PULSES

Sufficient pulses have been created in the laboratory that we can outline their form. Refer to the literature for details, especially the work of K. Balmain, et al. on scaling laws for discharge pulses; amplitudes and slew rates are well reported.

The largest pulses are those which remove the surface voltage of a highly charged insulator. Although not investigated yet, even larger pulses should be expected for high voltage power supplies. A one square meter insulator irradiated with 20 keV electrons has produced pulses which peaked at several hundred amperes and which discharged the insulator surface from initially 18 kV to nearly zero volts. It is presumed that larger pulses would occur for larger samples or for higher surface voltage.

However, small pulses are also seen, and only partial surface discharge occurs. It is presumed that the quantity of plasma produced by the failing dielectric was not sufficient to discharge the surface. Composite materials, such as fiberglass, have been seen to produce small pulses at a rate of a few per second to a few per minute, and continue to do so for days after the radiation ceased. The radio frequency noise of such structures should be considered.

Similar phenomena are intensively studied and reported in the electrical insulation literature under the heading Partial Discharges or Prebreakdown. It appears that all spacecraft events are of this class. In partial discharge only a portion, usually small, of the electric field is collapsed and the electrodes are not bridged by a full arc. After the partial discharge, the dielectric returns to normal and is fully serviceable.

Based on this phenomenology we have two design guidelines! Never allow a large electric field in a large space volume to occur adjacent to a dielectric which may be irradiated; both spacecraft charging and power supply related fields are to be avoided. And, be prepared for rf noise with composites.

- Rise time is controlled by rate of carrier injection into E field.
 - field injection
 - mass transport, pressure
 - avalanching
 - photons {cascade, losses}
 - recombination losses
- HEIGHT, 0 → 300 Amperes
- WIDTH, 0 → 10 Microseconds
- ENERGY, Will not exceed stored static energy so we have a DESIGN GUIDELINE.

METAL TO METAL ARCS ?

NOT LIKELY

Currents in space generally do not exceed a nanoampere per square centimeter. If a metal surface becomes highly charged and is associated with a large normal electric field, then one would expect (Fowler-Nordheim) tunneling emission from the surface to equilibrate with the incoming electron currents. The currents and voltages would not be sufficient to cause "vaporization" of the metal surface. Without the emission of large quantities of surface material, an arc in an evacuated space between electrodes will not occur. Tunneling currents will increase to cancel the effects of in-coming space electrons.

Satellites with high voltage power supplies may be another story. If emission from a surface reaches a certain level, then currents in the gap, accelerated by the power supply, may contain enough energy to "vaporize" some electrode surface, and thereby provide the source of ions and electrons to form an arc. A strong power supply is needed to do this. The most likely process, even for the power supply case, is an event triggered by an adjacent dielectric partial discharge pulse. The partial discharge introduces enough plasma so that acceleration by the power supply heats the metal electrode and generates more plasma directly from the electrode. Avalanche can then occur between the electrodes.

We need to definitively answer the question concerning the existence of direct metal to metal arcs. The work should be performed on actual, to be flown, metals because it is impurities characteristic of the metal surface which control the onset of arcing (as discussed in the literature on vacuum circuit breakers used for high voltage transmission line lightning protection.)

A great deal is already known from the high voltage power distribution community and direct arcs are very unlikely at the voltages encountered in space charging. But, perhaps the simultaneous irradiation by the high energy "tail" would activate some surface impurities or oxides to produce partial discharges.

The figure describes an experiment whereby a faraday cup is used to achieve high voltage. The secondary suppressor (see battery) can be used to control the steady state potential by controlling back emission of low energy electrons from the cup. A few high energy particles can penetrate the cup to irradiate the gap along with the bremsstrahlung, if such is desired.

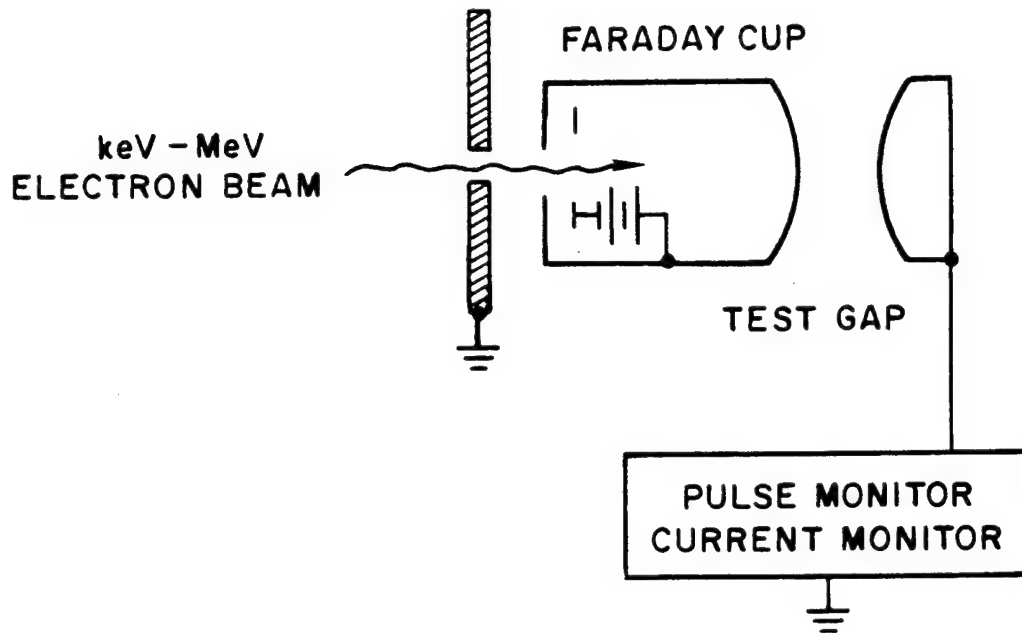
A control experiment should be simultaneously performed. The control should contain an irradiated dielectric adjacent to the metal gap. It is expected that the dielectric will induce many metal to metal current pulses, while the experiment without a dielectric will require inordinant voltage to induce pulses.

METAL TO METAL ARCS
NOT LIKELY

- Space currents do not exceed nanoamp per square cm.
- At high fields, Fowler-Nordheim emission equilibrates with space currents to reach steady state.
- Steady state current insufficient to vaporize metal, so no arc develops.
- BUT, a high voltage power source could vaporize metal to start arc.
- DIELECTRIC IS THE PROBLEM. Discharge in dielectric initiates vapor to start the arc, even in applied field case.

METAL TO METAL ARCS ?

EXPERIMENT



- Faraday cup contains secondary emission suppressor.
- Voltage of faraday cup is monitored using external field probes.
- Beam can partially penetrate if secondary electrons are needed.

INSULATOR FAILURE, STREAMERS

High Electric fields within the insulator interact with imperfections or impurities to initiate a local discharge. The initiated discharge continues to propagate because of amplification of the field strength (x100 in this case) at the sharp tip of the streamer. The amplified field ionizes molecules and the resulting plasma may be liberated to vacuum. The needle-like streamer continues to propagate as long as the field (x100) is sufficient to ionize at its tip, and plasma continues to be produced, escaping from the material where the streamer intersects the surface.

Energy from the electric field within the dielectric heats the plasma and the resulting pressure forces plasma to pass through the streamer to the exit point. The plasma collapses the electric field within itself. There is a radially directed electric field at the wall of the streamer tube which can erode the tube to larger diameter and add to the total plasma production. Recombination within the plasma may be of interest but has not been investigated. The dynamics of streamers is only now being studied, and the knowledge is not sufficient to help us predict what can happen with much certainty.

Externally monitored current pulses are very small when the plasma is collapsing only the fields within the streamer tube in the insulator. However, escaped plasma in the external vacuum is highly mobile and produces large current pulses if an electric field is present in the vacuum. Preventing streamers will prevent pulses.

- High E fields create Streamer type of discharge {not avalanche}.
- Streamers propagate as narrow tubes.
- Tubes of plasma escape the solid.
Pressure, Recombination, Erosion
- Escaped plasma collapses the external electric fields -- Large Pulses.
- Internal field collapse, small pulses

SOLUTION = Prevent Streamers !

PREVENT STREAMERS

Pulses are most generally eliminated, at least in dielectrics, by preventing streamers from developing. Experience has shown that prebreakdown pulses usually do not occur for applied fields below 10^4 V/cm. Since prebreakdown pulses are generally associated with small streamers in a local region of a dielectric near a void or imperfection, experiments imply that even with field amplification and field initiated defect growth, fields of 10^4 V/cm will not initiate a streamer.

For space radiation levels, the stopped charge induced fields will be kept to acceptable values if the dark conductivity within the insulator bulk is held to greater than 10^{-12} S/cm. For many insulators, this will occur only by modification of the material. Such modification is not well understood and its reliability in this environment is suspect. Such dark conductivity is the most important solution to the electric discharge anomaly problem,

Another solution is to make thin dielectrics, where they may serve a useful function, in place of thicker dielectrics. Firstly, it is not clear whether streamers will form and propagate for insulators thinner than one micron. Films of < 1000 angstrom thickness discharge or breakdown by other processes. Space radiations are not likely to ever induce sufficient fields in such thin insulators to initiate these other breakdown processes. Useful materials should be tested as a function of thickness using the standard electron beam technique.

In addition, thin films can have a higher conductivity than thick films because the mean free path before deep trapping may exceed the film thickness, and because the environment itself is the source of charge carriers. Thus, because of specific charge transport properties in the material, a thin film may not develop electric fields sufficiently strong to propagate a discharge.

Finally, thin films will have a larger average conductivity due to low energy particle bombardment and penetration, and thus are, again, less likely to support large electric fields.

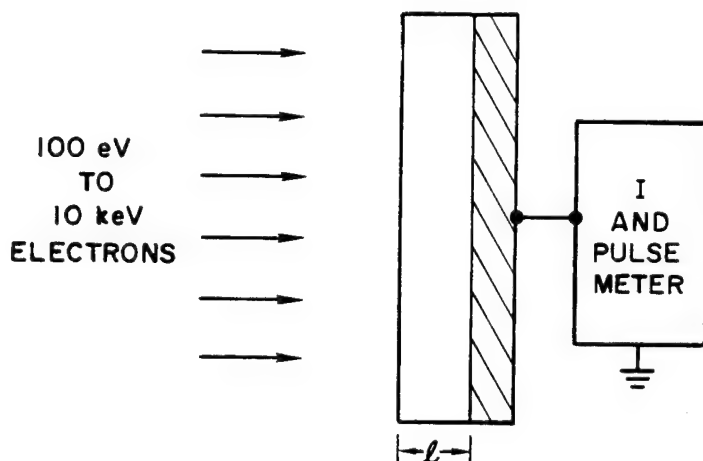
- Limit Fields to 10^4 V/cm
- Add Conductivity $> 10^{-12}$ S/cm
- Decrease Thickness < 1 micron ?
can streamers form ?
enhanced conductivity, mfp

THIN FILM EXPERIMENTS

Dielectrics in common use should be made as thin as possible. Even thick dielectrics can be made effectively thin for streamer purposes by burying a ground plane, say a 1000 Å thick metal film, below the dielectric surface at a depth, ℓ , such that discharges will not occur. The thickness dependence on ℓ for the onset of pulsing should be determined.

A number of spectra should be used to investigate a range of thicknesses ($1000\text{Å} < \ell < 10\text{ microns}$) in common dielectrics. For some spectra, a relatively large ℓ will be small enough to eliminate pulses while for other spectra only very thin dielectrics will eliminate pulses. We need a range of data in order to develop design guidelines.

This work should be performed taking into account that long term exposure to vacuum and low level radiation is likely to enhance the probability of pulsing.



- In Vacuum
- Vary Thickness, ℓ , from 1 to 25 microns
- At each ℓ , use 100 eV to 10 keV
- Find ℓ where pulses don't occur

DEVELOP BETTER MATERIALS

Conduction in polymeric dielectrics is becoming a well studied field. Useful concepts and information are steadily developing. Strongly conducting polymers are heavily studied for the obvious terrestrial applications, including superconductivity. The space community does not need to add to the fray in this discipline because progress is already rapid. But enhancing conductivity in good insulators, a need in space applications, sounds like nonsense to most people. The space community needs to help the work in this discipline (leaky insulators) because making normal dielectrics leaky is the best solution to the electric discharge anomaly problem.

The terrestrial applications include photoconductors and antistatic materials. A recent survey of possible new materials (this author with others published by AIAA) indicates that good spacecraft candidates include: polyvinylcarbazole, polyimide, polythiazyl, polypyrrole and polyacrylonitrile. But such materials require special development.

The rigors of the space environment are very different and usually more severe than on earth, at least for polymers. The material properties must be matched against these problems. Testing for space applications, at this time, does not take into consideration the effects of electric fields and radiation gradients on the materials. Electric fields will drive the reactants through the sample, over long time scales, producing different end of life results. Radiation chemistry in polymers must be addressed with respect to electric fields and with respect to effects on conductivity. This is a withered field which needs some fertilizer. As leaky materials are developed for space applications, proper testing is needed to predict the long term stability of the level of leakiness.

- Maintain Enough Conductivity
- Reliable > 10 Years
- Radiation Effects
- Other Damage
- Accelerated Testing

PARAMETERS TO TEST

Candidate materials (leaky insulators, paints, etc.) require realistic testing prior to launch. All the standard tests would be continued, of course. In addition, the following tests would need to be added:

- a) Amount and kinds of impurities desorbed while under UV, optical, proton and electron irradiation; all in the presence of both polarity electric fields up to 10^5 V/cm within the dielectric.
- b) Reaction rates at interfaces where electric fields accelerate flow of reactants to the interface. Perhaps a bond failure will be accelerated by this process.
- c) The relative levels of constituent atomic species emitted into vacuum under irradiation is an indication of the kinds of bond breaking created by radiation. This should be studied in the presence of extreme electric fields, $10^4 < E < 10^5$ V/cm.
- d) Radiation enhances conductivity by generating mobile charge carriers. Electric fields can sweep out such carriers or deposit them in sensitive regions. Alternatively, radiation can create traps and lower the number of mobile species. Transient conductivity might increase while dark conductivity decreases; both are important independently. The effects of electric fields on both forms of conductivity, over long radiation exposure times needs to be assessed for critical, actually used dielectrics.

- Typical such as strength, color, etc.
- Desorbed Impurities
- Desorbed Radicals
- Impurities, radicals react at rear attachment
- Atomic Species Emitted
- Long Term Dark Conductivity
- Field-Driven Reactant Currents

QUICK TESTS - DAYS

Some of the tests can be performed quickly, in a few days. Tests of the material to study its initial response, those effects which happen rapidly, can be done using electron or proton beams. Charging by the beams creates the electric fields. Irradiation at higher than space intensity speeds up some of the effects.

We should look at emission of atoms and molecules once the field has developed (10^5 rads) using mass spectrometers. Comparison to zero field and reverse field emissions should be made.

Conductivity, both dark and transient, should be made soon after and during irradiation. The method of measurement must quantitatively account for the fields of stopped charge to truly measure conductivity. Conductivity is likely to be a function of dose rate, accumulated dose, field strength, trap density, loss of ions to vacuum, radiation generated radicals, etc. Therefore, changes in conductivity should be noted over a period of time.

Electron emission should be measured immediately upon irradiation before the surface changes potential. Thereafter it should be measured periodically to see if radiation chemistry effects may have changed the surface. This should be done with differing internal fields so that the field driven radical effects can be discerned. Perhaps positive radicals do not change secondary emission whereas negative radicals do. Positive radicals are driven away from the surface by electron beam charging, so other methods (proton beam, rays, X-rays, applied bias) are required to send positive radicals to the surface.

SOME TESTS CAN BE DONE WITH ELECTRON BEAMS

- Initial Radical or Impurity Release, mass spectrometer
- Initial Test of Conductivity, S/cm
- Initial Electron Emission Level, secondary emission
- Above tests again later, after exposure to vacuum/radiation

LONG RANGE TEST PROBLEMS

There are long term problems, the interpretation of which lead us to further investigation of candidate materials. For many important processes, accelerated testing is very difficult. When we measure conductivity in these materials, what are we seeing? Very often we see short term mobility of radiation generated ions/radicals. Slowly, over time, the effect of these species can change by orders of magnitude. This is but one example of the classical materials ageing problem, addressed specifically to conductivity.

Conductivity caused by radicals and mobile ions can not be relied upon in space. There may not be an electrode on the dielectric surface to trap the mobile species inside. Yet charge exchange can occur, bonds broken, and thus the species can outgas. Only electronic carriers (holes, electrons, protons, ...) can be relied upon since space is a source of them, yet, they are not always sufficiently mobile. The measurement of conductivity must distinguish charged mass currents from electronic currents.

Charged mass (ions, etc.) must be carefully investigated for stability. Do they escape over time, do they bond and thus become inactive as carriers, are they a source of ageing/failure at interfaces, and are they driven to interfaces by electric fields? Temperature may play an important role. High temperatures may not be bad as it can allow annealing of damage created by radiation. All of these things need to be investigated under the influence of electric fields which can drive reactions into or out of specific regions of the material.

- Do conducting ions escape ?
- Do radicals escape ?
- Do radicals accumulate and change the material ?
- Does electric field drive atoms, radicals or impurities ?
- Slow Chemistry, field enhanced
- Conductivity Increases or Decreases ?
- Which is worse, hot or cold ?

ACCELERATED LIFE TESTS

Man-made leaky dielectrics form an essentially new class of material. Requiring them to have specific levels of conductivity over long times in difficult environments is an unusual requirement. Semiconductors are disrupted in the space environment by the creation, over long times, of displaced atom defects. Relative to insulators, semiconductors have very high concentrations of charge carriers, so the space environment does not appreciably alter the carrier concentration. In insulators, however, the environment can severely alter the charge carrier density as well as the material structure and carrier transport properties. There is little good information on carrier transport properties, nor on structural defects relating to carrier transport, in insulators.

We can not accelerate testing on leaky dielectrics, at this time, because we can not describe the physics/chemistry well enough to use short tests to predict long term behavior. Running an electron beam for a year is not practical, but the same effects, including generation of stopped charge fields, can be performed using radioisotopes such as cesium or cobalt. The long term exposure can be interrupted, perhaps monthly, to measure the properties of the material. Generally, electron beams will be the best probe to measure the properties.

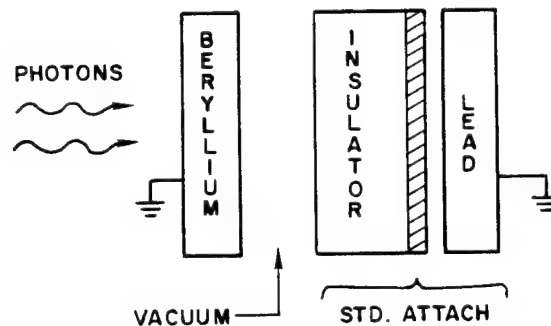
- Impossible, but let's try.
How about 1 year for 10 year life ?
- Use cobalt 60, cesium 137, or reactor
- Test at: 10^4 rads/hr. \rightarrow 10^{10} rads
 10^5 rads/hr. \rightarrow 10^9 rads
- Use high atomic number interface to produce large E field
- Periodically test for parameters using electron beam:
 - conductivity/breakdown
 - secondary emission
 - radical emission

CO 60 OR CS 137 TESTS

This is a method for creating large electric fields in insulators using gamma rays. I have created lichtenberg discharges using this technique. Windows in cobalt 60 cells have broken due to electrical discharges caused by an analog to this structure.

The beryllium, along with air in front, creates a strongly forward directed flux of high energy electrons, mostly compton electrons. Beryllium thicknesses of 3 mm to 10 mm are fine. The lead creates a flux of photo and compton electrons, a reasonable proportion of which are directed backwards into the insulator. Breakdown strength fields can be attained after as little as 10^5 roentgens exposure in this configuration. On the other hand, if carbon were to surround a polymeric insulator (carbon based, not silicon based) then large E fields would never be attained.

One can test the long term response of insulators to the combined action of radiation, vacuum and electric fields. Even a surface bond, such as glue or evaporated metal can be tested, as shown. The change in material properties would be monitored primarily by periodically removing the sample for short periods of testing. Electron beams would be a good probe to measure properties such as conductivity after the above radioisotope exposures are performed.



- Vacuum allows escape of mobile species.
- Be and Pb create divergent electron current, negative charge build-up.
- $> 10^5$ V/cm in good insulators
- Also tests "glue" or attach

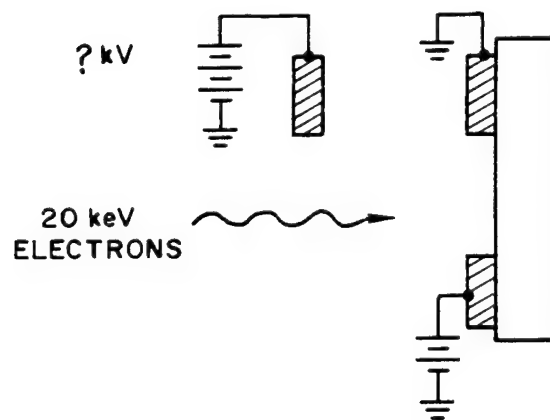
NEW PROBLEM

Some initial experiments have been performed by this author and coworkers which indicate that radiation can initiate electrical breakdown in capacitor structures. The process had been neglected because generalized "irradiate it and see what happens" experiments over the years found no statistically significant change in the probability of breakdown for insulators in or out of radiation.

We find that by choosing the radiation spectrum based on the electrode/-insulator geometry, one can quickly initiate full breakdown for some geometries. Much more work needs to be done. These results are in the process of writing and hopefully will appear in the literature next year. The electric fields in the insulator are caused by the combination of applied (power supply) voltage and deep charge induced fields. When the combined field initiates and propagates a streamer which spans the dielectric, then the electrodes are shorted by the plasma in the streamer, and full breakdown can occur. Space and ground experiments need to be performed.

Dielectric Discharges Next to a Power Line - Will this arc the power supply by initiating a wire to wire plasma arc ?

EXPERIMENT



Much more work needs to be done, but initial answer is YES !

RECOMMENDATIONS

1. Perform ground tests on dielectrics for the combined effects of total dose and electric fields upon the properties critical for surface charging calculations (such as in NASCAP).
2. Perform ground tests for long term effects of dose and electric field on conductivity of insulators used in space. Such measurements would be best if performed with electron beams as the measurement probe.
3. Perform space experiments on the long term conductivity of insulators in space. Satellite surface insulators as well as those inside the structure should be tested by periodically measuring the current between electrodes as a function of voltage applied. Interdigitated electrodes are preferred. Electron gun measurements would be ideal but would make the experiment much more complicated and limit the number of samples which can be tested.
4. With constant applied bias, monitor exposed dielectrics for electrode to electrode arcing caused by streamer propagation completely spanning the space between electrodes. Perform ground experiments first in order to scope the problem, and then design space experiments based on those experiments.
5. Develop new semi-insulating polymers for space applications. Several approaches look promising and some work is in progress. These materials must be tested for long term exposure to see if the conductivity remains stable. Space and ground tests are needed, remembering to be especially careful to test under all internal electric field conditions: positive, zero and negative fields adjacent to the surface.
6. Perform both space and ground experiments when a power supply produces the electric fields in the space adjacent to a dielectric. Irradiate the dielectric to create discharge pulses, and look for large currents to the power supply lines. Is there some power supply voltage which sustains an arc, once initiated?
7. Without dielectrics present, perform ground experiments to show that metal to metal arcs can, or cannot, occur. For typical spacecraft potentials, I predict that they cannot occur.
8. Perform ground tests of the thin film hypothesis; that very thin films can not produce an internal discharge and thus can be used even though their bulk conductivity is too low for thick film applications. Space tests would follow the ground tests, if successful.
9. Develop accelerated testing procedures using radioisotopes where one year exposure is not too expensive. These ground tests should be performed on existing insulators as well as on those developed for future use.
10. Determine the spectral distribution of radio frequency noise generated by irradiated composites.

BIBLIOGRAPHY

This briefing focuses on a broad range of materials and effects. The concepts come from exposure to many works and people from several communities. A concise reference list cannot be composed. Instead, the following basic concepts can be found by study of the appropriate literature.

1. Discharge pulses: IEEE Trans. Nuc. Sci. December issues from 1975 to the present. Proceedings of the Spacecraft Charging Conferences which appear as NASA documents CP-2071 (1978), TMX-73537 (1977), CP-2182 (1980), and CP-2359 (1983). The NTIS numbers for the NASA documents respectively are AD/A084626, AD/A045459, AD/A114426, and N85-22470.
2. Dielectric breakdown: IEEE Trans. Elec. Ins. and various proceedings of the international symposium on discharge and electrical insulation in vacuum.
3. Development of leaky materials and review of test procedures: Spacecraft Dielectric Material Properties and Spacecraft Charging by A. R. Frederickson et al., AIAA Progress in Astronautics and Aeronautics Vol. 107 (1986). This is a brief review and a compilation of literature citations, over 200 of them.
4. Electric fields in irradiated insulators. Same literature listed in 1. above.

AN OVERVIEW OF CHARGING ENVIRONMENTS

*S. B. Gabriel and H. B. Garrett
Jet Propulsion Laboratory
California Institute Of Technology
Pasadena, California*

NATURAL ENVIRONMENTS THAT CONTRIBUTE TO CHARGING

This paper presents a brief synopsis of the natural environments that play a role in spacecraft charging. Environments that cause both surface and internal charging are discussed along with the mechanisms involved. The geosynchronous and low altitude (< 1000 km) regions of the Earth's magnetosphere/ionosphere are considered and simple descriptions of each environment presented. As material properties are critical to the charging process, definition of material properties important to charging, which can be affected by the environment, will also be described. Finally, several space experiments are proposed that would help fill the gaps in our knowledge of the performance of materials in a charging environment.

Figure 1 lists the major natural environments that contribute to charging. This list is not comprehensive and has been selected on the basis of those environments that interact directly with surfaces (surface charging) or through surfaces (internal charging) to cause the production of high electric fields. Because of this rather restricted definition, environments such as contaminant molecules, x-rays, electron/ion beams, and cosmic rays have not been included.

Surface:

- Thermal Plasma
- High Energy Electrons (1-100 keV)
- UV/EUV Radiation
- Magnetic Field
- Neutral Particles

● Internal:

- High Energy Electrons (≥ 100 keV)

FIGURE 1

ROLE OF ENVIRONMENTS IN CHARGING

Figures 2 a) and b) show schematically the interactions between the environments and the surface that cause surface and internal charging, respectively. In surface charging, the process is governed by current balance (1) (i.e. in the steady-state, the net sum of all the currents to the surface must be zero and the equilibrium potential will satisfy this condition). To first order these currents comprise the currents from the thermal or low energy plasma (including any ram ions), the high energy electrons and ions, the secondary electrons emitted by impacting high energy electrons and ions and photo-electrons released due to the incident UV/EUV radiation. The presence of a magnetic field and space charge can affect the escape of low energy secondary/photoelectrons.

For internal charging, the primary process is the build up of negative charge (electrons) in or on isolated surfaces inside the spacecraft body caused by penetration of the external surfaces by high energy (> 100 keV) electrons (2). As shown in the figure, charge can accumulate on/in ungrounded conductors or insulators and cables as well. This charge can produce high electric fields and induce breakdown.

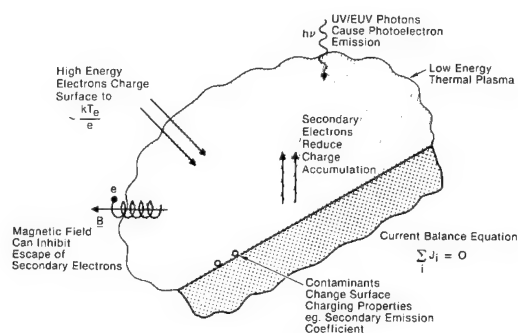


FIGURE 2a

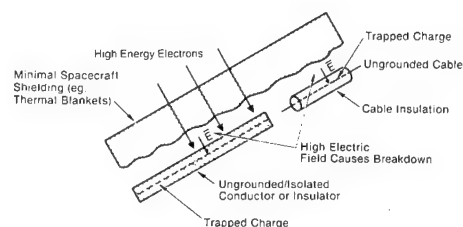


FIGURE 2b

THERMAL PLASMA

The presence of a high density, low energy plasma can significantly affect surface charging. Qualitatively, this can be understood by thinking of this plasma as a good conductor which "drains off" any charge accumulation thus preventing high surface potentials. Figures 3a) and b) (3) are presented to illustrate that the thermal plasma electron density varies by many orders of magnitude in the magnetosphere/ionosphere regions. At one extreme, in the geosynchronous region, densities are as low as 1 cm^{-3} while at 300 km in the F region they can be as high as 10^6 cm^{-3} . These large differences in density have 2 major implications:

- 1) At low altitudes ($< 1000 \text{ km}$), even in the presence of high energy electron population, ($\sim 10 \text{ keV}$) such as the precipitating electrons in the high latitude auroral oval regions, high spacecraft potentials are unlikely to occur.
- 2) Charging calculations are quite different in the two regions. At geosynchronous altitudes the ratio of characteristic dimension of the spacecraft to the Debye length (R) is $\ll 1$ whereas at 300 km the reverse is true (i.e. $R \geq 1$), leading to the so-called thick and thin sheath approximations. In the former, space-charge effects can be neglected (ie. the charge density in the sheath region can be set to 0) while the latter necessitates the inclusion of space-charge effects.

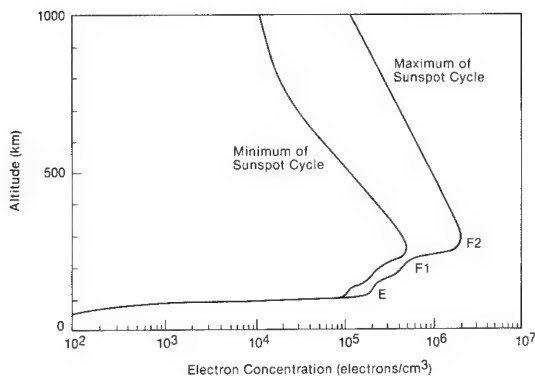


FIGURE 3a

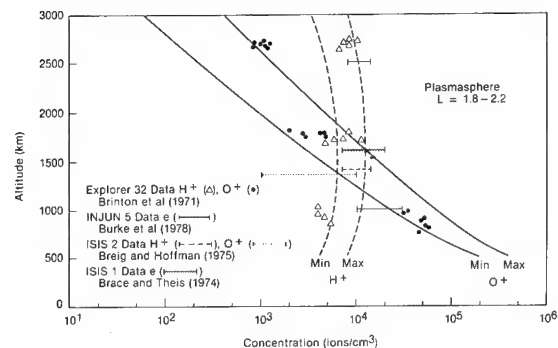


FIGURE 3b

HIGH ENERGY ELECTRONS

Figures 4a) and b) show representative spectra for the high energy electron population at geosynchronous (4) orbit and for a discrete auroral arc (5), respectively. With respect to surface charging, the most notable feature is the presence in both cases of electrons with energies of 10 keV and greater; typically one can describe these populations in terms of a Maxwellian distribution function with a characteristic temperature, T_e . Simple charging analysis demonstrates that, in the absence of significant thermal plasma and a photoelectron current, the spacecraft potential is directly proportional to the mean temperature of the electrons. As electron temperatures can vary from 1-20 keV, potentials of 1-20 kV are possible and indeed, have been observed.

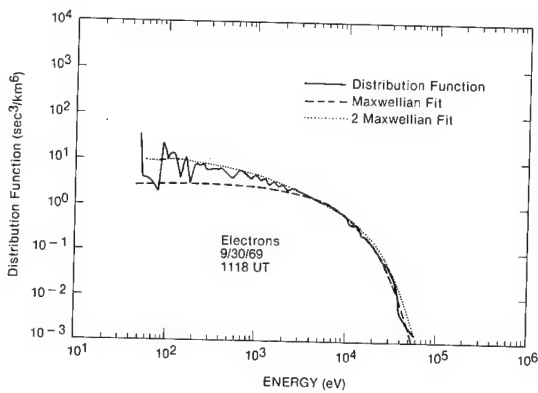


FIGURE 4a

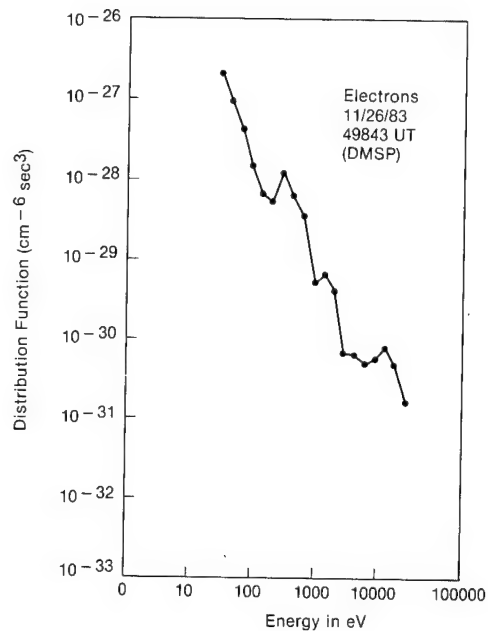


FIGURE 4b

The photoelectron current, emitted from the surface by the impact of the incident high energy photons, can make an important contribution to the overall current balance. This is particularly true at higher altitudes, where, for example, at geosynchronous altitude in the absence of a significant thermal plasma, the photoelectron current plays a dominant role. The photoelectron current is a function of satellite material, solar flux, solar incidence angle and satellite potential (6). In figure 5, adapted from reference 7, is a composite plot of: $W(E)$, the electron yield per photon; $S(E)$, the solar flux; and their product, $H(E)$, the total photoelectron yield, as a function of energy, E , for aluminum oxide.

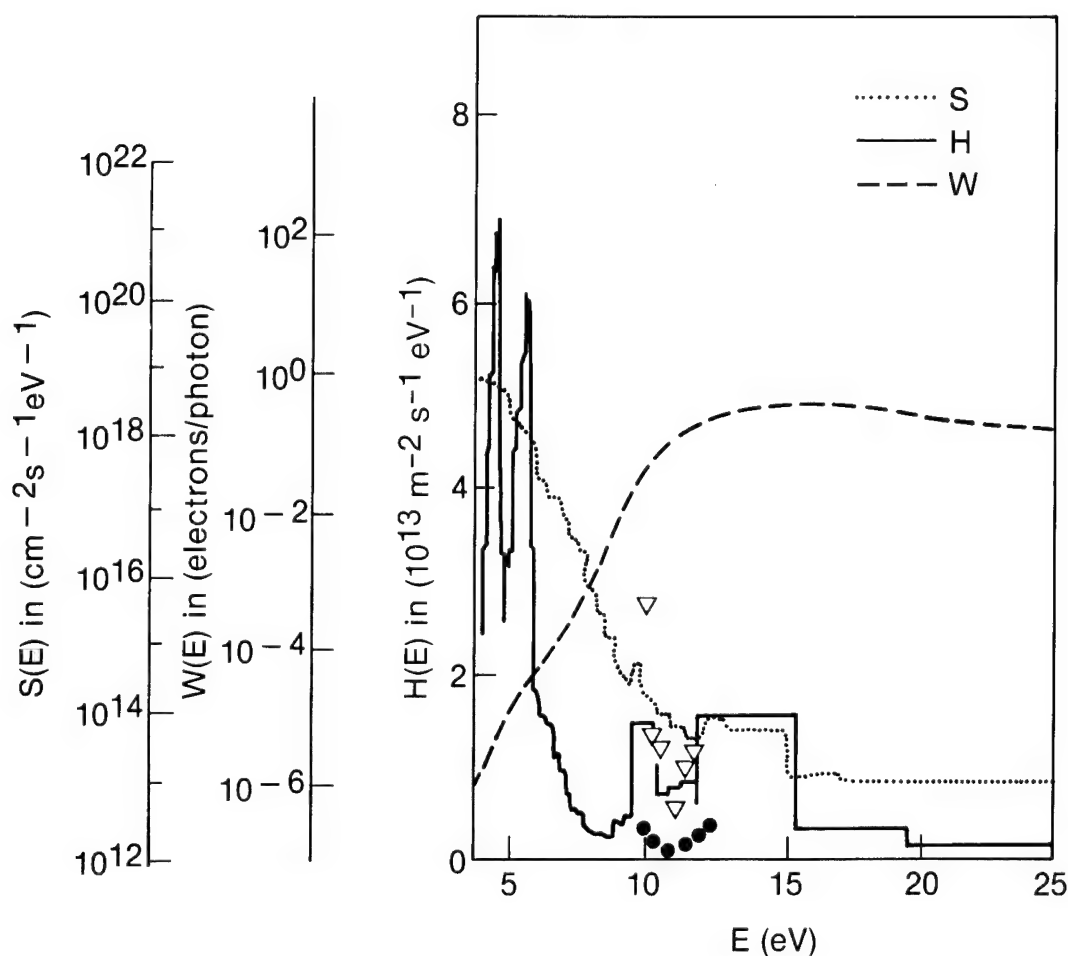


FIGURE 5

MAGNETIC FIELD

The Earth's magnetic field can be approximated by a magnetic dipole located near the centre of the Earth. The dipole moment is $M = 0.312 \text{ G } R_E^3$, where R_E is the radius of the Earth, and the dipole is directed so that the magnetic south pole on the Earth's surface is located in northern Greenland (geographic coordinates: 78.5° N , 291° E). The spatial distribution of the dipolar magnetic field strength beyond the surface of the Earth is given by (8):

$$B = B_E \left(\frac{R}{R_E} \right)^{-3} \frac{[4 - 3 \cos^2 \lambda]^{1/2}}{\cos^6 \lambda}$$

where R is the radial distance measured from the center of the Earth, $B_E = 0.312 \text{ G}$ is the equatorial field at $R = R_E$, and λ is the magnetic latitude.

Figure 6 shows a schematic of the Earth's magneto/ionosphere indicating the various domains. The solid lines represent the magnetic field lines which can be seen to be distorted from a purely dipolar pattern due to the interaction with the solar wind. In terms of charging environments, the magnetic field can be viewed as playing essentially three roles: 1) it is a major factor in determining the shape and location of the charging regions (i.e. the domains shown in figure 6); 2) it can affect the escape of photoelectrons or secondary electrons emitted from the surface (9) 3) it can introduce anisotropy in particle fluxes.

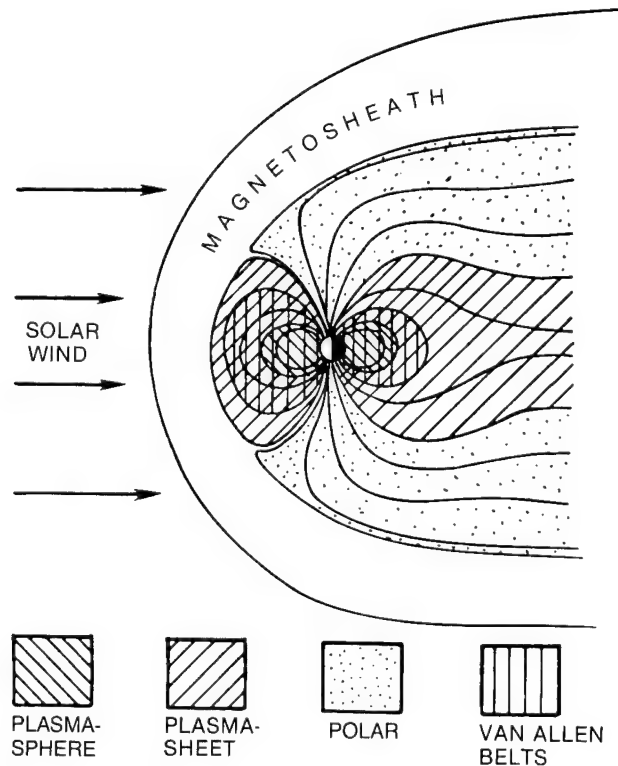


FIGURE 6

NEUTRAL ATMOSPHERE

Figure 7 shows the neutral atmosphere environment up to an altitude of 1000 km. The important feature of this environment is that the neutral density is approximately two to three orders of magnitude higher than the electron/ion density (i.e. the atmosphere is weakly ionized). At higher altitudes where the mean free path for collisions between neutrals and electrons is very large, collisionless probe theory can be applied to surface charging calculations, while at lower altitudes, collisional theory is probably needed and ionization may be of importance. Little attention has been paid to charging calculations at altitudes between 100-200 km where the thermal plasma density is low but where auroral precipitations of high energy electrons are still found. This may be because it has been assumed that the simultaneous increase in the local thermal plasma density caused by the precipitating auroral electrons is of sufficient magnitude to prevent significant charging. In addition, at these altitudes, satellites cannot orbit for long periods due to aerodynamic drag. However, with the advent of the proposed tethered satellite systems (e.g. TSS2) which will be able to trail a downward - deployed platform to altitudes of about 100 km, this problem warrants more detailed study.

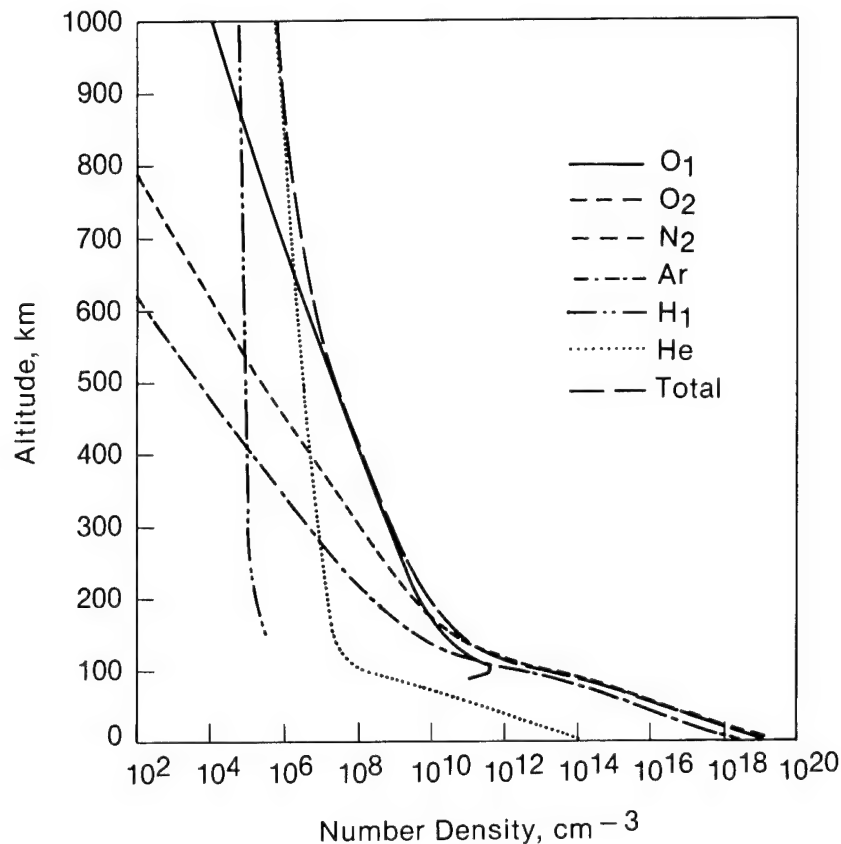


FIGURE 7

INTERNAL CHARGING
HIGH ENERGY TRAPPED ELECTRONS

Figure 8 (10) shows empirical radiation belt electron fluxes at $L = 1.4$. The important feature to note here, as far as internal charging is concerned, is the presence of significant fluxes at energies between 0.1 and 1.0 MeV. These energetic electrons can penetrate lightly shielded parts of the spacecraft and accumulate on ungrounded cables, conductors or insulators, located inside the spacecraft. If the resultant electric field rises to a high enough value, breakdown can occur. The ranges of 0.1 and 1.0 MeV electrons in aluminum are about 3 and 70 mils, respectively.

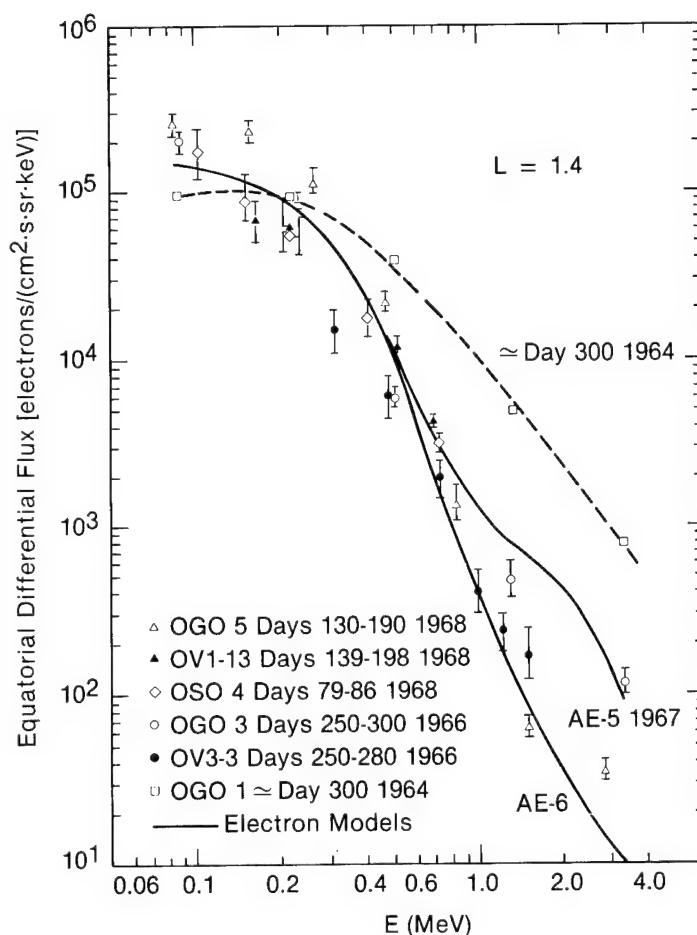


FIGURE 8

TIME VARIATIONS OF
GEOPHYSICAL PHENOMENA

Nearly all of the charging environments described previously show dynamic variations both temporally and spatially. Consequently, in many cases, modelling of an environment has to be done statistically with average and worst case environments being defined. Further, the environments are not independent but form a coupled and highly-complex interacting system. Figure 9 shows order of magnitude time variations for some of the phenomena associated with charging environments.

<u>Geophysical Event</u>	<u>Time Period</u>
1. Solar Cycle	11 Years
2. Geomagnetic Storms	1-10 Days
3. Substorms	1-3 Hours
4. Magnetic Pulsations	Sec-Min
5. Plasma Boundary Crossings	Sec-Min
6. Plasma Waves	mS - μ S

FIGURE 9

POTENTIAL IN SITU MATERIAL CHARGING EXPERIMENTS

For many of the adverse interactions between the space environments and spacecraft materials described here, the critical parameters required to accurately model the physical response are currently lacking or poorly known. In particular, for spacecraft charging, 6 key parameters are required as a function of material and, as some of the interactions result in long term variations in properties, time. These are

- 1) Bulk and surface electrical properties
- 2) Secondary emission coefficients for electrons and ions
- 3) Backscatter properties for electrons
- 4) Photoemission properties
- 5) Sputtering characteristics
- 6) Arc breakdown properties

To date, these properties are known only through ground tests or, in situ, by indirect methods--primarily through variations in parameters to fit charging observations. Given the hypothesized variations over time of these parameters due to radiation damage, contamination, etc., in situ measurements are vital to a proper understanding of how materials behave over the long term in a charging environment.

POTENTIAL IN SITU MATERIAL
CHARGING EXPERIMENTS

Three experiments are presented in Figure 10 that would make possible measurements of the in situ material properties relevant to spacecraft charging. First, for surface charging it is necessary to study the in situ secondary, backscatter, and photoemission properties. Although ground experiments are useful for this purpose, it is not likely that the in situ surfaces will actually retain their ground values following long term exposure to space. This experiment (referred to here as the Electrical Properties Degradation experiment) would alternately expose samples to the ambient environment and then to a probe capable of directly measuring the secondary emitted electrons and ions--one potential configuration would be a carousel tray for the samples with a commercially available secondary emission probe. The second experiment would measure natural and, if necessary, simulated surface arcs with the objective of locating them on the test surface and estimating the conducted and radiated emissions (referred to here as the ElectroStatic Discharge experiment). Such instruments have been flown in the past on SCATHA but, for various reasons, did not return sufficient information on the arc discharges to unambiguously define their characteristics or their locations.

- Electrical Properties Degradation Experiment
 - Secondary Emission Properties
 - Photoemission Rate
 - Surface Electrical Properties
- Electrostatic Discharge Experiment
 - Arc Properties
 - Surface Location
 - Surface Conditions at Time of Arc
 - Surface Damage
- Internal Discharge Monitor
 - Internal Arc Characteristics
 - Material Bulk Property Changes

FIGURE 10

POTENTIAL IN SITU MATERIAL
CHARGING EXPERIMENTS

The third experiment, the Internal Discharge Monitor, is planned to fly on the CRRES spacecraft in 1990 in a simplified form to monitor arc discharges on samples inside a protected tray assembly. As in the case of CRRES, more advanced forms of this instrument will also need to be flown through the radiation belts to obtain useful information in a short time period. All 3 instruments would need supporting environmental sensors to monitor the natural environment--particularly the relevant particle and EUV fluxes. Finally, while the EPD and ESD instruments might be suitable for low-altitude, short duration missions (although the longer the exposure, the better), the IDM will clearly require multi-year missions.

CONCLUSIONS

In this paper we have identified and provided brief descriptions of the major natural environments that contribute to charging. The intent has been to provide an overall picture of the charging environment but in a very short space. The result is a necessarily oversimplified and idealized view of a highly complex interdependent physical system; in essence, only allusions have been made to some of the realistic features such as temporal variability and particle flux anisotropies.

The importance of surface properties in determining charging levels makes it essential to measure these properties in the real environment. However, to correlate charging levels with the environment and surface characteristics, simultaneous monitoring of the environment will also be required.

REFERENCES

- 1) H. B. Garrett, "The Charging of Spacecraft Surfaces", *Reviews of Geophysics and Space Physics*, Vol. 19, 4, pp577-616, 1981.
- 2) A. R. Frederickson, "Radiation Induced Dielectric Charging", *Space Systems and Their Interactions with Earth's Space Environment*, ed. by H. B. Garrett and C. P. Pike, vol. 71, *Progress in Astronautics and Aeronautics*, 1980.
- 3) Chiu, Y. J. et al., "An Equilibrium Model of Plasmaspheric Composition and Density", *J. Geophys. Res.*, vol. 84, 1979, pp 909-916.
- 4) Garrett, H. B. and Spitale, G. C., "Magnetospheric Plasma Modelling (0- 100 keV)", *Journal of Spacecraft and Rockets*, vol. 22, 3, p231, 1985.
- 5) Gussenhoven, M. S. et al., "High-level spacecraft charging in the low-altitude polar environment", *J. Geophys. Res.*, 90, 11, 009, 1985.
- 6) Lucas, A. A., "Fundamental Processes in Particle and Photon Interactions with Surfaces", *Photon and Particle Interactions with Surfaces in Space*, ed. by R. J. L. Grard, D. Reidel, Hingham, MA, pp3-21, 1973.
- 7) Grard, R. J. L., "Properties of the satellite photoelectron sheath derived from photoemission laboratory measurements", *J. Geophys. Res.*, 78, pp 2885-2906, 1973.
- 8) Spjeldvik, W. N. and Rothwell, P. L. "The Earth's Radiation Belts", AFGL-7R-83-0240, 1983.
- 9) Laframboise, J. G., "Calculation of Escape Consents of Electrons Emitted from Negatively Charged Spacecraft Surfaces in a Magnetic Field", *J. Geophys. Res.*, 93, A3, pp1933-1943, 1988.
- 10) Teague, M. J. and Vette, J. I., "The Inner Zone Electron Model AE-5, NSSDC/WDC -A-R&S 72-10, NASA, Goddard Space Flight Center, Maryland (1972).

SURFACE PHENOMENA IN PLASMA ENVIRONMENTS*

C. K. PURVIS
D. C. FERGUSON
NASA LEWIS RESEARCH CENTER
CLEVELAND, OHIO

*Original figures not available at time of publication.

PLASMA-SYSTEM INTERACTIONS PHENOMENA

From the viewpoint of plasma interactions, a space system may be regarded as a collection of conducting and insulating surfaces with active power generation and distribution systems in motion through the ionospheric or magnetospheric plasma and the Earth's magnetic field. The system comes into electrical equilibrium with the plasma by acquiring surface potentials such that the net current to the system as a whole, and to individual insulating surfaces is zero. This equilibration establishes the system and surface potentials relative to the plasma. It is a dynamic equilibrium, and the potentials will change whenever there is a change in the current densities to surfaces or the system. Higher energy environment components (≥ 50 KeV) also cause charge deposition in insulators and radiation damage. These aspects are considered by others in this workshop and will not be discussed further here.

A SPACE SYSTEM IS A COLLECTION OF CONDUCTING AND INSULATING SURFACES WITH ACTIVE POWER GENERATION AND DISTRIBUTION COMPONENTS MOVING THROUGH AN ELECTRICALLY CHARGED "GAS" AND THE EARTH'S MAGNETIC FIELD.

- o SYSTEM EQUILIBRATES ELECTRICALLY WITH PLASMA
 - SUM OF CURRENTS = 0
 - "GLOBAL" FOR CONDUCTORS (MUST INCLUDE INDUCED $V_{B.L}$ POTENTIALS)
 - POINT-BY-POINT FOR INSULATION
- o ESTABLISHES SYSTEM AND SURFACE POTENTIALS RELATIVE TO PLASMA
- o EQUILIBRIUM IS DYNAMIC: CHANGES WITH ANY CHANGE IN CURRENT DENSITIES
 - NATURAL ENVIRONMENT
 - ORBITAL POSITION/ORIENTATION
 - EFFLUX
 - "APPLIED" VOLTAGE VARIATIONS
 - PARTICLE EMISSION BY VEHICLE
 - ARCING, IONIZATION IN SHEATH
 - ETC, ETC

HIGHER ENERGY ENVIRONMENT COMPONENTS ALSO CAUSE CHARGE DEPOSITION IN INSULATORS AND RADIATION DAMAGE

SYSTEM DRIVERS FOR PLASMA INTERACTIONS

The potentials and fields around orbital systems depend on the material properties which contribute to the currents which must be balanced (conductivities, secondary and photoelectron yields, dielectric properties, sputter yields, thickness of films, etc.), on local and overall geometry, and on electrical configuration, as well as on the plasma properties. Included in "local geometry" are the properties of adjacent materials, the presence of edges or holes in insulation, and local electric and magnetic fields produced by the system itself or by the equilibration process. Overall geometry includes the system and subsystem size and shape, and the orientation of surfaces to the system's orbital velocity vector, the Earth's magnetic field, and the Sun. Electrical configuration includes the system-produced voltage and current levels and frequencies, the insulation (or lack of same) of conductors from the plasma, and the electrical grounding scheme of the system. The importance of these various factors in determining the potential and field structures around the system will depend on the orbital altitude and inclination.

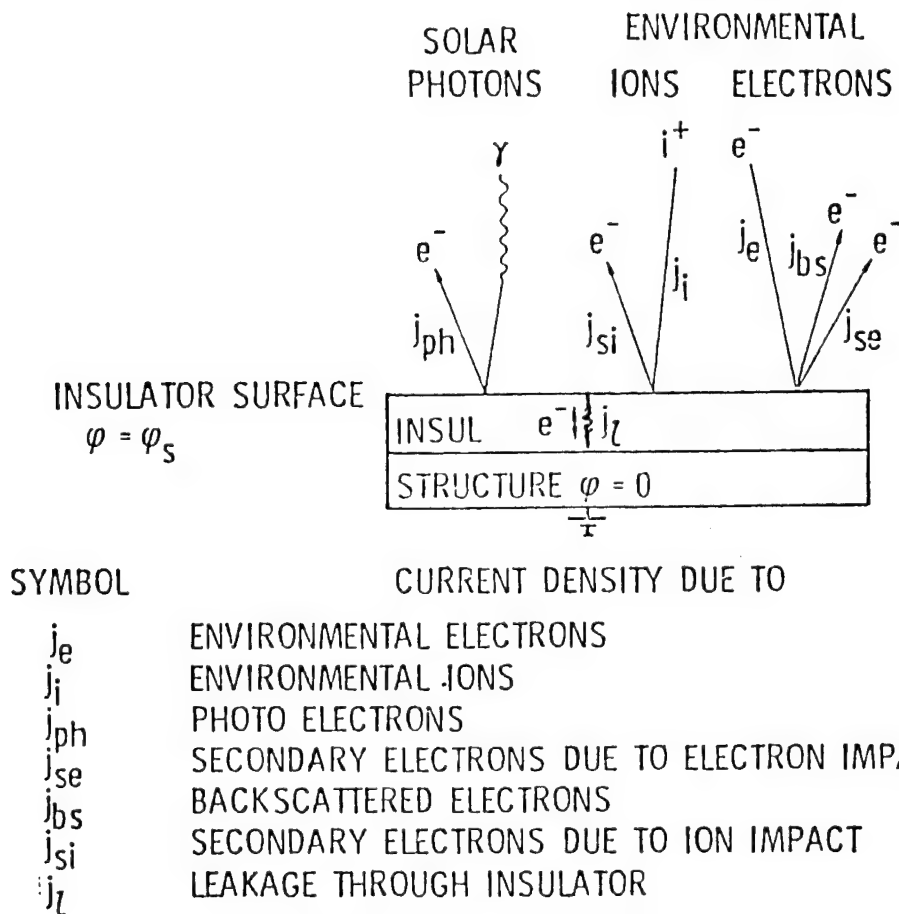
POTENTIALS AND FIELDS AROUND ORBITAL SYSTEMS DEPEND ON

- o MATERIAL PROPERTIES OF STRUCTURE AND SURFACES
 - CONDUCTIVITIES/RESISTIVITIES
 - SECONDARY AND PHOTOYIELDS
 - DIELECTRIC CONSTANT AND STRENGTH
 - CHEMISTRY
 - THICKNESS
- o GEOMETRY
 - LOCAL SURROUNDINGS
 - * ADJACENT MATERIALS
 - * EDGES, HOLES
 - * LOCAL \vec{E} AND \vec{B} FIELDS
 - OVERALL
 - * SYSTEM SUBSYSTEM SIZE
 - * ORIENTATION TO \vec{v}
 - * ORIENTATION TO \vec{B}_E
 - * ORIENTATION TO SUN (GEO)
- o ELECTRICAL CONFIGURATION
 - SYSTEM-PRODUCED VOLTAGE AND CURRENT LEVELS AND FREQUENCIES
 - * EXPOSED AND INSULATED
 - GROUNDING SCHEME

CHARGING RESPONSE

The charging response of a surface in a plasma may be illustrated by considering the simple case of an insulating surface element, and the current densities which must be balanced to obtain net zero current, as is shown in the figure. The sources of current density to the surface element are environmental electrons and ions, secondary and backscattered electrons produced by these primaries, leakage current through the insulator, and, if sunlit, photoelectrons. For an isolated surface in a plasma, i.e., ignoring photoelectrons and leakage current, the rule of thumb is that the surface will charge negatively to a potential of the order of the electron temperature. The surface charges negatively because the electrons are much less massive than the ions, and consequently their flux is larger. This assumes that the electron and ion temperatures are approximately the same, which is true within a factor of about two for the orbital environments considered here.

SIMPLE CASE; CURRENT DENSITIES TO INSULATING SURFACE ELEMENT



EQUILIBRIUM CONDITION:

$$j_{net} = \sum_n j_n = 0$$

CHARGING RESPONSE (Continued)

Thus, an isolated, shadowed body in a geosynchronous substorm environment, in which the electron temperatures are in the 10-15 KeV range, is expected to charge to kilovolts. This has been observed on the ATS-5, ATS-6 and Spacecraft Charging at High Altitudes (SCATHA) satellites in eclipse. Actually, these satellites charged to something less than the electron temperature because of secondary electron emission, but potentials of several kilovolts in eclipse were frequently observed; the record event charged ATS-6 to -19KV. In geosynchronous orbit, photoemission from sunlit surfaces is an important determinant of potentials because photoelectron current densities are of order 10^{-9} A/cm^2 , while environmental electron current densities are typically an order of magnitude less. Thus, in sunlight, the shadowed insulating surfaces of a spacecraft charge negatively while the sunlit surfaces stay near plasma potential until the negative potential on the shaded surfaces becomes large enough to form potential barriers on the sunlit side which suppress the emission of the low energy ($\sim 2 \text{ eV}$) photoelectrons, allowing the entire spacecraft to begin charging negatively. This process allows the development of kilovolt level differential potentials between various surfaces, with subsequent arc discharging and disruption of spacecraft systems as a consequence. In contrast to the geosynchronous case, the ionospheric plasma at low Earth orbit (LEO) has electron temperatures of order .1 eV, and electron current densities of order 10^{-5} A/cm^2 , so an isolated surface in this environment is expected to be within a volt of plasma potential, and photoemission does not play a large role. Another difference between the LEO and geosynchronous Earth orbit (GEO) cases is that the GEO plasma is so tenuous that potentials of a GEO system may be computed using Laplace's equation (i.e., ignoring space charge effects in the plasma) with appropriate boundary conditions on the surfaces and expressions for the current densities. However, in LEO, space charge plays an important role in sheath formation.

SHEATH RADIUS INCLUDING ELECTRON MOTION

A body immersed in a plasma will disturb the plasma in its vicinity. The region near the body in which the electric field is non-zero is the sheath. For a floating body, the scale size over which the plasma screens the charge on the body is the Debye length. For LEO plasmas the Debye length is on the order of cm. If a potential is applied to the body, the sheath dimension will be larger, and net current will be collected by the body. The figure illustrates a spherical space-charge limited sheath for the case of the applied potential, ϕ much larger than the electron and ion temperatures (θ_e and θ_i , respectively). This sphere is not in equilibrium with the plasma, but is collecting net electron current from it.

SPACE-CHARGE LIMITED SPHERICAL PROBE THEORY

sheath equations

$$\nabla^2 \phi = -\frac{\rho}{\epsilon_0}$$

$$\rho = e (n_i - n_e)$$

$$n_i = n_0 \exp(-\phi / \theta_i) \approx 0$$

$$n_e = \frac{j_e}{e v_e}$$

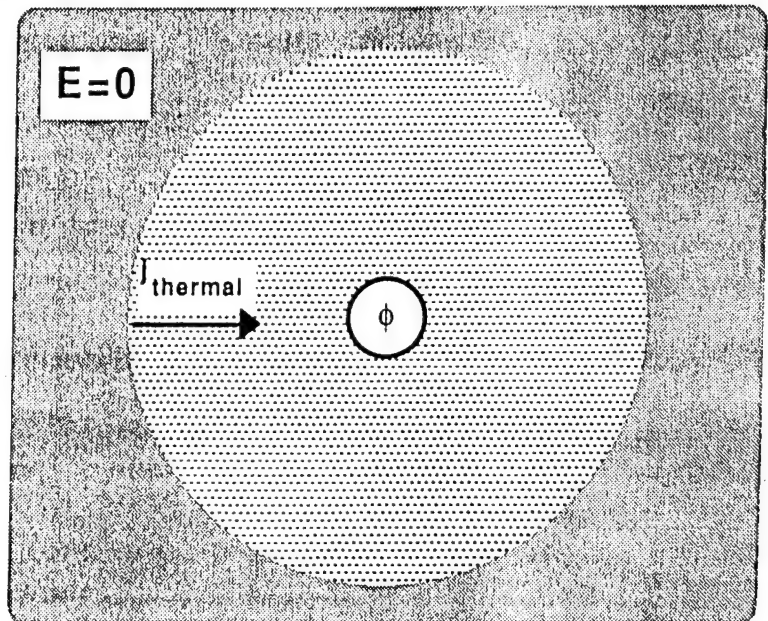
boundary conditions

$$\phi(r) = \phi_{\text{sphere}} \quad \phi(R_{\text{sheath}}) \approx \theta_e$$

$$j_e(R_{\text{sheath}}) \approx j_{\text{thermal}}$$

result

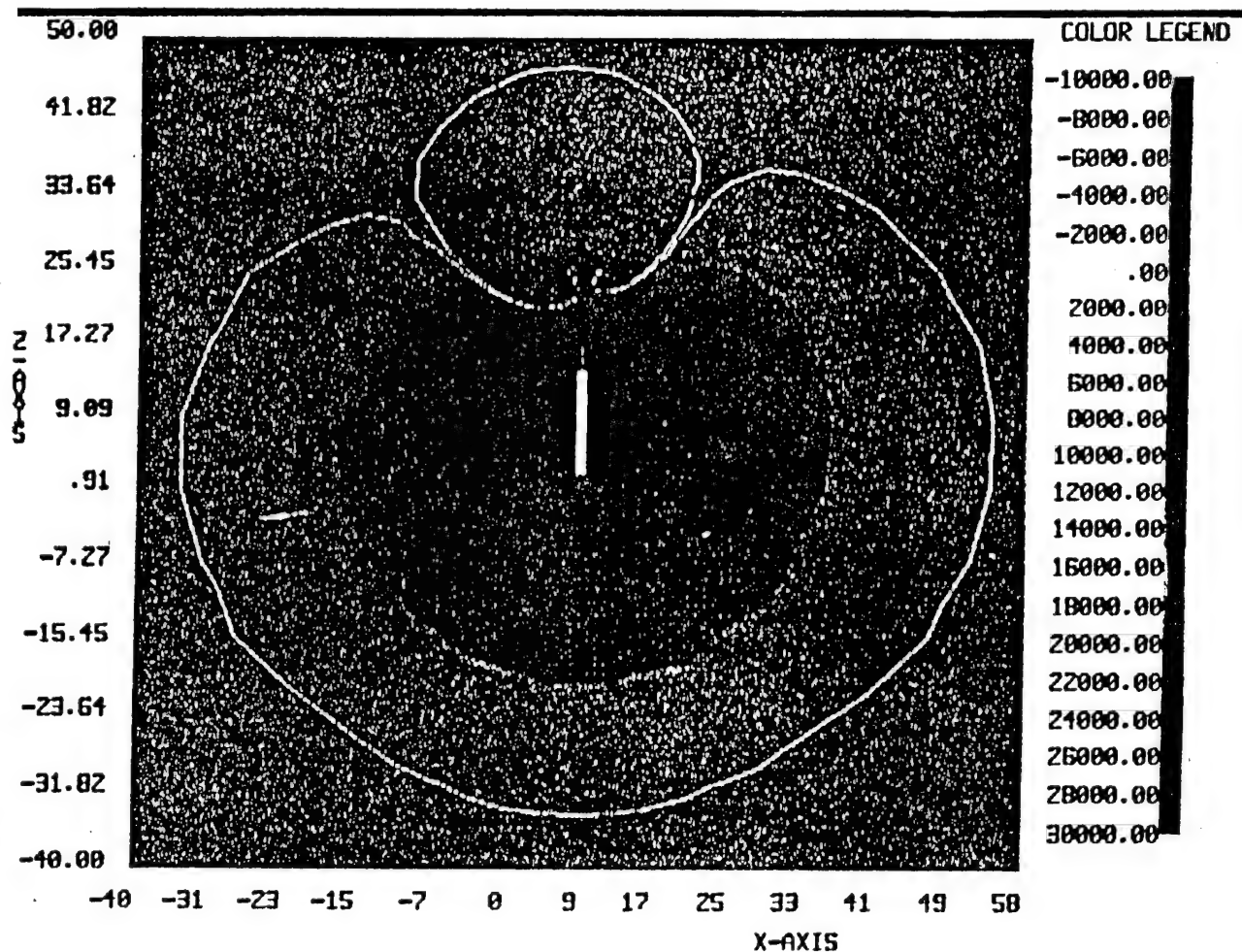
$$R_{\text{sheath}} = 9 m$$



S3-

* SEPAR I
NASCAP/LEO PLASMA SHEATH CALCULATION

A space system with a voltage applied between two parts will equilibrate by forming electron and ion sheaths such that (again!) the net current to the system is zero. The figure illustrates the electron and ion sheaths predicted around an object representing the SPEAR-I rocket experiment. The spheres on the top are biased positively with respect to the rocket body; the white lines show the sheath boundaries. Clearly, the sheath geometries are quite complex, even though the system geometry is relatively simple.



Minimum Potential = $-7.00E+03$ Maximum Potential = $2.60E+04$
 $-10.00 < X < 50.00$, $-10.00 < Z < 50.00$, CUTPLANE OFFSET Y = 9.00

* NASA Charging Analyzer Program

NASCAP/LEO CALCULATION OF ELECTRON COLLECTION BY NON-SYMMETRICAL SHEATH

An additional complexity arises when the magnetic field is introduced. This figure illustrates the role of the magnetic field in altering electron current collection in the nonsymmetrical sheath.

$$n_e = n_i = 3 \times 10^{10} \text{ m}^{-3}$$

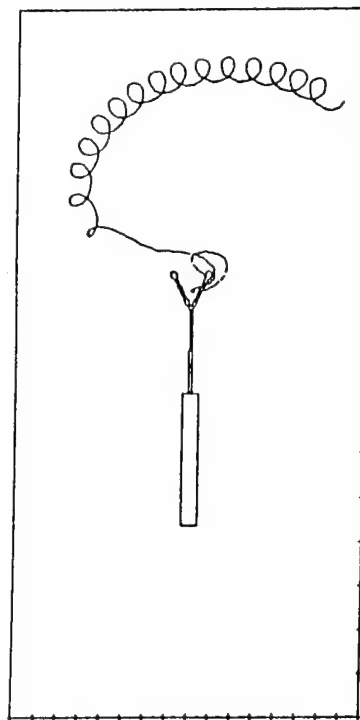
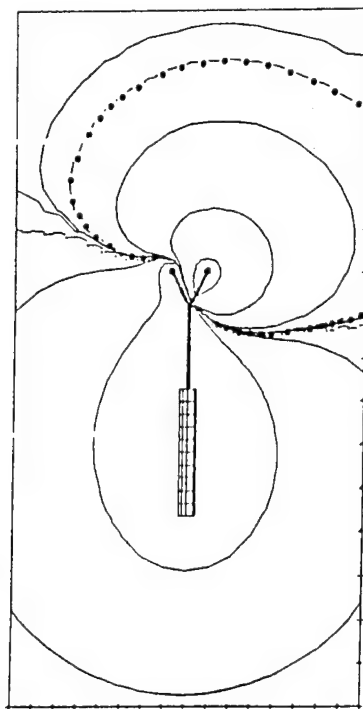
$$\theta_e = \theta_i = 0.1 \text{ eV}$$

$$B = 0.4 \text{ gauss}$$

$$\phi_{\text{sphere 1}} = 46 \text{ kV}$$

$$\phi_{\text{sphere 2}} = 0 \text{ kV}$$

$$\phi_{\text{ground}} = -6 \text{ kV}$$

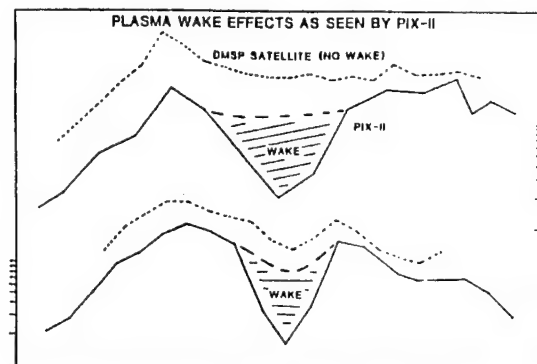
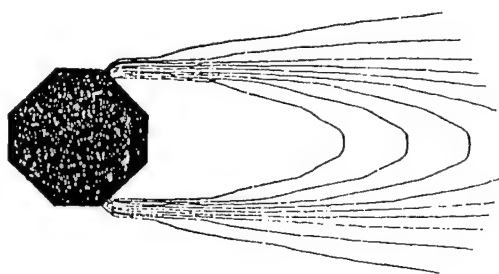


RAM/WAKE EFFECTS

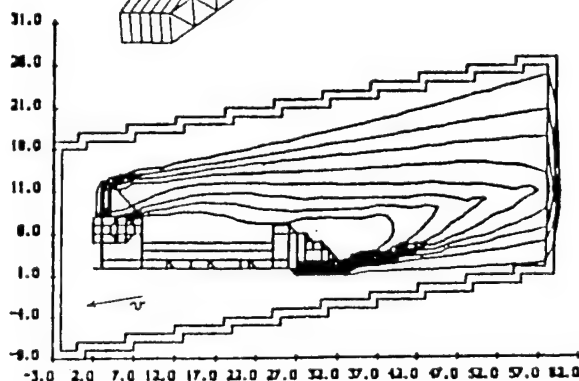
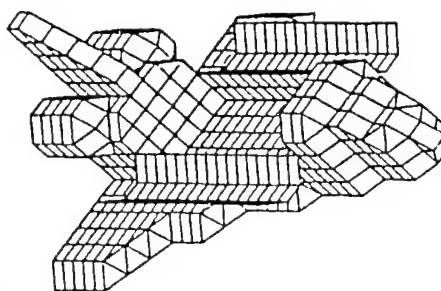
This chart illustrates the potential structures due to the motion of a simple (PIX-II) and a more complex (SHUTTLE) object through a plasma. Here, there are no applied biases nor any magnetic field. Evidently, the sheath structure around a "realistic" space system with applied biases (e.g., from the power system), in motion through the plasma and Earth's magnetic field is quite complex. Yet, a realistic assessment of plasma/charged particle interactions with surfaces demands an understanding of the local field structures.

POLAR CODE MODELING

PIX-II



SHUTTLE



CHARACTERISTIC MAGNITUDES

This chart indicates the characteristic length and potential scales for plasma phenomena in various Earth orbital regimes and indicates the factors which drive the determination of surface potentials and local fields.

In LEO, the characteristic plasma lengths are small, as are the naturally induced potentials which range from tenths of volts (the electron temperature), through tens of volts ($\vec{v} \times \vec{B}$ induced potentials for large systems). Wake potentials are also in this range. In this environment it is the system electrical and geometric configurations which dominate the interactions, with material properties a secondary consideration, except for the case of insulators near biased conductors. The naturally induced potentials are, however, large enough to create possible concern for thin films or coatings and for electrostatically enhanced contamination of sensitive surfaces (e.g., optics).

In GEO, the characteristic plasma lengths are hundreds of meters and the naturally induced potentials in the kilovolt range. Here, material properties and geometry (including shadowing) dominate the interactions, with system electrical configuration and a secondary consideration, except for very high voltage (>KV) systems.

Polar orbit represents a composite of the LEO and GEO cases and all factors must be considered.

LEO

- o SYSTEM SIZE \gg DEBYE LENGTH (CM)
- o SYSTEM VOLTAGES \gg NATURALLY INDUCED POTENTIALS (TENTHS TO TENS OF VOLTS)
 - SYSTEM ELECTRICAL AND GEOMETRIC CONFIGURATIONS DOMINATE INTERACTIONS
 - * IMPORTANCE OF MATERIAL PROPERTIES DEPENDS ON CONFIGURATIONS
 - * SYNERGISTIC EFFECTS (METEOROID DAMAGE, CHANGES TO MATERIAL ELECTRICAL PROPERTIES, ETC.) IMPORTANT
 - NATURALLY INDUCED POTENTIALS OF CONCERN FOR
 - * THIN FILMS OR COATINGS
 - * ELECTROSTATICALLY ENHANCED CONTAMINATION
 - * VERY LARGE SYSTEMS ($\geq 50m$)

GEO

- o SYSTEM SIZE \ll DEBYE LENGTH (100's OF m)
- o SYSTEM VOLTAGES \ll NATURALLY INDUCED POTENTIALS (KV)
 - SURFACE MATERIAL PROPERTIES AND GEOMETRIC CONFIGURATIONS DOMINATE INTERACTIONS
 - * ELECTRICAL CONFIGURATION OF SECONDARY IMPORTANCE

PEO (polar Earth orbit)

- o INTERMEDIATE CASE: CHARACTERISTIC LENGTHS AND POTENTIALS VARY WIDELY DEPENDING ON POSITION IN ORBIT AND AURORAL ACTIVITY
 - BOTH "LEO" AND "GEO" CASES MUST BE CONSIDERED

COLLECTION OF CHARGED SPECIES TO SURFACES

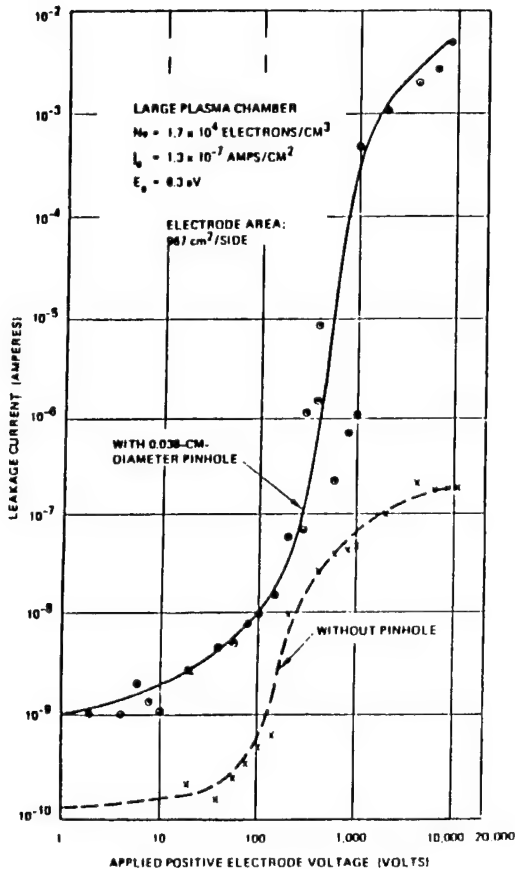
Let us leave the question of self-consistent determination of potentials relative to the plasma, and examine some of the phenomena associated with electron and ion collection, focusing on the role of materials and effects on them. This chart indicates phenomena associated with positive bias (electron collection). Note that in addition to phenomena associated with plasmas alone, the possibility of cascade ionization of neutral gases in the sheath must be considered.

ELECTRON COLLECTION:

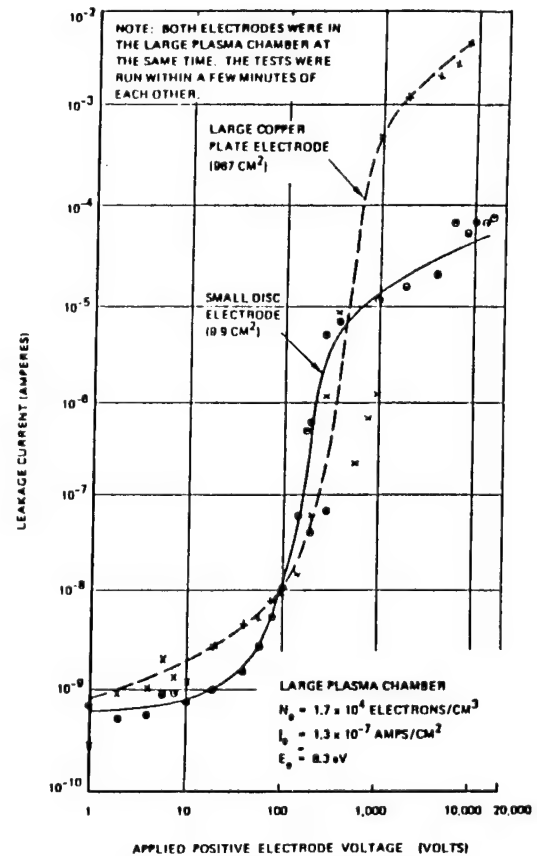
- 0 MAY HEAT SMALL AREAS
- 0 CURRENT DRAIN
- 0 MAY INFLUENCE SYSTEM FLOATING POTENTIAL DRASTICALLY BY SECONDARY ELECTRON EMISSION
 - Testing needed on secondary emission curves of many materials
- 0 WELL UNDERSTOOD TO BARE CONDUCTORS, SIMPLE GEOMETRIES
- 0 MAY BE INCREASED BY CASCADE IONIZATION OF SYSTEM GASEOUS EFFLUX
- 0 NOT KNOWN FOR ATOMIC OXYGEN (AO)-DEGRADED MATERIALS
 - Testing needed on degraded Kapton around pinholes, etc.

PINHOLE CURRENTS

This figure shows data (taken by K. Kennerud of Boeing) on electron currents collected by insulated electrodes with defects ("pinholes"). Note that the current rises sharply at applied voltages in the 100-1000 V range. The right-hand graph indicates that the level at which the current rise tapers off appears related to the size of the insulating surface area surrounding the pinhole. In the high-voltage regime, the current densities at the pinholes were large enough to cause severe degradation of the insulation near the holes.



LEAKAGE CURRENT COLLECTED BY A 10-INCH BY 15-INCH COPPER PLATE ENCAPSULATED IN 0.005-INCH THICK KAPTON - WITH AND WITHOUT A DEFECT



EFFECT OF ELECTRODE SIZE ON THE PLASMA LEAKAGE CURRENT COLLECTED BY A 0.015-INCH-DIAMETER PINHOLE IN 0.005-INCH-THICK KAPTON

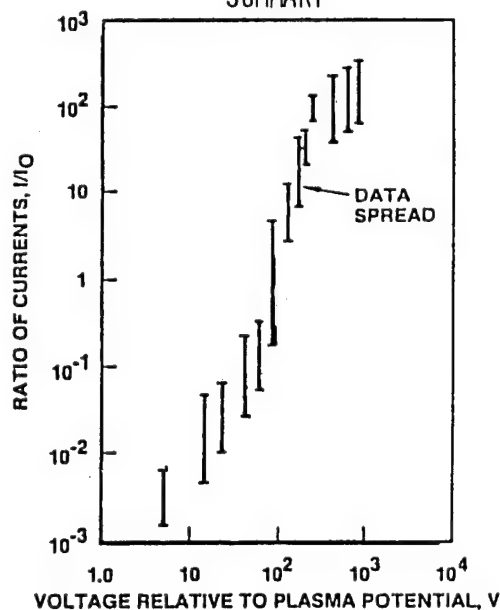
SOLAR ARRAY SURFACE VOLTAGE PROFILES AND COUPLING CURRENTS

I-V curves similar to those for "pinholes" are observed when solar array segments are biased in plasmas. Surface potential traces (right) indicate that the low current/low voltage and high current/high voltage regimes are associated with very different potential profiles across the surface. For voltages ≤ 100 V (top), the profiles show the dielectric coverslide surfaces having slightly negative potentials, with the interconnects standing out in sharp relief. This is what one expects if the coverslides are behaving as "isolated" surfaces (electron temperatures in these tests are about 1 eV). When high voltages are applied to the interconnects (bottom), the surfaces of the coverslides are seen to attain positive potentials comparable to (but somewhat less than) the nearby interconnects. The latter condition is associated with the enhanced current region of the I-V curve. Two interrelated phenomena are believed to be occurring: expansion of the sheath due to the large potentials on the coverslides; and collection of secondary electrons generated on the coverslides. This condition is made possible by the secondary electron characteristics of the coverslide.

POSITIVE APPLIED POTENTIALS

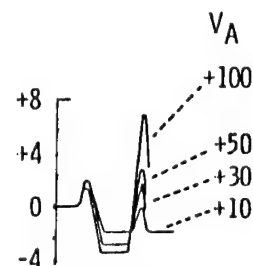
2x2 CM CELLS

LERC GROUND TEST CURRENTS
SUMMARY

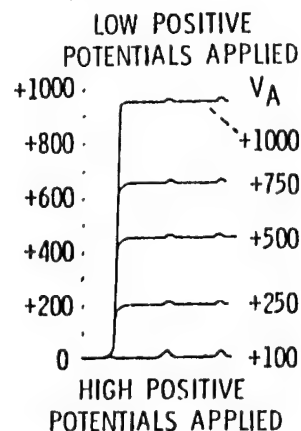


- 0 LOW VOLTAGE ENVELOPE: $I/I_0 \propto V^{3/2}$
- 0 CONSISTENT WITH $I/I_0 \propto \bar{\Phi}$, $\bar{\Phi} = f_i \phi_i + f_c \phi_c$ with $-5V \lesssim \phi_c < 0$
- 0 HIGH VOLTAGE BEHAVIOR: $I/I_0 \propto V^x$, $x \approx 1$

MEASURED SURFACE
POTENTIAL,
 V_m

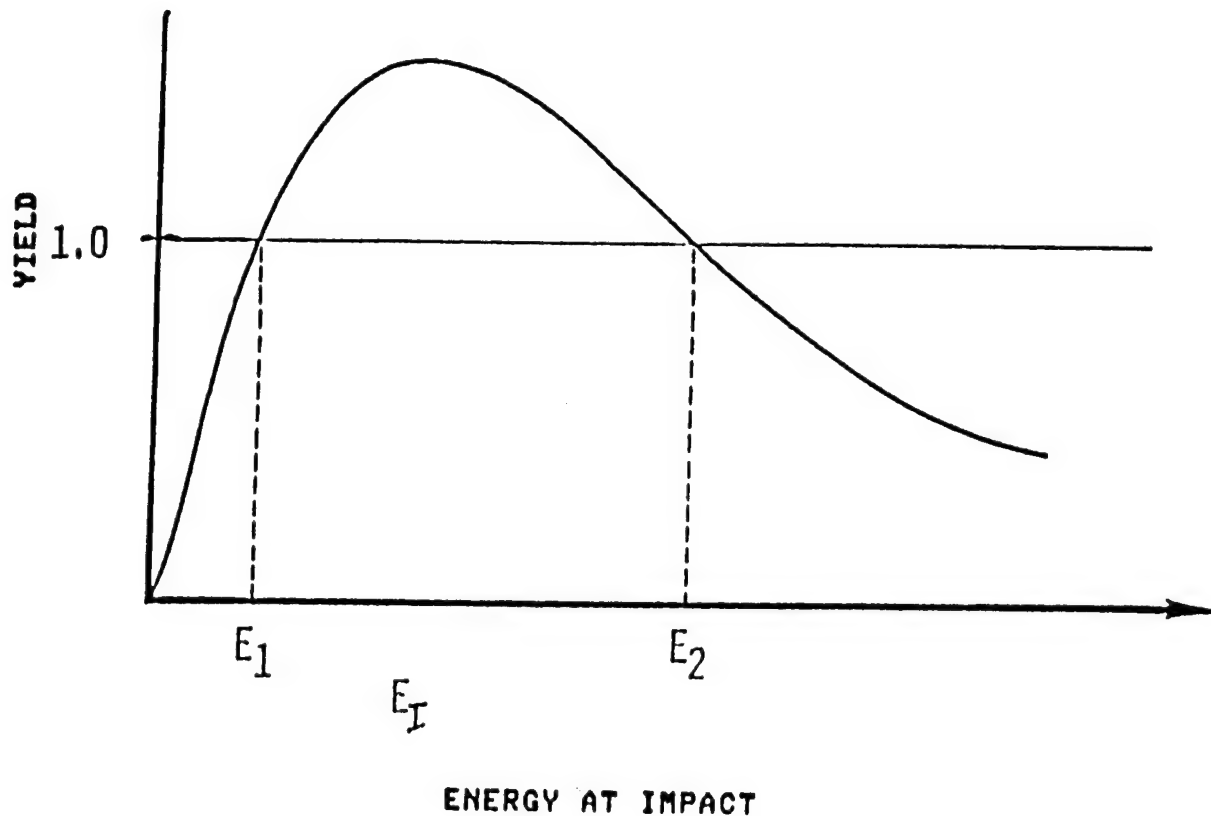


MEASURED SURFACE
POTENTIAL,
 V_m



SECONDARY ELECTRON YIELD VERSUS ENERGY

This figure illustrates a typical secondary electron yield due to electron impact curve for an insulating surface. Shown is yield (secondary electrons out per primary electron in) as a function of primary electron energy at impact. Note that there is a range of primary electron energies for which the yield of secondary electrons is greater than 1.



HIGH SECONDARY YIELDS

The fact that typical insulators have secondary electron emission yields greater than one for a range of primary electron energies means that the I-V curve for such a surface in a plasma environment for conditions under which all secondary electrons escape is multivalued; i.e., there is no unique voltage for which the net current to the surface is zero. This in turn implies that the potential actually attained by an insulating surface in a plasma will depend not only on the emission characteristics of the insulator but also on the local electric fields which will determine what fraction of the secondary electrons escape, and on the initial conditions. Thus, hysteresis effects and rate of change effects are expected to be important in determining the final potential of an insulating surface.

HIGH SECONDARY YIELDS IMPLY

MULTIPLE EQUILIBRIA POSSIBLE

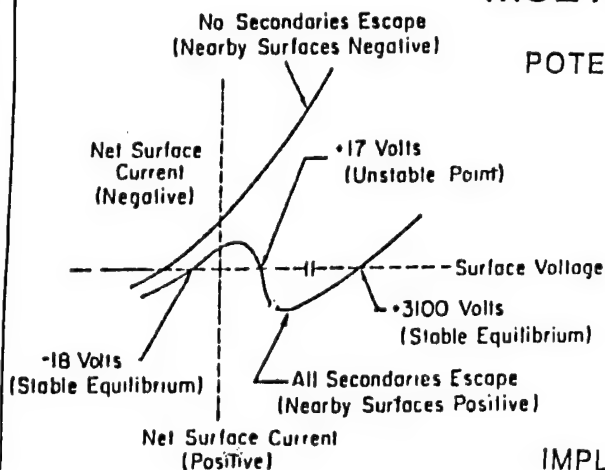
POTENTIAL ON INSULATING SURFACE DEPENDS ON

- o SECONDARY YIELD
- o PLASMA PROPERTIES
- o POTENTIALS OF NEARBY SURFACES
- o "INITIAL CONDITIONS"

IMPLIES POSSIBILITY OF

o HYSTERESIS EFFECTS IN CURRENT
AND VOLTAGE

o RATE OF CHANGE EFFECTS



BOUNDING I-V CURVES FOR

"SPACECRAFT" MATERIAL

IN A 10-eV MAXWELLIAN PLASMA

COLLECTION OF CHARGED SPECIES TO SURFACES

Turning now to negatively biased surfaces, we consider some of the effects of ion impact on surfaces. A brief discussion of arcing, which is observed on negatively biased systems in plasmas, will follow. Ions accelerated by local fields in the sheath will strike surfaces with an energy corresponding to the negative potential on them. Two consequences of ion impact which are important for surface materials are sputtering and chemical reactions enhanced by the energy of the accelerated ions. Oxygen erosion is generally attributed to atomic oxygen atoms because they are more numerous than are atomic oxygen ions. However, if the reaction rates increase strongly with impact energy, the ions may contribute significantly to the erosion process.

POSITIVE ION COLLECTION (IMPORTANT FOR INSULATORS UNDER AC BIAS, CONDUCTORS UNDER AC OR DC BIASES, INCLUDES COLLECTION AND IONIZATION OF GASEOUS EFFLUX):

0 SPUTTERING

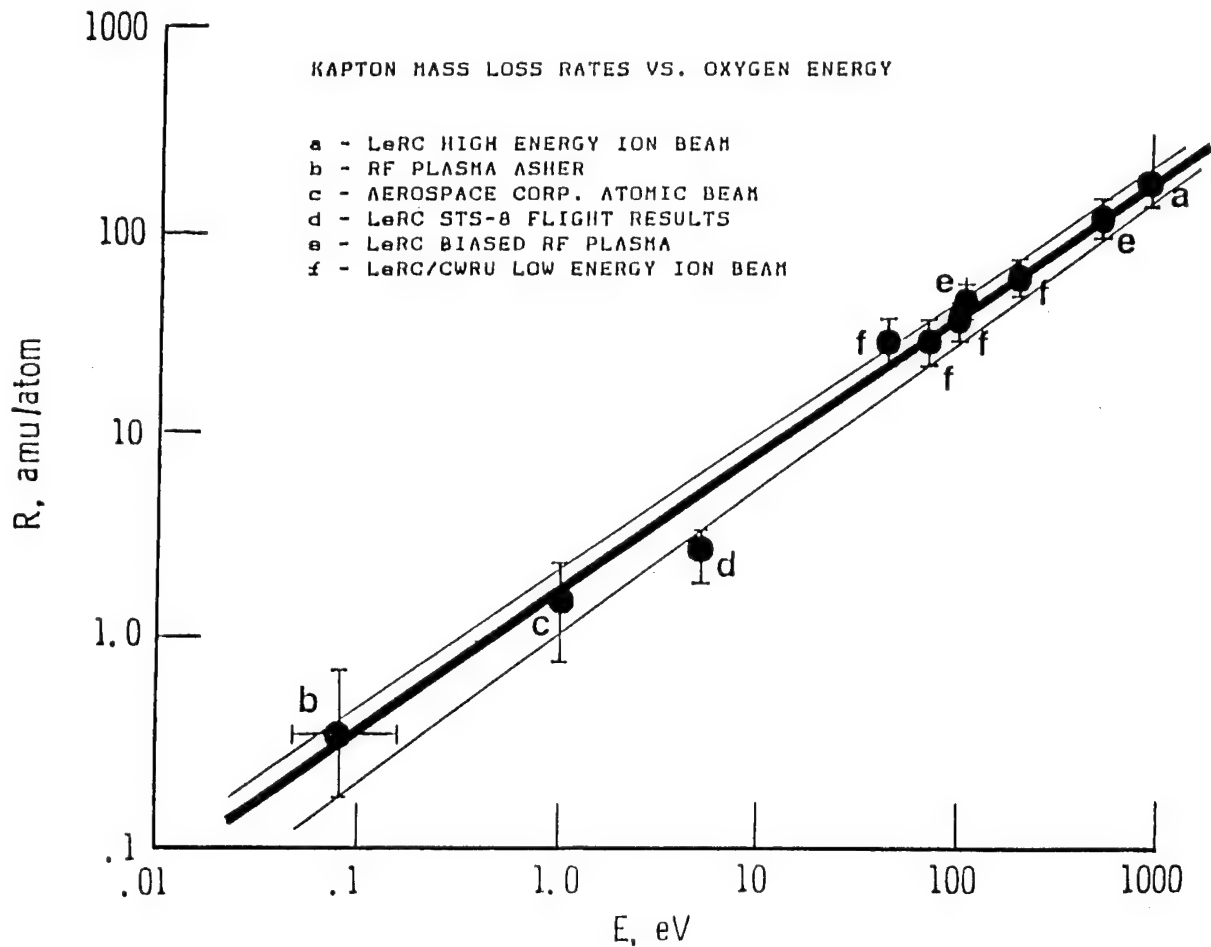
- LOSS OF MATERIAL, CHANGE OF SURFACE PROPERTIES
 - RATES POORLY KNOWN FOR OXYGEN IONS
 - CHEMICALLY AIDED SPUTTERING?
 - HIGHLY MATERIALS-SENSITIVE
- Testing needed on materials in energetic oxygen ion beams

0 ENHANCED CHEMISTRY

- LOSS OF MATERIAL, CHANGE OF SURFACE ELECTRICAL, MECHANICAL, OPTICAL, AND CHEMICAL PROPERTIES
 - OCCURS EVEN IN NON-RAM DIRECTIONS
 - ENHANCED AO REACTION RATES AT HIGH O ENERGIES MAY COMPENSATE FOR LOW ION DENSITY
- Materials-sensitive
- Tests needed on materials in energetic oxygen ion beams
- NITRIDIZATION AND HYDRIDIZATION OF METALS
- Tests needed on metals in energetic nitrogen and hydrogen ion beams

KAPTON MASS LOSS RATES VERSUS OXYGEN ENERGY

This figure shows a plot of mass loss rates versus beam energy for kapton based on data from various sources, including ground tests with both ion and neutral oxygen sources and results from the STS-8 flight experiment. The plot indicates that the mass loss rates indeed increase with increasing impact energy for kapton, so that at high voltages, atomic oxygen ions may contribute significantly to erosion of this material. Similar curves for other materials are needed to allow assessment of the possibility for enhanced erosion.



ARCING TO OR THROUGH THE PLASMA

Arcing of negatively biased samples in plasma has been observed at potentials in the few-hundred volt range both on the ground and in space. Such arcing is a concern both for system performance (electromagnetic interference (EMI), upsets) and for long-term integrating of materials. Arcing of systems in plasmas is not yet well understood, but it is known to be sensitive to materials and geometry.

ARCING TO LEO PLASMA FROM NEGATIVELY BIASED CONDUCTOR/INSULATOR INTERFACES EXPOSED TO THE PLASMA:

- 0 MAY CAUSE ELECTRICAL DISTURBANCES, EMI, LOSS OF SURFACE MATERIAL, CONTAMINATION OF OTHER SURFACES
- 0 THRESHOLD > 100 V, BUT MATERIALS-SENSITIVE
 - Copper threshold lower than for silver
 - More tests needed on other materials
 - May be sensitive to ion species (O^+ , H^+ tests needed)
- 0 PINHOLES IN INSULATORS A CONCERN
 - Micrometeoroids and debris rates needed

ARCING THROUGH PLASMA BETWEEN EXPOSED CONDUCTORS AT DIFFERING POTENTIALS:

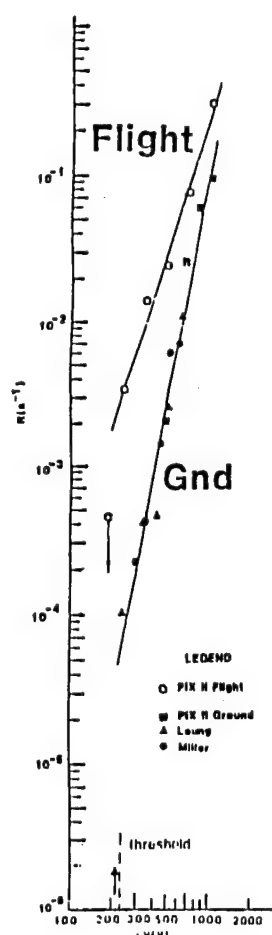
- 0 SIMILAR EFFECTS AS ARCING TO PLASMA
- 0 OCCURS, BUT NO INFORMATION ON THRESHOLDS, MATERIALS, OR ION SPECIES SENSITIVITIES
 - More testing needed

BREAKDOWN TO LEO PLASMA THROUGH THIN FILM DIELECTRICS

- 0 MAY DESTROY OR DAMAGE DIELECTRICS
- 0 DEPENDS ON DIELECTRIC STRENGTHS OF MATERIALS
- 0 PROBABLY DIFFERENT TO PLASMA THAN BETWEEN CAPACITOR PLATES
- 0 PROBABLY DIFFERENT TO AC VOLTAGES THAN DC, MAY DEPEND ON SIGN OF DC, AND ON ION SPECIES
 - Testing needed on representative materials in all relevant configurations and environments

ARC RATES ON SOLAR ARRAYS

This chart illustrates results of studies of arcing on solar cell arrays in ground chambers and in the PIX-II flight experiment. The data have been scaled according to the formula indicated. As can be seen, this scaling organizes the data from a number of ground experiments along a power law curve of arc rate versus negative voltage. The dependence of arc rate on voltage is different for the flight and ground test data--a result which is not presently understood. The "threshold" for arcing appears to be the same for the two data sets. The data available for newer technology solar cells (large area Si) suggest that the arc rates are also dependent on a power of the voltage. The exponent appears much larger when both sides of these samples, which featured **wraparound interconnects** and exposed copper on the back sides of the array segments, were exposed. This suggests that the rates (and perhaps the thresholds) for arcing are material dependent.

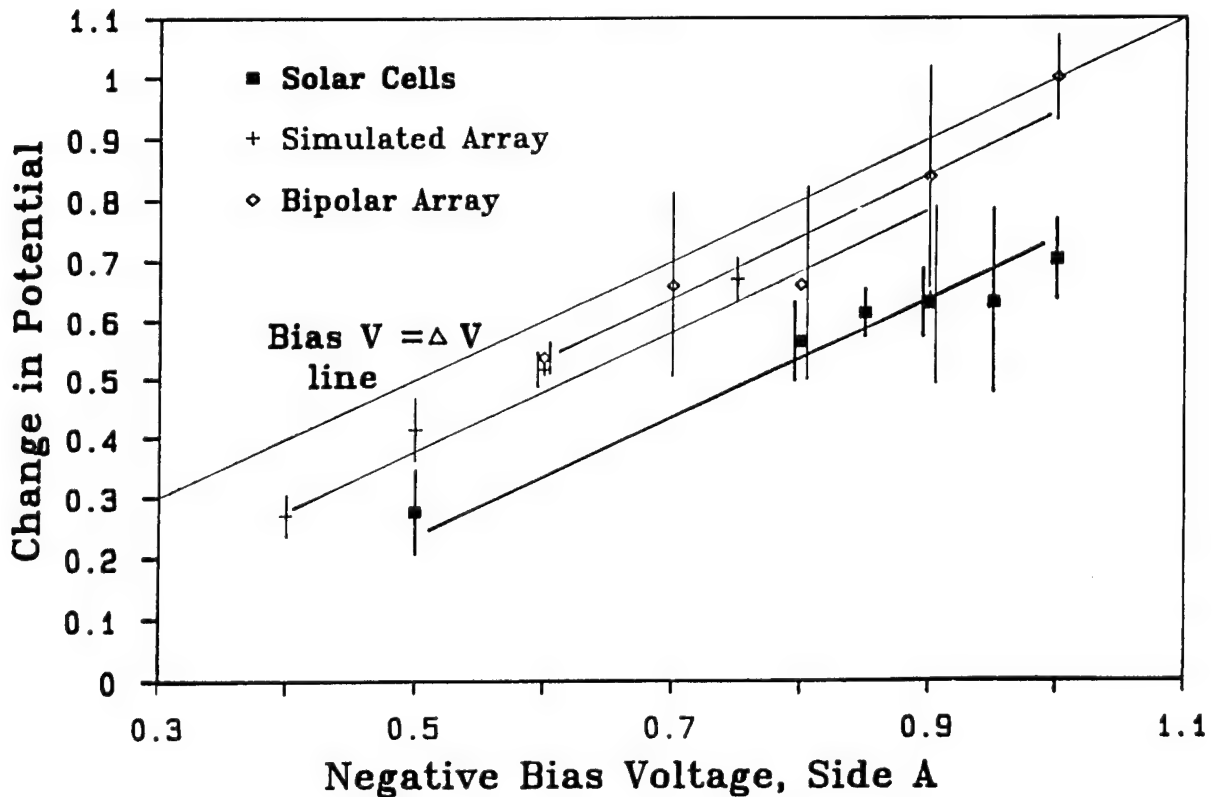


-GROUND VS. FLIGHT RESULTS-

- 0 SMALL AREA CELLS (2x2 AND 2x4 CM)
 - THRESHOLD IN -200 TO -250 V RANGE
 - ARC RATE $\propto n_i T_i^{0.5} M_i^{-0.5} V^a$ ABOVE THRESHOLD
 - $a \approx 3$ FOR FLIGHT DATA
 - $a \approx 5$ FOR GROUND DATA
 - FLIGHT ARC RATE $>$ GROUND ARC RATE
- 0 LARGE AREA CELLS (5.9 x 5.9 CM, WRAP AROUND)
 - GROUND TESTS ONLY
 - INSUFFICIENT DATA TO DETERMINE IF THRESHOLD EXISTS
 - RATE EXPONENTS:
 - $a \approx 5$ FRONT SIDE EXPOSED
 - $a \approx 8-10$ BOTH SIDES EXPOSED
- 0 IMPLICATIONS
 - ARC RATE SENSITIVE TO CELL TECHNOLOGY
 - GROUND TO SPACE SCALING VERY RISKY WITHOUT FLIGHT TESTS

CHARGE LOSS

This chart gives further evidence of dependence of arc behavior on materials and geometry. Shown is charge loss, as reflected in change of potential during arcs on biased samples which are "decoupled" from the power supply during the arcs. The data indicate that a given sample tends to end an arc with a characteristic potential, suggesting the existence of a cutoff voltage, which may indicate a threshold for the arcs. The solar cell sample, which had 2 x 2 cm cells of the same design as the PIX-II cells, tended to cease arcing with about 200 volts remaining on the sample. This is consistent with the 200-volt threshold inferred for these cells from the previous figure. The simulated array had a pattern of Kapton and copper exposed and ceased arcing with less voltage on the sample (about 100 volts), suggesting a lower threshold. The bipolar sample was able to transfer charge from one side to the other and lost nearly all of its charge during arcs. This implies that local geometry is important in determining arc strength.



BREAKDOWN OF OPTICAL COATINGS AND OTHER THIN INSULATORS

Arcing is generally associated with application of voltages in the >100-volt range in LEO and with development of large differential potential due to fluxes of hot particles in GEO and PEO. However, very thin insulating films on large systems may be subject to breakdown due to the 10's of volts of potential which can be generated by $v \times B$ or wake effects on these systems. Breakdown strengths of such insulators may well be different when one "electrode" is a plasma than when placed between physical electrodes. In addition, breakdown strengths and resistivities are expected to be different for positive and negative bias applied when one "electrode" is a plasma.

- 0 MAY HAPPEN AT EVEN LOW POTENTIALS BECAUSE OF HIGH FIELDS ACROSS VERY THIN FILMS
- 0 CHANGES IN SURFACE OPTICAL, ELECTRICAL, CHEMICAL PROPERTIES
 - MAY LOSE RESISTANCE TO AO DEGRADATION
 - MAY CHANGE REFLECTIVITY, ABSORPTANCE, RESISTIVITY
- 0 MEASUREMENTS NEEDED OF DIELECTRIC STRENGTH OF OPTICAL COATINGS, ETC. INTO PLASMA

ENHANCED COLLECTION OF DUST AND OTHER CONTAMINANTS

The local electric fields and surface charges developed in the sheath around a system can result in enhanced contamination of surfaces both by molecular and particulate contaminant sources. These processes are not well understood but may be significant, particularly for sensitive surfaces with long lifetime requirements.

- 0 POSSIBLE SOURCES INCLUDE MICROMETEORIDS, DEBRIS, SYSTEM EFFLUX, SPATTERED AND VOLATILE CHEMICALLY-PRODUCED PRODUCTS
- 0 MAY CAUSE ABRASION, OPTICAL CONTAMINATION, POINTS OF HIGH ELECTRIC FIELD FOR THIN FILM BREAKDOWNS
- 0 DUST AND CONTAMINANTS MAY BE COLLECTED ELECTROSTATICALLY IF CHARGED BY PHOTOELECTRIC EFFECT OR CHARGE EXCHANGE PROCESSES, OR EVEN UNCHARGED BY POLARIZATION OF CHARGE ON PARTICLE SURFACE
- 0 PHOTOELECTRON-YIELDS MEASUREMENTS NEEDED FOR POSSIBLE CONTAMINANTS, MICROMETEORIDS AND DEBRIS

MATERIALS RESEARCH NEEDED TO TREAT PLASMA EFFECTS

This chart presents a summary of materials studies needed to assess the effects of plasma interactions on surfaces in space. Ground-based studies can provide much needed information, but cannot stand alone. "Space truth" will be needed both to "calibrate" the ground experiments, which can never perfectly simulate orbital conditions, and to validate models.

- 0 ARCING THRESHOLDS INTO AND THROUGH PLASMA
 - ALL MATERIALS EXPOSED AT HIGH POTENTIALS
 - OXYGEN AND HYDROGEN PLASMAS
- 0 DIELECTRIC STRENGTHS IN A PLASMA
 - THIN FILM DIELECTRICS
 - OPTICAL COATINGS
 - AC AND DC POTENTIALS
 - OXYGEN AND HYDROGEN PLASMAS
- 0 PHOTOYIELDS AND SECONDARY ELECTRON YIELDS
 - ALL SURFACE MATERIALS AND COATINGS AND THEIR OXIDES
 - DEBRIS AND MICROMETEOROID MATERIALS
 - AS FUNCTION OF INCOMING ENERGY AND ANGLE
- 0 BULK CHANGES IN ELECTRICAL PROPERTIES THROUGH CHARGE DEPOSITION
 - ALL ELECTRICALLY IMPORTANT SURFACE MATERIALS
 - AS FUNCTION OF INCOMING ELECTRON ENERGY
- 0 SPUTTERING RATES IN OXYGEN ION BEAMS
 - ALL MATERIALS LIKELY TO BE AT HIGH POTENTIALS
 - AS FUNCTION OF ENERGY AND ANGLE
 - CHEMICALLY AIDED SPUTTERING?
- 0 ENERGY DEPENDENCE OF ATOMIC OXYGEN ION REACTIONS
 - METALS AND INSULATORS, ALL EXPOSED MATERIALS
- 0 RATES OF OTHER HIGH ENERGY ION CHEMICAL REACTIONS

CHARGED PARTICLE INTERACTIONS WITH SPACE MATERIALS SUMMARY

To summarize, plasma interactions and their effects on materials depend on a number of factors, including the pre-existing environment, the properties of surface materials and the characteristics of the system. An additional dimension is the question of mission: some payloads may be much more sensitive to plasma interactions than others. As an example, a payload whose objective is to measure the ambient environment will be more sensitive to any effects than will a power system. Material-specific effects include charging and its associated effects, which can result in short- and long-term damage. Selection of materials for a particular application requires consideration of all factors and assessment of effects due to all causes. Proper selection and suitability determination requires analysis to identify the actual environment combined with testing under exposure to single and combined environment factors.

INTERACTIONS AND IMPACTS DEPEND ON

- o ORBIT (NATURAL ENVIRONMENT)
- o MATERIAL PROPERTIES
- o SYSTEM
 - OPERATIONS (EFFLUX, CONTAMINANTS)
 - LOCAL AND OVERALL GEOMETRY
 - ELECTRICAL CONFIGURATION
- o MISSION

INTERACTIONS WITH MATERIALS INVOLVE

- o SURFACE AND BULK CHARGING
 - LOCAL FIELDS AND CURRENTS
 - ARCING, SPUTTERING
- o IRRADIATION

EFFECTS ON MATERIALS INCLUDE

- o SURFACE CONTAMINATION AND DAMAGE
- o BULK DEGRADATION

MATERIALS SELECTION/SUITABILITY DETERMINATION REQUIRES

- o CONSIDERATION OF ALL INTERACTION FACTORS
- o ASSESSMENT OF AGING EFFECTS DUE TO ALL CAUSES
- o ANALYSIS COMBINED WITH TESTING UNDER EXPOSURE TO SINGLE AND COMBINED ENVIRONMENT FACTORS

INFLUENCE OF CHARGING ENVIRONMENTS ON SPACECRAFT
MATERIALS AND SYSTEM PERFORMANCE

N. John Stevens
TRW Space and Technology Group
Engineering and Test Division
System Integration Laboratory
Redondo Beach, CA 90278

ENVIRONMENTALLY-INDUCED INTERACTIONS

The purpose of this paper is to present an overview of potential interactions that can occur on spacecraft operating in space environments. These interactions will be discussed in more detail in the accompanying papers.

The environment acts on spacecraft in such a way that charging of exterior surfaces occurs. The consequences from this charging then affect system operational performance. Hence, it is the coupling of this exterior charging to system performance that is of concern here. These interactions were first discovered in the spacecraft charging phenomena in which the geomagnetic substorms charged external surfaces to a level that discharges occurred. As a result of the discharge, electronic systems either changed logic state (anomalous switching) or failed.

These interactions can occur in all orbits. The type associated with geosynchronous orbits is called "passive" since the environment provides the charging mechanism (Reference 1). This type can also occur in polar orbits due to auroral charging environments. In low Earth orbits, the thermal plasma alleviates charging environment concerns, but system operations can induce similar effects ("active" interactions).

- o ENVIRONMENT ACTS ON SURFACE MATERIALS
 - RESULTS AFFECT SYSTEM PERFORMANCE
 - EXTERIOR SURFACE DISCHARGES COUPLE INTO ELECTRONIC SYSTEMS
- o INTERACTIONS OCCUR IN ALL ORBITS
 - ACTIVE: DUE TO SYSTEM OPERATION
 - EXAMPLES: HIGH VOLTAGE OPERATIONS, EFFLUENT
 - PASSIVE: DUE TO ENVIRONMENT
 - EXAMPLES: GEO AND POLAR-AURORAL CHARGING

GEO SUBSTORM CHARGING OF SPACECRAFT

This phenomena has been investigated for the past ten years (References 2-5). These studies have shown that there is a link between the exterior surface discharge and electronic system upsets (References 6, 7). The hazards with this spacecraft charging phenomena have been enhanced electrostatic contamination and plasma particle measurement disturbances. These studies have generated design guideline documents that provide guidance and suggested mitigation techniques (References 8, 9). The recommended mitigation techniques are to analyze to ascertain the extent of charging interaction, ground all exposed metallic surfaces to prevent discharge triggers, select minimal charging materials, filter sensitive system inputs, shield harnesses and control grounding techniques to minimize extraneous circuits. This document has been included in the revised edition of Military Standard 1541A (Reference 10).

- o HAZARDS ASSOCIATE WITH GEO SPACECRAFT CHARGING
 - DISCHARGES
EMI, ELECTRONIC SWITCHING AND FAILURE, MATERIAL DAMAGE
 - ENHANCED ELECTROSTATIC CONTAMINATION
 - DISTURB SPACE SCIENCE MEASUREMENTS
- o MITIGATION TECHNIQUES
 - ANALYZE FOR CHARGING EFFECTS
 - GROUND EXTERIOR METALLIC SURFACES
 - SELECT MINIMAL CHARGING EXTERIOR MATERIALS
 - PROTECT INTERIOR SYSTEMS
FILTER, SHIELD AND GROUND
- o INCORPORATED IN MIL STD 1541A

SPACECRAFT CHARGING IN FUTURE MISSIONS

The previous studies have resulted in the conclusion that the spacecraft charging issue has been settled. In the initial stages of the spacecraft charging investigation several companies claimed that "... there is no such thing as spacecraft charging, only bad design." These statements were wrong then just as this belief that all issues have been resolved is wrong now. The charging investigation covered only those materials and systems that were in use in the late seventies. The spacecraft of the future will not use those materials or systems. Charging anomalies arose because of the transition from relay to solid-state logic. This innovation reduced switching transients from long pulses at 15 volts to short pulses at less than 5 volts. The surface charging provided pulses which could switch and damage solid-state systems. The future missions want long mission duration at very high operating speed. In fact, the suggested operating speeds for future data buses correspond to the ringing frequency of today's standard structures. Hence, filtering is impossible. The future spacecraft will use new composite materials for structures. The behavior of these materials has not yet been determined. The only help that prior studies can provide is the recognition that the environment can cause interactions and that these must be assessed.

- o FUTURE MISSIONS REQUIRE ADDITIONAL EVALUATION
 - ELECTRONIC SYSTEM SPEED INCREASING
 - OPERATIONS AT STRUCTURE RESONANT FREQUENCY
 - CAN'T FILTER OUT NOISE
 - MATERIAL SELECTIONS
 - COMPOSITE BEHAVIOR UNKNOWN
 - COATING SELECTION PROVIDENCE OF THERMAL DESIGN
 - LONG TERM AGING EFFECTS ON MATERIAL PROPERTIES UNKNOWN
- o GUIDES EXIST BUT MAY NOT BE DIRECTLY APPLICABLE

LEO ORBIT INTERACTIONS

NASA is planning to build a very large Space Station* that will orbit at about 400 km. This Station will incorporate solar arrays that will generate 200 kw of power at a nominal operating voltage of 160 volts. This is the largest system yet conceived operating at a voltage larger than any previous satellite. This array voltage will determine the spacecraft floating potential relative to space. Whether or not this is serious has to be determined. Today's technology has trouble understanding its present data base of solar cell interactions obtained with 2 X 2 cm and 2 X 4 cm silicon cell segments tested only in limited areas of up to 1000 sq. cm. (References 11-13). The Station has baselined 8 X 8 cm solar cell for which there is no data on plasma effects.

The size of the Station also presents concerns for environmental interactions. There will be high voltage that may or may not be distributed over very large areas moving at orbital speeds through the Earth's magnetic field. The electronic systems must function at high operational rates. This Station is a complicated system and its interaction has to be understood in order to assure safe operations over the lifetime of the Station.

As complicated as the Space Station may appear, the SDI missions are far more complex. Here, the power levels rise to gigawatt levels which would be required instantaneously, anytime in their 10 year mission life. Clearly, this is a challenge to understanding complex interactions between space environments and spacecraft systems.

- o NASA SPACE STATION IN LEO
 - LONG MISSION LIFE (30 YEARS) AT HIGH POWER
 - 160 VOLT OPERATIONS
 - COMPLEX INTERACTION WITH ENVIRONMENT
- o TECHNOLOGY TO PREDICT BEHAVIOR UNPROVEN
 - NO LARGE SOLAR CELL DATA
 - NO LARGE STRUCTURE DATA
 - NO HIGH VOLTAGE DATA
 - NO LARGE COMPLEX STRUCTURE DATA
- o SDI MISSION AT HIGHER POWER LEVELS
 - VERY HIGH VOLTAGE PHENOMENA
 - EFFLUENTS FROM OPEN CYCLE OPERATIONS
 - LONG STORAGE TIME IN SPACE DIELECTRIC AGING

*Space Station Freedom

GROUND SIMULATION TECHNIQUES

Environmentally-induced effects have been studied in the past in ground simulation facilities (References 13-15). Such facilities allow a more complete testing of phenomena under controlled conditions. However, they suffer since they are normally poor simulations of the Earth's environment.

Geomagnetic substorm facilities normally operate with a monoenergetic electron beam irradiating a dielectric mounted on a grounded metal plate. Such tests can generate meaningful data on dielectric properties, but they can not be used to demonstrate space behavior. Floating or biasing the metal plate can be done, but this can influence the results.

Low Earth orbit simulation of the plasma environment also suffers in comparison to the actual environment. The space plasma temperature cannot be reproduced in chambers and the influence of the higher, ground simulation particle temperatures has not been determined. These facilities also limit the size of the sample that can be tested before the tank walls dominate the interaction.

Flight experiments provide the environment but the instrumentation is limited; the cost is high and the opportunities few.

The ideal situation would be to have the tools to model the interaction (engineering level as well as the more detailed techniques), conduct ground simulation tests to obtain needed information for the models, conduct flight experiments to validate the modeling technique and then use the models to predict the impact of the interaction on spacecraft systems behavior.

- o SUBSTORM SIMULATORS
 - MONOENERGETIC ELECTRON BEAMS
 - SMALL AREAS EXPOSED
 - TANK GROUND POTENTIAL REFERENCE
- o LEO SIMULATORS
 - POOR PLASMA ENVIRONMENT SIMULATION
 - SHEATH EFFECTS DOMINATE
 - FACILITY SMALL FOR PROJECTED SPACECRAFT DIMENSIONS
 - EFFLUENT FLOW CONSTRAINED BY WALLS
- o INTERPRETATION OF RESULTS DIFFICULT
- o ANALYTICAL MODELING TECHNIQUES NEEDED
 - SUPPORTED BY GROUND AND FLIGHT EXPERIMENTS

SUMMARY

This paper is intended to present an overview of the possible interactions between spacecraft system and charging environment. Encounters with such environments have resulted in system upsets and failure in the past and it is naive to believe that future systems would be immune to these interactions. The state of the art is not as well developed as the technical community believes. All spacecraft interact with the environment, many have had system difficulties, but only a limited number of events have been reported. A program leading to an analytical modeling technique is required to ascertain the impact of interactions on system designs. This program must be supported by ground and flight experiments.

- o SPACECRAFT SYSTEMS RESPOND TO ENVIRONMENTAL CONDITIONS
 - ELECTRONIC SWITCHING UPSETS, COMPONENT FAILURES AND MATERIAL DEGRADATION OCCURS
 - MOST SPACECRAFT HAVE ANOMALIES
 - FEW INCIDENTS ARE WELL-KNOWN
- o FUTURE SPACECRAFT ARE LARGER, USE FASTER ELECTRONIC SYSTEMS AND HAVE LONGER MISSION LIFE
 - ANOMALOUS BEHAVIOR WILL INCREASE
 - TECHNIQUES FOR MITIGATION UNPROVEN
- o DEVELOPMENT OF CONTROL TECHNIQUE REQUIRED
 - BASED ON UNDERSTANDING INTERACTION
 - DEMONSTRATED CAPABILITY TO PREDICT BEHAVIOR
 - DOCUMENTED MITIGATION TECHNIQUES

REFERENCES

1. Stevens, N. J.: Interactions Between Spacecraft and Charged-Particle Environments. Spacecraft Charging Technology - 1978. NASA CP-2071/AFGL-TR-79-0082, 1979, pp. 268-294.
2. Proceedings of the Spacecraft Charging Technology Conference. AFGL-TR-77-0051/NASA TMX-73537. C. P. Pike and R. R. Lovell, eds., 1977.
3. Spacecraft Charging Technology - 1980. NASA CP-2182/AFGL-TR-81-0270, 1981.
4. Spacecraft Environmental Interactions Technology - 1983. NASA CP-2359/AFGL-TR-85-0018, 1985.
5. Space Systems and Their Interactions with Earth's Space Environment. H. B. Garrett and C. P. Pike, eds. Progress in Astronautics and Aeronautics, Volume 71, AIAA, NY, 1980.
6. Stevens, N. J.; Barbay, M. R.; Viswanathan, R.: Modeling of Environmentally Induced Transients Within Satellites. Journal of Spacecraft and Rockets, Volume 24, No. 3, May-June 1987, pp. 257-263.
7. Woods, A. J., et al.: Model of Coupling of Discharges Into Spacecraft Structures. Spacecraft Charging Technology - 1980, op.cit., pp. 745-754.
8. Purvis, C. P., et al.: Design Guidelines for Assessing and Controlling Spacecraft Charging Effects. NASA TP-2361, September 1984.
9. Vampola, A. L., et al.: The Aerospace Spacecraft Charging Document. Aerospace Corp. Space Sciences Laboratory Report #SSL-84(4940-05) - 3 May 1984.
10. Military Standard. Electromagnetic Compatibility Requirements for Space Systems. MIL-STD-1541A (USAF), 30 December 1987.
11. Kennerud, K.: High Voltage Solar Array Experiments. NASA CR-121280, 1974.
12. Snyder, D.: Discharge Mechanisms in Solar Arrays - Experiment. AIAA Paper 86-0363, Aerospace Sciences Meeting, Reno, NV, January 1986.
13. Grier, N. T.: Experimental Results on Plasma Interactions With Large Surfaces at High Voltages. NASA TM-81423, 1980.
14. Berkopce, F. D.; Stevens, N. J.; Sturman, J. C.: The Lewis Research Center Geomagnetic Substorm Simulation Facility. NASA TMX-73602, 1976.
15. Williamson, W. S.: Spacecraft Dielectric Surface Charging Property Determination. NASA CR 180879, October 1987.

SECTION II-A

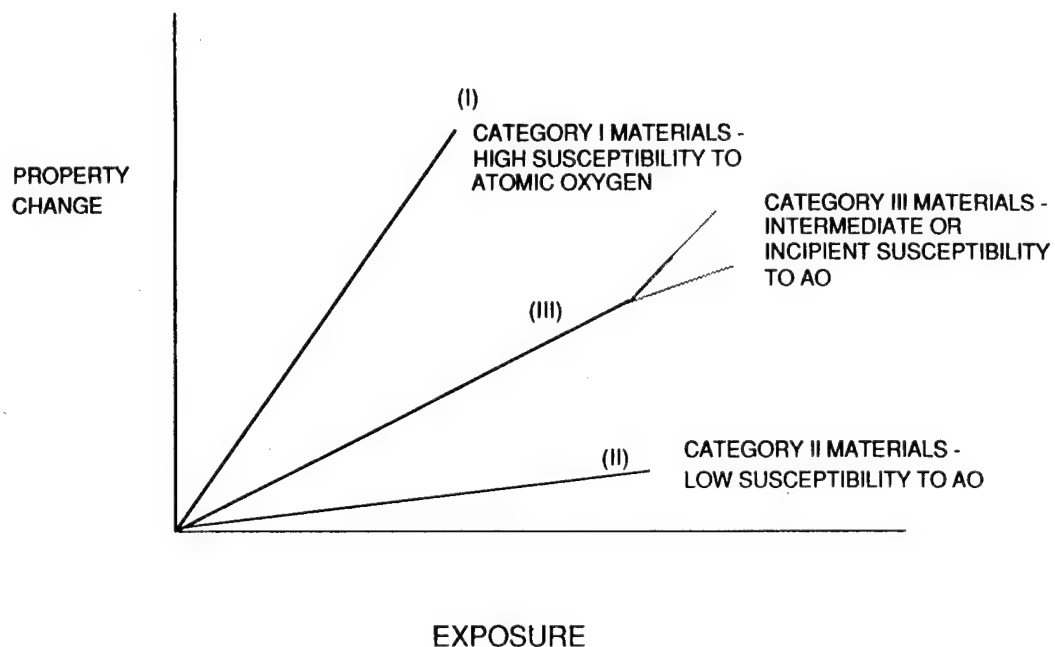
WORKING GROUP ORAL PRESENTATIONS *

*These presentations were given orally by the working group chairmen during the last day of the Workshop.

ATOMIC OXYGEN

LUBERT LEGER AND JAMES VISENTINE
NASA - JOHNSON SPACE CENTER
CHAIRMEN

MATERIAL PERFORMANCE CATEGORIES



WHAT MATERIALS ARE MOST VULNERABLE TO ATOMIC OXYGEN DEGRADATION?

- CATEGORY I AND III MATERIALS ARE MOST VULNERABLE; CATEGORY II MATERIALS ARE LEAST VULNERABLE
 - FOR SOME APPLICATIONS, EVEN SMALL DEGRADATION DUE TO AO INTERACTIONS MAY BE UNACCEPTABLE
 - MOST SENSITIVE ORBITS ARE THOSE LEO ORBITS WHERE AO NUMBER DENSITIES VARY BETWEEN 10^5 - 10^9 ATOMS/CM³
 - = DEGRADATION EFFECTS VARY IN RELATION TO EXPOSURE TIME (FLUENCE)
 - = MATERIAL APPLICATIONS AND SYSTEM PERFORMANCE REQUIREMENTS DETERMINE EXPOSURE CONDITIONS
 - PROLONGED EXPOSURE OF SENSITIVE MATERIALS WILL RESULT IN DEGRADED SYSTEM PERFORMANCE OR REQUIREMENTS FOR ON-ORBIT MAINTENANCE; BOTH CONDITIONS CONTRIBUTE TO INCREASED MISSION COST AND REDUCED MISSION OBJECTIVES

MATERIAL CLASSES FOR SPACECRAFT APPLICATIONS

<u>MATERIAL CLASS</u>	<u>PERFORMANCE CATEGORY</u>
• ORGANIC FILMS	I-II
• INORGANIC	II
• SILICONE PAINTS	II
• LUBRICANTS	I-II-III
• ORGANIC ADHESIVES	I
• ORGANIC COMPOSITES	I
• METAL MATRIX COMPOSITES	II
• THERMAL CONTROL COATINGS	I-II-III
• OPTICAL COATINGS	I-II-III

SPACECRAFT ORBITS SENSITIVE TO AO INTERACTIONS

- MINIMUM ALTITUDE IS 100 KM
- MAXIMUM ALTITUDE IS 700 KM, ALTHOUGH VERY SENSITIVE SYSTEMS MAY BE AFFECTED AT HIGHER ALTITUDES
- WHY? -- OXYGEN ATOM CONCENTRATIONS ARE DOMINANT WITHIN THESE ALTITUDE RANGES

CORRELATION OF AO EFFECTS ON MATERIALS

- LABORATORY AND FLIGHT EXPERIENCE REPRESENT RELATIVELY IMMATURE DATA BASE
 - FLIGHT DATA LIMITED IN FLUENCE AND ACCURACY OF FLUENCE ESTIMATES
 - LABORATORY SIMULATIONS ONLY RECENTLY AVAILABLE
 - QUALITATIVE CORRELATION OF LABORATORY AND FLIGHT DATA FOR VERY LIMITED NUMBER OF MATERIALS (REACTION EFFICIENCIES AND MORPHOLOGY CHANGES, ACTIVATION ENERGY)
- FUTURE FLIGHT EXPERIMENTS TO PROVIDE ACCURATE REACTION RATE MEASUREMENTS FOR COMPARISON TO GROUND-BASED RESULTS

CORRELATION OF SPACECRAFT GLOW EFFECTS

- CORRELATION BETWEEN GLOW FLIGHT EXPERIMENTS AND LABORATORY RESULTS
 - VISIBLE EMISSIONS
 - = MEASURED SPECTRUM SIMILAR TO LABORATORY NO₂
 - = PREDICTED PHENOMENA VERY DIFFICULT TO SIMULATE
 - = EFFECTS OF SURFACE PROPERTIES ON RECOMBINATION EFFICIENCY (INCLUDING STICKING EFFICIENCIES VS T_s) NEEDS STUDY
 - UV EMISSIONS
 - = MEASURED SPECTRUM (1400-1800) SIMILAR TO LABORATORY SURFACE RECOMBINATION (N₂ -LBH)
 - = NO GOOD FLIGHT UV DATA BASE
 - = PREDICTED PHENOMENOLOGY (1-5 EV N₂ ON SURFACE) HAS NOT BEEN DONE
 - IR EMISSIONS
 - = FLIGHT DATA SPARSE
 - = LABORATORY EXPERIMENTS OF MANY PREDICTED PHENOMENA CAN BE SIMULATED

DO WE KNOW ENOUGH TO LAUNCH FOR 10-30 YEARS OF SERVICE WITH CONFIDENCE?

- NO FLIGHT OR LABORATORY DATA BASE FOR FULL LIFE EXPOSURE; LIMITED EXPOSURE ONLY
- MATERIALS ARE AVAILABLE THAT APPEAR TO BE NON-REACTIVE TO AO
 - LIMITED KNOWLEDGE PLACES SEVERE CONSTRAINTS ON SYSTEM DESIGN
 - EACH APPLICATION REQUIRES SPECIAL CONSIDERATIONS AND UNDERSTANDING OF SYNERGISTIC EFFECTS
 - DESIGN SOLUTIONS FOR 5-YEAR LIFE HAVE BEEN DEVELOPED
 - ACCELERATED, FULL-LIFE TESTING OF PROTECTIVE COATING CONCEPTS TO BE CONDUCTED IN GROUND-BASED LABORATORIES
- SYNERGISTIC EFFECTS NOT ADEQUATELY UNDERSTOOD

ARE TERRESTRIAL LABORATORY FACILITIES ADEQUATE?

- AT LEAST TWO AO-BEAM FACILITIES HAVE ADEQUATE SIMULATION CAPABILITY

PHYSICAL SCIENCES CORP.

STRENGTHS

- LARGE BEAM (30-1,000 CM²)
- MULTIPLE SAMPLES
- HIGH ENERGY (5-12 EV)
- LONG EXPOSURES POSSIBLE
- HIGH FLUX (10¹⁸ - 10¹⁶ ATOMS/CM²)
- FLUENCE UP TO 10²¹ ATOMS/CM² HAVE BEEN ACHIEVED

WEAKNESSES

- PULSED SOURCE
- HIGH INSTANTANEOUS FLUX

LOS ALAMOS

- CONTINUOUS BEAM
- HIGH ENERGY (1-5 EV)
- HIGH INTENSITY (10¹⁷ ATOMS/CM²)
- LONG EXPOSURES (76 HRS)
- FLUENCES TO 2 X 10²² ATOMS/CM² HAVE BEEN ACHIEVED

- SMALL BEAM
- CONTAINS O₂ , INSERT GAS, 0° AND UV

- OTHER FACILITIES BEING DEVELOPED
- NEED TO PROVIDE HIGH QUALITY SIMULATION FACILITY TO COMMUNITY FOR MATERIAL EVALUATIONS

SYNERGISM WITH OTHER FACTORS

- SYNERGISM WITH OTHER FACTORS IMPORTANT RELATIVE TO MATERIAL EFFECTS
- MOST IMPORTANT APPEAR TO BE DAMAGE TO PROTECTIVE COATINGS FOLLOWED BY REACTION WITH SUBSTRATE
 - RADIATION INDUCED FAILURE OF COATING
 - MICROMETEOROID/SPACE DEBRIS (SMALL PARTICLES)
 - THERMAL CYCLING
 - CHARGING DAMAGE
- ACCELERATION OF REACTION RATES
- GLOW SYNERGISM WITH OTHER FACTORS
 - SURFACE CONTAMINATION
 - GAS RELEASES OF REACTIVE PRODUCTS
- HAS SYNERGISM BEEN TESTED OR EVALUATED?
 - INITIAL CONSIDERATION OF COUPLING, BUT VERY LIMITED EVALUATIONS
 - LABORATORY FACILITIES WITH COMBINED ENVIRONMENTS NOT AVAILABLE

NEED FOR SPACE EXPERIMENTS

- SPACE EXPERIMENTS ARE NEEDED FOR MATERIAL INTERACTION ASSESSMENT
 - VALIDATION OF GROUND-BASED MATERIAL EVALUATION SYSTEMS
 - ESTABLISH MATERIAL REACTION DATA BASE
 - ENHANCED UNDERSTANDING OF INTERACTION MECHANISMS LEADING TO CONFIDENCE IN DESIGN
- GLOW SPACE EXPERIMENTS ARE NEEDED
 - ESTABLISH DATA BASE ON GLOW CHARACTERISTICS ACROSS SPECTRAL REGIONS OF INTEREST
 - VALIDATED EXISTING MODELS

PROPOSED EXPERIMENTS

- LDEF RETRIEVAL
 - EXPANSION OF DATA BASE
 - HIGH FLUENCE EXPOSURE (1×10^{21} ATOMS/CM²)
 - FLUX EFFECTS (LOW FLUX OVER LONG EXPOSURE)
 - HARDWARE ASSESSMENTS
- EOIM-3
 - BENCHMARK REACTION RATE DATA BASE USING ON-BOARD MASS SPECTROMETER
 - DATA FOR CORRELATION WITH GROUND SIMULATION SYSTEMS
- DELTA STAR
 - ACTIVE SENSOR DEVELOPMENT AND PERFORMANCE ASSESSMENT
 - CORRELATION WITH GROUND-BASED SIMULATION FACILITIES
- SMALL SATELLITES (INCLUDING LDEF)
 - ORIENTATION CONTROLLED
 - REAL TIME DATA
 - RECOVERY (IN SOME CASES)
 - DEPLOY IN DIFFERENT ORBITS INCLUDING HIGH ALTITUDE, LONG EXPOSURES

PROPOSED EXPERIMENTS (CONTINUED)

- LDEF REFLIGHT
 - REAL TIME TELEMETRY DATA
 - EVALUATE ADVANCED MATERIAL CONCEPTS
- SATELLITE RETRIEVAL
 - RECOVERING EXISTING SATELLITES FOR POST-MISSION INSPECTION
 - SATELLITE ORBITS MAY NOT BE COMPATIBLE WITH STS MISSIONS--MAY REQUIRE SPECIAL PROVISION FOR SHUTTLE RECOVERY
- SPACECRAFT GLOW
 - NASA OAST OUTREACH EXPERIMENT
 - INFRARED GLOW MEASUREMENTS
 - CIV GLOW EFFECTS
- DEVELOPMENT OF LOW-COST SATELLITE BASE AND ACTIVE SENSORS

EXPERIMENT CHARACTERISTICS

- MATERIAL EFFECTS EXPERIMENTS
 - LONG DURATION EXPOSURES
 - CONTROLLED SPACECRAFT ORIENTATION
 - DISTURBANCE INDEPENDENT
 - PROVISIONS FOR ELECTRICAL POWER
 - TELEMETRY
 - GOOD CONTROL OF CONTAMINATION
- GLOW INVESTIGATIONS--SAME REQUIREMENTS AS MATERIAL EFFECTS, EXCEPT:
 - ELLIPTICAL ORBITS
 - LONG DURATION DURATION EXPOSURES NOT NECESSARY

VOLUME, WEIGHT, AND COMPLEXITY OF EXPERIMENTS

- MATERIAL EXPERIMENTS

- | | |
|-------------------|--|
| - EOIM-3 | - WEIGHT--1,000 LBS, WITH STS CARRIER |
| | - VOLUME--1/8 SHUTTLE PAYLOAD BAY |
| | - COMPLEXITY--MODERATE |
| | COMPLEXITY (RAM ORIENTATIONS REQUIRED) |
| - LDEF | - PREVIOUSLY DESCRIBED |
| - DELTA STAR | - WEIGHT--50 LBS |
| | - VOLUME--SEVERAL CUBIC FEET |
| | - COMPLEXITY--LOW (ACTIVE TRAY) |
| - SPACECRAFT GLOW | - WEIGHT--1,000 LPS, WITH STS CARRIER |
| | VOLUME - 10 CUBIC FEET |

MICROMETEOROIDS AND DEBRIS

ANDREW POTTER
NASA - JOHNSON SPACE CENTER
CHAIRMAN

SCOPE

- WHAT MATERIALS ARE VULNERABLE?
 - ALL VULNERABLE TO HYPERVELOCITY IMPACTS
 - IMPORTANCE OF IMPACT EFFECT DEPENDS ON FUNCTION OF MATERIAL:
 - = MIRROR (EROSION)
 - = PRESSURE VESSEL (EXPLOSION)
- LEO MOST SIGNIFICANT REGION RELATIVE TO ORBITAL DEBRIS
 - METEOROID ENVIRONMENT INDEPENDENT OF ORBIT
 - RELATIVE VELOCITIES DEBRIS IN GEO ARE LOW
- CONSEQUENCES OF ENVIRONMENT EFFECT
 - SMALL SIZES-DEGRADATION
 - LARGE SIZES-CATASTROPHE

CORRELATION BETWEEN LAB/THEORY AND ACTUAL EFFECTS

- HYPERVELOCITY IMPACT MEASUREMENTS SIMULATE DEBRIS IMPACTS
 - SMALL PARTICLES (< 100 MM) TO 10'S KM/SEC
 - LARGE PARTICLES LIMITED TO 7-8 KM/SEC
- CANNOT SIMULATE MICROMETEOROID IMPACTS VERY WELL
 - VELOCITIES TO 40 KM/SEC
 - LOW DENSITY PARTICLES
- MASSIVE COLLISIONS CAN BE SCALED AND MODELED
 - MAJOR EFFECTS PREDICTED
 - SIZE AND VELOCITY DISTRIBUTION OF SMALL PARTICLES NOT WELL KNOWN

RELATED TOPICS

- STUDY OF IMPACTS/COLLISIONS IN SPACE
 - GROUND-BASED, SPACE-BASED (IF POSSIBLE) OBSERVATIONS - SIZE AND VELOCITY OF DEBRIS
 - "MISSIONS OF OPPORTUNITY"
- MITIGATION MEASURES
 - SWEEPING SMALL DEBRIS
 - AVOIDANCE MANEUVERS
 - MOVABLE SHIELD
 - REMOVAL OF LARGE OBJECTS
 - IMPROVED SPACECRAFT PAINT
 - OPERATIONAL PROCEDURES TO MINIMIZE BREAKUPS

FLIGHT EXPERIMENT POSSIBILITIES

ENVIRONMENT DEFINITION

- NON-RETRIEVABLE SATELLITES (SOURCE ID DIFFICULT)
 - 1 MM AND LARGER-QUICKSAT (\$100M)
 - BELOW 1 MM
 - = OFF-THE-SHELF SENSORS
 - = EXISTING/PLANNED EXPERIMENTS (SERTS, EOIM)
- RETRIEVABLE SATELLITES (SOURCE ID POSSIBLE)
 - LDEF RECOVERY
 - FREE-FLYER "GAS-CAN"
 - = EXPANDABLE SURFACES FOR LARGE AREA
 - = REGULAR LAUNCHES (2-3 YEAR INTERVALS)
- COSMIC DUST FACILITY FOR SPACE STATION
 - > 10 YEARS AWAY

SPACE EXPERIMENT REQUIREMENTS

- ENVIRONMENT FOR SIZES BELOW 10 CM POORLY DEFINED
 - UNCERTAINTY FACTORS OF 3 TO 10 FOR DEBRIS
 - RAPID CHANGES OF DEBRIS POPULATION ARE POSSIBLE (AND LIKELY)
 - METEOROID ENVIRONMENT DEFINED WELL ENOUGH
- SYNERGISM AND CUMULATIVE EFFECTS NOT WHOLLY PREDICTABLE, AND HENCE MAY NOT ALL BE SIMULATABLE. FLIGHT EXPERIMENT EXERCISES ALL POSSIBILITIES
- CANNOT COMPLETELY SIMULATE/CALCULATE EFFECTS OF MASSIVE COLLISIONS IN SPACE

SYNERGISTIC EFFECTS

- MANY POSSIBILITIES-RELATIVE IMPORTANCE UNKNOWN
- EXAMPLES
 - ATOMIC OXYGEN EROSION INITIATED BY IMPACT
 - CONTAMINATION INDUCED BY VAPOR FROM IMPACT
 - SPACECRAFT CHARGING EFFECTS FACILITATED BY PENETRATIONS
 - THERMAL EFFECTS PRODUCED BY EROSION OF THERMAL CONTROL COATINGS
- CASCADES CONCEIVABLE

CONFIDENCE LEVEL

- CAN WE BUILD SATELLITES FOR 10-30 YEAR OPERATION?
 - NO FOR LARGE AREA, LONG LIFE SATELLITES
 - = DEBRIS ENVIRONMENT NOT WELL ENOUGH KNOWN
 - NO FOR SATELLITES WITH NEW FUNCTIONS
 - = DON'T KNOW SYNERGISTIC EFFECTS AND THEIR IMPORTANCE
 - YES FOR SATELLITES OF CONVENTIONAL DESIGN AND FUNCTION

FLIGHT EXPERIMENTS NEEDED

- FIRST PRIORITY: MEASURE LEO ENVIRONMENT FOR SIZES BELOW 1 CM (GROUND-BASED RADARS TO COVER > 1 CM OBJECTS)
 - VITAL DATA FOR DETERMINING SIGNIFICANCE
- SECOND PRIORITY: REPEAT THE MEASUREMENTS AT INTERVALS TO MONITOR CHANGES
- THIRD PRIORITY: ESTABLISH NATURE AND SIGNIFICANCE OF POSSIBLE SYNERGISTIC EFFECTS
- FOURTH PRIORITY: UNDERSTAND DETAILS OF MASSIVE COLLISIONS IN ORBITS (BETTER DEFINITION OF ENVIRONMENT)

FLIGHT EXPERIMENT POSSIBILITIES

SYNERGISM/ACCUMULATED EFFECTS

- NEED LONG-TERM EXPOSURE OF REAL SYSTEMS
- RECOVERY OF OLD SATELLITES FOLLOWED BY DETAILED INTERDISCIPLINARY ANALYSIS
 - LDEF ~ 5 YEARS OLD, CAPTURE PLANNED NOVEMBER 1989
 - SMM, SAGE ~ 10 YEARS OLD
 - = CAPTURE BY SHUTTLE
 - TIROS ~ 30 YEARS
 - = CAPTURE USING ELV
- COSTLY, DIFFICULT TO RETRIEVE SATELLITES
 - NEED INTERDISCIPLINARY JUSTIFICATION
- LDEF REMAINS PRIME CANDIDATE FOR RECOVERY
 - MAJOR SOURCE OF NEW DATA

CONTAMINATION

CARL MAAG JET PROPULSION LABORATORY CHAIRMAN

SCOPE

- CLASSES OF MATERIALS DID NOT SEEM APPROPRIATE FOR THIS ENVIRONMENTAL ISSUE
- WORKING GROUP CHOSE TO ACCEPT S/C SYSTEMS FOR SUBSYSTEMS AS THE MOST VULNERABLE
 - OPTICAL SYSTEMS
 - = SENSORS
 - = REFLECTIVE/REFRACTIVE OPTICS
 - THERMAL CONTROL SYSTEMS
 - SOLAR POWER
- ALL ORBITS NEED TO BE CONSIDERED
- CONCERNS ARE
 - CHANGES IN TRANSMITTANCE OF OPTICS
 - RADIATIVE PROPERTIES OF COATINGS

ISSUES

- WHICH MATERIALS OR CLASSES OF MATERIALS ARE MOST VULNERABLE? IN WHAT ORBITS? WHY? CAN GENERAL OR SPECIFIC CONSEQUENCES FOR LONG-TERM S/C OR SATELLITE PERFORMANCE BE IDENTIFIED?
- IS THERE ANY CORRELATION BETWEEN THEORY AND LAB EXPERIENCE (AND SPACE EXPERIENCE) SO THAT LONG-TERM PERFORMANCE CAN BE PREDICTED?
 - SOME THEORY/LABORATORY CORRELATIONS HAVE BEEN DEMONSTRATED
- DO WE KNOW ENOUGH, EVEN IF ONLY EMPIRICALLY, TO LAUNCH FOR 10 YEARS (OR 30 YEARS) OF SERVICE WITH CONFIDENCE?
 - VERY SHORT TERM DATA AVAILABLE
 - NOT ENOUGH CONFIDENCE FOR 10-YEAR LIFETIME

TERRESTRIAL LABORATORY FACILITIES

- AVAILABILITY OF LABORATORY SIMULATION FACILITIES
 - OUTGASSING - YES
 - PLUMES - NO
 - EFFECTS - PARTIAL

INTERACTION/SYNERGISM OF ENVIRONMENTAL EFFECTS

- IS SYNERGISM LIKELY? YES
- HAS SYNERGISM BEEN EVALUATED? IN A FEW CASES
- DO LABORATORY FACILITIES EXIST TO ASSESS SYNERGISM? VERY LIMITED FACILITIES
- SPACE EXPERIMENTS ARE REQUIRED; GROUND FACILITIES CANNOT SIMULATE ALL ENVIRONMENTAL CONDITIONS SIMULTANEOUSLY

REQUIRED SPACE EXPERIMENTS

- HIGH PRIORITY:
 - PLUME FLOWFIELD/CONTAMINATION
 - MOLECULAR BACKSCATTER

(NOTE: BOTH HIGH PRIORITY EXPERIMENTS COULD BE CONTAINED IN ONE PACKAGE - VOLUME $\sim 0.6 \text{ m}^3$, MASS $\sim 500 \text{ LBS.}$)
- MEDIUM TO HIGH PRIORITY:
 - PARTICLE RELEASE, DETECTION, AND REMOVAL

PLANNED AND DEPLOYED SPACE EXPERIMENTS

- SPACE SHUTTLE
 - IBS/SPAS (DEPLOY AND RECOVERY)
 - STAR LAB
 - CIRRIIS (IR TELESCOPE)
 - LDEF (DEPLOY AND RECOVERY)
 - IFCE (BACKSCATTER; NASA/ESA)
 - EOIM III
 - SPACE (DEPLOY AND RECOVERY)
- FREE FLYER:
 - P-888 (TEAL RUBY, IAPS, UV) SHUTTLE LAUNCH
 - SSTS NTFE (PROPOSED NEAR TERM FLIGHT EXPERIMENT)
 - SPIRIT II, III
 - DELTA STAR
 - GAS EJECTION PACKAGE

PLANNED AND DEPLOYED SPACE EXPERIMENTS **(CONTINUED)**

- STS PLATFORMS
 - GAS CAN
 - MPSS
 - HITCHHIKER G
 - SPAS
 - CTM (COLLAPSIBLE TUBE MAST)

SHUTTLE PACKAGE

- IOCM
- APM
- CMP II
- PACS

SPACE EXPERIMENT INSTRUMENTATION

- TQCM, CQCM
- CALORIMETER
- RODIOMETER
- MASS SPECTROMETER
- CAMERAS
 - VISIBLE (FILM, ELECTRONIC)
 - UV
 - IR
- SCATTEROMETERS
- PARTICLE DETECTORS
 - FLUX COUNTER
 - FOV SPIR
- PRESSURE/DENSITY GAGES

SPACE EXERIMENT

MOLECULAR

- E.1. PRIORITY
 2. DURATION
 3. RETRIEVAL
- F.1. VOLUME
 2. WEIGHT
 3. ASE/GSE
 4. PLATFORM
 CHARACTERS
- G.1. PLANNED
 2. DESIGNED
 3. BUILT

TRANSPORT	BACK SCATTER	SYNERGISTIC DEPOSITION RATES	REEMISSIONS	EFFECTS

TRAPPED RADIATION

AL VAMPOLA AND WAYNE STUCKEY
AEROSPACE CORPORATION
CHAIRMEN

SCOPE OF PROBLEM

- VULNERABLE MATERIALS/COMPONENTS
 - ORGANIC POLYMERS
 - OPTICS
 - INTEGRATED CIRCUITS
- ORBITS
 - PRIMARILY THE HIGHER ORBITS
 - = 2000 KM p⁺
 - = GEOSYNC e⁻
- CONSEQUENCES
 - POLYMERS: CROSS-LINKING, SCISSION
 - = EMBRITTLEMENT
 - = MODULUS CHANGES
 - = COEFFICIENT OF EXPANSION
 - OPTICS: DISLOCATIONS, IONIZATION
 - = DISCOLORATION
 - = DISTORTION (DUE TO DIFFERENTIAL EXPANSION)
 - CIRCUITS
 - = SEU
 - = LATCHUP
 - = BURNOUT
 - = DOSE EFFECTS

THEORY/EXPERIENCE

- NEW MATERIALS--NO SPACE EXPERIENCE
- POOR CORRELATION (QUANTITATIVE) BETWEEN THEORY AND LAB EXPERIENCE
 - FACTORS OF 2-5 SEU
 - NO QUANTITATIVE AGREEMENT LATCHUP/BURNOUT
 - DOSE/ANNEALING, TEST DATA ONLY
- BATCH PROPERTIES

PREDICTABILITY OF LONG-TERM PERFORMANCE

- QUALITATIVE ESTIMATES ONLY
- SYNERGISTIC EFFECTS ONLY GUESSED AT
- AT THIS POINT, IT IS PROBABLY NOT POSSIBLE TO PREDICT A GIVEN DESIGN WILL SURVIVE FOR 10 YEARS IN SPACE WITH A HIGH PROBABILITY

LAB FACILITIES

- AVAILABILITY
 - IN GENERAL, YES
 - BEING CLOSED DOWN
- ADEQUACY
 - IN GENERAL, NOT ADEQUATE
 - BEAM CHARACTERISTICS
 - MONOENERGETIC
 - UNIDIRECTIONAL
 - INTENSITY
 - SPECIES
- NEED DATA BASE
 - SYSTEMATIC, p^+
 - FOR DEVELOPMENT/TEST OF THEORY
- COMMITTEE TO OVERSEE LAB FACILITIES
- SREL?

SYNERGISMS

- SYNERGISTIC PARAMETER
 - THERMAL/RADIATION
 - UV/TRAPPED RADIATION
 - ALL THREE
- TESTING
 - THERMAL/RADIATION (SEU-YES)
 - UV/RADIATION (SOME)
- NO LAB FACILITIES, PER SE
 - FOR DEVELOPMENT/TEST OF THEORY
- COMMITTEE TO OVERSEE LAB FACILITIES
- SREL DATA?

SPACE EXPERIMENTS

- SPACE EXPERIMENT REQUIREMENTS
 - HIGHER ORBIT THAN SHUTTLE
 - LONGER DURATIONS THAN SHUTTLE
 - A NEED FOR RECOVERY
- PRIORITY
 - CAN IDENTIFY GENERIC TYPES
(E.G., LDEF - FOLLOW-ON)
 - CAN IDENTIFY LOCATIONS AND DURATIONS FOR SOME
 - FUTURE WORK/ADVANCES IN ELECTRONICS AND MATERIALS WILL BE THE DRIVER

APPENDIX

TRAPPED PARTICLE FLUX MODELS AT NSSDC/WDC-A-R&S

D. Bilitza, D.M. Sawyer, J.H. King

National Space Science Data Center, Goddard Space Flight
Center, Code 633, Greenbelt, Maryland 20771

Abstract

This is a document prepared for the NASA/SDIO Workshop on Space Environment Effects on Materials at Langley Research Center June 28-30, 1988. It summarizes our perception of what data are needed in the future for trapped particle modeling. We have also include a short summary of NSSDC's past and future modeling activities and a list of satellite data that have not yet been considered in the modeling efforts.

Introduction

This paper addresses the following questions:

- I. What is the present status of NSSDC's models ?
- II. Which data have become available since the last model up-date?
- III. What is needed to improve the models ?
- IV. What are NSSDC's future modeling activities ?

The answers are as follows:

Present Status of NSSDC's Models

NSSDC's trapped particle models describe the omnidirectional proton and electron fluxes in the inner and outer radiation belts in terms of energy, L-shell, and B/B₀.

	Name	Energy Range	L range	NSSDC Report
Electrons	AE-8	0.04 - 7 MeV	1.2 - 11	Appendix
Protons	AP-8	0.1 - 400 MeV	1.17-7	ref. 2)

AE-8 and AP-8 are the latest editions in a series of models that have been developed and continuously improved by J. I. Vette and his collaborators at NSSDC/WDC-A-R&S over the last decades. This is documented in several NSSDC reports and is summarized in ref.1 (Table 1) and the Appendix. For each species two model maps have been established, one for solar minimum conditions (epoch 1964) and one for solar maximum conditions (epoch 1970). The models are based on satellite data up to 1977 (see Figures 3,4,5 and 6 in ref. 1); this includes 27 satellites over a time span of almost 20 years. The data coverage in B/B₀ - L space is shown in Figures 1 and 2 of ref.1. The models provide time averages over half a year or more. The average enhancement due to magnetic storms during this period is included.

Data Available Since the Last Model Up-date

Low-altitude, circular orbits:

Space Shuttle, NASA, 250 to 450 km, 20 to 60 deg., several flights since 1981

Dosimeters at several locations on the shuttle and on the astronauts determined the accumulated dose per shuttle flight.

Trapped Ions in Space Experiment, J.H. Adams, NRL; shuttle flight: Oct 84, 245 km, 57 deg.

The stack of plastic track detectors allowed measurements of He/p ratio in the energy range 7 to 70 MeV/amu.

Long Duration Exposure Facility, R. Gualdoni, NASA HQ.

The free-flying LDEF module was released from the shuttle on 4/6/84 and will be recovered when shuttle flights resume; contains passive track detectors of F.J. Rich, AFGL (protons) and of J.H. Adams, NRL (heavy ions).

Circular, polar orbits:

DMSP, USAF, 840 km, 7 satellites since 1976

Silicon Dosimeter, J.B. Blake, Aerospace Corp.

4 detectors allow separation of electron and proton fluxes with different threshold energies.

TIROS & NOAA, NOAA, 850 km, 4 satellites since 1978,

Space Environment Monitor, D.J. Williams, NOAA

protons, 5 energy bands above 30 KeV

electrons, 3 energy bands above 30 KeV

Geostationary orbits:

SMS & GOES, NOAA, 6.67 Re, 8 satellites since July 1974, two satellites operate simultaneously at 75 and 135 west.

Energetic Particle Monitor, D.L. Williams, NOAA

solid state detector, protons from 0.8 to 500 MeV,

alpha particles from 4 to 392 MeV, electrons > 2 MeV.

Higbie, DOD, 6 satellites since 1976

Energetic Particle Detector, P.R. Higbie, Los Alamos

electrons from 0.03 to 2 MeV

protons from 0.05 to 150 MeV

alpha particles from 1.2 to 600 MeV (special mode)

Highly elliptical orbits:

S3-3, USAF, 246 - 7856 km, 97.5 deg., launched 7/8/76

Energetic Electron Spectrometer, A.L. Vampola, Aerospace Corp.

electrons from 0.0012 to 1.6 MeV

protons from 0.08 to 3 MeV, alpha > 4 MeV

ISEE-1,-2, NASA/ESA, 281 - 138120 km, 29 deg., 10/22/77

Medium Energy Particle Experiment, Williams, NOAA

electrons from 20 KeV to 1 MeV

protons from 0.02 to 1.2 MeV

SCATHA, DOD, 184 - 43905 km, 27 deg., 1/30/79

Energetic Proton Detector, J.B. Blake, Aerospace Corp.

protons from 0.02 to 2 MeV

Rapid Scan Particle Detector, D.A. Hardy, AFGL
 electrons from 50 eV to 1.1 MeV
 ions from 50 eV to 35 MeV
 High-Energy Particle Detector, J.B. Reagan, Lockheed
 electrons from 0.3 to 2.1 MeV
 protons from 1 to 100 MeV
 alpha particles from 6 to 60 MeV
 AMPTE/CCE, NASA, 550 - 49400 km, 5 deg., 8/16/84
 Medium Energy Particle Analyzer, R.W. McEntire, APL
 composition and spectra from 10 KeV/n to 6 MeV/n
 32 sector angular resolution.
 AMPTE/IRM, FRG, 550 - 112800 km, 29 deg., 8/16/84
 Suprathermal Ionic Charge Analyzer, D.K. Hovestadt, MPIE
 10 to 300 KeV/q; electron sensor: 35 to 220 KeV

High-altitude orbits:

NTS-2, NRL, 11000 n. miles, 63 deg., launched 7/17/77
 DMSP-type dosimeter, A.I. Cole, TRW Systems
 IUE, ESA/NASA, 26643 - 44951 km, 29 deg., 1/26/78
 Silicon detector, electrons > 1.3 MeV, protons > 15 MeV

Requirements for Model Improvement

The last page of ref. 1 is a modeler's wish list. Most of these 10-year old recommendations will be fulfilled with the long awaited CRRES satellite. Modeling needs a reliable data base large enough to allow the necessary statistical evaluation. Therefore it is important to insure (i) a long CRRES mission time, (ii) the resources to process all acquired raw data, (iii) follow-up satellite missions similar to CRRES. It would be also desirable to obtain direct flux measurements at shuttle/space station altitudes.

NSSDC's Future Modeling Activities

- completion of NSSDC report describing AE-8
- comparisons with some of the measurements listed in ref. 2.

The development of dynamic models can be envisaged for the time after the successful completion of the CRRES satellite mission.

References

1. Vette, J. I., K. W. Chan, and M. J. Teague, Problems in Modeling the Earth's Trapped Radiation Environment, Air Force Geophysics Lab report AFGL-TR-78-0130, Hanscom AFB, MA, 1978.
2. Short summary of AE-8 model; enclosed
3. D.M. Sawyer and J.I. Vette, AP-8 Trapped Proton Environment, NSSDC/WDC-A-R&S Report 76-06, 175 pages (1976).

Appendix: AE-8 Short Summary

The AE-8 (MAX and MIN) models were established from earlier AE models with some modifications (as indicated below).

Region	Solar Activity	Model	NSSDC Rep.	Modification
Outer zone ($L > 2.8$)	Solar minimum and maximum	AE-4	72-06	Energy spectra above 2 MeV increased based on ATS-6, AZUR, and OV1-19 data. B-cutoff based on AZUR data.
Inner zone ($L < 2.4$)	Solar minimum	AE-5	74-03	None
	Solar maximum	AE-6	76-04	None

An interpolation procedure was applied between $L=2.4$ and $L=2.8$ to obtain smooth transitions between the inner and outer zones at all energies. In comparison with earlier AE models you will find:

- somewhat lower fluxes at low altitudes (< 300 km)
- small modifications in the range $L=2.5$ to $L=2.7$
- the spectrum above 2 MeV in the outer zone is harder than AE-4

SOLAR RADIATION

**WAYNE S. SLEMP
NASA LANGLEY RESEARCH CENTER
CHAIRMAN**

CURRENT STATUS

- MOST MATERIALS DEGRADE TO SOLAR RADIATION
- INFORMATION AVAILABLE ON SHORT-TERM UV EFFECTS ON MATERIALS;
PROVIDES LIMITED DATA BASE
- FLIGHT DATA ON COATING DEGRADATION CONFUSED BY CONTAMINATION
- LITTLE CORRELATION BETWEEN TESTING LABORATORIES IN: UV EXPOSURE
CONDITIONS, CALIBRATION TECHNIQUES, AND DETECTORS
- FEW FACILITIES WITH EXTREME UV EXPOSURE CAPABILITY
- LIMITED DATA ON THERMAL CYCLING EFFECTS IN LAB AND IN SPACE

TECHNOLOGY DRIVERS

- 30-YEAR LIFETIME OF SPACE STATION
 - UV + AO + THERMAL CYCLING
- 5 TO 15 YEAR-LIFETIME OF SDI MISSIONS
 - UV + HIGH ENERGY RADIATION
 - UV + AO + THERMAL CYCLING
- MATERIALS AND SYSTEMS SURVIVABILITY FOR LONG-LIFE MISSIONS

TECHNOLOGY NEEDS

- DEVELOPMENT OF A UV TESTING METHODOLOGY WITH STANDARDIZED TEST PROCEDURES FOR ACCELERATED UV TESTING OF MATERIALS
- DATA BASE OF FLIGHT DATA FOR LONG-TERM MISSIONS - INCLUDES:
 - OPTICAL FILTERS, WINDOWS, THERMAL COATINGS, HARDENED COATINGS, POLYMERIC FILMS
- FLIGHT DATA BASE ON UV FLUX/DISTRIBUTION
- LONG-TERM THERMAL CYCLING DATA
 - LDEF COMPOSITES COULD PROVIDE 5-YEAR FLIGHT DATA

UV TESTING RECOMMENDATIONS

- NEED CONTINUUM UV SOURCE (FROM EUV TO VISIBLE) FOR LAB TESTING TO DETERMINE SPECTRAL SENSITIVITY OF MATERIALS
- A TEST FACILITY SHOULD BE CONSTRUCTED TO PROVIDE TEST DATA NEEDED TO STANDARDIZE UV SIMULATION SOURCES, FLUX MEASUREMENTS, AND TESTING PROCEDURES
- A FLIGHT EXPERIMENT (1 YEAR MINIMUM) SHOULD BE CONDUCTED FOR CORRELATION OF LAB SIMULATION
 - RADIOMETERS FOR UV MEASUREMENT
 - PROVIDE DATA ON SELECTED MATERIALS
 - EXPERIMENT RETURNED IN VACUUM FOR LAB TESTING

OTHER RECOMMENDATIONS

- QUARTERLY OR SEMI-ANNUAL MEETING OF COMMITTEE TO ADDRESS PROGRESS IN SPACE ENVIRONMENTAL SIMULATION AS REQUIRED FOR PERFORMANCE OF ONGOING AND PLANNED NASA/SDIO MISSIONS

SPACECRAFT CHARGING

N. JOHN STEVENS
TRW
CHAIRMAN

GENERAL COMMENTS

- SPACECRAFT CHARGING INTERACTIONS COUPLE ENVIRONMENT TO SYSTEM PERFORMANCE THROUGH MATERIALS
- TECHNOLOGY IS STILL DEVELOPING
 - CONCERN FOR BOTH ENVIRONMENT-DRIVEN & OPERATING SYSTEM - DRIVEN INTERACTIONS
- MEETING ADDRESSED ENVIRONMENT BUT LACKED SPECIFIC MISSION REQUIREMENTS
 - REQUIRE SYSTEM DEFINITION TO PRIORITIZE INTERACTIONS
 - RECOMMEND SDI BRIEF SYSTEMS REQUIREMENTS
- NEED ADDITIONAL GROUP SUPPORT WORK TO SUPPLEMENT FLIGHT EXPERIMENTS

MATERIAL PROPERTY CHANGES WITH ELECTRICAL STRESS

AND TIME IN SPACE ENVIRONMENT

- WHY PROBLEM:
 - STRESS ENHANCES AGING
 - RADIATION INDUCED INTERFACE FAILURES:
 - CURRENT SPACECRAFT BEHAVIOR STARTING TO BE UNDERSTOOD BUT MATERIALS AND OPERATING CONDITIONS CHANGING
 - LIFETIME EXTENDED
- GROUND TEST/THEORY CORRELATION:
 - DIELECTRIC COMMUNITY WORKING
 - SHORT TERM TESTING WITHOUT SPACE ENVIRONMENT
- WHAT IS STILL NEEDED
 - MATERIALS TESTING TO ESTABLISH RANGE OF INTERACTION

MATERIAL PROPERTY CHANGES WITH ELECTRICAL STRESS

AND TIME IN SPACE ENVIRONMENT (CONTINUED)

- WHY REQUIRE SPACE FLIGHT:
 - NEED SPACE ENVIRONMENT TO VERIFY BEHAVIOR
 - HIGH ALTITUDES OR POLAR FOR RADIATION
 - TIME IN ENVIRONMENT
- SUPPORTING WORK:
 - DIELECTRIC COMMUNITY
 - NOT DIRECTED TOWARDS SPACE APPLICATIONS

CANDIDATE EXPERIMENTS

- MATERIAL PROPERTY CHANGES WITH ELECTRICAL STRESS AND TIME IN SPACE ENVIRONMENT
- HIGH VOLTAGE SYSTEM INTERACTIONS
- THIN-FILM COATING INTERACTIONS
- DISCHARGE CHARACTERIZATION
- "TAILORED" MATERIALS
- HEAVY STRESSED POWER SYSTEM DIELECTRICS
- PULSED POWER SYSTEM INTERACTIONS
- COMPOSITE INTERNAL NOISE GENERATION
- ACTIVE CHARGE CONTROL
- "RADIATION BELT" CHARGING

RADIATION BELT CHARGING BY ENERGETIC PROTONS AND ELECTRONS

- WHY PROBLEM:
 - UPSET SEEMS TO OCCUR ON GPS
 - NO CHARGING MODEL EVALUATION
- GROUND TEST/THEORY CORRELATION
 - SHOULD BE ABLE TO TREAT BUT HASN'T BEEN YET
- WHAT IS STILL NEEDED:
 - EVALUATION OF EFFECT OF ENVIRONMENT
- WHY REQUIRE SPACE FLIGHT:
 - NEED ENVIRONMENT AND TIME IN SPACE

ACTIVE CHARGE CONTROL INTERACTIONS

- WHY PROBLEM:
 - THIS IS A CHARGING MITIGATION TECHNIQUE, BUT IT CAN DEGRADE COATINGS BY BOMBARDMENT TIME EFFECT
- GROUND TEST/THEORY CORRELATION:
 - SHORT TERM TESTING
 - MODEL EXISTS BUT NOT VALIDATED
- WHY REQUIRE SPACE FLIGHT:
 - LONG TERM STUDY IN SPACE WITHOUT WALLS
- SUPPORTING WORK:
 - AFGL CHARGE CONTROL SYSTEM (XENON)
 - IAPS (MERCURY)

PULSED POWER INTERACTION-SYSTEM DYNAMIC RESPONSE TO 1 TO 100/SEC POWER PULSE

- WHY PROBLEM:
 - BEHAVIOR IN PLASMA UNCERTAIN
 - AFFECTS SYSTEM PERFORMANCE
 - FLASHOVER
- GROUND TEST/THEORY CORRELATION:
 - THEORY BEING DEVELOPED
- WHAT IS STILL NEEDED:
 - THEORY AND TESTS DEMONSTRATION
- WHY REQUIRE SPACE FLIGHT:
 - NEED SPACE ENVIRONMENT
 - RADIATION ENVIRONMENT IMPORTANT
- SUPPORTING WORK:
 - SPEAR II
 - TEXAS TECH AND MAXWELL (TESTING)

NOISE GENERATED IN COMPOSITES
**(SPACE INDUCED CHARGING COUPLED WITH RADIATION
TO GENERATE NOISE IN MATERIALS)**

- WHY PROBLEM:
 - RF NOISE CAN COUPLE INTO COMMUNICATIONS AND SENSORS
- GROUND TEST/THEORY CORRELATION:
 - MEASURE RF LEVELS IN SMALL SAMPLES UNDER ELECTRICAL STRESS AND RADIATION
 - THEORY ADEQUATE BUT NUMBER OF PULSES UNKNOWN
- WHY REQUIRE SPACE FLIGHT:
 - NEED SPACE FLIGHT ENVIRONMENT
 - AURORAL OR HIGH ALTITUDE
 - CAN BE ADDED TO EXISTING S/C HAVING RF DETECTION SYSTEMS

HEAVY STRESSED POWER SYSTEM DIELECTRIC
**(SDI APPLICATIONS UNDER HIGH VOLTAGE AND LARGE
CURRENTS)**

- WHY PROBLEM:
 - STRONG ELECTRICAL STRESS AND INDUCED MAGNETIC FIELD REDUCE BREAKDOWN THRESHOLDS
- GROUND TEST/THEORY CORRELATION:
 - COMPONENTS UNDER STUDY
- WHAT IS STILL NEEDED:
 - COMBINED SYSTEM EFFECTS
 - SPACE ENVIRONMENT DEMONSTRATION
- WHY REQUIRE SPACE FLIGHT:
 - TOTAL SPACE ENVIRONMENT EFFECT
 - TIME IN SPACE

SYSTEM INTERACTIONS

- SCOPE:
 - HIGH VOLTAGE
 - = HIGH VOLTAGE SOLAR ARRAYS
 - = STRUCTURE COLLECTION IN PLASMAS
 - = SCALING LAWS FOR SIZE, VOLTAGE, POWER FREQUENCY
 - = SHEATH EFFECTS
- WHY PROBLEM:
 - SYSTEM FLOATS ELECTRICALLY IN PLASMA ENVIRONMENT
 - BREAKDOWNS IN HIGH VOLTAGE SYSTEMS
- GROUND TEST/THEORY CORRELATION:
 - SMALL SCALE SAMPLE CORRELATES WITH THEORY
- WHAT IS STILL NEEDED:
 - SIZE, VOLTAGE, POWER, FREQUENCY SCALING
- WHY REQUIRE SPACE FLIGHT:
 - NEED COMPLETE SPACE ENVIRONMENT
 - CAN'T SIMULATE ON GROUND
- SUPPORTING WORK:
 - GROUND SUPPORT WORK
 - JAPANESE SPACE EXPERIMENT

THIN FILM COATING-STABILITY OF THIN-FILM OPTICAL AND ELECTRICAL COATINGS IN SPACE ENVIRONMENT

- WHY PROBLEM:
 - COATING APPLIED FOR SPECIFIC OPTICAL OR ELECTRICAL PURPOSE SPACE--
- SPACE
 - SPACE CHARGING INTERACTION COUPLED WITH SPUTTERING OR CONTAMINATION MAY DESTROY COATING CHARACTERISTICS
- GROUND TEST/THEORY CORRELATION:
 - SHORT TERM TESTING
 - FLIGHT DATA NOT INSTRUMENTED FOR DETAILED EXAMINATION
- WHAT IS STILL NEEDED:
 - IDENTIFICATION OF COATINGS
- WHY REQUIRE SPACE FLIGHT:
 - NEED SPACE ENVIRONMENT

DISCHARGE CHARACTERIZATION

- SOURCES:
 - WHAT ARE CONDITIONS FOR DISCHARGE INITIATION
- CHARACTER:
 - FREQUENCY, AMPLITUDES, REP RATE, TRANSFER FUNCTION, AND CHANGES WITH TIME IN SPACE
- WHY PROBLEM:
 - PROTECTION OF SYSTEM CIRCUITS DEPENDS ON KNOWLEDGE OF DISCHARGES
- GROUND TEST/THEORY CORRELATION:
 - DEDUCE DISCHARGE BEHAVIOR IN SPACE
 - CHARACTERISTICS NOT REPEATABLE
- WHAT IS STILL NEEDED:
 - THEORY AND TEST CORRELATION
- WHY REQUIRE SPACE FLIGHT:
 - NEED TOTAL ENVIRONMENT AND SPACECRAFT CONFIGURATIONS

"TAILORED" MATERIALS

- SCOPE:
 - MATERIALS DEVELOPED FOR PROPERTIES TO MINIMIZE CHARGING LEVELS
 - CONDUCTIVITIES IN RANGE 10^{-8} TO 10^{-10} S/M²
- WHY PROBLEM:
 - CAN MITIGATE CHARGING CONCERNS
- GROUND TEST/THEORY CORRELATION:
 - QUASI-CONDUCTIVE MATERIALS UNDER DEVELOPMENT
- WHAT IS STILL NEEDED:
 - BETTER MATERIALS FOR THIS APPLICATION
 - DEMONSTRATE STABILITY IN SPACE ENVIRONMENT
- WHY REQUIRE SPACE FLIGHT:
 - DEMONSTRATE BEHAVIOR IN SPACE ENVIRONMENT
- SUPPORTING WORK:
 - GSFC
 - VIRGINIA TECH

SUMMARY

- IDENTIFIED INTERACTIONS THAT WOULD AFFECT SYSTEM PERFORMANCE
- BETTER DEFINITION OF SYSTEM/MISSIONS REQUIRED
- GENERAL APPROACH FOR THIS AREA:
 - SMALL SCALE GROUND TESTS
 - MODELING OF INTERACTION
 - UNDERSTANDING
 - SCALING
 - FLIGHT VERIFICATION TEST

SECTION II-B

WORKING GROUP WRITTEN PRESENTATIONS *

- * These presentations were submitted to the compilers of this document by the working group chairmen in the weeks following the Workshop.

WORKING GROUP WRITTEN PRESENTATION

ATOMIC OXYGEN

Co-chairmen: Lubert J. Leger and James T. Visentine
NASA Johnson Space Center

Earlier Shuttle flight experiments have shown NASA and SDIO spacecraft designed for operation in low-Earth orbit (LEO) must take into consideration the highly oxidative characteristics of the ambient flight environment. Although the number densities of atomic oxygen (AO) at altitudes where spacecraft typically operate (300-600 km) are quite low (10^9 - 10^7 atoms/cm³), the high orbital speed of the spacecraft can result in incident fluxes (10^{14} - 10^{15} atoms/S cm²), and collisional energies (translational energies equivalent to ~60,000 °K) large enough to interact with and degrade many different kinds of material surfaces.

Materials most adversely affected by atomic oxygen interactions include organic films, advanced (carbon-based) composites, thermal control coatings, organic-based paints, optical coatings, and thermal control blankets commonly used in spacecraft applications. In addition to causing changes in the mechanical, electrical, and optical properties of these materials, atomic oxygen can also interact with spacecraft surfaces to produce chemiluminescence, or "glow" within the ultraviolet (1400-4000 Å), visible (4000-8000 Å), and infrared (1.2-5.5 µm) wavelength ranges. These emissions can, in turn, interfere with or obscure low-light level observations made aboard Space Station Freedom and obtained from SDI target acquisition satellites. To obtain a more basic understanding of these and other environmental interaction effects, NASA has scheduled retrieval of the LDEF (Long Duration Exposure Facility) when the Shuttle flights resume, and now has under development the EOIM-3 (Evaluation of Oxygen Interactions with Materials, third series) flight experiment to obtain accurate reaction rate measurements for a large number of materials used in spacecraft applications, and an OAST spacecraft glow experiment to quantify glow brightness as functions of orbital altitude and surface temperature and study the interaction mechanisms responsible for the glow emissions.

Earlier results of NASA flight experiments have shown prolonged exposure of sensitive spacecraft materials to the LEO environment will result in degraded systems performance or, more importantly, lead to requirements for excessive on-orbit maintenance, with both conditions contributing significantly to increased mission costs and reduced mission objectives. These problems are especially important for SDI space-based platforms launched by expendable vehicles and delivered to orbits not easily accessible for maintenance by the Space Shuttle. In addition, our laboratory and flight results represent a relatively

immature data base, and the synergistic aspects of atomic oxygen, UV radiation, ionizing radiation, and micrometeoroid/space debris impacts are not adequately understood.

Flight data obtained from previous Space Shuttle missions and results of the Solar Max recovery mission are limited in terms of atomic oxygen exposure and accuracy of fluence estimates. The results of laboratory studies to investigate the long-term (15-30 yrs.) effects of AO exposure on spacecraft surfaces are only recently available, and qualitative correlations of laboratory results with flight results have been obtained for only a limited number of materials. To resolve these limitations to our data base, the Atomic Oxygen Working Group has recommended flight experiments be developed jointly by NASA and SDIO to improve the accuracy of the data base, provide an enhanced understanding of the interaction mechanisms and establish increased confidences in system designs. These flight experiments, in order of priority, are identified as follows:

- LDEF retrieval
- EOIM-3 Atomic Oxygen Effects experiment
- Delta Star materials studies
- Small, recoverable (mini-LDEF) satellites
- LDEF re-flight
- Retrieval of operational satellites
- OAST spacecraft glow experiment

The working group has also recommended the most promising ground-based laboratories now under development be made operational as soon as possible to study the full-life (15-30 yrs.) effects of atomic oxygen exposure on spacecraft systems. These laboratories should have adequate diagnostics to fully characterize the oxygen beam, and must produce atomic oxygen fluxes sufficiently high to accomplish full-life exposure studies within reasonable periods of time. The fidelity and accuracy of these exposures would later be determined by comparing their measurement results to results obtained from the EOIM-3 and Delta Star flight experiments.

WORKING GROUP WRITTEN PRESENTATION

METEOROID/ORBITAL DEBRIS EFFECTS ON MATERIALS

Chairman: Andrew Potter
NASA Johnson Space Center

1. Background

Low earth orbit (LEO) is the most significant region relative to orbital debris, since the flux of orbital debris peaks in the region from 800 to 1000 kilometers, and the relative velocities of objects in LEO are about 10 kilometers per second.

The flux and relative velocities of objects in geosynchronous orbit (GEO) are small, so that debris is not considered to be a problem in GEO.

The meteoroid environment is independent of orbit or altitude, so that its effects are the same in LEO and GEO.

The effects of orbital debris and meteoroid impacts can be divided into two broad regions:

(a) Erosion and pitting. Small particles (less than 100 microns) are very numerous. Impacts from these generally do not lead to penetration of surfaces, but cause pitting and erosion. The Solar Max surfaces were peppered with thousands of tiny impact pits.

(b) Catastrophic impacts. Large debris particles are few in number relative to small debris, so that the probability of an impact is low. However, the effects of an impact of a large particle at 10 kilometers per second are devastating. It is estimated that a 40 square meter spacecraft in LEO would suffer one impact from a 1 centimeter particle every 100 years. While the likelihood of this event is small, an impact of this kind would destroy most spacecraft. There is of course, an intermediate region where either effect can predominate, depending on the system being impacted. The impact of a 1 millimeter particle on a space suit will cause a catastrophic puncture of the life support system, while the impact of a 1 millimeter particle on the Shuttle Orbiter will cause some pitting damage, but nothing of great significance.

2. What materials are vulnerable?

All types of materials can be pitted or penetrated by hypervelocity impacts from meteoroids or orbital debris. Whether or not these impacts are important depends on the function of the material. For example, a mirror could be affected by pitting and erosion caused by the impact of very small particles which would not be a problem for structural materials. A pressure vessel could be damaged catastrophically by the impact of a particle large enough to penetrate its wall, while some other systems could tolerate similar penetrations without difficulty.

3. Correlation between actual effects and laboratory and theoretical simulations.

Material retrieved from the Solar Max satellite, the Palapa and Westar satellites, and the Shuttle Orbiter windows are the only available samples which show the actual effect of the meteoroid/debris environment on materials. These materials show impact pits from both micrometeoroids and very small orbital debris particles, the latter identified as mostly paint flakes and aluminum oxide particles. Microscopic examination of these pits shows shapes and fracture patterns identical to those observed in laboratory hypervelocity impact tests. By analysis of these shapes and patterns, it has been possible in some cases to deduce the size and velocity of the impacting particles. However, there are no laboratory hypervelocity impact tests for comparison with high velocity meteoroid impacts, due to the lack of a capability to make such measurements.

4. Capability for laboratory simulation and theoretical modelling of impact effects.

The effects of orbital debris impacts can be simulated in the laboratory by firing solid projectiles at test targets. Several methods exist for accelerating particles to the necessary high velocities. Van de Graaf electrostatic accelerators can be used to raise small (less than 1 micron) particles to velocities of tens of kilometers per second. One such accelerator exists at the Los Alamos National Laboratory, and another in West Germany. Shock tubes are also capable of accelerating small particles to hypervelocity, but most if not all such facilities are currently mothballed. Light gas guns can accelerate solid particles a centimeter and more in diameter up to velocities of about 7 km/sec. There are a number of such guns in operation in the U.S. In order to accelerate moderate size projectiles to velocities greater than 7 km/sec, the only proven method is the shaped charge gun, which generates velocities up to 11 km/sec. Electromagnetic accelerators, or rail guns, have so far not realized their promise of high velocities. Finally, a pulsed laser can be used to simulate the energy deposition resulting from a hypervelocity impact, and thus simulate the effects of the impact.

The laboratory results obtained at currently available impact velocities can be extrapolated to higher velocities by the use of models whose empirical constants are adjusted to fit the low velocity results. At the present time, this method fails or works poorly with complex materials, such as foams or composites. It is also difficult to deal with complex geometries.

Simulation of meteoroid impacts is more difficult. The impact velocities of micrometeoroids are higher than debris, up to 72 km/sec, and the particles are mostly low-density "snowflake" structures. There is no satisfactory way for laboratory simulation of this

combination of properties, although modeling of the impacts is possible.

Synergistic effects can be simulated, where they are known to exist. Examples include the effects of impact pits on the protective coatings for atomic oxygen and stress crack initiation at impact pit sites.

On-orbit collisions which result in total breakup of the colliding objects can be modeled approximately using current theory. However, the size and velocity distribution of the small particles generated in the collision are not well known. This information is essential for predicting the future growth of the debris population, since theory predicts that at some future date, runaway growth of the debris population could occur as a result of cascading collisions.

5. Synergistic Effects.

There are many possibilities for synergistic effects, but their significance for long-term space flight are not known. Examples of such effects include the following:

- a. Atomic oxygen erosion initiated by impact on a protective coating. Laboratory studies of protective coatings have shown that atomic oxygen can attack the substrate over a large area through a small break in the coating.
- b. Thermal effects could be produced by erosion of thermal control coatings.
- c. Spacecraft charging effects can be facilitated by penetrations.
- d. Contamination can be induced by vapor from the impact.
- e. Impact pits can serve as initiation points for stress cracks produced by thermal cycling.
- f. Cascades of effects are conceivable, in which several effects follow one another.

6. Confidence level: Can we build satellites for 10-30 year lifetime?

The answer is probably yes for small conventional satellites (less than about 40 square meters area), where the expected effects of erosion and pitting are taken into account by appropriate protective surfaces. The answer is a qualified no for satellites with large areas (5000 square meters or more) expected to operate for up to 30 years without malfunction. The reason is the debris environment in the size range (up to 1 centimeter) expected to impact a spacecraft of this size is not well enough known, so that the shielding used on the spacecraft may not be adequate. In principle, the spacecraft can be designed with a sufficiently massive shield to cover all possibilities, but in practice, the weight and volume costs for this approach are large, and may become prohibitive as the debris environment becomes more severe in the future.

The answer is also a qualified no for satellites with radically new functions or materials. In these cases, we don't know the synergistic effects, or their importance.

7. Space experiment requirements.

The U.S. Space Command tracks and catalogs all objects in LEO with diameters larger than about 10 centimeters. The orbital debris environment for smaller sizes is poorly defined, with an uncertainty factor of at least 3. The population data for very small debris (less than 100 micron size) in LEO is anchored by only one set of data-- that from analysis of the surfaces from the Solar Max satellite. There also exists one limited set of optical data for sizes down to about 2 centimeters. There is no data at all for sizes between 100 microns and 2 centimeters. Rapid changes of the debris environment can occur when new breakups take place, making these few measurements obsolete overnight. Experiments are needed to define the small debris environment below the 10 centimeter level to a degree of confidence significantly better than the current uncertainty factor of three.

Synergism and cumulative effects, particularly from the small debris which cause erosion and pitting, are not wholly predictable, and hence may not all be capable of simulation. A flight experiment which included other materials experiments would exercise all possibilities.

It should be noted that we cannot completely simulate or calculate the effects of hypervelocity collisions of objects in space. In the event that such an event is deliberately planned as part of a space experiment, then every effort should be made to measure the particle sizes and velocities resulting from the collision. Since any instrumentation on the colliding spacecraft will be destroyed by the collision, either ground-based sensors, or sensors aboard a co-orbiting satellite would be required to make these measurements.

The meteoroid environment is better understood than the debris environment, and there is general agreement concerning the definition of an environment suitable for engineering calculations. No further space experiments are needed for assessing the effects of the meteoroid environment on materials.

8. Flight experiments needed.

The first priority is to measure the LEO environment for sizes below 1 centimeter. It is expected that a ground-based radar currently under development will be capable of monitoring the debris environment for sizes above 1 centimeter.

The second priority is to repeat the measurements at intervals to monitor changes which are expected to occur as the rate of space activity increases in the future.

The third priority is to establish the nature and significance of possible synergistic effects.

9. Possibilities for flight experiments: Environment definition

For debris sizes of 1 millimeter and larger, it would be possible to build a dedicated debris sensor satellite. JPL has designed a debris sensor system consisting of two 10-inch telescopes and CCD image detectors which would be capable of monitoring the debris population in orbit down to sizes of 1 millimeter. The cost of building and launching such a satellite has been estimated at \$100M. For small debris (100 microns or less), off-the-shelf micrometeoroid sensors are capable of measuring the environment. The Space Electric Rocket Test (SERT) satellite is equipped with a small micrometeoroid experiment, which is probably still functional. Planned EOIM satellite experiments may also provide some new information. Measurements of these kinds provide information on the flux of debris particles, but do not identify their source.

Surfaces which are retrieved from the space environment provide unique information, in that the source of the debris can be identified by chemical analysis of material in the impact pits. Such material retrieved from the Solar Max satellite has provided a wealth of new information on the small debris environment. When LDEF is recovered in 1989, it will have been in LEO for about 5 years. An enormous number of impact pits will be available for analysis, and a new and more exact picture of the small debris environment will emerge from analysis of the LDEF surfaces. The information available from LDEF could be extended in future years by the development of a free-flyer "gas-can" type of experiment, in which an expandable surface would be deployed from the "gas can" to expose a large area to the space environment. After exposure for several months, the surface would be pulled back into the "gas can", retrieved, and returned to Earth for laboratory study. This type of experiment could be repeated at intervals of 2 to 4 years.

The Cosmic Dust Facility planned for Space Station Freedom is intended to measure the flux of micrometeoroids with great accuracy. It will inevitably measure some orbital debris as well, although the experiment is being carefully designed to minimize the count rate of orbital debris.

10. Flight experiment possibilities: Synergism and accumulated effects.

For this problem area, it is necessary to obtain long-term exposure of real spacecraft systems, recover them, and perform detailed interdisciplinary analysis of the kind done on the recovered Solar Max hardware.

One such approach would be to recover old satellites by capture from the Shuttle Orbiter. A survey of candidate satellites for capture by the Orbiter shows surprisingly few possibilities. The best appear to be the Solar Max and SAGE. Both are about 10 years old. SAGE is small enough that it could be recovered in its entirety, but it is likely that Solar Max would have to be dismantled, and only

parts retrieved, since it is a large satellite. There are no other candidate satellites with longer exposures available to the Orbiter. There are several TIROS satellites which have been in orbit up to 30 years, but their orbits are such that an ELV mission would be required for recovery. Capture and retrieval of an old satellite is a costly and difficult operation. Strong interdisciplinary justification would be needed to support such a mission.

11. Related topics.

There was considerable discussion in the Workshop concerning measures that could be taken to mitigate the growth of the orbital debris environment. In order of increasing cost and difficulty, these included:

- a. Operational procedures to minimize breakups.
- b. Improved spacecraft paint
- c. Avoidance maneuvers
- d. Removal of large satellites
- e. Movable shields
- f. "Sweeping" of small debris

The most practical and cost-effective measure was considered to be the introduction of operational procedures to minimize future breakups.

CONTAMINATION*

Chairman: C. Maag
Jet Propulsion Laboratory

* This working group written presentation was not available at time of publication.

WORKING GROUP WRITTEN PRESENTATION

TRAPPED RADIATION EFFECTS

A working group report prepared for the Space Environmental Effects on Materials Workshop-

A. L. Vampola and W. K. Stuckey, Chairmen; D. Coulter, E. J. Friebele, K. J. Hand,

D. A. Hardy, P. Higby, W. A. Kolasinski, R. T. Santoro, and S. S. Tompkins

ABSTRACT

This report presents the results of the Trapped Radiation Effects Panel for the Space Environmental Effects on Materials Workshop held at the NASA Langley Research Center in Hampton, Virginia in June, 1988. It lists the needs of the space community for new data regarding effects of the space environment on materials, including electronics, as perceived by the panel during their discussions. It addresses a series of questions asked of each of the panels at the workshop. It also suggests areas of research which should be pursued to satisfy the requirements for better knowledge of the environment and better understanding of the effects of the energetic charged particle environment on new materials and advanced electronics technology.

INTRODUCTION

The various panels at the Space Environmental Effects on Materials Workshop were asked to address a number of issues. In the case of the Trapped Radiation Effects Panel, the assessment was taken to include all direct effects on materials induced by the energetic particles, including dose effects, dose-rate effects, and Single Event Upset (SEU). The italicized introductions to each of the panel's responses below are quotations of the questions submitted to the panels for elucidation.

A. In your topic area: Which materials or classes of materials are most vulnerable? In what orbits? Why? And can you identify general or specific consequences on long term spacecraft or satellite performance?

Our current areas of highest concern are:

- a) Microcircuits
- b) Optics (glass, ceramics)
- c) Organic materials

Reasons:

Microcircuits

- i. Trend is toward smaller geometries and higher speeds, resulting in lower signal levels for circuit upset, thereby increasing the vulnerability to SEU.
- ii. Difference between theory and practice for SEU is a factor of 2 to 5.

- iii. No correlation between latchup/burnout and SEU.
- iv. Significant lot-to-lot variations in total dose hardness.
- v. Only empirical data available, no theory or prediction on dose and annealing effects.
- vi. Basic physics parameters not readily available for calculation--e.g., proton inelastic interactions.

Optics and Organic Polymers

- i. Serious effects in discoloration, embrittlement.
- ii. Swelling, gas production.
- iii. Changes in the coefficient of expansion, density changes, surface deformation.

Orbits of Concern

Basically, for all orbits above about 500 km the trapped particle population is of concern. The energetic proton environment is encountered in the region of the South Atlantic Anomaly on all orbits. These energetic protons ($E_p > 100$ MeV) which can't be shielded out of circuitry, can produce SEU in the most sensitive circuits. With a low probability, they also produce inelastic collisions ("star" events) which can upset even more resistant circuits. With the trend to smaller circuit element geometries, the probability of upset from this mechanism increases. For very long term missions, the integrated dose to optical and organic polymer elements may also be of concern. For orbits above 1000 km, the dose from the energetic protons and moderate energy electrons (50 keV to 1 MeV) also becomes a significant consideration. For orbits in the outer electron zone (altitudes greater than 10000 km), the radiation dose may be the controlling factor for mission lifetime. At geosynchronous orbit, the electron dose is still severe, although not as severe as in the 15000 to 25000 km orbits. At geosynchronous orbit, lightly shielded components can receive doses on the order of 50000 rads/year.

Consequences of Long-Term Spacecraft Operation

Electronic circuits:

- a) SEU
- b) Latchup
- c) Burnout
- d) Dose effects
- e) Microelectronics degradation through attrition to parts

Long term radiation effects on solar panels are well known and the design of the power system includes the radiation degradation factors. Electronic circuitry is usually designed with size, speed, and power in mind and radiation resistance is either ignored or attempts are made to build it into the device almost as an afterthought, usually through processing methods. Once the circuits are built, radiation tolerance is partially achieved either through shielding (usually bulk methods even though chip shielding uses two orders of magnitude less mass), or operationally with powered-down redundancy, or signal processing. Some thought is being given to increasing the annealing rate in dose effects through heating circuitry up to increase the mobility of trapped charge carriers.

Glass optics:

- a) Atomic displacements, ionization, dielectric breakdown
- b) Optical degradation through discoloration and defocussing (figure-of-merit degradation)
- c) Distortion (due to compaction)

Radiation effects are seen in glasses and glass-ceramics for optical components in the form of darkening and densification. For example, fused quartz compacts 20 ppm at 5 Mrads, its absorption coefficient in the 200-300 nm wavelength range has increased to ~ 5 cm⁻¹, and it has turned faintly

purplish in color. These effects become more intense with dose. Darkening is especially detrimental in fiber optics due to the long path lengths involved (especially for the fiber gyroscope). Because of the competing darkening and recovery processes, irradiation at low dose rate results in lower incremental attenuation than at high dose rate. Typically, the loss induced in a fiber at $1.3\ \mu\text{m}$ by a natural space background low dose rate irradiation (1-10 rads/day) is $\sim 1\ \text{dB/km-krad}$ if the fiber is maintained at $23\ ^\circ\text{C}$. The loss induced at $0.85\ \mu\text{m}$ is approximately 5 times greater. Note, however, that dose rates of the order of 1 krad/hr have been observed in the outer electron zone behind nominal amounts of shielding ($0.035\ \text{g/cm}^2\ \text{Al}$), and of the order of 75 rads/day behind shielding an order of magnitude thicker. AR or HR dielectric coatings on optics tend to make an optic more sensitive to radiation.

Figure 1 shows quantitatively the effect of radiation on the deformation of optical materials. In the figure, the dose appears to be quite high. However, optical surfaces are apt to be exposed to the space environment where surface doses in excess of 1 rad per second can occur. Also, the deformation displayed is enormous compared to the distortions which would significantly degrade performance of a large space mirror (a quarter of a wavelength of light over the diameter of the mirror).

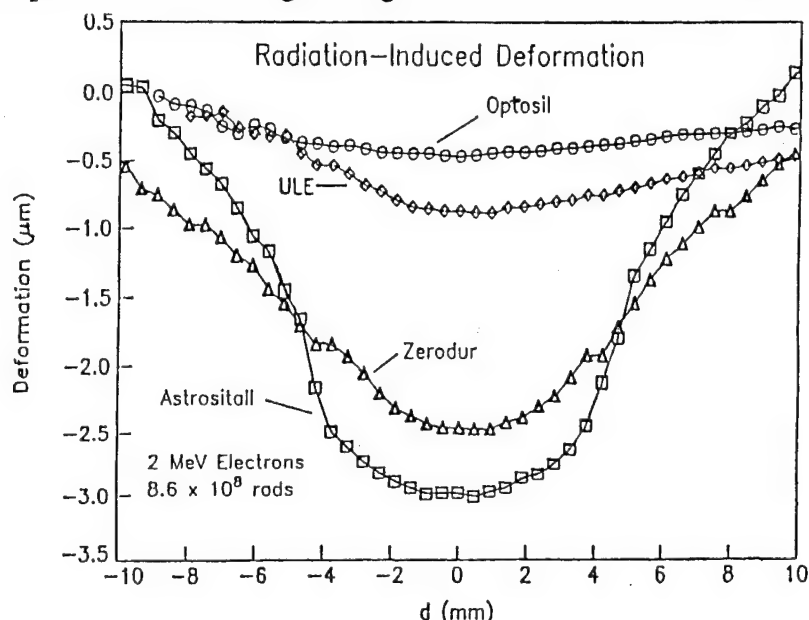


Figure 1. Radiation induced deformation of optical materials.

Organic Polymers:

- a) Cross-linking, scission
- b) Embrittlement
- c) Modulus changes
- d) Coefficient of expansion changes
- e) Significant structural changes due to asymmetric changes in ceramic/glass/polymer structures

Doses in the range of the high 10^5 to 10^6 rads produce embrittlement, modulus changes, and discoloration of the binders. For light pipes, changes occur in the kilorad range--changes of coefficient of expansion, dislocations in various glasses; swelling and gas production. Data on the effects of energetic protons don't exist in the volumes that are needed. They haven't been done systematically. We need the response function of materials for electronics; we need ground testing and modeling, and we need cross-section data. Any long-term mission has a problem with proton-induced activation. We need an NDEF equivalent for proton interaction cross-sections to correlate the effects of P^+ inelastic on spacecraft materials. We need a list of materials categorized by vulnerability in rads.

Many organic polymeric materials will be used in the space environment on future missions in the form of structural composites, adhesives, seals, coatings, optics, etc. In general, these materials are more sensitive to radiation than are inorganics and metallics. Cross-linking and chain scission, the two principal manifestations of radiation damage in polymers, cause significant degradation of a variety of properties including strength, color, modulus, and T_g . The reported thresholds for physical changes for most polymers are in the range of 1 to 100 megarads. These dose levels are not inconsistent with what could be experienced by long term missions in certain high orbits. Figure 2 displays graphically the radiation level at which significant deterioration of material properties occur.

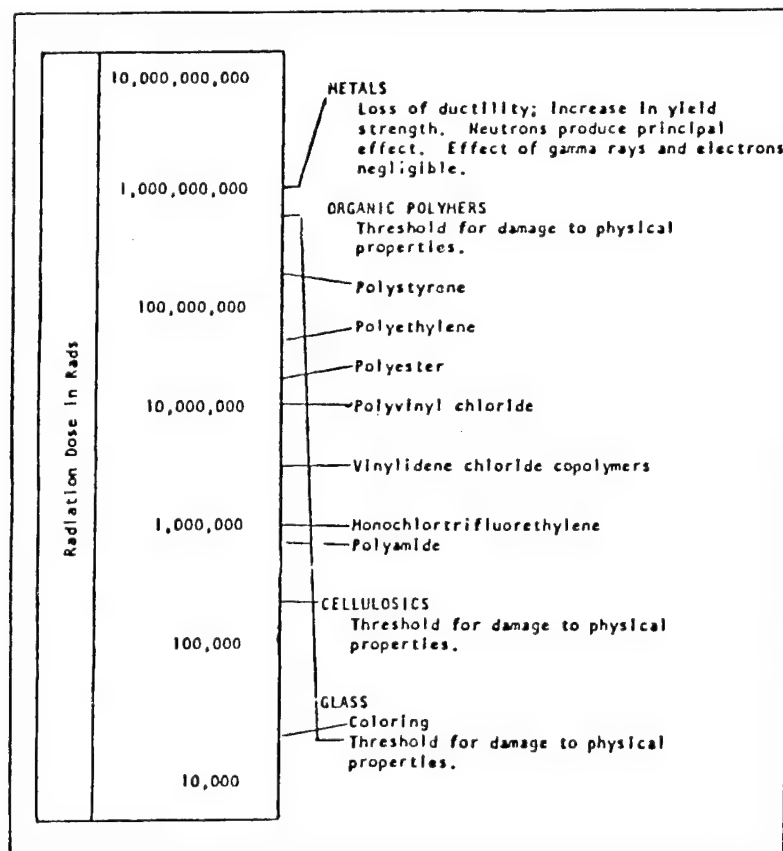


Figure 2. Relative sensitivity of materials to radiation.

Very little data exists on space radiation exposure for polymers. What does exist is poorly characterized as to dose and exposure conditions (temperature, UV, atomic oxygen, etc.). This is because few long term missions have flown and returned incorporating these materials. What is required is an exposure experiment in a known environment followed by analysis upon return of samples on selected materials from several basic classes of polymers (thermosets, thermoplastics, rubbers, etc.)

Areas of Concern

Basic physics data is not available to properly predict the SEU/materials effects:

- P⁺ cross-sections/interactions have not been done systematically
- P⁺ + Be > 2 α produces distortions in Be mirrors
- Long-term missions will have an activation problem.

Comments:

- a) Long-term missions will produce high integrated fluences which will have serious effects on optical elements/ceramics/glasses--misalignment of structures, defocussing, etc.
- b) Flight tests of model structures to get experience on omnidirectional loading, complex spectral effects needed.
- c) A well-organized ground test program is required.
- d) What happened to all of the information gleaned from SREL activities in the 60's and the 70's?
- e) More effort in the modeling area is required.
- f) Recommendation for a bench-mark test site.

Is there any correlation between theory and lab experience (and space experience) so that long term performance can be predicted?

The difference between theory and practice for SEU in CMOS/SOS and CMOS/EPI is a factor of 2 to 5. There is no correlation between latchup/burnout and theory. The same is true for annealing/dose effects. We can't predict the effects, we can only test for them. Bulk properties not as well known as fiber optics, still in the "getting data" stage. Effects on materials/polymers is still basically in the empirical (qualitative) stage. Correlation between theory and practice to predict long-term performance: Space data base very sparse; new circuits and materials being introduced all need to be tested; Prediction (except for continued degradation in performance) not possible--at least not quantitatively.

Do we know enough, even if only empirically, to launch for 10 years (or 30 years) of service with confidence?

NO! Current practice shows that the 5-year+ spacecraft lifetime is the exception rather than the rule and that new technologies are less reliable because of the increased complexity. At this point, we can probably say that 10 years of service is improbable and 30 years is probably impossible.

Comments on the predictability of long-term performance:

- a) Qualitative estimates only
- b) Synergistic effects only guessed at
- c) At this point, it is probably not possible to predict a given design will survive for 10 years in space with a high probability

B. In general, are terrestrial lab facilities available? Adequate?

Not really. They exist "in general" or "in principle", and that is precisely the problem, especially where proton accelerators with potential for simulating inner-zone and solar flare protons are concerned. These facilities are scattered all over the country, and no single accelerator can provide the complete range of energies, intensities, and spatial distributions needed to adequately simulate the effects of protons in space. Each group using a given facility has to perform its own studies of beam properties and develop special tuning techniques to obtain the desired beam. This results in much duplication of effort, unnecessary expense and waste of accelerator time, the availability of which is often very limited. Furthermore, most facilities are paid by each group for beam actually used and have no long term funding to develop generally applicable capabilities for conducting research on space radiation effects. As their usefulness to DOE nuclear physics programs declines, operation of the facilities is curtailed and eventually they become permanently shut down and dismantled. Under these circumstances, the

availability of ground facilities to support space research is sporadic at best, and makes planning and development of long-term programs a high risk operation.

We need ground test facilities; should set up a committee with funding to oversee this area. (This could be either by discipline or by environmental effect). New technologies have made a more urgent requirement for ground testing than existed previously. The industry should have a national facility for space environmental effects testing.

Comments on lab facilities:

- a) Availability
 - in general, yes
 - being closed down
- b) Adequacy
 - in general, not adequate
 - problems with the beam characteristics
 - monoenergetic
 - unidirectional
 - intensity
 - species
- c) We need data bases
 - systematic, p+
 - for test/development of theory
- d) Need a committee to oversee facilities

Without being exhaustive, please identify major facilities and their strengths and weaknesses.

Some of the currently operating particle accelerators which are of potential use to the space program are

Radiation Facilities (Partial List)

Heavy Ions:

Brookhaven	Tandem Van de Graaff	20 MV
Oak Ridge	Holifield Heavy Ion Facility	20 MV
Law. Berkeley Lab	88-Inch Cyclotron	20 MeV/nuc
Law. Berkeley Lab	Bevelac	>1 GeV/nuc

Protons:

Oak Ridge	Isochronous Cyclotron	70 MeV
Law. Berkeley Lab	88-Inch Cyclotron	50 MeV
Law. Berkeley Lab	Bevelac	>1 GeV
UC Davis	Cyclotron	45 MeV
UCLA	Cyclotron	45 MeV
Harvard	Cyclotron	150 MeV
Brookhaven	AGS	>350 MeV
Argonne	LINAC	50 MeV

Electrons:

NRL	LINAC	10-60 MeV
NRL	FEBETRON	0.5 MeV
RADC	LINAC	2-20 MeV

ORELA
GSFC

Tandem Van de Graaff

150 MeV
2 MeV

Other Radiation Facilities:

NRL
RADC
Savannah River

Co60, 50-100 kV X-Rays, Excimer Laser
Co60, Van de Graaff, Dynamitron, Ion Beam
Hot Co60

C. Having heard a short tutorial on the major space environment factors: Is there likely to be interaction or synergism between your factor and one or more of the other factors?

Any discussion of synergism at the present time is speculative (except for temperature effects on SEU and latchup, and temperature/total dose effects on radiation-hardened RAMs, rad-soft circuits, and polymers). However, the suspected synergisms are

- a) UV/particle radiation (in polymers, optics)
- b) Temperature/UV/particle radiation (in thin materials, surfaces)
- c) Temperature/trapped radiation (in electronic circuits, sensors, materials)

Has that interaction or synergism been tested and evaluated, or is it only speculative?

Some testing of the synergism between thermal effects and trapped radiation, particularly in the SEU effects area and total dose in MOS circuitry have been done. Some SEU and latchup radiation testing has been done as a function of temperature. Also, for some materials the synergism between trapped radiation and UV has been tested.

Do any lab facilities exist to test such interaction/synergism?

We know of no lab facilities, per se, that exist, although some synergisms can be tested in the lab--the general problem is that the energy spectrum and the angle of incidence for the particles cannot be properly simulated.

D. Are space experiments needed to assess the vulnerability of materials to long term exposure to your environmental factor? Why? (Possible reasons include validation or calibration of terrestrial experiments, identification of interactions or synergisms not possible to schedule on Earth, absence of equipment to duplicate an environment with real time and accelerated exposure capabilities, etc...)

Yes, additional space experiments are needed, but the need is for higher orbits and longer durations than Shuttle permits. There is a need to get samples back, not only for materials and optics, but also for microcircuits. In the case of malfunctioning circuits, there is a need for an "autopsy" in order to determine the cause and mechanism of failure. Ground measurements are also required. A recommendation: Boost a test vehicle up to the center of the inner zone (2000 km at low inclination), stay for a year, then deboost and retrieve the test vehicle with the Shuttle. There is also a need for tests intended to validate ground based experiment, theory, and models.

Other Requirements:

Analytic/Theoretical Capabilities: Development of computational capability for pre- and post-experiment analysis of trapped radiation (protons, electrons, and possibly weapons radiation pumped belts) effects on materials and electronics.

Data: Evaluated charged-particle cross section data to predict atomic displacements, gas production (p,p; p, α ; α ,p; α , α ; etc.) and single event upset phenomena (SEU, latchup, burnout, etc.) Considerable data are required to predict bond breaking in organic materials, optical property effects, fiber optic response data, etc.

Facilities: Dedicated electron, proton, α -particle, and heavy ion accelerators for measurement of cross-section and damage data. Beam energies and intensities sufficient to replicate Van Allen belt proton and electron energy spectra.

Experiments: Carefully tailored and designed ground and space experiments to quantify radiation damage to materials and electronics.

Staffing: Multilaboratory, multidisciplinary committee to organize, design and classify needs and supporting experiments.

Modeling: Modeling capabilities to a) accurately model satellite and the environments; b) component representation (electronics); c) macro- and micro-material properties (?).

Computer Capabilities: Dedicated facilities a'la Livermore fusion computing center, etc. for the entire NASA/SDIO community.

E. Identify in priority order those experiments that must be conducted and can only be conducted in space. What duration(s) will be necessary? Is retrieval necessary? After what interval?

It is not possible to prioritize experiments at this time; that is probably best left to individual programs which recognize a need for basic data related to the operations of their specific missions. However, it is possible to indicate the generic types of experiments which should be conducted and their locations. The highest priority has to be given to CRRES, but since that already has a dedicated launch, emphasis can be placed on other high priority missions. Retrieval of LDEF is extremely important. A follow-up to LDEF, using information gleaned from LDEF and incorporating new materials not available when LDEF was designed. Although future work/advances in electronics and materials will be the driver in defining the space tests that must be done, we can identify orbit locations and durations for some experiments.

Tests of materials in which a varied angle-of-incidence of the particles produce special effects (stress in structures, deformations), tests in which a real cosmic ray spectrum is required (high-energy heavy ion production of SEUs, latchup, etc.) and long duration exposures to particles of varied energy at a low level (degradation of fiber optics, organic polymers) all need to be done in space with durations of a few months to a year. For glasses and polymers and possibly for other materials, we need to get megarads/year exposures. We could probably start with "quick and dirty" flights, then use a long-term program to follow up on what is initially learned.

F. Estimate, by order of magnitude, the volume, weight and complexity of each experiment and necessary auxiliary gear. Also identify platform characteristics essential to your experiment (orientation in the RAM direction or toward the sun, unmanned and adrift to prevent any disturbances, power for active experimentation, telemetry equipment to obviate retrieval, etc.)

The panel did not address this in much detail because specific experiments (other than CRRES, LDEF, LDEF-follow-on) were not identified. But it was the consensus that for valid testing of particulate radiation effects on materials, the orbit has to be at least 500 km; a boost-deboost mission is required; and

environmental monitors should be installed on all flights, whether test or operational. For any space test, the energetic particle environment must be known because of synergistic effects of the energetic particles on the other environmental parameters being tested (which we did not address). For operational spacecraft, environmental monitors are needed to provide the data base which is required to determine the cause of a failure on the space system.

G. Does your technical community have any experiments planned/designed/built for early access to space? If so, please describe.

The technical community does have available experiments in this area. The CRRES mission, which is described elsewhere in this Proceedings, will make simultaneous measurements of the particle environment, the dose from that environment, and effects in circuits and materials from that dose. The effects that will be measured are the degradation of solar panels, microcircuit damage, SEUs, and electrostatic discharges due to the embedding of charge in cables and circuit boards. Other than CRRES, the only resource known to this panel is the reservoir of space instruments/experiments which exist in laboratories and museums which were at one time prototypes or backups for completed missions or flight units from cancelled missions.

Panel Recommendations

- A. The panel recommends that a benchmark site for radiation effects on materials be established.
- B. It is recommended that an interagency committee at the national level be formed to assess in depth the long term radiation effects testing requirements and act as a coordinator in the efficient utilization of the above and other facilities as the needs for their use rise.
- C. A well-organized ground test program is required.
- D. More effort in the modeling area is required.
- E. Flight tests of model structures to get experience on omnidirectional loading, complex spectral effects needed.
- F. All space vehicles should carry environmental monitors in order to assist in determining the cause of any degradation in performance or failures in orbit.

WORKING GROUP WRITTEN PRESENTATION

SOLAR RADIATION

Chairman: WAYNE S. SLEMP
NASA LANGLEY RESEARCH CENTER

CURRENT STATUS

Ultraviolet (UV) radiation testing of materials and coatings has been conducted for over 30 years. A substantial data base is available for laboratory exposure of thermal control coatings using simple UV sources such as mercury vapor or xenon arc lamps. These exposures typically cover a wavelength range down to 180 nm because of atmospheric absorption and the transmission of quartz windows. Limited data is available on the effects of lower wavelength UV radiation on materials and coatings. These laboratory data are also of short duration - typically 500 to 1,000 hours at one to two solar constants. Most testing laboratories have constructed their own UV simulation and testing systems, and little correlation can be established between exposure conditions, calibration techniques, and UV detectors. This difference in equipment leads to different test results on similar materials and coatings. There also are few facilities with extreme ultraviolet (EUV) (below 180 nm) exposure capability. Since these wavelengths are present at low flux levels in space solar radiation, the need for these wavelength sources in laboratory testing has not been established. Little laboratory data is available on synergistic effects of UV with thermal cycling or of UV, thermal cycling, and particulate radiation. These combined exposures are found in all space flights. The need for laboratory simulation of the combined space environment must be established to better predict material and coating performance in long-duration missions.

Most of the available flight data on coatings and materials was conducted prior to 1980. These data are confused by spacecraft contamination. Many coatings tended to degrade rapidly in the first few weeks of flight and then change the degradation rate. This rapid degradation was not experienced in most laboratory tests and was therefore attributed to spacecraft contamination. The effect of atomic oxygen in space on coatings and contamination has not been established in laboratory testing but is known to "bleach" UV degradation in some white paint coatings. This is another combined space environment parameter which is not available in current laboratory simulators.

TECHNOLOGY DRIVERS

The major technology drivers for solar radiation testing are the long design lifetimes of Space Station Freedom and other future space missions. All of these missions, whether in low Earth orbit or higher altitudes, will experience solar radiation exposure. The limitation of only 5-year duration flight data and less than 1-year laboratory exposure data requires extrapolation to an unacceptable degree. When the full environment of UV, atomic oxygen, and thermal cycling with a low dose of particulate radiation is considered for Space Station Freedom, then an understanding of each of these individual effects and their synergistic efforts needs to be established.

TECHNOLOGY NEEDS

The members of the Solar Radiation Working Group arrived at two major solar radiation technology needs: 1) generation of a long-term flight data base, and 2) development of a standardized UV testing methodology. The flight data base should include 1- to 5-year exposure of optical filters, windows, thermal control coatings, hardened coatings, polymeric films, and structural composites. The UV flux and wavelength distribution, as well as particulate radiation flux and energy, should be measured during this flight exposure. A standard testing methodology is needed to establish techniques for highly accelerated UV exposure which will correlate well with flight test data. Currently, UV can only be accelerated to about 3 solar constants and can correlate well with flight exposure data. With space missions to 30 years, acceleration rates of 30 to 100X are needed for efficient laboratory testing.

UV TESTING RECOMMENDATIONS

The Working Group recommendations for solar UV testing follow the technology needs. A series of flight experiments with 1 year minimum duration should be conducted in the proposed service environments. These experiments should have radiometers for UV measurement and detectors for particulate radiation detectors for flux and energy. Provision should also be made for the specimens to be returned in vacuum. This information is necessary for correlation of laboratory simulation on Earth.

Since many materials are sensitive to UV radiation of specific wavelengths, the committee recommended that a continuum UV source be developed covering the range from the extreme ultraviolet to the visible. The continuum source would incorporate multiple lamps to cover this large UV spectrum.

The other major recommendation was the construction of a test facility to provide the data needed to standardize UV simulation sources, detectors for flux measurement, and testing procedures. Such a facility would be a national resource for evaluation of UV sources, detectors, and optical measuring equipment as well as conducting studies of UV effects on materials.

WORKING GROUP WRITTEN PRESENTATION

SPACECRAFT CHARGING

Chairman: N. John Stevens
TRW

Issue Summary -

A. 1. Materials vulnerability and orbits. Spacecraft system performance

Spacecraft Charging Interactions Couple Environment Factors To System Operations Through Material Behavior.

The concern here is for possible interactions that result from the natural environment action on the spacecraft materials (e.g. GEO spacecraft charging) and for interactions caused by on-board system operations (e.g. high voltage solar arrays in low Earth orbits). Therefore, all orbits have possible spacecraft charging effects. This technology is still developing.

Specific effects on system performance are electromagnetic noise generation, anomalous electronic switching, electronic parts and thermal control coating degradation, dielectric electrical property change, power system losses and system failures.

These effects have all been documented in previous spacecraft flight data. Biggest data base is in GEO.

2. Correlation between theory and lab experience.

Previously defined charging interactions have been modeled and lab experiences indicate validity of models. This includes surface and bulk dielectric charging, effect of material configuration and some aspects of high voltage solar array/plasma interactions. The trouble with long-term predictive capability is that the systems are changing and what was tested in the past will not be flown in the future.

3. Can we predict for 10 or 30 years?

No, not with confidence. Present long-lived satellites are not the result of predictive confidence; they just occurred. In families of supposedly identical satellites, the lifetime varies because each is, in reality, individual satellites.

B. Facilities

There are facilities that can do pieces of this investigation. However, a facility has not been identified that can do all environments required simultaneously. Also, since these interactions are dependent on the configuration of materials, there is no facility that can handle the size of sample necessary to understand the very large spacecraft behavior in the space environment. Simulation

of actual space environments is very poor as is simulation of sample grounding. Facility ground is not the same as space. The available facilities exist at NASA-Lewis, Hughes, TRW, Boeing, G.E., and NASA-JSC.

C. 1. Synergism

Spacecraft Charging is the result of the other environmental factors acting on spacecraft materials. Therefore, all of the other factors are important:

- Atomic Oxygen - Changes insulators, films and coatings of properties.
- Meteoroid/Debris - Erodes and punctures dielectrics allowing structure potential electric fields to interact with plasmas.
- Trapped Radiation - Charges dielectrics and structure.
- Solar Radiation - Sunlit/shaded surfaces promote differential charging.
- Contamination - Changes surface properties.

Atomic oxygen and debris are low altitude phenomena (<1000 km for oxygen and 2500 km for debris); meteoroid and solar at all altitudes; trapped radiation at >800 km and polar orbits; contamination at all altitudes.

2. Testing of Synergism

Some aspects tested, but not all. Charging environments and solar effects documented by ground test and flight data (SCATHA). Pinholes in insulators in high voltage systems documented in laboratory. Influence of contamination on charged samples observed in laboratory tests and SCATHA flight data.

3. Available Facilities for Testing Synergism

Since these interactions are so all-inclusive, there are no facilities to do testing for all aspects of synergism.

D. Need for Space Experiments

The primary reason for space experiments is because the environment simulation is poor. The interactions to be studied require high energy electrons and protons, thermal plasmas, and sunlight for high orbits. For lower orbits the electrons and protons are replaced by atomic oxygen and debris. The physical size relationships that have to be studied, coupled with the power and voltages, demand space flight experiments.

This does not mean that only space flights must be conducted. Ground tests of individual aspects of interactions must be conducted. Analytical modeling of these tests must be validated and this modeling used to extrapolate to other interactions and size/power effects. This approach forms a data base to design meaningful spaceflight experiments. Flight experiments will have the proper environment, but instrumentation is limited and the experiment must be designed well to maximize the output.

E. Prioritized List of Experiments

The working group identified 10 interaction topics which are arranged in priority order in attached sheets. These fall into materials experiments (1,3,5,8) and materials related systems experiments (2,4,6,7,9 and 10). Since our interactions are normally prioritized against the impact on system performance, we should have had a better briefing on SDI system and technology requirements. It is recommended that this be done.

The experiments all should be run for extended periods of time in space. Some, like high voltage system interactions, can be done in days, while those dependent on radiation damage to materials require years to build up total dose effects. It would be nice to retrieve but it is not necessary. None of these experiments should be conducted within the Shuttle bay. It should be elevated away from the sides.

This general list of experiments can be further condensed into three:

1. Material Property Determination With Time in Space Environment With Material Under Electrical Stress

This is a radiation, UV, meteoroid-type experiment requiring high altitudes and long life. Materials include conductors, dielectrics, composites, and thin film coatings.

2. High Voltage System Interactions With Plasmas

This would be a low altitude experiment and would evaluate electric and magnetic stress as well as coupling in space. This would be a material configuration effect experiment.

3. Discharge Monitors

High altitude or polar satellites should carry these monitors along with environment sensors to quantify effect of environmentally-induced effects.

F. Experiment Design

These are usually designed for the specific set of interactions desired. There probably can be a generic bus with interchangeable payloads. These can be tailored as piggyback, GAS or free-flyers. Only those experiments requiring low altitude information can be run at Shuttle/Space-Station Freedom altitudes. Those requiring radiation dose effects must be above 800 km.

G. Available Experiments

Concur with need for retrieving and reducing LDEF data.

Require future flight information at available altitudes.

1. Material performance under electrical stress and space radiation environments.

No experiment to do this has been identified.

2. High Voltage Systems

- a. SPEAR flight program underway (Space Plasma Experiments Aboard Rockets). These are very short duration, pulsed power experiments that provide information on system but not material behavior. Three minutes is not adequate to design multiyear life.
- ** b. NASA Planned Solar Array-Plasma Interaction Experiment. This must be conducted now. Such experiments have been planned in the past, started and then canceled. The data are mandatory.
- c. Japanese plan experiment for 1992 time frame. No further information available.

SPACECRAFT CHARGING WORKING GROUP REPORT

CANDIDATE EXPERIMENTS

1. Material Property Changes With Electrical Stress and Time in Space Environment
2. High Voltage System Interactions
3. Thin-Film Coating Interactions
4. Discharge Characterization
5. "Tailored" Materials
6. Heavy Stressed Power System Dielectrics
7. Pulsed Power System Interactions
8. Composite Internal Noise Generation
9. Active Charge Control
10. "Radiation Belt" Charging

Interaction: Material Property Changes With Electrical Stress and Time in Space Environment

- Stress Enhances Aging by Driving Solid State Chemical Interactions
- Radiation Induced Interface Failures

Why Problem: ◦ Current Spacecraft Behavior Starting To Be Understood but Materials and Operating Conditions Changing

- Lifetime Extended

Ground Test/Theory Correlation:

- Dielectric Community Working
- Short Term Testing Without Space Environment

What Is Still Needed: Materials Testing To Establish Range of Interaction

Why Require Spaceflight:

- Need Space Environment to Verify
- High Altitudes or Polar for Radiation
- Time in Environment

Supporting Work: Dielectric Community
Not Directed Towards Space Applications

Interaction: High Voltage System Interactions

- High Voltage Solar Arrays
- Structure Collection in Plasmas
- Scaling Laws for Size, Voltage, Power, Frequency
- Sheath Effects

Why Problem: System Floats Electrically in Plasma Environment
Breakdowns in High Voltage Systems

Ground Test/Theory Correlation: Small Scale Sample Correlates With Theory.

What Is Still Needed: Size, Voltage, Power, Frequency Scaling.

Why Require Spaceflight: Need Complete Space Environment.
Can't Simulate On Ground

Supporting Work: Ground Support Work
Japanese Space Experiment

Interaction: Thin-Film Coatings
Stability of Thin-Film Optical and Electrical Coatings in Space
Environment

Why Problem: Applied for Specific Optical or Electrical Purpose
Charging Interaction Coupled With Sputtering or Contamination May
Destroy

Ground Test/Theory Correlation:

- Short-Term Testing
- Flight Data Not Instrumented For Detailed Examination

What Is Still Needed:

- Identification of Coatings

Why Require Spaceflight:

- Need Space Environment

Interaction: Discharge Characterization

Sources - Conditions for Discharge Initiation, High Power
Character - Frequency, Amplitudes, Rep Rate, Transfer Function and
Changes With Time in Space

Why Problem: Protection of System Circuits Depends on Knowledge of Discharges

Ground Test/Theory Correlation:

- Deducing Discharge Behavior in Space by Effect
- Characteristics Not Repeatable

What Is Still Needed:

- Theory and Test Correlation

Why Require Spaceflight: Need Total Environment and Spacecraft Configurations

Interaction: "Tailored" Materials

- Materials Developed for Properties To Minimize Charging Levels
- Conductivities in Range 10^{-8} to 10^{-10} S/cm²

Why Problem: Can Mitigate Charging Concerns

Ground Test/Theory Correlation:

- Quasi-Conductive Materials Under Development

What Is Still Needed: ◦ Better Materials for This Application
 ◦ Demonstrate Stability in Space Environment

Why Require Spaceflight: Demonstrate Behavior in Space Environment

Supporting Work: GSFC, VA. Tech

Interaction: Heavy Stressed Power System Dielectric SDI Applications Under High
Voltage and Large Current

Why Problem: Strong Electrical Stress and Induced Magnetic for Reduce Breakdown
Thresholds

Ground Test/Theory Correlation:

- Pieces Under Study

What Is Still Needed: Combined System Effects
Space Environment Demonstration

Why Require Spaceflight: Total Space Environment Effect
Time in Space

Interaction: Pulsed Power Interaction
System Dynamic Response to 1 to 100 μ sec Power Pulse

Why Problem: Behavior in Plasma Uncertain
Affects System Performance
Flashover

Ground Test/Theory Correlation: Theory Being Developed

What Is Still Needed: Theory and Test Demonstration

Why Require Spaceflight: Need Space Environment
Radiation Environment Important

Supporting Work: SPEAR II
Texas Tech and Maxwell (Testing)

Interaction: Noise Generated in Composites
Space Induced Charging Coupled With
Radiation Generates Noise in Materials

Why Problem: RF Noise Can Couple Into Communications and Sensors

Ground Test/Theory Correlation: Measure RF Levels in Small Samples Under Electrical
Stress and Radiation Theory Adequate but Number
of Pulses Unknown

What Is Still Needed: Pulses Expected in Samples Scaling

Why Require Spaceflight: Need Spaceflight Environment
Auroral or High Altitude
Can Be Added to Existing S/C
Systems Having R.F. Detection

Interaction: Active Charge Control Interactions

Why Problem: Mitigation Technique but Can Degrade Coatings by Bombardment - Time
Effect

Ground Test/Theory Correlation: Short Term Testing
Model Exists but Not Validated

Why Require Spaceflight: Long Term Study in Space Without Walls

Supporting Work: AFGL Charge Control System (Xenon)
IAPS (Mercury)

Interaction: "Radiation Bolt" Charging
Energetic Proton and Electron Environment - Variable in Orbits

Why Problem: Upsets Seem To Occur on GPS
No Charging Model Evaluation

Ground Test/Theory Correlation:
Should Be Able To Treat but Hasn't Been Yet

What Is Still Needed: Evaluation of Effect of Environment

Why Require Spaceflight: Need Environment and Time In Space

SPACECRAFT CHARGING WORKING GROUP REPORT

SUMMARY -

- Identified Interactions That Would Affect System Performance
- Better Definition of System/Missions Required
- General Approach for This Area:
 - Small Scale Ground Tests
 - Modeling of Interaction
 - Understanding
 - Scaling
 - Flight Verification Test

SECTION II-C

WORKSHOP CONCLUSIONS AND RECOMMENDATIONS
TO NASA AND SDIO

WORKSHOP CONCLUSIONS AND RECOMMENDATIONS
TO NASA AND SDIO

As summarized by
William Hong
Institute for Defense Analysis

A consensus that can be said to fairly represent all of the major environmental factors discussed at this Workshop is that present knowledge of Earth orbit environments is inadequate to confidently design space systems for long lifetimes. Much of our data from past space experience is too limited in scope to correlate properly with present ground testing and simulation capabilities and becomes more obsolescent as new materials and systems are developed. An unquestioned need exists to carefully design additional spaceborne missions to develop a modern data base and validate ground testing methodologies.

In particular, LDEF was seen by several of the workshop groups (AO, Debris, Solar Radiation, Contamination) as representing a valuable, if inadvertent, source of long duration data, as it will have been in low Earth orbit for over five years when finally recovered. The loss of several experiments due to the long exposure can be mitigated by the wealth of additional findings on other panels, which could only have been gained by an orbit time in LEO that is a significant fraction of the anticipated lifetimes for SDI and NASA systems. Estimates of total AO and radiation fluence levels, microdebris distributions, analyses of outgassing contaminants, and thermal cycling effects are among the types of information that LDEF could provide.

Several additional options were proposed as a means to expand knowledge of both the space environment and its effects on materials. These included minisatellites designed as generic, retrievable platforms building upon the LDEF concept. The development of standard flight packages (possibly as piggyback modules on other satellites) carrying environment sensors was also suggested; these systems could prove valuable in correlating and diagnosing satellite failures. More sophisticated systems could also be designed to provide active data on materials, either as functions of the natural environment or from imposed satellite conditions. Nonretrievable, diagnostic or active systems require telemetry capabilities for gathered data.

Finally, the possibility was discussed of continuing the efforts started at this Workshop by holding future yearly Symposia on specific topics in space environmental effects. It was felt that a series such as this would build upon the increasing awareness in both the NASA and SDI space communities of the future challenges in building long-life space systems. The opportunities for enhanced communication among these communities that was begun at this Workshop would enable increased coordination in designing future space experiments to more efficiently address the wide range of needs presented here.

1. Report No. NASA CP-3035, Part 2		2. Government Accession No.		3. Recipient's Catalog No.	
4. Title and Subtitle NASA/SDIO Space Environmental Effects on Materials Workshop				5. Report Date May 1989	
				6. Performing Organization Code	
7. Author(s) Louis A. Teichman and Bland A. Stein, Compilers				8. Performing Organization Report No. L-16575	
				10. Work Unit No. 506-43-21-04	
9. Performing Organization Name and Address NASA Langley Research Center Hampton, Virginia 23665-5225 and				11. Contract or Grant No.	
				13. Type of Report and Period Covered Conference Publication	
12. Sponsoring Agency Name and Address National Aeronautics and Space Administration Washington, DC 20546-0001 and Department of Defense - Strategic Defense Initiative Organization, Washington, DC 20301-7100				14. Sponsoring Agency Code	
15. Supplementary Notes					
16. Abstract The National Aeronautics and Space Administration (NASA) and the Strategic Defense Initiative Organization (SDIO) cosponsored a workshop on Space Environmental Effects on Materials at the NASA Langley Research Center from June 28 to July 1, 1988. The joint workshop was designed to inform participants of the present state of knowledge regarding space environmental effects on materials and to identify knowledge gaps that prevent informed decisions on the best use of advanced materials in space for long-duration NASA and SDIO missions. Establishing priorities for future ground-based and space-based materials research was a major goal of the workshop. The end product of the workshop was an assessment of the current state-of-the-art in space environmental effects on materials in order to develop a national plan for spaceflight experiments. The workshop was intended for participation by expert applied researchers, systems technologists, and program managers for spacecraft systems.					
17. Key Words (Suggested by Author(s)) Space environmental effects on materials Atomic oxygen Micrometeoroids and debris Contamination Thermal and ultraviolet (UV) radiation Particulate radiation and cosmic rays				18. Distribution Statement 18. Distribution Statement Unclassified - Unlimited Subject Category 23	
19. Security Classif. (of this report) Unclassified		20. Security Classif. (of this page) Unclassified		21. No. of pages 265	
				22. Price A12	